

Functional Characterisation of the Eukaryotic
Translation Elongation Factor 1By in
Aspergillus fumigatus; A Proteomic Systems
Approach

Gráinne O' Keeffe BSc



NUI MAYNOOTH

Ollscoil na hÉireann Má Nuad

Thesis submitted to the
National University of Ireland
for the degree of
Doctor of Philosophy
October 2011

Supervisor:

Prof. Sean Doyle,

National Institute for Cellular Biotechnology,

National University of Ireland Maynooth,

Co. Kildare.

Head of Department:

Prof. Kay Ohlendieck

Table of Contents

Declaration of Authorship.....	xiv
Acknowledgements.....	xv
Publications and Presentations.....	xvi
Abbreviations.....	xviii
Summary.....	xxii

Chapter 1. Introduction

1.1	<i>Aspergillus fumigatus</i>	1
1.1.1	General description.....	1
1.1.2	Pathogenesis.....	3
1.1.3	Virulence factors.....	6
1.1.4	Genome.....	10
1.2	Functional Genomics.....	11
1.3	Comparative proteomics.....	15
1.4	Systems biology.....	19
1.5	Protein synthesis in eukaryotes.....	21
1.6	Eukaryotic elongation factor 1 complex.....	27
1.7	Eukaryotic elongation factor 1B γ	31
1.8	eEF1B γ in <i>A. fumigatus</i>	34
1.9	Glutathione <i>s</i> -transferases.....	37
1.9.1	GST function.....	37
1.9.2	GST classification.....	40
1.9.3	GSTs in <i>A. fumigatus</i>	41
1.10	Oxidative stress.....	44
1.11	Transcription factors in redox regulation.....	49
1.12	Degradation of “damaged” and misfolded proteins.....	51

1.13	Thesis rationale and objectives.....	53
------	--------------------------------------	----

Chapter 2. Materials and Methods

2.1	Materials.....	55
2.1.1	<i>Aspergillus</i> Media and Agar.....	55
2.1.1.1	Sabouraud Dextrose Broth.....	55
2.1.1.2	Sabouraud Agar.....	55
2.1.1.3	Malt Extract Agar.....	55
2.1.1.4	<i>Aspergillus</i> Minimal Media (AMM).....	56
2.1.1.4.1	<i>Aspergillus</i> Trace Elements.....	56
2.1.1.4.2	<i>Aspergillus</i> Salt Solution.....	56
2.1.1.4.3	100 X Ammonium Tartrate.....	56
2.1.1.4.4	AMM Liquid Media.....	57
2.1.1.4.5	AMM Agar.....	57
2.1.1.5	Regeneration Agar.....	57
2.1.1.5.1	1.8% (w/v) Regeneration Agar.....	57
2.1.1.5.2	0.7% (w/v) Regeneration Agar.....	58
2.1.1.6	RPMI 1640 containing 2 % (w/v) glucose.....	58
2.1.2	Solutions for pH Adjustment.....	58
2.1.2.1	5 M Hydrochloric Acid (HCl).....	58
2.1.2.2	5 M Sodium Hydroxide (NaOH).....	58
2.1.3	Phosphate Buffer Saline (PBS).....	59
2.1.4	Phosphate Buffer Saline-Tween 20 (0.05% (v/v)) (PBST 0.05%)....	59
2.1.5	Phosphate Buffer Saline-Tween 20 (0.1% (v/v)) (PBST 0.1%).....	59
2.1.6	Plate Assays.....	59
2.1.7	Luria-Bertani Broth (LB Broth).....	59
2.1.8	Luria-Bertani Agar (LB Agar).....	61

2.1.9	80 % (v/v) Glycerol.....	61
2.1.10	10% (w/v) Sodium Dodecyl Sulphate (SDS).....	61
2.1.11	20 % (w/v) SDS.....	61
2.1.12	Antibiotics and Supplements.....	62
2.1.13	DNA Electrophoresis Reagents.....	62
2.1.13.1	50 X Tris-Acetate Buffer (TAE).....	62
2.1.13.2	1 X Tris Acetate Buffer (TAE).....	62
2.1.13.3	Ethidium Bromide.....	63
2.1.13.4	6 X DNA Loading Dye.....	63
2.1.14	DNA Reagents.....	63
2.1.14.1	100 % (v/v) Ethanol (ice-cold).....	63
2.1.14.2	70 % (v/v) Ethanol (ice-cold).....	63
2.1.14.3	3 M Sodium Acetate.....	63
2.1.14.4	Table of primers.....	63
2.1.15	RNA Electrophoresis Reagents.....	65
2.1.15.1	RNA Glassware.....	65
2.1.15.2	0.5 M EDTA.....	65
2.1.15.3	10 X Formaldehyde Agarose (FA) Gel Buffer.....	65
2.1.15.4	1 X Formaldehyde Agarose (FA) Running Buffer.....	65
2.1.16	Aspergillus Transformation Reagents.....	66
2.1.16.1	0.7 M Potassium Chloride.....	66
2.1.16.2	25 mM Potassium Phosphate Monobasic.....	66
2.1.16.3	25 mM Potassium Phosphate Dibasic.....	66
2.1.16.4	Lysis Buffer.....	66
2.1.16.5	Lysis Buffer containing Lytic Enzymes.....	66
2.1.16.6	Buffer L6.....	67
2.1.16.7	Buffer L7.....	67

2.1.17	Southern Blot Reagents.....	67
2.1.17.1	Southern Transfer Buffer.....	67
2.1.17.2	20 X SSC.....	67
2.1.17.3	2 X SSC.....	68
2.1.17.4	Dig Buffer 1.....	68
2.1.17.5	Blocking Reagent.....	68
2.1.17.6	10 % (w/v) Laurosarcosine.....	68
2.1.17.7	Membrane Pre-Hybridisation Buffer.....	68
2.1.17.8	1 X SSC/ 0.1 % (w/v) SDS.....	69
2.1.17.9	Dig Wash Buffer (0.3 % (v/v) Tween-20 in Dig Buffer 1).....	69
2.1.17.10	Dig Buffer 2.....	69
2.1.17.11	Dig Buffer 3.....	69
2.1.17.12	Anti-Digoxigenin-Alkaline Phosphatase (AP), Fab fragment conjugate.....	70
2.1.17.13	Chemiluminescent Substrate Phosphate Detection (CSPD) Substrate.....	70
2.1.17.14	DIG-labelled deoxynucleotide triphosphates (dNTP's).....	70
2.1.18	Chemicals for Photography.....	70
2.1.18.1	Developer Solution.....	70
2.1.18.2	Fixer Solution.....	70
2.1.19	SDS-PAGE Reagents.....	71
2.1.19.1	1.5 M Tris-HCl, pH 8.8.....	71
2.1.19.2	0.5 M Tris-HCl, pH 6.8.....	71
2.1.19.3	10 % (w/v) Ammonium Persulphate.....	71
2.1.19.4	30 % (w/v) Acrylamide/Bis.....	71
2.1.19.5	0.5 % (w/v) Bromophenol Blue.....	71
2.1.19.6	5 X Solubilisation Buffer; reducing.....	72
2.1.19.7	4 X Solubilisation Buffer; non-reducing.....	72

2.1.19.8	5 X Electrode Running Buffer.....	72
2.1.19.9	1 X Electrode Running Buffer.....	72
2.1.19.10	Coomassie® Blue Stain Solution.....	73
2.1.19.11	Destain Solution.....	73
2.1.19.12	Colloidal Coomassie® Blue Stain Solutions.....	73
2.1.19.12.1	Fixing Solution.....	73
2.1.19.12.2	Incubation Buffer.....	73
2.1.19.12.3	Stain Solution.....	74
2.1.20	Western Blot Reagents.....	74
2.1.20.1	Towbin Electrotransfer Buffer.....	74
2.1.20.2	Blocking Solution.....	74
2.1.20.3	Antibody Buffer.....	74
2.1.20.4	ECL.....	74
2.1.21	Lysis Reagents.....	75
2.1.21.1	<i>A. fumigatus</i> Mycelia Lysis Buffer.....	75
2.1.21.2	<i>A. fumigatus</i> Mycelia Lysis Buffer; non-reducing.....	75
2.1.22	Bradford Solution.....	75
2.1.23	2D-PAGE Solutions.....	75
2.1.23.1	Trichloroacetic Acid 100 % (w/v) (100 % TCA).....	75
2.1.23.2	Trichloroacetic Acid 10 % (w/v) (10 % TCA).....	76
2.1.23.3	Isoelectric focusing Buffer (IEF).....	76
2.1.23.4	IPG Equilibration Buffer.....	76
2.1.23.5	Reduction Buffer.....	76
2.1.23.6	Alkylation Buffer.....	77
2.1.23.7	Agarose Sealing Solution.....	77
2.1.24	Mass Spectrometry Reagents.....	77
2.1.24.1	100 mM Ammonium bicarbonate (NH ₄ HCO ₃).....	77

2.1.24.2	100 mM Ammonium bicarbonate / Acetonitrile (1:1 (v/v)).....	77
2.1.24.3	10 mM Ammonium bicarbonate containing acetonitrile 10% (v/v)..	78
2.1.24.4	Trypsin Solution.....	78
2.1.24.5	0.1 % (v/v) Formic Acid in LC-MS Grade Water.....	78
2.1.24.6	0.1 % (v/v) Formic Acid in 90 % (v/v) LC-MS Grade Acetonitrile..	78
2.1.24.7	0.1% (v/v) Trifluoroacetic acid.....	78
2.1.25	Reverse-Phase High Performance liquid Chromatography (RP-HPLC) Solvents.....	79
2.1.25.1	Solvent A (0.1 % (v/v) Trifluoroacetic Acid in HPLC Grade H ₂ O)..	79
2.1.25.2	Solvent B (0.1 % (v/v) Trifluoroacetic Acid in HPLC Grade Acetonitrile).....	79
2.1.26	Intracellular Glutathione measurement.....	79
2.1.26.1	125 mM Sodium Phosphate monobasic.....	79
2.1.26.2	125 mM Sodium Phosphate dibasic.....	79
2.1.26.3	GSH/GSSG Assay Buffer (125 mM Sodium Phosphate (pH 7.5) 6.3 mM EDTA.....	80
2.1.26.4	5 % (w/v) 5'5-sulfosalicylic acid (5 % SSA).....	80
2.1.26.5	50 % (v/v) Triethanolamine.....	80
2.1.26.6	20 % (v/v) 2-vinylpyridine.....	80
2.1.26.7	10 mM 5,5'-dithio-bis(2-nitrobenzoic acid) (DTNB).....	80
2.1.26.8	DTNB containing 1 UN Glutathione Reductase.....	81
2.1.26.9	30 mM β -nicotinamide adenine dinucleotide 2'-phosphate reduced tetrasodium salt hydrate (NADPH).....	81
2.1.26.10	5 mM NADPH.....	81
2.1.26.11	1 mg/ml Glutathione.....	81
2.1.26.12	2 mg/ml Glutathione disulfide.....	81
2.1.27	Biotinylation of Glutathione disulfide.....	82
2.1.27.1	Sulfo-NHS-LC-Biotin.....	82
2.1.27.2	1 M Tris-HCl (pH 7.2).....	82

2.1.28	Confocal Imaging.....	82
2.1.28.1	50 mM Sodium Phosphate Monobasic.....	82
2.1.28.2	50 mM Sodium Phosphate Dibasic.....	82
2.1.28.3	50 mM Sodium Phosphate Buffer (pH 7.4).....	82
2.1.28.4	4 % (v/v) Formaldehyde, 50 mM Sodium Phosphate Buffer (pH 7.4).....	83
2.1.28.5	Confocal Buffer (50 mg/ml BSA in PBS).....	83
2.1.29	50 mM Sodium Phosphate Buffer (pH 7.4) containing 150 mM NaCl.....	83
2.2	Methods.....	84
2.2.1	Microbiological Methods- strain storage and growth.....	84
2.2.1.1	<i>A. fumigatus</i> growth, maintenance and storage.....	84
2.2.1.2	<i>E. coli</i> Growth, Maintenance and Storage.....	87
2.2.2	Molecular Biological Methods.....	87
2.2.2.1	Isolation of Genomic DNA from <i>A. fumigatus</i>	87
2.2.2.2	DNA Precipitation.....	88
2.2.2.3	Polymerase Chain Reaction (PCR).....	89
2.2.2.4	Agarose Gel Electrophoresis.....	91
2.2.2.5	DNA Gel Electrophoresis.....	91
2.2.2.6	DNA Gel Extraction.....	92
2.2.3	Cloning.....	93
2.2.3.1	TOPO TA Cloning.....	93
2.2.3.2	Colony PCR.....	94
2.2.3.3	Small Scale Plasmid Purification.....	96
2.2.3.4	DNA Sequencing.....	97
2.2.4	RNA Analysis.....	97
2.2.4.1	RNA Isolation.....	97
2.2.4.2	RNA Gel Electrophoresis.....	98

2.2.4.3	DNase Treatment of RNA.....	99
2.2.4.4	cDNA Synthesis.....	99
2.2.4.5	Semi-quantitative RT-PCR.....	101
2.2.5	Restriction Enzyme Digests.....	101
2.2.6	De-phosphorylation of blunt-end restriction digests.....	102
2.2.7	Filling in overhangs from restriction digests.....	103
2.2.8	Ligation of DNA fragments.....	103
2.2.9	Generation of <i>A. fumigatus elfA</i> deletion and complementation strains.....	104
2.2.9.1	Deletion of <i>elfA</i> in <i>A. fumigatus</i>	104
2.2.9.1.1	Generation of <i>A. fumigatus elfA</i> deletion constructs.....	107
2.2.9.2	Complementation of <i>A. fumigatus ΔelfA</i>	110
2.2.9.2.1	Generation of the complementation construct.....	111
2.2.9.3	<i>A. fumigatus</i> protoplast production and transformation.....	114
2.2.9.3.1	<i>A. fumigatus</i> protoplast production.....	114
2.2.9.3.2	<i>A. fumigatus</i> protoplast transformation with gene deletion constructs.....	115
2.2.9.3.3	Plating transformed protoplasts on appropriate selection media.....	115
2.2.9.3.4	Isolation of <i>A. fumigatus</i> transformed colonies.....	116
2.2.9.3.5	Single-spore isolation of <i>A. fumigatus</i> transformants.....	117
2.2.10	Southern Blot Analysis.....	117
2.2.10.1	Transfer of Nucleic Acid.....	117
2.2.10.2	Disassembly of the Southern Tower.....	121
2.2.10.3	Digoxygenin (DIG) – Detection of hybridised Nucleic Acids.....	121
2.2.10.3.1	Generation of DIG- labelled probes.....	121
2.2.10.3.2	Pre-hybridisation of Nylon membrane.....	122
2.2.10.3.3	Hybridisation of Nylon membrane with DIG-labelled probe.....	122
2.2.10.3.4	DIG Detection.....	122

2.2.11	Developing Blots that used a chemiluminescent substrate.....	123
2.2.12	Bradford Protein Assay.....	124
2.2.13	Sodium Dodecyl Sulphate Polyacrylamide Gel Electrophoresis (SDS-PAGE).....	124
2.2.14	Colloidal Coomassie Blue Staining.....	126
2.2.15	Western Blot Analysis; Semi-Dry.....	126
2.2.16	Protein Extraction from <i>A. fumigatus</i>	127
2.2.16.1	Whole Cell Protein Extraction for 2D Analysis of <i>A. fumigatus</i>	127
2.2.16.2	Whole Cell Protein extraction from <i>A. fumigatus</i> ; Small scale.....	128
2.2.16.3	Whole cell protein extraction from <i>A. fumigatus</i> ; Large scale.....	128
2.2.16.4	Whole Cell Protein Extraction from <i>A. fumigatus</i> germlings.....	129
2.2.17	TCA/Acetone precipitation before 2D-PAGE.....	129
2.2.18	Isoelectric Focussing (IEF) and 2D-PAGE.....	130
2.2.19	In-Gel Digestion of Protein Spots from 2D-PAGE Gels.....	132
2.2.20	MALDI-ToF Mass Spectrometry.....	132
2.2.20.1	Matrix (a-cyano-4-hydroxycinnamic acid) (4-HCCA) Preparation.....	132
2.2.20.2	Target preparation and MS analysis.....	133
2.2.21	Liquid Chromatography Mass Spectrometry (LC-MS).....	134
2.2.21.1	Sample Preparation.....	134
2.2.21.2	Sample Analysis.....	134
2.2.22	Biotinylation of Glutathione disulfide (Biotin-GSSG).....	135
2.2.23	Reverse Phase – High Performance Liquid Chromatography Analysis.....	135
2.2.24	Investigating protein glutathionylation using Biotin-GSSG.....	136
2.2.24.1	Western blot analysis of protein glutathionylation.....	136
2.2.25	Intracellular Glutathione Measurement.....	136
2.2.25.1	Sample Preparation.....	136
2.2.25.2	GSH Standard Preparation.....	137

2.2.25.3	GSSG Standard Preparation.....	137
2.2.25.4	Pre-treatment of GSSG samples.....	138
2.2.25.5	Glutathione Assay.....	138
2.2.25.6	Comparative Hydrophobicity Assay.....	139
2.2.25.7	<i>A. fumigatus</i> Germination Assay.....	139
2.2.25.8	MIC of Voriconazole.....	140
2.2.25.9	Confocal Microscopy.....	140
2.2.25.10	Statistical analysis.....	141
2.2.25.11	Multiple sequence alignment.....	141

Chapter 3. Deletion and Complementation of *A. fumigatus* Δ elfA

3.1	Introduction.....	142
3.2	Results.....	147
3.2.1	Generation of deletion constructs for the transformation of <i>A. fumigatus</i>	147
3.2.2	Generation of Digoxigenin (DIG)-labelled probes for Southern blot analysis.....	152
3.2.3	Transformation of <i>A. fumigatus</i> resulted in the deletion of <i>elfA</i> in ATCC46645 and Δ <i>akuB</i>	154
3.2.4	Generation of construct for complementation of Δ elfA.....	160
3.2.5	Re-insertion of <i>elfA</i> into Δ elfA complements its deletion.....	166
3.2.6	RT-PCR confirms expression of <i>A. fumigatus</i> <i>elfA</i> in ATCC46645 and <i>elfA</i> ^C and absence of expression in Δ elfA.....	171
3.3	Discussion.....	173

Chapter 4. Functional Characterisation of *A. fumigatus* Δ elfA

4.1	Introduction.....	178
-----	-------------------	-----

4.2	Results.....	186
4.2.1	Multiple sequence alignment of <i>A. fumigatus</i> <i>elfA</i> and other eEF1B γ proteins.....	186
4.2.2	Phenotypic analysis of <i>A. fumigatus</i> Δ <i>elfA</i>	190
4.2.2.1	Phenotypic analysis of <i>A. fumigatus</i> Δ <i>elfA</i> in response to amphotericin B.....	192
4.2.2.2	Phenotypic analysis of <i>A. fumigatus</i> Δ <i>elfA</i> in response to gliotoxin.....	192
4.2.2.3	Phenotypic analysis of <i>A. fumigatus</i> Δ <i>elfA</i> in response to Glycerol-induced osmotic stress.....	194
4.2.2.4	Analysis of <i>A. fumigatus</i> Δ <i>elfA</i> protease secretory capacity.....	194
4.2.2.5	Phenotypic analysis of <i>A. fumigatus</i> Δ <i>elfA</i> in response to DTT.....	196
4.2.2.6	Phenotypic analysis of <i>A. fumigatus</i> Δ <i>elfA</i> in response to voriconazole.....	196
4.2.2.8	Phenotypic analysis of <i>A. fumigatus</i> Δ <i>elfA</i> in response to oxidative stress.....	198
4.2.3	Intracellular glutathione measurement.....	203
4.2.3.1	GSH and GSSG determination.....	203
4.2.3.2	Measurement of the intracellular GSH and GSSG levels in <i>A. fumigatus</i> strains under normal growth conditions.....	205
4.2.3.3	Investigation of intracellular GSH and GSSG levels in <i>A. fumigatus</i> Δ <i>elfA</i> after exposure to H ₂ O ₂	207
4.2.3.4	Determination of an altered redox status in <i>A. fumigatus</i> Δ <i>gliT</i>	211
4.2.4	Protein glutathionylation investigation.....	214
4.2.4.1	Synthesis of biotin-GSSG.....	214
4.2.4.2	Investigating protein glutathionylation in <i>A. fumigatus</i> ATCC46645 and Δ <i>elfA</i>	220
4.3	Discussion.....	224

Chapter 5. Comparative proteomic investigation of *A. fumigatus* wild-type versus $\Delta elfA$

5.1	Introduction.....	233
5.2	Results.....	237
5.2.1	2D-PAGE of <i>A. fumigatus</i> ATCC46645 and $\Delta elfA$ under normal growth conditions.....	237
5.2.2	Mass spectrometry analysis of differentially expressed proteins....	240
5.2.3	Identification of a unique protein in <i>A. fumigatus</i> $\Delta elfA$ corresponding to the selection marker <i>ptrA</i>	245
5.2.4	2D-PAGE of <i>A. fumigatus</i> ATCC46645 and $\Delta elfA$ following exposure to H ₂ O ₂	248
5.2.5	LC-MS/MS analysis of differentially expressed proteins.....	251
5.3	Discussion.....	257

Chapter 6. Comparative proteomics elucidation of additional gene function in *A. fumigatus*

6.1	Introduction.....	275
6.2	Results.....	281
6.2.1	Comparative proteomic analysis of <i>A. fumigatus</i> ATCC46645 and <i>A. fumigatus</i> $\Delta pes3$	281
6.2.2	LC-MS/MS analysis of differentially expressed proteins.....	284
6.2.3	Identification of thiazole synthase, which is encoded by the selection marker <i>ptrA</i> , in <i>A. fumigatus</i> $\Delta pes3$ germlings only.....	289
6.2.4	Confocal Imaging of (1,3)- β -glucan in <i>A. fumigatus</i> ATC46645 and <i>A. fumigatus</i> $\Delta pes3$	291
6.2.5	<i>A. fumigatus</i> $\Delta pes3$ germinated at a slower rate than <i>A. fumigatus</i> ATCC46645 under static conditions.....	294
6.2.6	Investigation of hydrophobicity of <i>A. fumigatus</i> $\Delta pes3$ conidia.....	296
6.2.7	Determining the MIC of voriconazole for <i>A. fumigatus</i> $\Delta pes3$	296

6.3	Discussion.....	298
	Chapter 7. Discussion.....	307
	Chapter 8. Bibliography.....	322

Declaration of Authorship

This thesis has not previously been submitted in whole or in part to this or any other University for any other degree. This thesis is the sole work of the author, with the exception of the generation of the *A. fumigatus pes3* mutant, which was generated by Dr. Deirdre Stack.

Gráinne O' Keeffe BSc.

Acknowledgements

First and foremost I would like to thank my supervisor Professor Sean Doyle for all the guidance, advice, support and encouragement I have received throughout this PhD. I would also like to thank Dr. Christoph Jöchl and Dr. Markus Schrettl for the expert training I received at the start of this work. Also, sincere thanks to Dr. Stephen Carberry for his training and advice. I would also like to extend thanks to Caroline Batchelor for assistance with LC-MS and Ica Dix for assistance with confocal microscopy. I would like to thank IRCSET and the Department of Biology, NUI Maynooth, for funding this PhD.

To all the members of the Biotechnology Lab, past and present; Rebecca, Cindy, Carol, Karen, Lorna, Luke, Natasha, and John and Karen T. (honorary Biotech members!!), thank you for all the help, advice, and laughs which made this PhD an enjoyable experience. In addition I would like to thank my colleagues in the department for allowing me to borrow and use reagents and equipment when needed, in particular the Medical Mycology Lab.

A special thanks to my closest friends; Colette, Michelle, Mark, Eilish, Orlaith and Gemma. Your listening ears and willingness to provide distractions have kept me somewhat sane throughout this PhD and your patience when I fell off the face of the planet in the past few months is much appreciated!

Finally, I would like to thank my family. To my sisters, Sinéad and Róisín, your “unique” encouragement throughout this PhD was most helpful! To my parents, Con and Annamay, thank you for your unwavering support and encouragement, not only throughout this PhD, but in everything I do.

Publications and Presentations

Research Publications

O'Hanlon, K.A., Cairns, T., Stack, D., Schrettl, M., Bignell, E.M., Kavanagh, K., Miggin, S. M., **O'Keeffe, G.**, Larsen, T. O., Doyle, S. (2011) Targeted Disruption of Non-Ribosomal Peptide Synthetase *pes3* Augments the Virulence of *Aspergillus fumigatus*. *Infect. Immun.* 79(10)3978-3992.

Carberry, S., Molloy, E., Hammel, S., **O'Keeffe, G.**, Jones, G.W., Kavanagh, K. and Doyle, S. 2011. Gliotoxin Effects on Fungal Growth: Mechanisms and Exploitation. *Fungal Genet Biol.* Submitted 12 October 2011.

O'Keeffe, G., Jöchl, C., Kavanagh, K. and Doyle, S. Functional Characterisation of the Eukaryotic Translation Elongation Factor 1B γ in *A. fumigatus*. In preparation.

Oral Presentations

Genomic and proteomic approaches implicate an EF1B γ elongation factor in protein synthesis and redox control in *Aspergillus fumigatus*. Irish Fungal Society Meeting, Trinity College Dublin, 16th - 17th June 2011.

Using Proteomics to Characterise Gene Function in *Aspergillus fumigatus*. Annual Irish Mass Spectrometry Society Meeting, Dublin, Ireland. 12th May 2010.

Characterisation of a putative translation elongation factor in *Aspergillus fumigatus*. Departmental Symposium, NUI Maynooth, 3rd June 2010.

Functional Proteomic Analysis in *Aspergillus fumigatus*. Departmental Symposium, NUI Maynooth, 27th May 2009.

Poster Presentations

Genomic and proteomic approaches implicate an EF1B γ elongation factor in protein synthesis and redox control in *Aspergillus fumigatus*. Fourth FEBS Advanced Lecture Course on Human Fungal Pathogens. La Colle sur Loup, France, 7th – 13th May 2011.

Targeted functional proteomics: A putative translation elongation factor with glutathione s-transferase activity protects *Aspergillus fumigatus* against oxidative stress. Irish Fungal Meeting, UCC Cork, 17th June 2010.

Targeted functional proteomics: A putative translation elongation factor with glutathione s-transferase activity protects *Aspergillus fumigatus* against oxidative stress. 10th European Conference on Fungal Genetics, Leeuwenhorst, The Netherlands, 30th March 2010.

Targeted functional proteomics: A putative translation elongation factor with glutathione s-transferase activity protects *Aspergillus fumigatus* against oxidative stress. Asperfest 2010 Leeuwenhorst, The Netherlands, 27th March 2010.

Dual-function protein: a putative translation elongation factor with glutathione s-transferase activity protects *Aspergillus fumigatus* against oxidative stress. Irish Fungal Meeting, UCD Dublin, 26th June 2009.

Dual-function protein: a putative translation elongation factor with glutathione s-transferase activity protects *Aspergillus fumigatus* against oxidative stress. Third FEBS Advanced Lecture Course on Human Fungal Pathogens. La Colle sur Loup, France, 13th May 2009. Awarded Young Investigator Award.

Abbreviations

2D-PAGE	Two dimensional polyacrylamide gel electrophoresis
aa	Amino acid
ABPA	Allergic bronchopulmonary aspergillosis
AMM	Aspergillus minimal media
AmpB	Amphotericin B
AMT	<i>Agrobacterium</i> -mediated transformation
AP	Alkaline phosphatase
ATCC	American Type Cell Culture
ATP	Adenosine triphosphate
bp	Base pairs
BSA	Bovine serum albumin
bZIP	Basic leucine zipper
CADRE	Central <i>Aspergillus</i> Data Respository
cDNA	Complementary deoxyribonucleic acid
CDNB	1-chloro-2,4-nitrobenzene
cds	Coding sequence
CGD	Chronic granulomatous disease
CIAP	Calf intestine alkaline phosphatase
CoA	Coenzyme A
CRD	Cysteine rich domain
CSPD	Chemiluminescent substrate phosphate detection
DIG	Digoxigenin
DIGE	Differential gel electrophoresis

DMSO	Dimethyl sulfoxide
DNA	Deoxyribonucleic acid
DTNB	5,5'-dithiobis-(2-nitrobenzoic acid)
ECL	Enhanced chemiluminescent
EDTA	Ethylenediaminetetraacetic acid
eEF1	Eukaryotic elongation factor 1
eIF	Eukaryotic initiation factor
EF	Elongation factor
ER	Endoplasmic reticulum
eRF	Eukaryotic termination release factor
ERAD	Endoplasmic reticulum associated degradation
FA	Formaldehyde agarose
gDNA	genomic deoxyribonucleic acid
GEF	Nucleotide exchange factor
GOI	Gene of interest
GR	Glutathione reductase
GST	Glutathione <i>s</i> -transferase
GSH	Glutathione
GSSG	Glutathione disulphide
H ₂ O ₂	Hydrogen peroxide
HCCA	α -cyano-4-hydroxycinnamic acid
HR	Homologous recombination
IA	Invasive Aspergillosis
IEF	isoelectric focusing
Kb	Kilobase

kDa	Kilodalton
LB	Luria Bertani
LC-MS	Liquid chromatography mass spectrometry
MALDI-ToF MS	Matrix assisted laser desorption time of flight mass spectrometry
ME	Malt extract
MIC	Minimum inhibitory concentration
MOPS	3-(N-morpholino)propanesulfonic acid
MRP	Multidrug resistance associated protein
NADH	Nicotinamide adenine dinucleotide
NADPH	Nicotinamide adenine dinucleotide phosphate
NCP	Nitrocellulose paper
NETs	Neutrophil extracellular traps
NHEJ	Non-homologous end joining
nm	Nanometer
NRP	Non ribosomal peptide
NRPS	Non ribosomal peptide synthetase
OD	Optical density
ORF	Open reading frame
PBS	Phosphate buffered saline
PBST	Phosphate buffered saline-Tween
PCR	Polymerase chain reaction
PEG	Polyethylene glycol
PMSF	Phenylmethylsulfonyl fluoride
PMT	Protoplast-mediated transformation

RNA	Ribonucleic acid
ROS	Reactive oxygen species
RP-HPLC	Reverse-phase High performance liquid chromatography
RPM	Revolutions per minute
RT-PCR	Reverse-transcriptase polymerase chain reaction
SAM	s-adenosyl methionine
SDS	Sodium dodecyl sulphate
SDS-PAGE	Sodium dodecyl sulphate polyacrylamide gel electrophoresis
SEM	Scanning electron microscopy
SM	Selection marker
SSA	5'5-sulfosalicylic acid
TAE	Tris:acetate:EDTA
TCA	Trichloroacetic acid
TFA	Trifluoroacetic acid
Ti	Tumour-inducing
tRNA	transfer RNA
UPR	Unfolded protein response
UTR	Untranslated region
UV	Ultraviolet
v/v	volume per volume
w/v	weight per volume
X-gal	1,5-bromo-4-chloro-3-indoyl- β -DNA-galactosidase

Summary

The opportunistic pathogen *Aspergillus fumigatus* is ubiquitous in the environment and predominantly infects immunocompromised patients. Sequencing of the fungal genome has led to an increased understanding of the organism; however the functions of many genes remain unknown. A putative translation elongation factor 1B γ (eEF1B γ , termed *elfA*; 750 bp) is expressed, and exhibits glutathione *s*-transferase activity, in *A. fumigatus*. The work presented here demonstrates the role of ElfA in protein synthesis, but also that it plays a key role in the oxidative stress response and may be involved in actin cytoskeleton organisation. Phenotypic analysis demonstrates that an *elfA* deficient strain (*A. fumigatus* Δ *elfA*) was significantly more sensitive to the oxidants H₂O₂ (> 1 mM) (p = 0.0003), diamide (> 0.5 mM) (p < 0.001), and 4, 4'-dithiodipyridine (> 7.5 μ M) (p = 0.0056), and was significantly more resistant to voriconazole (> 0.5 μ g/ml) (p = 0.0251) than the wild-type. Comparative proteomics, under basal and oxidative stress conditions, revealed significantly (p < 0.05) altered expression of proteins involved in protein synthesis, the oxidative stress response and actin cytoskeleton organization. In parallel, comparative proteomics of *A. fumigatus* Δ *pes3*, a non-ribosomal peptide synthetase deficient strain, supports a structural role for this peptide with the altered expression of proteins functioning in morphogenesis and germination. *A. fumigatus* Δ *pes3* exhibited a reduced germination rate in static cultures and confocal microscopy revealed not only shorter germ tubes but reduced surface (1,3)- β -glucan in this mutant. Moreover, the reduced surface (1,3)- β -glucan explains the lower MIC of *A. fumigatus* Δ *pes3* to voriconazole measured in this study as surface (1,3)- β -glucan sequesters azoles preventing entry into the cell. Overall, this work highlights the diverse roles of *A. fumigatus* *elfA*, with respect to protein synthesis, oxidative stress and actin cytoskeleton organisation. In addition to this, the advantages of combining targeted gene deletion with comparative proteomics for elucidating the role of proteins of unknown function are also revealed.

1. Introduction

1.1 *Aspergillus fumigatus*

1.1.1 General description

The ascomycete *Aspergillus fumigatus* is an opportunistic human pathogen (Brakhage and Langfelder, 2002). *A. fumigatus* is a saprotroph and plays an important role in recycling environmental carbon and nitrogen in its natural ecological niche, the soil (Latge, 1999). In the laboratory, *A. fumigatus* can grow rapidly on minimal agar plates containing a carbon source (e.g., glucose), a nitrogen source (e.g., nitrate), and trace elements (Brakhage and Langfelder, 2002). *A. fumigatus* can be recognised by its grey-green conidia (Figure 1.1). The conidia are 2.5 to 3 µm in size, which not only enables them to become and remain airborne, but also facilitates their entry into the lung alveoli (Brakhage and Langfelder, 2002; Latge, 1999). *A. fumigatus* is a thermotolerant fungus and can grow at temperatures up to 55 °C, while the conidia can survive at temperatures up to 70 °C (Bhabhra and Askew, 2005; Latge, 1999)

Reproduction in *A. fumigatus* occurs asexually via haploid conidia, although recently, sexual reproduction has been described (O’Gorman *et al.*, 2009). The asexual lifecycle of *A. fumigatus* is as follows; (i) the conidia germinate into septate mycelia, (ii) conidiophores are produced by the mycelia, (iii) the conidia are released from the conidiophores and the cycle continues (Figure 1.1). Following the sequencing of the *A. fumigatus* genome, studies identified genes involved in sexual reproduction (Galagan *et al.*, 2005; Nierman *et al.*, 2005; Paoletti *et al.*, 2005).

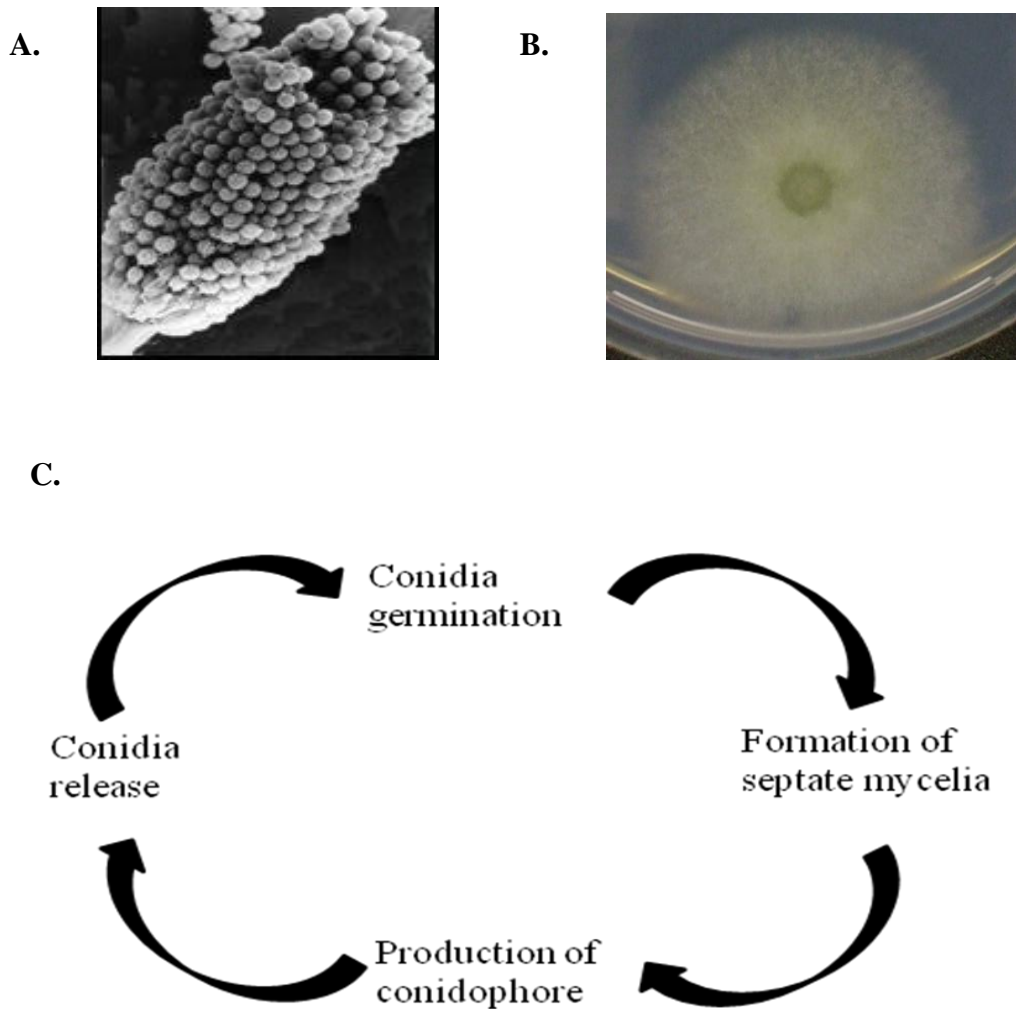


Figure 1.1: The life cycle of *A. fumigatus*.

- A. Scanning electron microscopy of *A. fumigatus* conidial head releasing asexual conidia. (Image from www.aspergillus.org.uk)
- B. *A. fumigatus* ATCC46645 colony growing on *Aspergillus minimum* media.
- C. Germinating conidia form septate mycelia, which then form conidiophores. Conidia are released from the conidiophores and germinate continuing the cycle.

The mating-type (MAT) genes associated with sexual reproduction along with genes involved in pheromone production and detection were identified (Galagan *et al.*, 2005; Paoletti *et al.*, 2005). O' Gorman *et al.* (2009) experimentally verified the existence of a sexual cycle in *A. fumigatus*, and described the telomorph; *Neosartorya fumigata*.

1.1.2 Pathogenesis

There are approximately two hundred species of *Aspergillus*, of which less than twenty cause disease in humans (Hohl and Feldmesser, 2007). *A. fumigatus* is the most pathogenic, followed by *A. flavus*, *A. terreus*, *A. niger* and *A. nidulans* (Dagenais and Keller, 2009). *A. fumigatus* not only causes invasive disease in immunocompromised patients, but also allergic disease in patients with atopic immune systems (Denning *et al.*, 2002). *A. fumigatus* is responsible for 4 % of patient deaths in European teaching hospitals and is the principal infectious agent causing death in leukaemia and bone marrow transplant patients (Denning *et al.*, 2002). *A. fumigatus* infections have increased in the past twenty years as the number of immunosuppressed patients increased. Increases in organ transplants, the use of immunosuppressive therapy and the population of HIV infected individuals has contributed to this increase in *A. fumigatus* infections (Dagenais and Keller, 2009; Hohl and Feldmesser, 2007; Brakhage and Langfelder, 2002).

In the environment, conidia are estimated to be present at concentrations of 1 – 100 conidia per m³ (Denning *et al.*, 2002) and humans are thought to inhale hundreds of these conidia each day (Latge, 1999). Once inhaled, due to their small

size, conidia can travel to the alveoli and so, most *Aspergillus* infections occur in the respiratory tract (McCormick *et al.*, 2010). In immunocompetent individuals these conidia do not pose a threat as the innate immune system is able to eliminate them (Latge, 1999). Conidia that are not removed by mucociliary clearance are subjected to the innate immune system in the form of alveolar macrophages (Dagenais and Keller, 2009). Alveolar macrophages phagocytose and kill the conidia in an NADPH oxidase dependent manner and also recruit neutrophils by initiating a proinflammatory response (Dagenais and Keller, 2009; Hohl and Feldmesser, 2007). Conidia that have evaded both mucociliary clearance and the alveolar macrophages germinate to form hyphae, which are too large to be destroyed by macrophages (Dagenais and Keller, 2009). These hyphae are targeted by neutrophils, which release microbicidal molecules and reactive oxygen species (McCormick *et al.*, 2010; Hohl and Feldmesser, 2007). Neutrophils also release neutrophil extracellular traps (NETs) when they are dying which are composed of nuclear DNA decorated with fungicidal proteins (Bruns *et al.*, 2010b). The NETs are fungistatic and restrict hyphal growth but do not eliminate the fungus (Bruns *et al.*, 2010b).

In individuals with a compromised immune system, *A. fumigatus* germinates and causes infection, known as aspergillosis, which depending on the site of infection can be classified into three categories; (i) allergic bronchopulmonary aspergillosis (ABPA), (ii) aspergilloma and (iii) invasive aspergillosis (IA) (Latge, 1999). ABPA is a hypersensitivity-type lung disease wherein *A. fumigatus* germinates in the bronchi and elicits a continued immune response (Knutsen and Slavin, 2011; Latge, 1999). It mainly affects patients suffering from asthma or cystic

fibrosis, where the increased levels of viscous mucus facilitate germination (Dagenais and Keller, 2009; Latge, 1999). Diagnosis of ABPA is difficult, and if left untreated can result in airway destruction, pulmonary fibrosis and ultimately respiratory failure (Knutsen and Slavin, 2011; Latge, 1999).

Aspergilloma, also known as “fungus ball” or mycetoma, occurs in pre-existing lung cavities that may have resulted from another pulmonary disease such as tuberculosis (Knutsen and Slavin, 2011; Dagenais and Keller, 2009). The aspergilloma is composed of a spherical mass of hyphae which are embedded in a proteinaceous matrix with sporulating structures to the periphery of the “fungus ball” (Latge, 1999). Hemoptysis is a common symptom of aspergilloma and results from the disruption of blood vessels by the fungus in the cavity wall or the bronchus (Knutsen and Slavin, 2011; Latge, 1999). This happens centimetres from the aspergilloma and results in internal bleeding which ultimately may become fatal (Latge, 1999). Aspergillomas are detected by chest radiographs and treatment involves antifungals and surgery to remove the fungal mass (Knutsen and Slavin, 2011).

Invasive aspergillosis (IA) is the most serious of the diseases resulting from *Aspergillus* infection. It affects patients with suppressed immune systems (neutropenia and corticosteroid-induced immunosuppression) due to treatment for leukaemia, solid-organ transplantation, graft-versus-host disease and other hematological conditions (Dagenais and Keller, 2009). Due to the immunosuppression, *A. fumigatus* conidia germinate and rapid hyphal growth colonises the surrounding tissue and invades the blood vessels resulting in

thrombosis, haemorrhage and dissemination to other organs (McCormick *et al.*, 2010; Dagenais and Keller, 2009; Latge, 1999). Diagnosis of IA is difficult and requires isolation of the *A. fumigatus* from biopsy, however due to the severe illness in the patient, suitable samples are usually unobtainable (Thornton, 2010). Culturing from sputum samples invites possible contamination from airborne conidia, and may not be reliable (Latge, 1999). Definitive diagnosis of IA sometimes only occurs at autopsy. Treatment of IA involves the administration of antifungals such as voriconazole and amphotericin B (Knutsen and Slavin, 2011). In high-risk populations, the mortality rates for IA patients are usually between 40 – 90 % (Dagenais and Keller, 2009).

1.1.3 Virulence factors

Virulence in *A. fumigatus* is multi-factorial, with no single defined virulence factor so far identified, however a number of different adaptive factors that contribute to the virulence of this organism have been elucidated (McCormick *et al.*, 2010; Latge, 1999). Basic traits, including the small size of conidia, thermotolerance, stress resistance and adaptive capabilities, cell wall composition, nutrient acquisition ability, secreted proteases and secondary metabolites all contribute to the virulence of *A. fumigatus* (Abad *et al.*, 2010; Dagenais and Keller, 2009; Hohl and Feldmesser, 2007; Latge, 1999). As described earlier, the small size of the *A. fumigatus* conidia enables them to travel deep into the respiratory system to the alveoli, whereas the larger conidia of other *Aspergillus spp.* are easily removed from the upper respiratory tract by mucociliary clearance (Dagenais and Keller, 2009).

As described earlier, the thermotolerant nature of *A. fumigatus* enables it to grow not only at 37 °C but also at temperatures up to 55 °C. As other environmental moulds are unable to grow at temperatures above 35 °C, it has been proposed that thermotolerance may be one of the reasons *A. fumigatus* is a successful human pathogen (Bhabhra and Askew, 2005). Disruption of *A. fumigatus crgA*, which encodes a protein associated with thermotolerance, ribosome biogenesis and virulence, resulted in a strain that grew normally at 25 °C but had reduced growth at higher temperatures (Bhabhra *et al.*, 2004). This disruption strain had attenuated virulence in a murine model (at 37 °C) but not in a *Drosophila melanogaster* model of infection (at 25 °C) (Bhabhra *et al.*, 2004). It has been proposed that genes involved in thermotolerance also influence the stress response and possibly contribute to the virulence of *A. fumigatus* (Dagenais and Keller, 2009; Bhabhra and Askew, 2005). A comparative proteomic study of the heat shock response in *A. fumigatus* identified proteins involved in translation, protein folding, cytoskeletal organisation, metabolism the oxidative stress response (Albrecht *et al.*, 2010b).

A. fumigatus encounters various different stresses including reactive oxygen species (ROS), hypoxia and nutrient starvation in a host. Alveolar macrophages destroy conidia that have been phagocytosed in a ROS-dependent manner, while neutrophils attack hyphae with microcidal molecules and ROS (McCormick *et al.*, 2010; Dagenais and Keller, 2009; Hohl and Feldmesser, 2007). Yet, disruption of various genes involved in the oxidative stress response (e.g., *Afyap1* (Lessing *et al.*, 2007), *catA* (Paris *et al.*, 2003) and the four superoxide dismutase genes (Lambou *et al.*, 2010)) did not lead to attenuated virulence. However, the significance of the

ability of *A. fumigatus* to neutralise ROS is particularly evident in patients suffering from chronic granulomatous disease (CGD). CGD sufferers lack a functional NADPH activity and are susceptible to *Aspergillus* infection, particularly IA (Hartmann *et al.*, 2011). As well as the oxidative stress response, *A. fumigatus* produces the pigment melanin, which plays a role in protecting conidia by scavenging ROS (Dagenais and Keller, 2009). White conidia, which lack melanin, have been shown to be less virulent in a murine model of invasive aspergillosis (Jahn *et al.*, 1997). Melanin also aids the virulence of *A. fumigatus* by reducing fungal cell phagocytosis and intracellular trafficking to acidified compartments (Hohl and Feldmesser, 2007).

During infection, *A. fumigatus* encounters low levels of oxygen and therefore must adapt to hypoxic conditions (Willger *et al.*, 2008). Sterol regulatory element-binding proteins (SREBPs) are required for adaptation to hypoxic environments as oxygen sensors via sterol synthesis (Hartmann *et al.*, 2011). In *A. fumigatus* the deletion of *srbA* resulted in a strain that was not only unable to grow in hypoxic conditions (1 % O₂, 5% CO₂), but was sensitive to azoles and most importantly, was unable to cause disease in two murine models of IA (Willger *et al.*, 2008). Therefore the ability to adapt to hypoxic conditions is necessary for virulence in *A. fumigatus*.

One of the defence mechanisms of the host involves nutrient deprivation, so the ability of *A. fumigatus* to acquire essential nutrients in this environment is important for virulence (Abad *et al.*, 2010; Hohl and Feldmesser, 2007). *A. fumigatus* secretes enzymes, the majority of which are proteases that degrade host proteins providing nutrients but also break down physical barriers in the host

allowing for increased growth (Abad *et al.*, 2010). Individual proteases have not been identified as virulence factors and it is thought that proteases play an overlapping role in virulence (Abad *et al.*, 2010). However, a deletion strain for methylcitrate synthase, a key enzyme in the metabolism of the by-product of amino acid degradation, had attenuated virulence in a murine model of IA indicating that amino acid degradation is an important feature of virulence (Ibrahim-Granet *et al.*, 2008).

The ability of *A. fumigatus* to sequester iron in the host has contributed to the virulence of this pathogen. Iron is important as it acts as a cofactor in enzymatic reactions and also as a catalyst in electron transport systems (Dagenais and Keller, 2009). *A. fumigatus* acquires iron by two processes, (i) siderophore-mediated iron uptake and (ii) reductive iron assimilation (Schrettl and Haas, 2011; Schrettl *et al.*, 2007). Reductive iron assimilation has been determined as dispensable for virulence, however siderophore-mediated iron uptake is essential (Schrettl *et al.*, 2007; Schrettl *et al.*, 2004). Mutant strains for genes involved in siderophore biosynthesis; *A. fumigatus sidA*, *sidC*, *sidD* and *sidF*, all had decreased virulence in neutropenic mice models of IA (Schrettl *et al.*, 2007). The mutant for *A. fumigatus sidA*, which catalyses the first step in biosynthesis, was avirulent in both neutropenic and non-neutropenic models of IA, indicating the importance of iron acquisition in *A. fumigatus* virulence (Hissen *et al.*, 2005; Schrettl *et al.*, 2004).

A. fumigatus secretes various secondary metabolites some of which have been implicated in virulence (Dagenais and Keller, 2009). These secondary metabolites produced in *A. fumigatus* include gliotoxin, fumagillin, fumitremorgins,

fumitoxin, fumigaclavines among others (Latge, 1999). Of these secondary metabolites, gliotoxin, the most potent toxin produced by *A. fumigatus*, has been characterised the best (Kwon-Chung and Sugui, 2009). Gliotoxin has been detected in insect and animal models of IA and also in the sera of patients with IA (Dagenais and Keller, 2009). Gliotoxin contributes to *A. fumigatus* virulence in preventing macrophage and neutrophil phagocytosis, inhibiting the NADPH of neutrophils and suppressing ROS production in neutrophils, and ciliary movement of epithelial cells (Abad *et al.*, 2010; Dagenais and Keller, 2009; Kwon-Chung and Sugui, 2009).

Investigation of the pathogenesis and multi-factorial virulence of *A. fumigatus* has been aided greatly by the sequencing of the whole genome of this fungus (Nierman *et al.*, 2005) (Section 1.1.4).

1.1.4 *A. fumigatus* Genome

The genome sequence of *A. fumigatus* Af293 was published in 2005 (Nierman *et al.*, 2005). Following sequencing, the genome was found to be 29.4 Mb in size and contained 9,926 predicted genes present on eight chromosomes (Nierman *et al.*, 2005). The genome sequence of *A. fumigatus* Af293 is available online in the Central *Aspergillus* Data Repository (CADRE) (Mabey *et al.*, 2004). The genome sequences of eight *Aspergillus spp* in total; *A. clavatus*, *A. flavus*, *A. nidulans*, *A. niger*, *A. oryzae*, *A. terreus* and *A. fumigatus*; Af293, A1163, are available on CADRE (www.cadre-genomes.org.uk). CADRE assigns each gene with a unique CADRE identification number and provides transcript information regarding, for example, the exon location, cDNA sequence and predicted protein sequence.

Studies have compared the genome sequences of different *Aspergillus spp.* providing information regarding genes related to pathogenicity, sexual reproduction, and also identification of a translocation event between two strains of *A. fumigatus* (Fedorova *et al.*, 2008; Galagan *et al.*, 2005). Fedorova *et al.* (2008) compared the *A. fumigatus* Af293 and A1163 genome sequences and identified a translocation event that took place between Chromosomes 1 and 6 of Af293 and a genomic region of A1163. In a comparison of the genome sequences of *A. fumigatus*, *A. nidulans* and *A. oryzae*, the genome of *A. fumigatus* was the smallest followed by *A. oryzae* (37 Mb) and *A. nidulans* (30 Mb). The three species of *Aspergilli* shared approximately 70 % amino acid identity for orthologous proteins (Galagan *et al.*, 2005). *A. fumigatus* contained approximately 500 genes that were found to have no orthologues in *A. nidulans* or *A. niger* (Nierman *et al.*, 2005). Many of these genes related to secondary metabolite production and were found in clusters (Nierman *et al.*, 2005).

The availability of the genome sequence of *A. fumigatus* has accommodated both genome-wide transcriptional analysis and proteomic investigations of *A. fumigatus* (Kniemeyer, 2011; Schrettl *et al.*, 2008; Perrin *et al.*, 2007).

1.2 Functional Genomics

Sequencing of the *A. fumigatus* genome, along with the advent of efficient genetic transformation techniques, has facilitated functional genomics investigations in filamentous fungi, including *A. fumigatus* (Meyer *et al.*, 2011). Functional genomics is a research tool used to define the biological function of genes and their

products (Hieter and Boguski, 1997). It analyses and characterises the responses in the proteome and/or the transcriptome to elucidate gene function.

One of the strategies for the elucidation of gene function is gene deletion and this has been deployed extensively in *A. fumigatus* (Davis *et al.*, 2011a; Schrettl *et al.*, 2010; Dagenais and Keller, 2009; Lessing *et al.*, 2007). Over the course of the past decade, gene deletion strategies have improved considerably due to the development of efficient gene transformation techniques, increased availability of selection markers, and the development of strains deficient for the non-homologous end joining pathway which resulted in increased gene targeting efficiencies (Meyer *et al.*, 2011; da Silva Ferreira *et al.*, 2006; Brakhage and Langfelder, 2002; Kubodera *et al.*, 2002). These topics will be discussed in more detail in Chapter 3.

Upon deletion of a gene of interest, comparative phenotypic analysis between the wild-type and the deletion strain is carried out to identify phenotypes associated with the loss of the gene of interest (Doyle, 2011). Comparative phenotypic analysis involves exposing both the wild-type and deletion strains to physical and chemical stresses (e.g., temperature, oxidative stress, antifungal drugs and cell wall perturbants) (Doyle, 2011). While comparative phenotypic analysis provides information towards possible gene functions, it does not offer an insight into the consequences of the gene deletion in the cell. To determine the effects of a gene deletion on the cell, the transcriptomes or proteomes of the wild-type and the gene deletion strains, respectively, need to be compared (Doyle, 2011; Willger *et al.*, 2008; Lessing *et al.*, 2007; Perrin *et al.*, 2007).

In *A. fumigatus*, LaeA is a transcriptional regulator of secondary metabolite gene clusters (Perrin *et al.*, 2007). A comparison of the transcriptional profiles of the wild-type strain and an *A. fumigatus* $\Delta laeA$ strain revealed that 943 genes, representing 9.5 % of the genome, were differentially expressed between the two strains (Perrin *et al.*, 2007). These genes were involved in processes including secondary metabolism, cell wall biogenesis and carbohydrate metabolism. The most significant observation was that genes associated with 13 of the 26 secondary metabolite biosynthesis clusters in *A. fumigatus* were expressed at lower levels in *A. fumigatus* $\Delta laeA$ compared to the wild-type strain confirming the regulatory role of *A. fumigatus* *laeA*. As secondary metabolites in *A. fumigatus* have been implicated in virulence, *A. fumigatus* *laeA* represents a novel target on the basis of its influence on secondary metabolism.

It has been hypothesised that *A. fumigatus* encounters hypoxic microenvironments in the host due to the influx of phagocytes and neutrophils, and necrosis of tissue (Willger *et al.*, 2008). The transcription factors, sterol regulatory element-binding proteins, which include *A. fumigatus* *srbA*, have been associated with hypoxia adaptation (Willger *et al.*, 2008). The transcriptomes of wild-type and *A. fumigatus* $\Delta srbA$ exposed to hypoxia were analysed and compared and 87 genes were differentially regulated (Willger *et al.*, 2008). Genes involved in sterol biosynthesis, cell wall biosynthesis and hyphal morphology were repressed in *A. fumigatus* $\Delta srbA$. The implications of the repression of these genes were increased sensitivity of *A. fumigatus* $\Delta srbA$ to azoles and reduced virulence in two murine models of IA. This study determined that hypoxia adaptation was possible in *A.*

fumigatus and most likely contributes to its pathogenicity, warranting further study in terms of azole drug resistance mechanisms, sterol metabolism and hypoxia adaptation (Willger *et al.*, 2008).

Alternatively, comparison of secreted metabolites from wild-type and gene deletion strains may also provide insight into gene function. This was the case with *A. fumigatus gliG*, a putative glutathione *s*-transferase that is part of the gliotoxin biosynthetic cluster (Davis *et al.*, 2011a; Gardiner *et al.*, 2005). A comparison of the secreted metabolites from *A. fumigatus* Δ *gliG* with the wild-type strain revealed the absence of gliotoxin in *A. fumigatus* Δ *gliG* but the presence of an alternative metabolite (Davis *et al.*, 2011a). Characterisation of this metabolite determined it as a gliotoxin precursor and therefore it was confirmed that *A. fumigatus gliG* is essential for gliotoxin biosynthesis in *A. fumigatus* (Davis *et al.*, 2011a).

In addition to its use in elucidating gene function in *A. fumigatus*, functional genomics has also been employed to investigate the interactions of human bronchial epithelial cells with *A. fumigatus* conidia (Gomez *et al.*, 2010). Gomez *et al.* (2010) analysed the transcriptomic response of the human bronchial epithelial cells following interaction with *A. fumigatus* conidia and identified increased transcripts of genes involved in repair and inflammatory processes, while the transcripts of genes involved with mitosis were decreased. This study demonstrated the ability of functional genomics to provide information regarding the host response to *A. fumigatus*, of which a greater understanding may provide new drug targets and improve drug development.

1.3 Comparative proteomics

Although relatively new in *A. fumigatus* study, comparative proteomics investigations have gained momentum in recent years. Improvements in protein extraction techniques, the availability of sequenced genomes, and finally the availability of proteomics technologies such as Liquid Chromatography Mass Spectrometry (LC-MS/MS) have aided the progression of proteome studies (Doyle, 2011; Kniemeyer, 2011). In *A. fumigatus* in particular, the development of strategies for efficient protein extraction from mycelia, which is difficult due to the presence of a robust cell wall, has been important for the development of this area of research (Carberry and Doyle, 2007; Kniemeyer *et al.*, 2006).

Some of the first proteomic studies in *A. fumigatus* were involved with mapping and cataloguing the fungal proteome and subproteomes (Vodisch *et al.*, 2009; Carberry *et al.*, 2006). Using two-dimensional polyacrylamide gel electrophoresis (2D-PAGE) and Matrix Assisted Laser Desorption Ionisation Time of Flight Mass Spectrometry (MALDI-ToF MS), Carberry *et al.* (2006) mapped and identified 50 proteins in the *A. fumigatus* proteome. In the same study, Carberry *et al.* (2006) used GSH-Sepharose affinity chromatography to selectively detect and purify glutathione binding proteins in *A. fumigatus* prior to 2D-PAGE. Vodisch *et al.* (2009) combined 2D-PAGE with MALDI-ToF-MS/MS to identify 334 proteins in *A. fumigatus*. They also mapped the mitochondrial proteome in the same study, identifying 147 proteins (Vodisch *et al.*, 2009). The proteome of dormant conidia has also been characterised using 2D-PAGE with MALDI-ToF-MS/MS (Teutschbein *et*

al., 2010). In total 449 proteins were identified involved in processes including translation, energy, metabolism and the stress response (Teutschbein *et al.*, 2010).

Comparative proteomics comprises the separation of proteins using 2D-PAGE, followed by image analysis to determine differentially expressed proteins, which are then identified by mass spectrometry (Kniemeyer *et al.*, 2009; Carberry and Doyle, 2007). Image analysis software compares stained gels and detects protein spots that are present at different intensities between gels. Alternatively, protein samples can be labelled with fluorescent dyes in Differential Gel Electrophoresis (DIGE) (Unlu *et al.*, 1997). With DIGE, protein extracts are pre-labelled with different fluorescent cyanine dyes. The protein extracts are then separated on the same IEF strip and, following 2D-PAGE, are scanned using a fluorescent scanner and the proteins are quantified according to the fluorescence intensity of the protein spots. Three different dyes are available for labelling, allowing for the comparison of three different protein extracts (Minden *et al.*, 2009).

Comparative proteomic studies have been undertaken to investigate changes in the proteome due to the addition of stress (e.g., heat shock (Albrecht *et al.*, 2010b) and H₂O₂ (Lessing *et al.*, 2007)), antifungals (e.g., amphotericin B (Gautam *et al.*, 2008) and caspofungin (Cagas *et al.*, 2011)) and also to complement gene deletion studies (Sato *et al.*, 2009). Comparative proteomics to explore the effect of H₂O₂ on the *A. fumigatus* proteome identified 27 proteins with up-regulated expression and 17 proteins with down-regulated expression (Lessing *et al.*, 2007). The predominant increased expression of a mitochondrial peroxiredoxin Prx1 and Allergen Asp f3, which have been classified as thioredoxin peroxidases, indicated the importance of

the thioredoxin system in response to oxidative stress (Lessing *et al.*, 2007). Lessing *et al.* (2007) also used comparative proteomics to investigate the effects of deleting the transcription factor *Afyap1*, involved in the oxidative stress response, in *A. fumigatus*. This led to the identification of 29 proteins whose expression was down-regulated in *A. fumigatus* Δ *yap1*. Interestingly, these proteins were found to be increased in expression in *A. fumigatus* in response to H₂O₂, confirming *Afyap1* involvement in the regulation of these proteins.

In *A. nidulans*, comparative proteomics was employed to investigate the deletion of a glutathione reductase (*glrA*) (Sato *et al.*, 2009). *A. nidulans* Δ *glrA* displayed reduced resistance to oxidative stress, decreased intracellular glutathione and was sensitive to temperature. Following 2D-PAGE and comparative image analysis, 13 and 7 proteins were up-regulated and down-regulated respectively. Proteins involved in the oxidative stress response were identified, among them a thioredoxin reductase, a cytochrome *c* peroxidase, catalase B and a glutathione *s*-transferase. This revealed interplay between the glutathione systems and both the thioredoxin system and the hydrogen peroxide defence mechanisms.

Comparative proteomics was used to investigate the effect of the antifungal amphotericin B on *A. fumigatus* (Gautam *et al.*, 2008). The exact mechanism by which amphotericin B acts as an antifungal is unknown, however it is known that it targets and forms pores in the cell membrane (Baginski *et al.*, 2006). Increased expression of 76 proteins and decreased expression of 9 proteins was observed in *A. fumigatus* upon exposure to amphotericin B (Gautam *et al.*, 2008). Proteins associated with ergosterol biosynthesis, cell wall maintenance, cell stress and

transport were all differentially expressed. As amphotericin B targets ergosterol biosynthesis the identification of ERG13 as one of the up-regulated proteins suggested its increased expression is to overcome the stress caused by amphotericin B. Gautam *et al.* (2008) also investigated the transcriptome of *A. fumigatus* in the presence and absence of amphotericin B by microarray analysis. The expression of 295 genes were differentially expressed, 165 genes were up-regulated while 130 genes were down-regulated. These genes belonged to the same functional categories as observed for the differentially regulated proteins.

Other studies have employed both comparative proteomics and transcriptomics to investigate the effects of gene deletion or applied stress (e.g., heat shock (Albrecht *et al.*, 2010b)). However poor correlation between mRNA levels and protein expression levels have been observed in *Aspergillus* and yeast (Albrecht *et al.*, 2010b; Greenbaum *et al.*, 2003). In examining the effects of heat shock in *A. fumigatus*, only 32 proteins and the respective transcripts correlated in their differential regulation despite the differential expression of 91 proteins, although it should be noted that the proteome and transcriptome were profiled by two different groups (Albrecht *et al.*, 2010b; Nierman *et al.*, 2005). In a functional profiling study of the *A. fumigatus* biofilm, poor correlation between the transcriptome and proteome was observed (Bruns *et al.*, 2010a). Bruns *et al.* (2010a) observed good correlation for genes and proteins involved in protein and amino acid metabolism, however, in the case of heat shock proteins, gene expression was the reverse of protein expression. There are a number of factors that may contribute to the poor correlation between proteomic and transcriptomic data. A delay between

transcription and translation may account for the presence of a gene in the transcriptome but its absence at the protein level (Greenbaum *et al.*, 2003). Additionally, if the response to a stress (e.g., heat shock or oxidative stress) is being investigated, translation may be repressed under these conditions. So while a gene may be up-regulated at the transcript level, it may not be translated and consequently the protein levels do not correlate (Albrecht *et al.*, 2010b).

While the transcriptome provides significant information regarding mRNA expression levels in a cell in response to a stress, ultimately it is the protein levels and concomitant interactions that are the facilitatory agents in the cell with regard adaptation to a new environment (Greenbaum *et al.*, 2003). For this reason, comparative proteomics is a powerful tool for investigating the impact a gene deletion has on the cell as a whole, that is, for studying fungal systems biology.

1.4 Systems biology

Genomics, transcriptomics and proteomics along with metabolomics all contribute to a systems understanding of cellular processes and responses (Andersen and Nielsen, 2009). The integration of information from genomic, transcriptomic, proteomic and metabolomic studies increases knowledge at the different levels; from gene to protein and also metabolic fluxes, and how this influences the interaction of different components in the cell (Zhang *et al.*, 2010). Because regulation in the cell occurs on the transcriptomic, proteomic and metabolomic level, it is important to take a holistic view of the cellular system (Andersen and Nielsen, 2009).

Systems biology is more advanced in bacterial research however advances are being made in fungal research (Albrecht *et al.*, 2011). A functional map of *S. cerevisiae* has been published recently which contains genetic interaction profiles for 75 % of genome (Costanzo *et al.*, 2010). This functional map provides a wealth of information on the links between genotypes and phenotypes. In *A. niger* a metabolic network comprising 2240 enzymatic reactions was constructed providing a comprehensive overview of *A. niger* metabolism (Andersen *et al.*, 2008). This metabolic map has potential to aid the development of high-yield production platforms in *A. niger* (Andersen *et al.*, 2008).

In *A. fumigatus*, systems biology studies in transcriptomics and proteomics have been carried out (Gautam *et al.*, 2008; Willger *et al.*, 2008; Lessing *et al.*, 2007), however genetic modelling of a network encompassing the data obtained from the systems studies has yet to be developed (Albrecht *et al.*, 2011). The establishment of a data warehouse, *Omnifung* (www.omnifung.hki-jena.de), storing data from microarrays and 2D-PAGE (Priebe *et al.*, 2011), and the *Aspergillus* Genome Database (www.aspergillusgenome.org) (Arnaud *et al.*, 2010), containing gene and protein sequence data aid researchers however an integrated data warehouse combining this information is required for the complete systems biology of *A. fumigatus* (Kniemeyer, 2011). Understanding the systems of *A. fumigatus* will lead to a greater understanding of pathogenicity and responses to host immune system, leading on to the prediction of drug targets, and the potential for development of vaccines (Albrecht *et al.*, 2011; Andersen and Nielsen, 2009). One area in which there is a deficit in information is protein synthesis in *A. fumigatus*

with respect to the functions of the individual components of this process and their roles in the overall system of the organism.

1.5 Protein synthesis in eukaryotes

Protein synthesis is a fundamental process that is divided into four stages; initiation, elongation, termination and ribosome recycling (Deplazes *et al.*, 2009; Rodnina and Wintermeyer, 2009; Preiss and Hentze, 2003). It is carried out by ribosomes and translation factors which include; eukaryotic initiation factors (eIF), elongation factors (EF) and termination release factors (eRF) (Deplazes *et al.*, 2009; Valouev *et al.*, 2009; Preiss and Hentze, 2003). Protein synthesis is regulated in response to intracellular growth, extracellular signals and stress conditions (Deplazes *et al.*, 2009). This regulation of protein synthesis primarily occurs at the initiation stage, however regulation has also been seen to occur during elongation (Jackson *et al.*, 2010; Deplazes *et al.*, 2009; Shenton *et al.*, 2006). In response to stress, protein synthesis is usually reduced to prevent translation errors and in addition to this, molecular chaperone systems are often up-regulated to deal with any increase in denatured or misfolded proteins (Deplazes *et al.*, 2009; Shenton *et al.*, 2006).

Ribosomes are large ribonucleoprotein assemblies that carry out protein synthesis (Rodnina and Wintermeyer, 2009; Preiss and Hentze, 2003). The eukaryotic ribosome is composed of two subunits, the 40S subunit and the 60S subunit (Figure 1.2) (Zemp and Kutay, 2007).

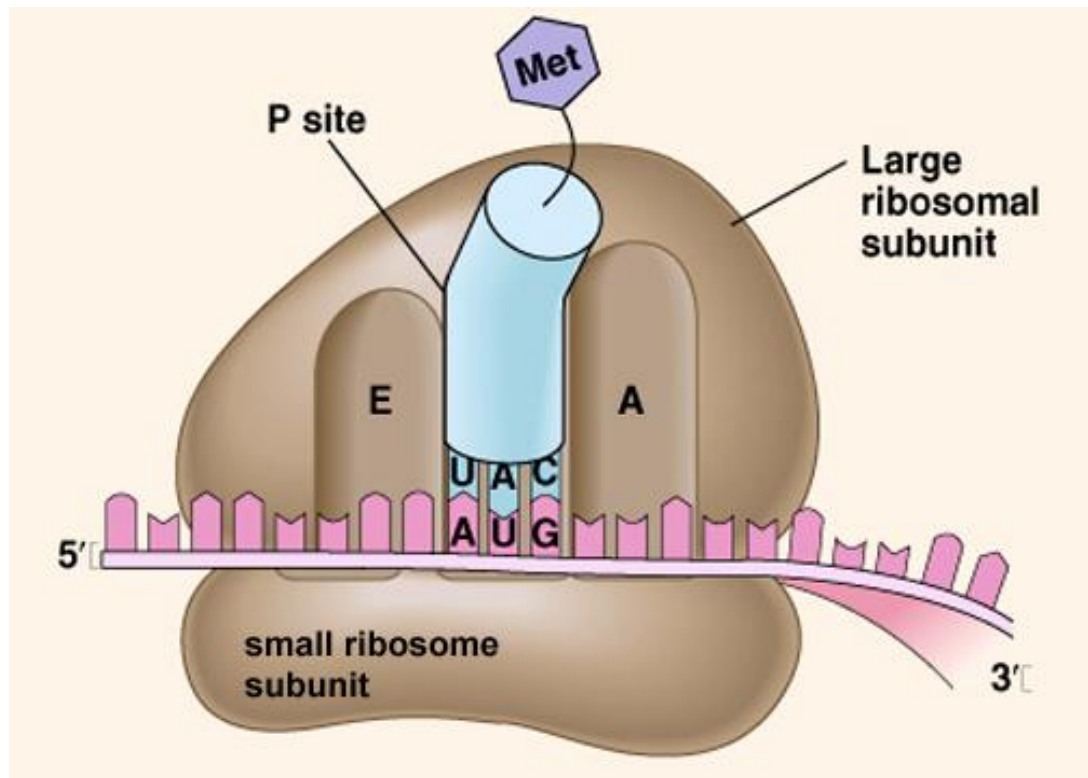


Figure 1.2: Schematic representation of the ribosome. Incoming aminoacyl-tRNA enters the A site, the P site holds the tRNA that is linked to the peptidyl-tRNA, while the E site holds the deacylated tRNA. Image taken from www.sgugenetics.pbworks.com.

The decoding of mRNA by aminoacyl-tRNA occurs at the small 40S subunit, while the large 60S subunit is responsible for catalysing the formation of peptide bonds (Rodnina and Wintermeyer, 2009)

The ribosome has three sites; P, A, and E, that are directly involved in translation (Figure 1.2). The P site holds the tRNA that is linked to the peptidyl-tRNA, the A site accommodates the incoming aminoacyl-tRNA, and the E site houses deacylated tRNA prior to its release from the ribosome (Jackson *et al.*, 2010). Protein synthesis is usually carried out by polysomes where multiple ribosomes translate the mRNA (Merrick, 2010).

Translation initiation is the most complex step of translation and therefore can often be the rate-limiting step (Gallie, 2002). Translation initiation can be divided into four steps; (i) the formation of the 43S complex, (ii) recruitment of the 43S complex to the capped 5' end of the mRNA, (iii) scanning of the 5' untranslated region (5' UTR) of the mRNA for the start codon, and (iv) assembly of the 80S ribosome by the joining of the 60S subunit (Figure 1.3) (Preiss and Hentze, 2003). In the cell, the 40S and 60S subunits of the ribosome form the 80S ribosome, which is favoured by physiological conditions (Jackson *et al.*, 2010; Preiss and Hentze, 2003). The first step in the formation of the 43S complex is the dissociation of the 80S ribosome into the 40S and 60S subunits by eIF3, eIF1 and eIF1A (Jackson *et al.*, 2010; Preiss and Hentze, 2003). The ternary complex comprised of eIF2 and initiator Met-tRNA_i^{Met} binds the 40S subunit to form the 43S complex (Jackson *et al.*, 2010; Deplazes *et al.*, 2009; Preiss and Hentze, 2003; Gallie, 2002).

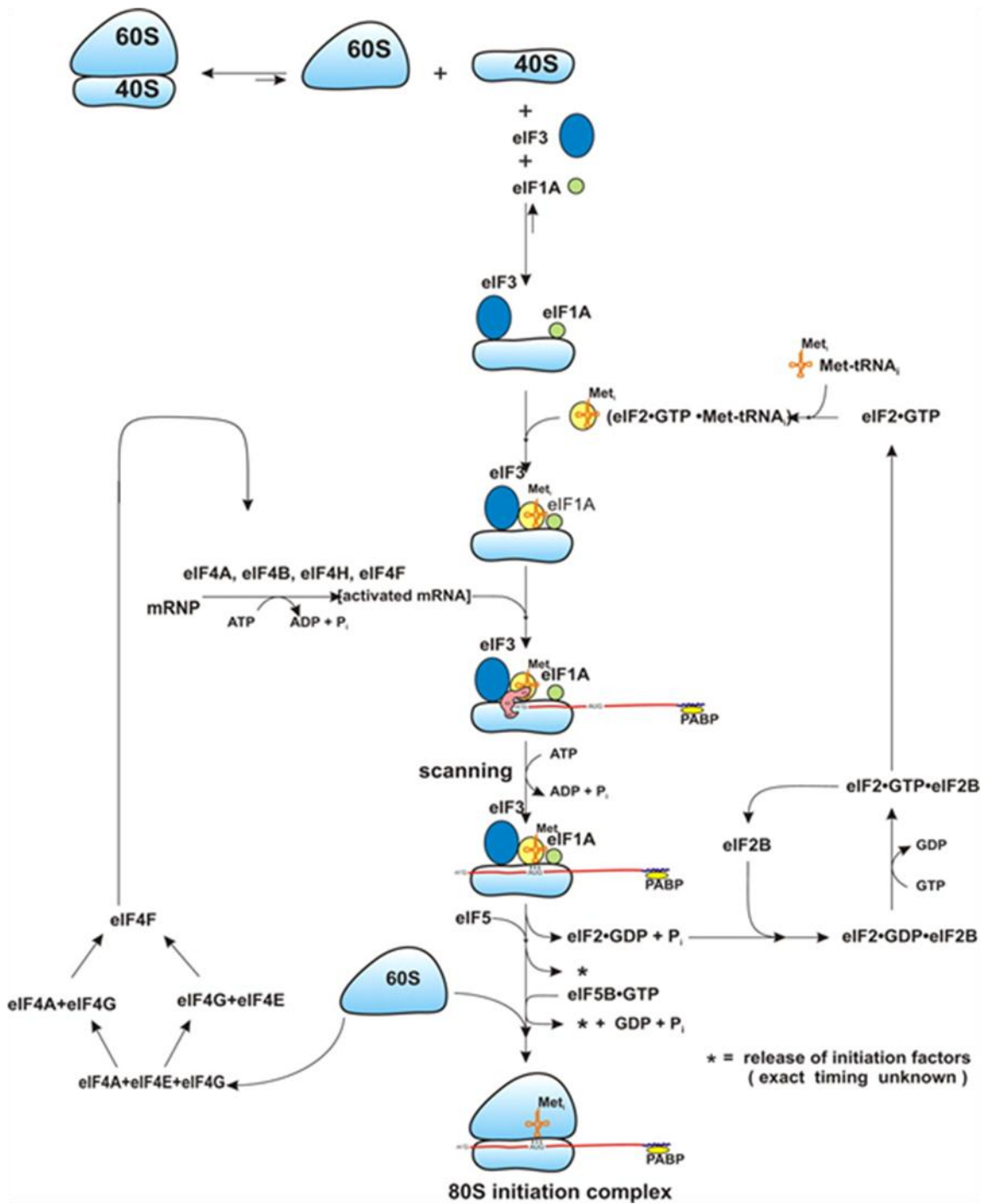


Figure 1.3: Schematic overview of translation initiation in eukaryotes taken from Merrick (2010).

The 43S complex then scans the 5' UTR until the start codon is positioned at the 40S subunit. Codon/anti-codon interaction results in GTP hydrolysis of eIF2-GTP reducing its affinity for Met-tRNA_i^{Met} and resulting in the partial dissociation of eIF2 from the 40S subunit. Finally hydrolysis of eIF5B-bound GTP results in the release of initiation factors from the 40S subunit and joining of the 60S subunit to form the 80S ribosome required for elongation.

Translation elongation can be separated into three steps; decoding of the mRNA codon by aminoacyl-tRNA, formation of the peptide bond, and finally translocation of the peptidyl-tRNA from the A site to the P site in the ribosome (Rodnina and Wintermeyer, 2009).

Relevant to the work presented in this thesis, eukaryotic translation elongation factor 1A (eEF1A) binds and recruits aminoacyl-tRNA to the A site of the ribosome where, once a codon/anticodon match is detected, it deposits the aminoacyl-tRNA (Mateyak and Kinzy, 2010; Ozturk and Kinzy, 2008). eEF1A will be discussed in more detail in Section 1.6. Once aminoacyl-tRNA has been deposited in the A site, a peptide bond is formed with the P-site peptidyl tRNA (Mateyak and Kinzy, 2010; Rodnina and Wintermeyer, 2009). The 60S subunit catalyses the transfer of the peptidyl moiety from the peptidyl tRNA in the P site to the aminoacyl-tRNA in the A site resulting in the formation of a peptide bond (Taylor *et al.*, 2007). The final step of translation elongation is the translocation of the peptidyl-tRNA from the A and P sites to the P and E sites, respectively, to position the next codon in the A site for decoding by eEF1A (Mateyak and Kinzy, 2010; Taylor *et al.*, 2007). Translocation is catalysed by eEF2 in a GTP hydrolysis reaction (Taylor *et*

al., 2007; Ejiri, 2002). These three steps of translation repeat until a stop codon enters the A site.

Translation termination is controlled by the translation releasing factor (eRF) and the presence of a stop codon in the A site of the ribosome (Valouev *et al.*, 2009; Alkalaeva *et al.*, 2006). eRF is composed of two subunits; eRF1 which recognises the three stop codons and catalyses the hydrolysis of the P site peptidyl-tRNA releasing the complete polypeptide chain, and eRF3 which provides the GTPase activity for eRF1 (Rodnina and Wintermeyer, 2009; Valouev *et al.*, 2009; Han *et al.*, 2005). GTP hydrolysis by eRF3 couples eRF1 recognition of the stop codon and peptidyl-tRNA hydrolysis and ensures that hydrolysis of peptidyl-tRNA by eRF1 is rapid (Alkalaeva *et al.*, 2006).

Ribosome recycling is the dissociation of the 80S ribosome into the 40S and 60S subunits allowing for their participation in translation initiation once more (Jackson *et al.*, 2010). As described for translation initiation, eIF3, eIF3j, eIF1 and eIF1A are all involved in the dissociation of the 80S ribosome into the 40S and 60S subunits (Pisarev *et al.*, 2007; Preiss and Hentze, 2003). The P site deacylated-tRNA is released by eIF1, while eIF3j removes bound mRNA. It is thought that eIF3, eIF1 and eIF1A remain bound to the 40S subunit to prevent its reassociation with the 60S subunit and allow for its binding to the ternary complex to form the 43S complex in translation initiation (Pisarev *et al.*, 2007).

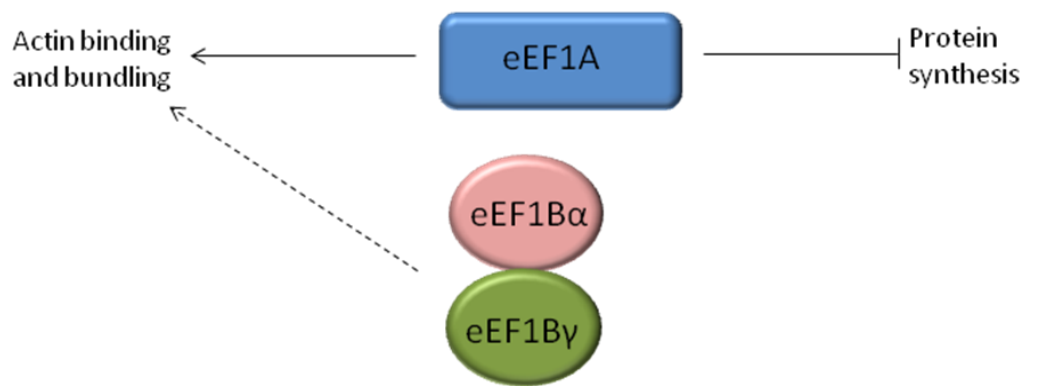
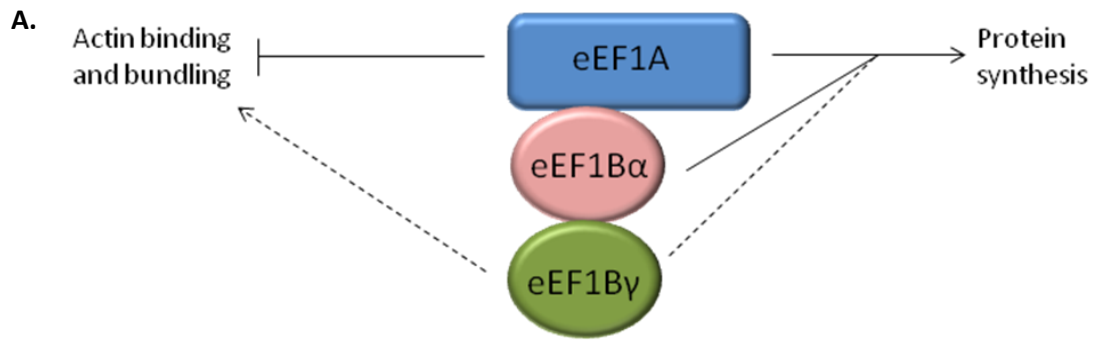
1.6 Eukaryotic elongation factor 1 complex

The eukaryotic elongation factor 1 (eEF1) complex delivers all aminoacyl-tRNAs to the ribosome with the exception of the initiator tRNA and selenocysteine tRNAs (Mateyak and Kinzy, 2010). The eEF1 complex is composed of two subunits, eEF1A and eEF1B (Pittman *et al.*, 2009). eEF1A binds and delivers aminoacyl-tRNA to the A site of the ribosome. eEF1A is a G-protein and requires a guanine nucleotide exchange factor (GEF). eEF1B is the GEF for eEF1A and is itself composed of two subunits; eEF1B α and eEF1B γ (Figure 1.4a) (Ozturk and Kinzy, 2008). In metazoans, a third subunit of eEF1B, eEF1B β , is present (Ozturk and Kinzy, 2008; Jeppesen *et al.*, 2003). In *S. cerevisiae*, the eEF1B α subunit is the nucleotide exchange factor, while the function of eEF1B γ has not been fully elucidated (Pittman *et al.*, 2009). eEF1B γ will be discussed in more detail in Section 1.7.

One of the most abundant protein synthesis factors in the cell is eEF1A (Mateyak and Kinzy, 2010). The canonical function of eEF1A is the delivery of aminoacyl-tRNA to the elongating ribosome. eEF1A binds aminoacyl-tRNA in a GTP-dependent manner and delivers it to the A site of the ribosome (Mateyak and Kinzy, 2010; Rodnina and Wintermeyer, 2009). Once a codon/anticodon match takes place, the ribosome acts as a GTPase-activating factor resulting in GTP hydrolysis (Pittman *et al.*, 2009). Because it is now bound to GDP, eEF1A “switches” to its inactive state and is released from the ribosome (Pittman *et al.*, 2009). GEFs catalyse the release of GDP from G-proteins as follows; the GEF binds to the G-protein and releases the phosphate groups, which in turn dissociates the nucleotides (Ozturk and

Kinzy, 2008; Bos *et al.*, 2007). eEF1B α catalyses this nucleotide exchange facilitating eEF1A to bind to GTP enabling it to bind aminoacyl-tRNA once more. The crystal structure of eEF1A from *S. cerevisiae* has elucidated that it is divided into three domains; domain I, domain II and domain III (Figure 1.4b) (Andersen *et al.*, 2001). Domain I binds GTP, domain II binds aminoacyl-tRNA and finally domains I and III interact with aminoacyl-tRNA (Mateyak and Kinzy, 2010; Ejiri, 2002; Andersen *et al.*, 2001).

In addition to delivering aminoacyl-tRNA to the elongating ribosome, eEF1A is also an actin binding and bundling protein, an interaction that is conserved from yeast to mammals (Pittman *et al.*, 2009; Gross and Kinzy, 2005). It has been estimated that greater than 60 % of eEF1A in the cell is associated with the actin cytoskeleton (Gross and Kinzy, 2005). Actin is an essential component of the cytoskeleton involved in a variety of cellular processes ranging from growth and differentiation to stress response (Farah *et al.*, 2011; Kummasook *et al.*, 2011). The actin binding and bundling activity of eEF1A is independent of GTP and does not take place in the presence of aminoacyl-tRNA suggesting mutual exclusiveness of these two binding factors (Figure 1.4a) (Edmonds *et al.*, 1998; Liu *et al.*, 1996). Actin binds to domains II and III of eEF1A in *S. cerevisiae* (Gross and Kinzy, 2007; Gross and Kinzy, 2005). eEF1B α also binds to Domain II of eEF1A and Pittman *et al.* (2009) have shown that *in vitro*, eEF1B α reduces the actin bundling activity of eEF1A and may act as a regulator in directing eEF1A function to translation elongation.



B.

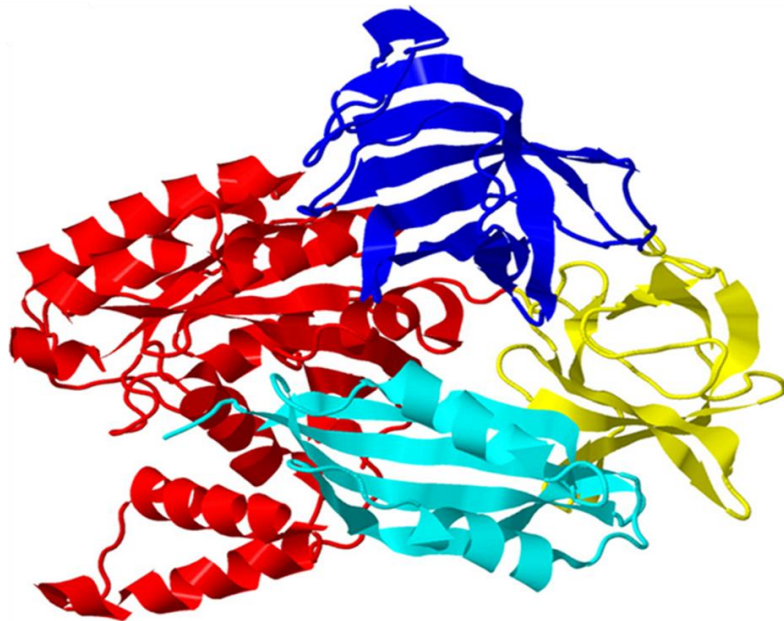


Figure 1.4: The eEF1 complex

- A.** The eEF1 complex is composed of eEF1A and eEF1B. eEF1B is composed of two subunits; eEF1B α and eEF1B γ . eEF1A delivers aminoacyl-tRNA to the elongating ribosome. eEF1B α is the nucleotide exchange factor for eEF1A, while eEF1B γ may stimulate this reaction. eEF1A also binds and bundles actin, however this is mutually exclusive of aminoacyl-tRNA binding. eEF1B α and actin bind to the same domain in eEF1A therefore eEF1B α may regulate the actin binding activity of eEF1A. eEF1B γ has been shown to bind keratin in epithelial cells. The dashed arrows indicate putative interactions.
- B.** The structural organisation of eEF1A from *S. cerevisiae*. Domain I (Red) binds GTP, domain II (Yellow) binds aminoacyl-tRNA, and domains II and III (Dark Blue) interact with actin. eEF1B α (Light Blue) binds to domains I and II of eEF1A. Figure taken from Mateyak and Kinzy (2010).

The regulation of the actin bundling activity of eEF1A by eEF1B α is very important for cytoskeleton organisation as mutant strains of eEF1B α in *S. cerevisiae* with a lowered affinity for eEF1A, induced actin disorganisation which was in the form of the loss of actin cables and an increased cell size compared to wild-type cells (Pittman *et al.*, 2009). It has also been demonstrated that disruptions to the actin cytoskeleton can result in a block in translation initiation (Gross and Kinzy, 2007). Two specific mutations of eEF1A (F308L and S405P) in *S. cerevisiae* not only exhibited actin cytoskeleton disorganisation, but also an increased 80S ribosome/polysome ratio which is indicative of a defect in translation initiation (Gross and Kinzy, 2007). This suggests that eEF1A actin organisation influences translation initiation in yeast.

eEF1A, along with eEF1B α , has an important function not only in translation elongation but also in actin cytoskeleton organisation. The function of eEF1B γ in the eEF1 complex has not been fully elucidated and will be discussed in more detail in Section 1.7.

1.7 Eukaryotic elongation factor 1B γ

eEF1B γ along with eEF1B α form the eEF1B complex that provides eEF1A with GEF activity. Studies have shown that eEF1B α is the GEF, whereas eEF1B γ does not carry out any GEF activity suggesting that it may have a stimulatory function for eEF1B α (Esposito and Kinzy, 2010; Le Sourd *et al.*, 2006; Janssen and Moller, 1988). In *S. cerevisiae*, eEF1B γ is encoded by two genes; *TEF3* and *TEF4* (Valouev *et al.*, 2009; Olarewaju *et al.*, 2004). eEF1B γ proteins encoded by both of

these genes were found, along with eEF1B α , to interact with the release factors eRF1 and eRF3, indicating that eEF1B provides GEF activity for translation termination (Valouev *et al.*, 2009). Deletion of either or both of the *TEF3* and *TEF4* genes did not have any significant effect on total translation or protein synthesis in *S. cerevisiae* (Olairewaju *et al.*, 2004).

The crystal structure of the N-terminal region of *S. cerevisiae* eEF1B γ contains a glutathione *s*-transferase (GST) -like domain, although GST activity was not observed for this domain (Jeppesen *et al.*, 2003). Prior to this, multiple alignment analysis, sequence motif searching along with tertiary structure modelling determined that eEF1B γ contained an N-terminal that was related to the theta class of GSTs (Koonin *et al.*, 1994). GST activity, however, has been observed in eEF1B γ proteins from different organisms. Specifically, eEF1B γ from *A. fumigatus*, purified by GSH-affinity chromatography exhibited GST activity for the substrates 1-chloro-2,4-dinitrobenzene (CDNB) and ethacrynic acid (Carberry *et al.*, 2006). In addition to *A. fumigatus* eEF1B γ , orthologues from rice and the silk worm *Bombyx mori*, expressed in *E. coli*, were also amenable to GSH-affinity purification (Kamiie *et al.*, 2002; Kobayashi *et al.*, 2001), and the eEF1B γ proteins from both of these organisms exhibited GST activity. The eEF1B γ protein from *Trypanosoma cruzi* detoxified lipophilic compounds in a GST-like manner (Billaut-Mulot *et al.*, 1997). It was suggested that the GST activity of eEF1B γ from *T. cruzi* may be involved in protecting lipids from peroxidation in this parasite and consequently contributed to its resistance to the lipophilic compound clomipramine (Billaut-Mulot *et al.*, 1997). It has also been hypothesised that the presence of a GST domain in eEF1B γ may act

to protect the elongating ribosome against oxidative stress (Carberry *et al.*, 2006), to control translation in response to oxidative stress (Ejiri, 2002), or indeed may act to regulate protein folding in a chaperone like manner (Koonin *et al.*, 1994). Given that GST activity has already been demonstrated in eEF1B γ proteins, further studies are required to fully understand the presence of a GST domain in eEF1B γ .

Esposito and Kinzy (2010) observed dramatic changes in protein expression patterns upon the deletion of both *TEF3* and *TEF4* in *S. cerevisiae* although the overall rate of protein synthesis was the same as the wild-type. There was an altered expression of heat shock proteins in the strain lacking eEF1B γ . This altered heat shock protein expression has been implicated in the increased resistance to oxidative stress observed with the absence of eEF1B γ in *S. cerevisiae* (Olawajaju *et al.*, 2004). eEF1B γ in *S. cerevisiae* was first identified through a screen for calcium dependent membrane-binding protein (Le Sourd *et al.*, 2006; Kambouris *et al.*, 1993). In the absence of eEF1B γ in yeast, morphological defects in vacuoles were observed along with a defect in vacuolar protein turnover (Esposito and Kinzy, 2010). The eEF1B γ deletion strain was also sensitive to tunicamycin, which suggested that there was also a defect in the ER-associated degradation (ERAD) pathway. Both vacuolar protein turnover and the ERAD pathway are involved in degrading oxidised proteins (Wang *et al.*, 2010). It was observed that there was an increase in oxidised proteins accumulated in the eEF1B γ strain, due to the defective vacuolar protein turnover and ERAD pathways (Esposito and Kinzy, 2010). The results observed in this study by Esposito and Kinzy (2010) suggest that in *S. cerevisiae*, eEF1B γ is involved in a membrane-associated function in the cell.

eEF1B γ has also been linked to the cytoskeleton in mammalian cells where it has been observed to interact with keratin in epithelial cells (Kim and Coulombe, 2010; Kim *et al.*, 2007). *In vitro*, eEF1B γ purified from epithelial cells cross-links keratin intermediate filament assemblies, while *in vivo* eEF1B γ increased the formation of keratin intermediate filament bundles in the epithelial cells (Kim *et al.*, 2007). Overexpression of eEF1B γ in epithelial cells resulted in a disrupted interaction between eEF1B γ and keratin, and also reduced protein synthesis. This suggested that the physical link between eEF1B γ and keratin has a functional role in translation in epithelial cells (Kim and Coulombe, 2010; Kim *et al.*, 2007).

1.8 eEF1B γ in *A. fumigatus*

As mentioned in Section 1.7, eEF1B γ was identified in *A. fumigatus* following isolation as a GSH-binding protein (Carberry *et al.*, 2006). In *A. fumigatus*, eEF1B γ is encoded by *A. fumigatus elfA*. Proteins in *A. fumigatus* selected by GSH-Sepharose affinity chromatography were separated by 2D-PAGE and ElfA was identified as the most abundant protein and was present as two distinct spots (Carberry *et al.*, 2006). Further analysis by Carberry *et al.* (2006) determined that ElfA was present as a monomer in the cell and is approximately 20 kDa. GST activity was demonstrated in native ElfA, representing the first demonstration of GST activity in native eEF1B γ , as previous to this GST activity had only been determined in recombinantly produced eEF1B γ (Carberry *et al.*, 2006; Kamiie *et al.*, 2002; Kobayashi *et al.*, 2001). Phylogenetic analysis of ElfA along with 28 predicted

GST proteins from a range of fungal species showed that ElfA clustered in the EF1B γ -like group (Figure 1.5) (Carberry *et al.*, 2006).

In microarray analysis of *A. fumigatus* gene expression in response to heat shock, *A. fumigatus elfA* was up-regulated two-fold after 1 h of a temperature shift from 30 °C – 48 °C, suggesting a possible role in protection against heat shock (Nierman *et al.*, 2005). However in a follow-up study examining the changes in the *A. fumigatus* proteome in response to the same heat shock, ElfA was not identified as being differentially expressed, indicating that while the transcript may have been up-regulated, this was not translated at the protein level (Albrecht *et al.*, 2010b).

In a comparative proteomic study of an *A. fumigatus yap1* deletion strain, *A. fumigatus elfA* was down-regulated in *A. fumigatus $\Delta yap1$* following exposure to H₂O₂ (Lessing *et al.*, 2007). As *A. fumigatus yap1* is a transcription factor involved in the regulation of the response to oxidative stress, Lessing *et al.* (2007) suggested that the proteins down-regulated in *A. fumigatus $\Delta yap1$* in response to H₂O₂ may be under the regulation of *A. fumigatus yap1*. This indicates that *A. fumigatus elfA* may be involved in the response to oxidative stress however this has not been explored to date.

Furthermore, in *A. nidulans*, an orthologue of *A. fumigatus* ElfA was up-regulated in a glutathione reductase deletion strain ($\Delta glrA$) (Sato *et al.*, 2009), again suggesting a possible link with the oxidative stress response.

Overall, there is very little information available regarding the role of *A. fumigatus* *elfA* in translation elongation. It is known that the *A. fumigatus* *elfA* GST domain is enzymatically active (Carberry *et al.*, 2006), however the relevance of the presence of a GST domain in an elongation factor needs further investigation with respect to a possible role in redox control and oxidative stress. In other organisms (e.g., *S. cerevisiae* and mammalian epithelial cells) eEF1B γ has been shown to interact with membranes and the cytoskeleton (Esposito and Kinzy, 2010; Kim *et al.*, 2007), however it is not known whether *A. fumigatus* *elfA* has any interactions with either the membrane network or the actin cytoskeleton. Thus, it is clear that there remains a lot to be explored regarding *A. fumigatus* *elfA*. Although the GST activity of ElfA will not be directly evaluated in this thesis nonetheless GST functionality merits consideration giving their expanding role in fungal systems.

1.9 Glutathione *s*-transferases

1.9.1 GST function

GSTs (EC 2.5.1.18) are a superfamily of multifunctional proteins functioning in cellular detoxification of a wide range of exogenous and endogenous compounds (Frova, 2006). GSTs are phase II detoxification enzymes and they function by catalysing the nucleophilic attack of glutathione (GSH: γ -Glu-Cys-Gly) on non-polar compounds that contain an electrophilic carbon, nitrogen or sulphur atom forming

more soluble non-toxic peptide derivatives (Frova, 2006; Hayes *et al.*, 2005). These GSH conjugated xenobiotics are removed from the intracellular space by ABC transporters that pump them into intracellular vacuoles (McGoldrick *et al.*, 2005). GSTs contribute to the metabolism of oxidative stress products such as peroxides, drugs, pesticides and other xenobiotics (Oakley, 2005).

The detoxification of these xenobiotics occurs in three distinct phases; phase I, phase II and phase III (Sheehan *et al.*, 2001). Phase I involves the conversion of the xenobiotics into more polar metabolites through the unmasking or *de novo* formation of a functional group (e.g., a thiol group) (Jancova *et al.*, 2010). Phase I reactions, of which one of the major reactions is oxidation, are generally catalysed by cytochrome P450 enzymes (Jancova *et al.*, 2010; Sheehan *et al.*, 2001). Quantitatively, the major phase II reaction is the conjugation of the activated xenobiotics to GSH, which is catalysed by GSTs (Figure 1.6) (Sheehan *et al.*, 2001). The electrophilic site of the activated xenobiotic reacts with the thiolate group of GSH forming a less toxic and more water soluble compound (Dourado *et al.*, 2008). Phase III involves the active removal of this water soluble conjugated compound from the cell (Sheehan *et al.*, 2001).

Fungal GSTs mainly appear to be involved in protecting against damage caused by oxidative stress, heavy metals and antifungals (Morel *et al.*, 2009), however recent studies have also implicated a fungal GST to have a biosynthetic role in gliotoxin production (Davis *et al.*, 2011a; Scharf *et al.*, 2011). Fungal GSTs, in particular those found in *A. fumigatus* will only be discussed here.

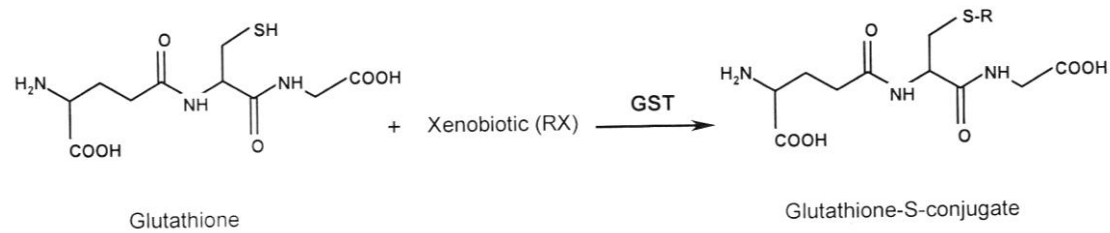


Figure 1.6: Conjugation of glutathione to xenobiotics. The activated xenobiotic reacts with the thiol group of GSH forming the glutathione conjugate (Jancova *et al.*, 2010).

1.9.2 GST classification

GSTs are classified according to (i) sequence similarity and subsequent immunological reactivity, (ii) substrate specificity and (iii) structural characteristics (Hayes *et al.*, 2005; Sheehan *et al.*, 2001). In order to be included in the same class, two GSTs must share a minimum of 40 % sequence identity, and if this identity is less than 30 % they are allocated to different classes (McGoldrick *et al.*, 2005). The N-terminus is quite conserved and contains the specific residues required for GSH binding (Morel *et al.*, 2009; Frova, 2006). Catalytically active tyrosine, serine or cysteine residues, located within the N-terminus are required for binding the thiol group of GSH (Frova, 2006). Due to its conservation within a class, the N-terminus is generally used to determine structural similarities.

Classification of fungal GSTs has advanced in recent years due to the increase availability of sequenced fungal genomes (Morel *et al.*, 2009). Initially, characterisation of *S. cerevisiae* GSTs divided them into the classes; omega, GTT, Ure2p, MAK16 and EF1B γ (Morel *et al.*, 2009; Garcera *et al.*, 2006; Rai *et al.*, 2003; Choi *et al.*, 1998; Koonin *et al.*, 1994). McGoldrick *et al.* (2005) identified five clusters of GST-like proteins following comparative multiple sequence alignment of 67 GST-like sequences from 21 fungal species. These classes were cluster 1, cluster 2, EF1B γ , Ure2p and MAK16. The latter three classes had previously been identified and related to the GST superfamily (McGoldrick *et al.*, 2005). Following this, Morel *et al.* 2009 described seven fungal GST classes in total; omega, GTT1, GTT2, Ure2p, EF1B γ , MAK16 and GTE. The cluster 1 class identified by McGoldrick *et al.* (2005) was shown to contain GTT1 from *S.*

cerevisiae (Morel *et al.*, 2009). Furthermore the GTT class was split into two classes; GTT1 and GTT2, both of which are fungal specific (Morel *et al.*, 2009). Cluster 2 was found to contain an Ure2p-related GST from *A. nidulans*; GSTA (Morel *et al.*, 2009). The newly identified class, GTE (glutathione transferase etherase-related), shares sequence homology with bacterial etherases (Morel *et al.*, 2009). In summary, there are now seven fungal GST classes; omega, GTT1, GTT2, Ure2p, EF1B γ , MAK16 and GTE.

1.9.3 GSTs in *A. fumigatus*

A. fumigatus contains twenty five putative GSTs (Davis, 2011b), of which only five have confirmed GST activity; GstA, GstB, GstC, GliG and ElfA (Table 1.1) (Davis *et al.*, 2011a; Scharf *et al.*, 2011; Carberry *et al.*, 2006; Burns *et al.*, 2005). Burns *et al.* (2005) demonstrated that recombinant GstA, GstB and GstC exhibited GST activity. Furthermore, RT-PCR of *A. fumigatus* *gstA*, *gstB* and *gstC* expression showed increased expression of all three genes in response to 1-chloro-2,4-nitrobenzene (CDNB) exposure, while *A. fumigatus* *gstA* and *gstC* were up-regulated in response to H₂O₂ (Burns *et al.*, 2005). *A. fumigatus* *gstB* expression was not induced upon exposure to H₂O₂ indicating that these three GSTs may have different roles with respect environmental stress in *A. fumigatus* (Burns *et al.*, 2005).

A. fumigatus *gliG* is a member of the gliotoxin gene cluster and was predicted to encode a GST (Davis *et al.*, 2011a; Gardiner *et al.*, 2005). Davis *et al.* (2011) demonstrated that recombinant GliG expressed in *E. coli* exhibited both GST activity and glutathione reductase activity. As described in Section 1.2, *A. fumigatus* *gliG*

was found to be essential for gliotoxin biosynthesis and was proposed to mediate GSH addition to an intermediate in the gliotoxin biosynthetic pathway (Davis *et al.*, 2011a; Scharf *et al.*, 2011). This biosynthetic function of GliG and the presence of a GST in *A. fumigatus elfA* highlight the possibility that GSTs in *A. fumigatus* are involved in an array of different roles in this fungus, as has been observed in other organisms (Frova, 2006; Hayes *et al.*, 2005).

Given that GST activity has already been determined in native *A. fumigatus* ElfA (Carberry *et al.*, 2006), the work described in this thesis will focus on the further characterisation of *A. fumigatus elfA*, in particular with respect to a possible function in the oxidative stress response, to elucidate its role in the organism.

Table 1.1: Characterised GSTs in *A. fumigatus*

<i>A. fumigatus</i> gene	GST Activity	Reference
<i>gstA</i>	Recombinant protein	Burns <i>et al.</i> (2005)
<i>gstB</i>	Recombinant protein	Burns <i>et al.</i> (2005)
<i>gstC</i>	Recombinant protein	Burns <i>et al.</i> (2005)
<i>elfA</i>	Native protein	Carberry <i>et al.</i> (2006)
<i>gliG</i>	Recombinant protein	Davis <i>et al.</i> (2011a)

1.10 Oxidative Stress

As a consequence of aerobic respiration, oxidative metabolism results in the generation of ROS which comprise the superoxide anion ($O_2^{\cdot-}$), the hydroxyl radical ($\cdot OH$) and hydrogen peroxide (H_2O_2) (Farah *et al.*, 2011). The majority of ROS in the cell, approximately 90 %, is produced by the electron-transport chain (Lushchak, 2011). In order to function properly, the cell is required to strictly monitor and control the levels of these ROS (Winyard *et al.*, 2005). If the intracellular levels of ROS increase, the cell is undergoing oxidative stress (Lushchak, 2011; Winyard *et al.*, 2005). In addition to endogenous sources of ROS (i.e., by-products of mitochondrial, peroxisomal and ER-localised oxidative metabolism), exogenous sources from the environment or host cell defence also result in oxidative stress (López-Mirabal and Winther, 2008; Winyard *et al.*, 2005). ROS are severely damaging, resulting in impairment of protein function, damage to DNA and peroxidation of lipids, ultimately causing disruption of cellular functions and possible cell death (López-Mirabal and Winther, 2008; Wheeler and Grant, 2004; Hayes and McLellan, 1999). Organisms have in place many different mechanisms to sense, respond to and ultimately defend against ROS and oxidative stress, some of which will be discussed in further detail here.

Glutathione is present in its reduced form (GSH) in larger quantities in the cell than the oxidised form (GSSG) (Anderson *et al.*, 1999). Oxidative stress can be identified by a disruption in the GSH/GSSG redox balance. The GSH/GSSG redox pair is considered to be a biological redox buffer due to the high concentration of glutathione in the cell and also because it can potentially influence the intracellular

protein thiol redox state (López-Mirabal and Winther, 2008). During oxidative stress, the concentrations of GSSG can increase resulting in disruption of the redox balance (i.e., decreased GSH/GSSG ratio) as the intracellular conditions become more oxidising (Rahman *et al.*, 2006). Thiol groups in proteins are oxidised in a number of ways when in the presence of ROS. Protein thiols exposed to ROS (e.g., H₂O₂) can be oxidised to form sulfenic acid (R-SOH), which in the presence of free thiols, such as GSH, is easily converted to disulphide which may be intramolecular, intermolecular or mixed disulphides with GSH (RS-SG) (Figure 1.7) (López-Mirabal and Winther, 2008). Alternatively, sulfenic acid can be further oxidised to sulfinic acid (RSOOH), which can be converted back into reduced thiols by the enzyme sulfiredoxin, or sulfonic acid (RSOOOH) which is irreversible (López-Mirabal and Winther, 2008; Biswas *et al.*, 2006). Glutathionylated substrates (RS-SG) can be reduced by the enzyme glutaredoxin (Grx), and in the process, GSSG is formed. The reaction of GSH with oxidised proteins, and the formation of GSSG following their subsequent reduction, disrupt the GSH/GSSG redox balance in the cell. The redox-active sulphhydryl group of GSH also directly scavenges ROS and acts as a cofactor for the enzyme glutathione peroxidase (Wheeler and Grant, 2004). GSH which is oxidised in this manner forms GSSG, again disrupting the GSH/GSSG redox balance in the cell (Wheeler and Grant, 2004).

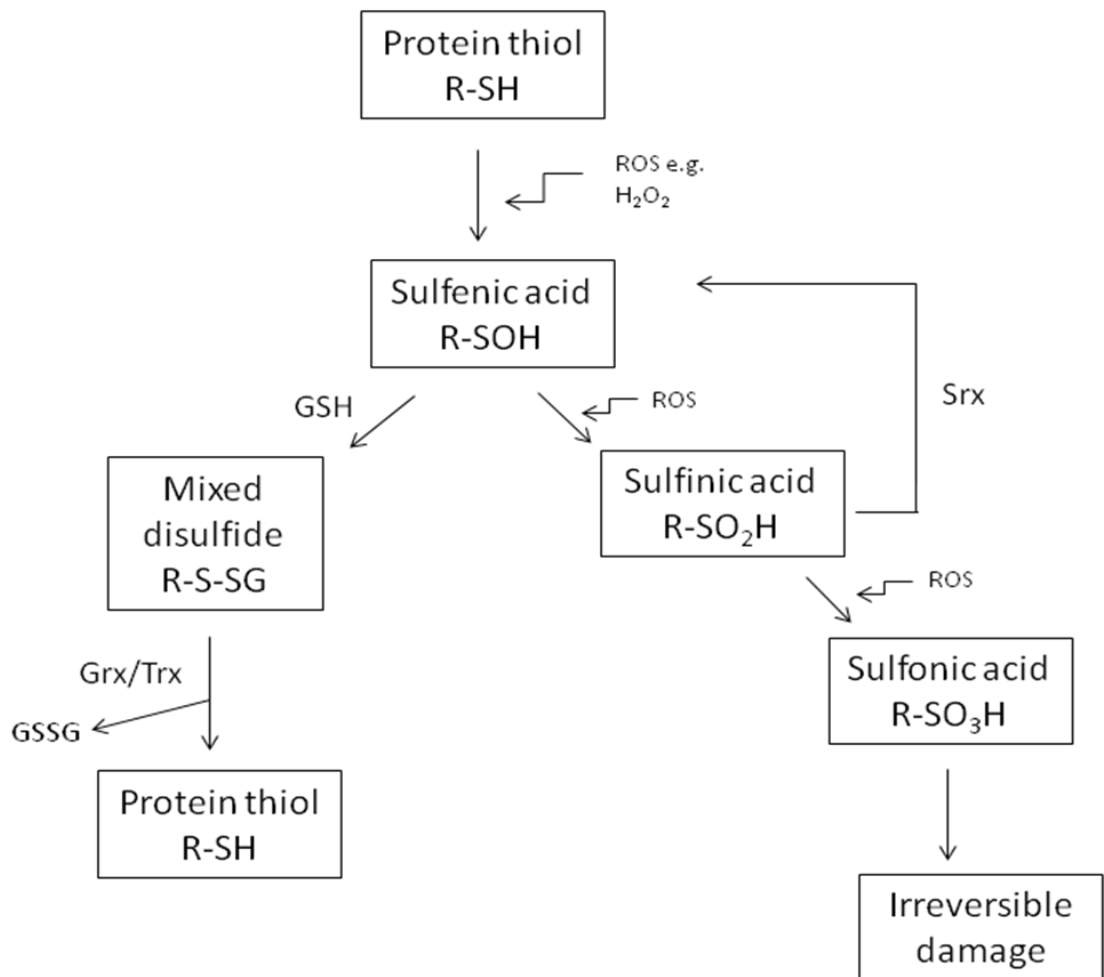


Figure 1.7: Protein thiol modifications due to oxidative stress. In the presence of ROS the thiol group forms a sulfenic acid derivative. This is a reversible modification if it is converted into a mixed disulphide as this can be reduced by glutaredoxin (Grx) or thioredoxin (Trx). Alternatively if the sulfenic acid derivative is oxidised further to sulfinic acid or sulfonic acid derivatives, this damage is generally irreversible. However in some cases, sulfinic acid can be converted back to sulfenic acid by Srx.

Oxidation of proteins can either be reversible or irreversible (Sheehan, 2006; Ghezzi, 2005). The oxidation of protein thiol groups to sulfonic acid species is irreversible and these “damaged” proteins must be degraded (Biswas *et al.*, 2006). The formation of mixed disulphides between proteins and glutathione is known as glutathionylation (Gao *et al.*, 2009; Ghezzi, 2005). Glutathionylation is a component of the oxidative stress response in that it protects sensitive thiol groups from irreversible oxidation and in doing so allows the cell to restore the cognate function of the protein once the oxidative stress conditions have abated (Sheehan, 2006; Ghezzi, 2005; Sies *et al.*, 1998). In addition to this, glutathionylation also functions to provide storage of intracellular glutathione which could be mobilised quickly under conditions of glutathione demand, and also to modulate protein function (Gao *et al.*, 2009; Sies *et al.*, 1998). The reversibility of protein glutathionylation is a means of controlling the GSH/GSSG balance (Ghezzi, 2005).

De-glutathionylation is catalysed by the family of protein disulphide oxidoreductases, as exchange between thiols and disulphides is very slow (Biswas *et al.*, 2006; Ghezzi, 2005). Three members of this family; glutaredoxin (Grx), thioredoxins (Trx) and sulphiredoxins (Srx) have been implicated in de-glutathionylation (Greetham *et al.*, 2010). Glutaredoxins form part of the glutaredoxin system, which includes NADPH, GSH and glutathione reductase which transfers electrons from NADPH to Grx by GSH (Collinson and Grant, 2003). Glutaredoxins have been proposed to be the most efficient enzymes for de-glutathionylation (Greetham *et al.*, 2010). Glutaredoxins contain the redox-active CXXC motif and the two cysteines in the active site form a monothiol or a dithiol

intermediate after undergoing reversible oxidoreduction (Ghezzi, 2005). Grx therefore catalyses the reduction of the protein disulphide to their respective sulphhydryls and in doing so becomes oxidised by forming an intramolecular disulphide in the CXXC active site (Biswas *et al.*, 2006; Ghezzi, 2005). Oxidised Grx is then reduced by GSH and consequently Grx is dependent on GSH (López-Mirabal and Winther, 2008).

Thioredoxins are members of the oxidoreductase family of enzymes (Ghezzi, 2005). The thioredoxin system comprises thioredoxin, thioredoxin reductase and NADPH (Biswas *et al.*, 2006). Thioredoxins catalyse the reduction of protein disulphides into their corresponding sulphhydryls in the same manner as that described for glutaredoxins (Ghezzi, 2005). Following deglutathionylation, the oxidised disulphide form of thioredoxin is reduced directly by NADPH and thioredoxin reductase (Greetham *et al.*, 2010).

It was generally accepted that protein thiols oxidised to form sulfinic acid derivatives were irreversibly damaged, however an ATP-dependent enzyme, sulfiredoxin, was identified that was capable of reducing the sulfinic acid derivative of yeast peroxiredoxins (Biswas *et al.*, 2006; Biteau *et al.*, 2003). Sulfiredoxin reduces the sulfinic acid derivative to peroxiredoxin-sulfenate and a sulfiredoxin-disulphide (Biteau *et al.*, 2003).

The enzymes and processes described here, along with others not discussed, are involved in maintaining the intracellular GSH/GSSG redox balance. Given that *A. fumigatus* ElfA has a GST domain it suggests that this protein may have a role in the oxidative stress response possibly with regard to protein glutathionylation. The

enzymes and proteins involved in the maintenance of this redox balance are regulated by transcription factors acting as sensors for oxidative stress conditions, which will be discussed in Section 1.11.

1.11 Transcription factors in redox regulation

The response to stress conditions in the cell is primarily initiated at the genetic level and ultimately involves the synthesis of proteins that protect the cell and restore redox homeostasis (Paulsen and Carroll, 2009). One of the central regulators of the oxidative stress response is the transcription factor Yap1, a basic leucine zipper (bZIP) transcription factor (Paulsen and Carroll, 2009). The bZIP domain is located at the N-terminal end, while located at the C-terminal end is a highly conserved cysteine-rich domain (CRD) (Qiao *et al.*, 2008). In the absence of oxidative stress Yap1 is located in the cytoplasm, however upon exposure to oxidative stress, Yap1 locates to the nucleus (Rodrigues-Pousada *et al.*, 2010; Qiao *et al.*, 2008). The location of Yap1 is dependent of the CRD and the nuclear export factor Crm1 (Rodrigues-Pousada *et al.*, 2010; Qiao *et al.*, 2008). In the absence of oxidative stress, Crm1 interacts with the CRD of Yap1 transporting it into the cytoplasm. However, upon exposure to oxidative stress, two cysteines in CRD are oxidised forming an intramolecular disulphide bond disrupting the interaction of Crm1 with CRD resulting in the retention of Yap1 in the nucleus (Rodrigues-Pousada *et al.*, 2010; Paulsen and Carroll, 2009).

In *A. fumigatus*, both Lessing *et al.* (2007) and Qiao *et al.* (2008) have demonstrated that *Afyap1* is the major regulator of the response to ROS. Deletion of

Afyap1 resulted in a strain sensitive to several oxidants including; H₂O₂, diamide, and menadione (Qiao *et al.*, 2008; Lessing *et al.*, 2007). Lessing *et al.* (2007) identified putative Yap1 targets, which included proteins directly involved in the oxidative stress response; mitochondrial peroxiredoxin, catalase and cytochrome *c* peroxidase, along with proteins required for protein biosynthesis (e.g., eEF1B γ , EF-3 and EIF5A), heat shock and metabolism. In the same study, it was also confirmed that the nuclear localisation of Yap1 is dependent on the presence of oxidative stress.

In *A. nidulans*, the CCAAT-binding factor, termed AnCF, consists of three subunits; HapB, HapC and HapE (Thön *et al.*, 2010; Brakhage *et al.*, 1999). HapC forms a stable heterodimer with HapE, which is then bound by HapB facilitating its transport into the nucleus (Thön *et al.*, 2010). AnCF senses the redox status of the cell via the HapC subunit which contains thiol groups (Thön *et al.*, 2010). In an oxidised environment, the thiol groups of HapC form intramolecular or intermolecular disulphide bonds preventing the formation of the heterodimer with HapE. Consequently AnCF is unable to localise to the nucleus. *A. nidulans napA* is the ortholog of the Yap1 transcription factor (Asano *et al.*, 2007). Under normal reduced conditions in the cell AnCF prevents the full expression of *A. nidulans napA* (Thön *et al.*, 2010). Because AnCF is unable to localise to the nucleus under oxidative stress, it no longer represses *napA* expression which is the main regulator of the oxidative stress response (Thön *et al.*, 2010).

1.12 Degradation of “damaged” and misfolded proteins

The endoplasmic reticulum (ER) provides the location for the majority of the protein folding events in the cell. Proteins are translocated into the lumen of the ER in an unfolded state before, with the aid of ER-resident chaperones, folding enzymes and post-translational modifications, acquisition of 3D confirmation (Richie *et al.*, 2009; Malhotra and Kaufman, 2007). The levels of unfolded proteins in the ER needs to be carefully monitored as unfolded proteins can form toxic aggregates that interfere with the function of normal proteins (Richie *et al.*, 2009). Disruption to the redox balance (e.g., under oxidative stress conditions) can also lead to a build up of unfolded proteins which ultimately results in ER stress (Malhotra and Kaufman, 2007). ER stress results from an imbalance between the amount of unfolded proteins in the ER and the capacity of the ER to deal with them (Ron and Walter, 2007). In the event of ER stress, the unfolded protein response (UPR) is initiated (Ron and Walter, 2007). The UPR is a conserved eukaryotic signalling pathway in the ER which transmits information regarding the protein folding capacity of the ER to the nucleus (Richie *et al.*, 2009).

The level of unfolded proteins is detected by a bifunctional protein call Ire1p (Malhotra and Kaufman, 2007). Under non-stressed ER conditions, Ire1p is bound to the protein chaperone BiP and is maintained in an inactive state (Malhotra and Kaufman, 2007). Under ER stress conditions, the accumulated misfolded proteins bind to BiP and Ire1p is released in an active state (Malhotra and Kaufman, 2007). Ire1p possesses both a protein kinase and an endoribonuclease (Ron and Walter, 2007; Ma and Hendershot, 2001). The endoribonuclease excises an intron from the

only substrate for Ire1p, *hac1*, and in doing so enables translation of this transcription factor which activates UPR target genes (Malhotra and Kaufman, 2007; Ron and Walter, 2007; Ma and Hendershot, 2001). The endoribonuclease activity of Ire1p is regulated by the intrinsic kinase module (Ron and Walter, 2007). Higher eukaryotes also contain two additional ER stress transducers; AFT6 and PERK (Malhotra and Kaufman, 2007; Ron and Walter, 2007), the functions of which will not be discussed here.

Activation of the UPR reduces protein synthesis and translocation to the ER, consequently reducing the amount of unfolded proteins entering the ER (Ron and Walter, 2007). In addition to this, up-regulation of UPR target genes involved in the ER protein-folding machinery increases the capacity of the ER to accommodate unfolded proteins (Ron and Walter, 2007). Targets of the UPR also includes genes involved in ER-associated protein degradation (ERAD) (Malhotra and Kaufman, 2007; Ron and Walter, 2007). ERAD is involved in the retro-translocation of unfolded proteins from the ER lumen to the cytosol where they are degraded by the ubiquitin-proteasome system (Goeckeler and Brodsky, 2010). In *A. fumigatus* the UPR is required for virulence and antifungal tolerance (Richie *et al.*, 2009). An *A. fumigatus* deletion strain for *hacA*, the ortholog of *hac1*, displayed increased sensitivity to antifungals, and also had attenuated virulence in different mouse models of IA (Richie *et al.*, 2009).

1.13 Thesis Rationale and objectives

A eukaryotic elongation factor 1B γ in *A. fumigatus* has been shown to exhibit GST activity suggesting a possible role in the oxidative stress response (Carberry *et al.*, 2006). eEF1B γ is a member of the eEF1 complex required for the elongation step of protein biosynthesis. In *S. cerevisiae*, eEF1B γ is not essential for translation to occur (Pittman *et al.*, 2009), and little information is available pertaining to the role of eEF1B γ during protein biosynthesis. The identification of GST activity in this protein raises questions regarding the function of *A. fumigatus elfA*. It has been speculated that the presence of a GST domain in eEF1B γ may contribute to protection of the elongating ribosome against oxidative stress (Carberry *et al.*, 2006), or control of translation in response to oxidative stress (Ejiri, 2002). This intriguing relationship between eEF1B γ and GST requires investigation to determine if *A. fumigatus elfA* functions in the oxidative stress response.

Comparative proteomics, as described in Section 1.3, is an important and useful tool for examining the effects of the loss of a protein on the whole proteome with a view to identifying possible functions for the protein. In addition to using comparative proteomics to investigate the function of ElfA it will also be used to investigate the systems interactions in *A. fumigatus* $\Delta pes3$. *A. fumigatus pes3* will be discussed in more detail in Chapter 6.

Therefore, the overall work objectives presented in this thesis are as follows;

- (i) The targeted deletion of *A. fumigatus elfA* in the ATCC46645 strain and the subsequent complementation of *A. fumigatus* $\Delta elfA$ to facilitate functional studies.

- (ii) Phenotypic characterisation of *A. fumigatus* $\Delta elfA$ in response to various stresses and investigation of the GSH/GSSG redox balance in *A. fumigatus* in response to hydrogen peroxide.
- (iii) Comparative proteomic analysis of *A. fumigatus* ATCC46645 and $\Delta elfA$ under both normal growth conditions and following exposure to hydrogen peroxide to determine the effect of the absence of *A. fumigatus* *elfA* on the proteome in order to elucidate possible functions.
- (iv) Application of comparative proteomics to *A. fumigatus* ATCC46645 and $\Delta pes3$ to elucidate a possible function for this nonribosomal peptide synthetase.

2.1 Materials

All chemicals were purchased from Sigma-Aldrich Chemical Co. Ltd. (UK), unless otherwise stated.

2.1.1 *Aspergillus* Media and Agar

2.1.1.1 Sabouraud Dextrose Broth

Sabouraud-dextrose broth (30 g) (Oxoid, Cambridge, UK) was added to 1 L distilled water, and dissolved. The solution was autoclaved and stored at 4 °C.

2.1.1.2 Sabouraud Agar

Sabouraud agar (65 g) (Oxoid, Cambridge, UK) was added to 1 L distilled water and dissolved. The solution was autoclaved and allowed to cool to ~50 °C. Agar (25 ml) was then poured into 90 mm sterile petri dishes, under sterile conditions. The plates were allowed to set and stored at 4 °C.

2.1.1.3 Malt Extract Agar

Malt extract agar (50 g) (Difco, Maryland, USA) was added to 1 L distilled water, and dissolved. The solution was autoclaved and allowed to cool to ~50 °C. Agar (25 ml) was then poured into 90 mm sterile petri dishes, under sterile conditions. The plates were allowed to set and stored at 4 °C.

2.1.1.4 *Aspergillus* Minimal Media (AMM)

2.1.1.4.1 *Aspergillus* Trace Elements

$\text{Na}_2\text{B}_4\text{O}_7 \cdot 7\text{H}_2\text{O}$ (40 mg), $\text{CuSO}_4 \cdot 5\text{H}_2\text{O}$ (400 mg), $\text{FeSO}_4 \cdot 7\text{H}_2\text{O}$ (800 mg), $\text{Na}_2\text{MoO}_4 \cdot 2\text{H}_2\text{O}$ (800 mg), and $\text{ZnSO}_4 \cdot 7\text{H}_2\text{O}$ (8 g) were dissolved in order, in 800 ml distilled water, allowing each to dissolve completely before addition of the next component. A few drops of concentrated HCl were added to maintain the solution. The solution was brought to a final volume of 1 L with distilled water. The solution was filter sterilised into aliquots (50 ml) and stored at $-20\text{ }^\circ\text{C}$.

2.1.1.4.2 *Aspergillus* Salt Solution

KCl (26 g), $\text{MgSO}_4 \cdot 7\text{H}_2\text{O}$ (26 g), KH_2PO_4 (76 g) and *Aspergillus* trace elements (50 ml) (Section 2.1.1.4.1) were added to 800 ml distilled water and dissolved. The solution was made up to 1 L with distilled water and autoclaved. The solution was stored at room temperature.

2.1.1.4.3 100 X Ammonium Tartrate

Ammonium tartrate (92 g) was dissolved in 1 L distilled water. The solution was autoclaved and stored at room temperature.

2.1.1.4.4 AMM Liquid Media

Ammonium tartrate (100 X, 10 ml) (Section 2.1.1.4.3), Salt Solution (50 X, 20ml) (Section 2.1.1.4.2), and glucose (10 g) were added to 800 ml distilled water and dissolved. The pH of the solution was adjusted to pH 6.8 and made up to a final volume of 1 L with distilled water. The solution was autoclaved at 105 °C for 30 min and stored at room temperature.

2.1.1.4.5 AMM Agar

Agar (20 g) (Fischer) was added to 1 L of AMM Liquid media (Section 2.1.1.4.4), before it was autoclaved, and stirred. The solution was autoclaved at 105 °C for 30 min and allowed to cool to ~50 °C before being poured (25 ml) into 90 mm sterile petri dishes, under sterile conditions. The plates were allowed to set and stored at 4 °C.

2.1.1.5 Regeneration Agar

2.1.1.5.1 1.8 % (w/v) Regeneration Agar

Salt Solution (50 X, 20 ml) (Section 2.1.1.4.2) and ammonium tartrate (100 X, 10 ml) (Section 2.1.1.4.3) were added to 800 ml distilled water and mixed. The solution was adjusted to pH 6.8. Sucrose (342 g) was added and dissolved. The solution was made to a final volume of 1 L with distilled water. Agar (18 g) (Fischer) was added to the solution. The solution was autoclaved and kept at 65 °C until required.

2.1.1.5.2 0.7 % (w/v) Regeneration Agar

Salt Solution (50 X, 20 ml) (Section 2.1.1.4.2) and ammonium tartrate (100 X, 10 ml) (Section 2.1.1.4.3) were added to 800 ml distilled water and mixed. The solution was adjusted to pH 6.8. Sucrose (342 g) was added and dissolved. The solution was made to a final volume of 1 L with distilled water. Agar (7 g) (Fischer) was added to the solution. The solution was autoclaved and kept at 65 °C until required.

2.1.1.6 RPMI 1640 containing 2 % (w/v) glucose

Glucose (2 g) was dissolved in RPMI 1640 (100 ml). The solution was filtered through a sterile 0.22 µm filter and stored at 4 °C until required for use.

2.1.2 Solutions for pH Adjustment

2.1.2.1 5 M Hydrochloric Acid (HCl)

Deionised water (40 ml) and HCl (43.64 ml) were added slowly to a glass graduated cylinder. The final volume was adjusted to 100 ml with deionised water. The solution was stored at room temperature.

2.1.2.2 5 M Sodium Hydroxide (NaOH)

NaOH pellets (20 g) were added to deionised water (80 ml) and dissolved by stirring. The final volume was adjusted to 100 ml with deionised water. The solution was stored at room temperature.

2.1.3 Phosphate Buffer Saline (PBS)

One PBS tablet (20 X) was added to 200 ml of distilled water and dissolved by stirring. The solution was autoclaved and stored at room temperature.

2.1.4 Phosphate Buffer Saline-Tween 20 (0.05 % (v/v)) (PBST 0.05 %)

Tween-20 (0.5 ml) was added to 1 L PBS (Section 2.1.3). The solution was mixed and stored at room temperature.

2.1.5 Phosphate Buffer Saline-Tween 20 (0.1 % (v/v)) (PBST 0.1 %)

Tween-20 (1.0 ml) was added to 1 L PBS (Section 2.1.3). The solution was mixed and stored at room temperature.

2.1.6 Plate Assays

The reagents and the concentrations at which they were used are listed in Table 2.1.

2.1.7 Luria-Bertani Broth (LB Broth)

LB Broth (25 g) (Difco, Maryland, USA) was dissolved in 1 L distilled water. The solution was autoclaved and stored at 4 °C.

Table 2.1: Reagents and concentrations used in Plate Assays to test for phenotypic alterations in *A. fumigatus*.

Condition Tested	Reagent added	Concentrations tested
Oxidative Stress	H ₂ O ₂	0 – 5 mM
	Diamide	0 – 4 mM
	Menadione	0 – 50 µM
Sensitivity to thiol-reactive reagent	4,4'-dithiodipyridine	0 – 7.5 µM
Sensitivity to reducing agent	DTT	0 – 5 mM
Sensitivity to antifungals	Voriconazole	0 – 1 µg/ml
	Amphotericin B	0 – 1 µg/ml
Sensitivity to gliotoxin	Gliotoxin	0 – 10 µg/ml
Osmotic stress	Glycerol	0 – 10 % (v/v)
Secreted proteases	Skimmed Milk	0 – 0.5 % (w/v)

2.1.8 Luria-Bertani Agar (LB Agar)

LB Agar (40 g) (Difco, Maryland, USA) was dissolved in 1 L distilled water. The solution was autoclaved and allowed to cool to ~50 °C. Agar (25 ml) was poured into sterile 90 mm petri dishes, under sterile conditions and allowed to set. They were stored at 4 °C.

2.1.9 80 % (v/v) Glycerol

Glycerol (80 ml) was added to 20 ml deionised water. The solution was autoclaved and stored at 4 °C.

2.1.10 10 % (w/v) Sodium Dodecyl Sulphate (SDS)

SDS (10 g) was added to 100 ml of deionised water, and dissolved. This solution was stored at room temperature. If the SDS precipitated, the solution was placed at 37 °C until the SDS had returned into solution.

2.1.11 20 % (w/v) SDS

SDS (20 g) was added to 100 ml of deionised water, and dissolved. This solution was stored at room temperature. If the SDS precipitated, the solution was placed at 37 °C until the SDS had returned into solution.

2.1.12 Antibiotics and Supplements

Hygromycin B was supplied by Melford Laboratories Ltd., Suffolk, UK. Antibiotics were prepared in water and stored at -20 °C, with the exception of hygromycin B, which was stored at 4 °C. See Table 2.2.

Table 2.2: Common antibiotics and supplements with working concentrations

Antibiotic	Diluent	Stock Concentration	Typical Working Concentration
Ampicillin	Water	100 mg/ml	100 µg/ml
Hygromycin B	Water	400 mg/ml	250 µg/ml
Pyriithiamine	Water	100 µg/ml	100 ng/ml

2.1.13 DNA Electrophoresis Reagents

2.1.13.1 50 X Tris-Acetate Buffer (TAE)

Trizma base (242 g) was added to 57.1 ml glacial acetic acid and 100 ml of 0.5 M EDTA, pH 8.0. The volume was adjusted to 1 L with distilled water. The solution was stored at room temperature.

2.1.13.2 1 X Tris Acetate Buffer (TAE)

50 X TAE (20 ml) (Section 2.1.13.1) was added to distilled water (980 ml). The solution was stored at room temperature.

2.1.13.3 Ethidium Bromide

Ethidium bromide was supplied at 10 mg/ml, of which 3 μ l was used per 100 ml agarose gel.

2.1.13.4 6 X DNA Loading Dye

Loading dye (Promega, Southampton, UK) was used at the concentration supplied.

2.1.14 DNA Reagents

2.1.14.1 100 % (v/v) Ethanol (ice-cold)

Molecular Biology Grade Ethanol (100 % (v/v)) was poured into a sterile 50 ml falcon tube and stored at – 20 °C.

2.1.14.2 70 % (v/v) Ethanol (ice-cold)

Molecular Biology Grade Ethanol (35 ml) was added to 15 ml of Molecular Biology Grade H₂O in a sterile 50 ml falcon tube and the solution was stored at – 20°C.

2.1.14.3 3 M Sodium Acetate

Sodium acetate (12.3 g) was dissolved in 50 ml of Molecular Grade H₂O and the pH was adjusted to pH 5.2. The solution was stored at room temperature.

2.1.14.4 Table of primers

All the primers used are listed in Table 2.3

Table 2.3: List of primers and sequences used in this study.

Primer Name	Sequence 5' – 3'
elfA 5' <i>Pst</i>I	TGTCTGCAGGTTAGGAGGTAGATTGCTC
elfA 3' <i>Ase</i>I	ATTATTAATGCCCAACCTGTGAATGAG
elfA 5'	AGACCCAACTCTCTCTCC
elfA 3'	CATAGAAGGGTTTCGCGC
elfA 5' nest	CTCCAGCCCACATTCTTG
elfA 3' nest	TAGCGTGTGGAGTTGAGG
optrA1	GAGGACCTGGACAAGTAC
optrA2	GTACCACTGGTCACGATG
5'elfA 02/10 dig	GGGTCATGAAGGTACGTAC
3' elfA 02/10 dig	AGCCTTGGGAATCTCACG
5'elfA RT-PCR	ATTTCTCGCCAAGTTCCC
3' elfA RT-PCR	AGCCTTGGGAATCTCACG
calm F	CCGAGTACAAGGAAGCTTTCTC
calm R	GAATCATCTCGTCGATTCGTCGTCTCAGT

2.1.15 RNA Electrophoresis Reagents

2.1.15.1 RNA Glassware

All glassware required for RNA reagent preparation and RNA extraction was autoclaved twice before use.

2.1.15.2 0.5 M EDTA

EDTA (18.612 g) was dissolved in twice autoclaved distilled water (100 ml).

2.1.15.3 10 X Formaldehyde Agarose (FA) Gel Buffer

MOPS (41.9 g) (0.2 M), sodium acetate (6.8 g) (82 mM) and 0.5 M EDTA pH 8.0 (20 ml) (Section 2.1.15.2) were dissolved in 800 ml twice autoclaved distilled H₂O. The pH of the solution was adjusted to pH 7.0 and the volume was adjusted to 1 L with twice autoclaved distilled H₂O. The solution was autoclaved and stored at room temperature.

2.1.15.4 1 X Formaldehyde Agarose (FA) Running Buffer

10 X FA gel buffer (100 ml) (Section 2.1.15.3), 37 % (v/v) formaldehyde (20 ml) and twice autoclaved distilled H₂O, to a final volume of 1 L, were mixed by stirring. The solution was stored at room temperature.

2.1.16 Aspergillus Transformation Reagents

2.1.16.1 0.7 M Potassium Chloride

KCl (26.1 g) was dissolved in 500 ml distilled water. The solution was autoclaved and stored at room temperature.

2.1.16.2 25 mM Potassium Phosphate Monobasic

KH₂PO₄ (1.7 g) was dissolved in 500 ml distilled water.

2.1.16.3 25 mM Potassium Phosphate Dibasic

K₂HPO₄ (0.87 g) was dissolved in 200 ml distilled water.

2.1.16.4 Lysis Buffer

KCl (26.1 g) was dissolved in 25 mM KH₂PO₄ (350 ml) (Section 2.1.16.2). The pH was adjusted to pH 5.8 with 25 mM K₂HPO₄ (Section 2.1.16.3). The solution was brought to a final volume of 500 ml with distilled water.

2.1.16.5 Lysis Buffer containing Lytic Enzymes

Lytic enzymes from *Trichoderma harzianum* (0.45 g) were added to 15 ml Lysis Buffer (Section 2.1.16.4) and dissolved. The solution was filter sterilised using 0.45 µm filters.

2.1.16.6 Buffer L6

Sorbitol (72.88 g), Tris-HCl (0.484 g), and CaCl₂·2H₂O (0.588 g) were dissolved in 400 ml distilled water. The pH was adjusted to pH 7.5. The solution was autoclaved and stored at room temperature.

2.1.16.7 Buffer L7

PEG 6000 (60 g) was added to distilled water (40 ml). Tris-HCl (0.157 g) and CaCl₂·6H₂O (0.219 g) was added. Concentrated HCl was added to aid dissolving. The pH was adjusted to pH 7.5. The solution was autoclaved and stored at room temperature.

2.1.17 Southern Blot Reagents

2.1.17.1 Southern Transfer Buffer

Sodium hydroxide (0.6 M, 16 g) and sodium chloride (0.4 M, 35.07 g) were dissolved in 800 ml distilled water. The volume was adjusted to 1 L with distilled water.

2.1.17.2 20 X SSC

Sodium chloride (175.3 g) and sodium citrate (88.2 g) were added to distilled water (800 ml). The pH was adjusted to pH 7.0. The final volume was adjusted to 1 L with distilled water. The solution was autoclaved and stored at room temperature.

2.1.17.3 2 X SSC

20 X SSC (100 ml) (Section 2.1.17.2) was added to 900 ml distilled water and stored at room temperature.

2.1.17.4 Dig Buffer 1

Maleic Acid (2.322 g) and sodium chloride (1.75 g) were added to distilled water (150 ml). NaOH (5 M) (Section 2.1.2.2) was added to aid dissolving. The pH was adjusted to pH 7.5. The final volume was adjusted to 200 ml with distilled water. The solution was filter sterilised and stored at room temperature.

2.1.17.5 Blocking Reagent

Blocking reagent was obtained from Roche Applied Science (Mannheim, Germany)

2.1.17.6 10 % (w/v) Lauroylsarcosine

Lauroylsarcosine (1 g) was dissolved in 10 ml distilled water.

2.1.17.7 Membrane Pre-Hybridisation Buffer

SDS (35 g), formamide (250 ml), 10 % (w/v) blocking reagent (Roche Applied Science) (100 ml), 10 % (w/v) laurylosarcosine (5 ml) (Section 2.1.17.6) and 20 X SSC (125 ml) (Section 2.1.17.2) were dissolved in water to give a final volume of 500 ml. The solution was stirred well and autoclaved. The solution was stored at 4 °C.

2.1.17.8 1 X SSC 0.1 % (w/v) SDS

20 X SSC (50 ml) (Section 2.1.17.2) and 10 % (w/v) SDS (4 ml) (Section 2.1.10) were added to distilled water (946 ml). The solution was mixed and stored at room temperature.

2.1.17.9 Dig Wash Buffer (0.3 % (v/v) Tween-20 in Dig Buffer 1)

Tween-20 (0.15 g) was added to Dig Buffer 1 (50 ml) (Section 2.1.17.4). The solution was mixed and filter sterilised (0.22 µm filter). It was stored at room temperature.

2.1.17.10 Dig Buffer 2

Blocking reagent (0.2 g) (Section 2.1.17.5) was dissolved in Dig Buffer 1 (20 ml) (Section 2.1.17.4) by stirring with low heat. The solution was filter sterilised (0.22 µm filter) and used immediately.

2.1.17.11 Dig Buffer 3

Tris-HCl (1.575 g), NaCl (0.584 g) and MgCl₂ (1.02 g) were dissolved in distilled water (90 ml). The pH was adjusted to pH 9.5 and the final volume adjusted to 100 ml with distilled water. The solution was filter sterilised (0.22 µm filter) and stored at room temperature.

2.1.17.12 Anti-Digoxigenin-Alkaline Phosphatase (AP), Fab fragment conjugate

Anti-Digoxigenin-AP, Fab fragments (Roche Applied Science, Mannheim, Germany) (2 µl) was added to 20 ml Dig Buffer 2 (Section 2.1.17.10).

2.1.17.13 Chemiluminescent Substrate Phosphate Detection (CSPD) Substrate

CSPD (50 µl) (Roche Applied Science, Mannheim, Germany) was added to Dig Buffer 3 (5 ml) (Section 2.1.17.11).

2.1.17.14 DIG-labelled deoxynucleotide triphosphates (dNTP's)

Pre-mixed DIG-labelled dNTPs were purchased from Roche Applied Science and used according to the supplied recommendations for the generation of DIG-labelled probes for Southern Blot detection.

2.1.18 Chemicals for Photography

2.1.18.1 Developer Solution

The Developer (Kodak) was diluted 1/4 in distilled water and stored in a tinfoil covered glass bottle in a dark room.

2.1.18.2 Fixer Solution

The Fixer (Kodak) was diluted 1/5 in distilled water and stored in a tinfoil covered glass bottle in a dark room.

2.1.19 SDS-PAGE Reagents

2.1.19.1 1.5 M Tris-HCl, pH 8.8

Trizma base (18.15 g) was dissolved in 75 ml deionised water. The pH was adjusted to pH 8.8. The final volume was adjusted to 100 ml with deionised water. The solution was stored at 4 °C.

2.1.19.2 0.5 M Tris-HCl, pH 6.8

Trizma base (6.05 g) was dissolved in 75 ml deionised water. The pH was adjusted to pH 6.8. The final volume was adjusted to 100 ml with deionised water. The solution was stored at 4 °C.

2.1.19.3 10 % (w/v) Ammonium Persulphate

Ammonium persulphate (0.1 g) was added to 1 ml deionised water. The solution was mixed, stored at 4 °C and used immediately.

2.1.19.4 30 % (w/v) Acrylamide/Bis

Protogel was obtained from National Diagnostics (Hessle Hull, England) and contained 30 % (w/v) acrylamide: 0.8 % (w/v) bis-acrylamide.

2.1.19.5 0.5 % (w/v) Bromophenol Blue

Bromophenol blue (0.1 g) was added to deionised water (20 ml). The solution was stored at 4 °C.

2.1.19.6 5 X Solubilisation Buffer; reducing

Glycerol (10 ml), 10 % (w/v) SDS (1.6 ml) (Section 2.1.10), 0.5 M Tris-HCl, pH 6.8 (1 ml) (Section 2.1.19.2) was added to deionised water (1.4 ml). The solution was mixed and then 2-mercaptoethanol (0.4 ml) was added along with 0.5 % (w/v) Bromophenol blue solution (0.2 ml) (Section 2.1.19.5). The solution was mixed again, aliquoted and stored at -20 °C.

2.1.19.7 4 X Solubilisation Buffer; non-reducing

Glycerol (3 ml) and 20 % (w/v) SDS (1 ml) (Section 2.1.11) were added to 0.5 M Tris-HCl, pH 6.8 (1.25 ml) (Section 2.1.19.2). 0.5 % (w/v) Bromophenol blue solution (0.1 ml) (Section 2.1.19.5) was added and the solution was mixed. It was aliquoted and stored at – 20 °C.

2.1.19.8 5 X Electrode Running Buffer

Trizma base (15 g), glycine (72 g) and SDS (5 g) were dissolved in deionised water (800 ml). The final volume was adjusted to 1 L. The solution was stored at room temperature.

2.1.19.9 1 X Electrode Running Buffer

5 X Electrode Running Buffer (200 ml) (Section 2.1.19.8) was added to 800 ml distilled water. The solution was stored at room temperature.

2.1.19.10 Coomassie® Blue Stain Solution

Coomassie® Brilliant Blue R (2 g), glacial acetic acid (100 ml), methanol (450 ml) and deionised water (50 ml) were added to a glass bottle and mixed. The solution was brought to a final volume of 1 L with deionised water. The solution was stored at room temperature.

2.1.19.11 Destain Solution

Glacial acetic acid (100 ml) and methanol (300 ml) was added to deionised water (600 ml). The solution was stored at room temperature.

2.1.19.12 Colloidal Coomassie® Blue Stain Solutions

2.1.19.12.1 Fixing Solution

Ethanol (500 ml) and phosphoric acid (30 ml) was added to deionised water (470 ml). The solution was mixed. The solution was made up fresh on the day.

2.1.19.12.2 Incubation Buffer

Methanol (340 ml), phosphoric acid (30 ml) and ammonium sulphate (170 g) were added to deionised water (630 ml). The solution was mixed. The solution was made up fresh on the day.

2.1.19.12.3 Stain Solution

Methanol (340 ml), phosphoric acid (30 ml), ammonium sulphate (170 g) and Colloidal Coomassie® Blue G-250 (0.35 g) (Serva Electrophoresis, Germany) were added to deionised water (630 ml). The solution was mixed. The solution was made up fresh on the day.

2.1.20 Western Blot Reagents

2.1.20.1 Towbin Electrotransfer Buffer

Trizma base (30.3 g) and glycine (144 g) were added to 3 L deionised water and 1 L methanol. The pH was adjusted to pH 8 – 8.5. The final volume was adjusted to 5 L with deionised water. The solution was stored at room temperature.

2.1.20.2 Blocking Solution

Marvel® (Powdered Milk) (5 g) was added to 100 ml PBST 0.05% (Section 2.1.4).

2.1.20.3 Antibody Buffer

Marvel® (Powdered Milk) (1 g) was added to 100 ml PBST 0.05% (Section 2.1.4).

2.1.20.4 ECL

SuperSignal® West Pico Chemiluminescent Substrate (Pierce) was used. Equal volumes of the SuperSignal® West Pico Stable Peroxide Solution and SuperSignal® West Pico Luminol/Enhancer Solution were mixed just before use.

2.1.21 Lysis Reagents

2.1.21.1 *A. fumigatus* Mycelia Lysis Buffer

Tris-HCl (12.5 g), NaCl (2.9 g), EDTA (7.44 g), 10 % Glycerol (100 ml) was added to 800 ml of deionised water. The pH was adjusted to pH 7.5 using 5 M HCl. The final volume was adjusted to 1 L with deionised water. The solution was stored at 4 °C. DTT (30 mM, final conc.), PMSF (1 mM, final conc.) and Pepstatin A (1 µg/ml, final conc.) were added directly before use.

2.1.21.2 *A. fumigatus* Mycelia Lysis Buffer; non-reducing

Tris-HCl (12.5 g), NaCl (2.9 g), EDTA (7.44 g), 10 % (v/v) Glycerol (100 ml) was added to 800 ml of deionised water. The pH was adjusted to pH 7.5. The final volume was adjusted to 1 L with deionised water. The solution was stored at 4 °C. PMSF (1 mM, final conc.) and Pepstatin A (1 µg/ml, final conc.) were added directly before use.

2.1.22 Bradford Solution

Bradford Reagent (BioRad) was diluted 1/5 in PBS. This was stored at 4 °C for up to one week.

2.1.23 2D-PAGE Solutions

2.1.23.1 Trichloroacetic Acid 100 % (w/v) (100 % TCA)

Trichloroacetic Acid (100 g) was dissolved in water (45.4 ml).

2.1.23.2 Trichloroacetic Acid 10 % (w/v) (10 % TCA)

100 % TCA (Section 2.1.23.1) (10 ml) was added to water (90 ml).

2.1.23.3 Isoelectric focusing Buffer (IEF)

Urea (48 g), thiourea (15.2 g), CHAPS (4 g), Triton X-100 (1 ml), and Trizma base (0.12 g) were dissolved in 50 ml deionised water. The final volume was adjusted to 100 ml with deionised water. The solution was aliquoted into 1 ml aliquots which were stored at – 20 °C until use. After thawing, DTT (0.01 g) and the appropriate Ampholytes (8 µl/ml) (GE Healthcare) were added.

2.1.23.4 IPG Equilibration Buffer

Glycerol (150 ml), SDS (10 g), urea (180 g), and Trizma Base (3 g) were added to 400 ml deionised water. The pH was adjusted to pH 6.8. The final volume was adjusted to 500 ml. The solution was frozen in 50 ml aliquots at – 20 °C until use.

2.1.23.5 Reduction Buffer

A 50 ml aliquot of the IPG Equilibration Buffer (Section 2.1.23.4) was thawed and the pH checked to ensure it was still pH 6.8. DTT (1 g) was dissolved into the buffer. The solution was made up fresh on the day.

2.1.23.6 Alkylation Buffer

A 50 ml aliquot of the IPG Equilibration Buffer (Section 2.1.23.4) was thawed and the pH checked to ensure it was still pH 6.8. Iodoacetamide (1.25 g) was dissolved into the buffer. Bromophenol Blue (200 µl of 0.5 % (w/v) solution) (Section 2.1.19.5) was also added. The solution was made up fresh on the day.

2.1.23.7 Agarose Sealing Solution

Trizma Base (1.5 g), glycine (7.2 g) and SDS (0.5 g) were dissolved in deionised water (80 ml). Agarose (0.5 g) and bromophenol blue (400 µl of 0.5 % (w/v) solution) (Section 2.1.19.5) was added. The final volume was adjusted to 100 ml with deionised water.

2.1.24 Mass Spectrometry Reagents

2.1.24.1 100 mM Ammonium bicarbonate (NH₄HCO₃)

NH₄HCO₃ (400 mg) was dissolved in HPLC-grade water (50 ml). The solution was made up fresh on the day.

2.1.24.2 100 mM Ammonium bicarbonate / Acetonitrile (1:1 (v/v))

100 mM ammonium bicarbonate (5 ml) (Section 2.1.24.1) was added to acetonitrile (5 ml). The solution was made up fresh on the day.

2.1.24.3 10 mM Ammonium bicarbonate containing acetonitrile 10 % (v/v)

100 mM ammonium bicarbonate (1 ml) (Section 2.1.24.1) and acetonitrile (1 ml) was added to deionised water (8 ml). This solution was made up fresh on the day.

2.1.24.4 Trypsin Solution

10 mM ammonium bicarbonate containing acetonitrile 10 % (v/v) (1.5 ml) (Section 2.1.24.3) was added to 20 µg of Sequencing Grade Trypsin (Promega) and briefly vortexed until dissolved.

2.1.24.5 0.1 % (v/v) Formic Acid in LC-MS Grade Water

Formic Acid (1 ml) was added to of LC-MS Grade water (999 ml) using a glass pipette. The bottle was inverted to mix, taking care not to create air bubbles.

2.1.24.6 0.1 % (v/v) Formic Acid in 90 % (v/v) LC-MS Grade Acetonitrile

LC-MS Grade Water (100 ml) was added to LC-MS Grade acetonitrile (900 ml) in a darkened bottle. 1 ml of this was removed and formic acid (1 ml) was added to this using a glass pipette. The bottle was inverted to mix, taking care not to create air bubbles.

2.1.24.7 0.1% (v/v) Trifluoroacetic acid

Trifluoroacetic acid (TFA) (10 µl) was added to deionised water (9.99 ml). The solution was prepared freshly before each use.

2.1.25 Reverse-Phase High Performance liquid Chromatography (RP-HPLC)

Solvents

2.1.25.1 Solvent A (0.1 % (v/v) Trifluoroacetic Acid in HPLC Grade H₂O)

TFA (1 ml) was added to 999 ml HPLC Grade water to give a 0.1 % (v/v) TFA and water solution. The solution was prepared freshly before each use.

2.1.25.2 Solvent B (0.1 % (v/v) Trifluoroacetic Acid in HPLC Grade Acetonitrile)

TFA (1 ml) was added to 999 ml HPLC Grade acetonitrile to give a 0.1 % (v/v) TFA and acetonitrile solution. The solution was prepared freshly before each use.

2.1.26 Intracellular Glutathione measurement

2.1.26.1 125 mM Sodium Phosphate monobasic

Sodium Phosphate Monobasic (1.5 g) was dissolved in distilled water (100 ml). It was stored at 4 °C until required for use.

2.1.26.2 125 mM Sodium Phosphate dibasic

Sodium Phosphate dibasic (1.7745 g) was dissolved in distilled water (100 ml). It was stored at 4 °C until required for use.

2.1.26.3 GSH/GSSG Assay Buffer (125 mM Sodium Phosphate (pH 7.5)

6.3 mM EDTA

125 mM sodium phosphate monobasic (Section 2.1.26.1) was added, dropwise, to 125 mM sodium phosphate dibasic (100 ml) (Section 2.1.26.2), until the pH was adjusted to pH 7.5. EDTA (0.2345 g) was dissolved in 100 ml of this sodium phosphate buffer. It was stored at 4 °C until required for use.

2.1.26.4 5 % (w/v) 5'5-sulfosalicylic acid (5 % SSA)

SSA (0.5 g) was dissolved in GSH/GSSG Assay Buffer (10 ml) (Section 2.1.26.3). The solution was stored on ice.

2.1.26.5 50 % (v/v) Triethanolamine

Triethanolamine (250 µl) was mixed with GSH/GSSG Assay Buffer (250 µl) (Section 2.1.26.3).

2.1.26.6 20 % (v/v) 2-vinylpyridine

2-vinylpyridine (20 µl) was mixed with GSH/GSSG Assay Buffer (80 µl) (Section 2.1.26.3). This was carried out in a fumehood.

2.1.26.7 10 mM 5,5'-dithio-bis(2-nitrobenzoic acid) (DTNB)

DTNB (11.89 mg) was dissolved in GSH/GSSG Assay Buffer (3 ml) (Section 2.1.26.3). This was covered in tinfoil and stored on ice.

2.1.26.8 DTNB containing 1 UN Glutathione Reductase

For every well to be assayed, 1 UN of glutathione reductase was added to 42 μ l of 10 mM DTNB (Section 2.1.26.7).

2.1.26.9 30 mM β -nicotinamide adenine dinucleotide 2'-phosphate reduced tetrasodium salt hydrate (NADPH)

NADPH (25 mg) was dissolved in GSH/GSSG Assay Buffer (1 ml) (Section 2.1.26.3). This was aliquoted into smaller volumes, covered in tinfoil and stored at -20°C until required for use.

2.1.26.10 5 mM NADPH

1 volume of 30 mM NADPH (Section 2.1.26.9) was added to 5 volumes of GSH/GSSG Assay Buffer (Section 2.1.26.3). This was covered in tinfoil and stored on ice.

2.1.26.11 1 mg/ml Glutathione

Glutathione (1 mg) was dissolved in GSH/GSSG Assay Buffer (1 ml) (Section 2.1.26.3). This was covered in tinfoil and stored on ice.

2.1.26.12 2 mg/ml Glutathione disulfide

Glutathione disulfide (2 mg) was dissolved in GSH/GSSG Assay Buffer (1 ml) (Section 2.1.25.3). This was covered in tinfoil and stored on ice.

2.1.27 Biotinylation of Glutathione disulfide

2.1.27.1 Sulfo-NHS-LC-Biotin

Sulfo-NHS-LC-Biotin was obtained from Proteochem (Denver, USA).

2.1.27.2 1 M Tris-HCl (pH 7.2)

Tris-HCl (7.88 g) was dissolved in water (30 ml). The pH was adjusted to pH 7.2 and the final volume adjusted to 50 ml with water.

2.1.28 Confocal Imaging

2.1.28.1 50 mM Sodium Phosphate Monobasic

Sodium phosphate monobasic (0.6 g) was dissolved in distilled water (100 ml). It was stored at 4 °C until required for use.

2.1.28.2 50 mM Sodium Phosphate Dibasic

Sodium phosphate dibasic (0.7098 g) was dissolved in distilled water (100 ml). It was stored at 4 °C until required for use.

2.1.28.3 50 mM Sodium Phosphate Buffer (pH 7.4)

50 mM sodium phosphate monobasic (Section 2.1.28.1) was added, dropwise, to 50 mM sodium phosphate dibasic (100 ml) (Section 2.1.28.2), until the pH was adjusted to pH 7.4.

2.1.28.4 4 % (v/v) Formaldehyde, 50 mM Sodium Phosphate Buffer (pH 7.4)

37 % (v/v) formaldehyde (1.81 ml) was added to 50 mM sodium phosphate buffer (8.19 ml) (Section 2.1.28.3).

2.1.28.5 Confocal Buffer (50 mg/ml BSA in PBS)

BSA (0.5 g) was dissolved in PBS (10 ml) (Section 2.1.3).

2.1.29 50 mM Sodium Phosphate Buffer (pH 7.4) containing 150 mM NaCl

NaCl (0.8766 g) was dissolved in 50 mM Sodium Phosphate Buffer (pH 7.4) (100 ml) (Section 2.1.28.3).

2.2 Methods

2.2.1 Microbiological Methods- strain storage and growth

The fungal and bacterial strains used in this study are listed in Table 2.3.

2.2.1.1 *A. fumigatus* growth, maintenance and storage

A. fumigatus strains were maintained on Malt extract (ME) agar (Section 2.1.1.3) or AMM (*Aspergillus* minimal media) agar (Section 2.1.1.4.5). A loop of spores from a stock spore solution was spread onto a culture plate. Plates were incubated at 37 °C for 5-7 days with periodic checking. Once fully grown, the plates were sealed with parafilm, and stored inverted in a sealed plastic bag at 4 °C. For permanent storage of *Aspergillus* spores, freshly grown spores were harvested from agar plates by adding 10 ml of sterile PBST 0.1% (Section 2.1.5) to the conidial culture and rubbing the surface with a disposable spreader to dislodge the spores. The spores were transferred to a 50 ml sterile tube using a sterile Pasteur pipette. They were centrifuged at 2000 g for 10 min. The supernatant was removed and the conidia were resuspended in sterile PBS (Section 2.1.3) and stored at 4 °C until required. Aliquots of the conidial suspensions (500 µl) were added to 500 µl of sterile 80 % glycerol (Section 2.1.9). The tubes were vortexed and rapid-frozen in liquid nitrogen before transferring to -80 °C for long-term storage.

Table 2.4: Fungal and Bacterial Strains used, including antibiotics and supplements used.

Species	Strain	Antibiotics/Supplements	Reference
<i>A. fumigatus</i>	ATCC46645	N/A	ATCC collection
<i>A. fumigatus</i>	\DeltaakuB	Hygromycin (250 $\mu\text{g/ml}$)	(da Silva Ferreira <i>et al.</i> , 2006)
<i>A. fumigatus</i>	\DeltaelfA^{46645}	Pyriithiamine (100 ng/ml)	This study
<i>A. fumigatus</i>	$\DeltaakuB:\DeltaelfA$	Pyriithiamine (100 ng/ml)	This study
<i>A. fumigatus</i>	$\DeltaelfA^{46645}:\text{elfA}^C$	Hygromycin (200 $\mu\text{g/ml}$)	This study
<i>A. fumigatus</i>	$\Delta pes3^{46645}$	Pyriithiamine (100 ng/ml)	(O'Hanlon <i>et al.</i> , 2011)
<i>E. coli</i>	TOP10	Ampicillin (100 $\mu\text{g/ml}$)	N/a

Table 2.5: Plasmids including antibiotics and supplements used.

Plasmid	Antibiotics/Supplements
pCR®2.1-TOPO	Ampicillin (100 µg/ml)
pSK275	Pyriithiamine (100 ng/ml)
pAN7.1	Hygromycin B (200 µg/ml)

2.2.1.2 *E. coli* Growth, Maintenance and Storage

E. coli strains were grown on Luria-Bertani agar (Section 2.1.8) overnight at 37 °C or in Luria-Bertani broth (Section 2.1.7) overnight at 37 °C with shaking at 200 rpm. Where appropriate, the media was supplemented with the suitable antibiotic (Table 2.3). Bacterial strains were stored at 4 °C for short-term storage. For long term storage, 500 µl of freshly grown liquid culture of the desired strain was mixed with 500 µl of 40 % (v/v) glycerol. Tubes were rapid-frozen in liquid nitrogen before transferring to – 80 °C. To regenerate bacterial strains, tubes were thawed in iced. A sterile was used to streak the culture onto a LB agar plate containing the appropriate antibiotic.

2.2.2 Molecular Biological Methods

2.2.2.1 Isolation of Genomic DNA from *A. fumigatus*

A. fumigatus conidia were harvested from five day old plates using PBST 0.1% (10 ml) (Section 2.1.5). An aliquot of the conidial suspension (50 µl) was used to inoculate 100 ml cultures of Sabouraud Dextrose Broth (Section 2.1.1.1). The cultures were incubated for 24 h, at 37 °C, with constant shaking at 200 rpm. The cultures were then filtered through autoclaved miracloth, washed with sterile water and the mycelia collected. The mycelial mass was wrapped in tinfoil, rapid frozen in liquid Nitrogen and ground to a fine powder using a pestle and mortar. DNA extractions were carried out using the ZR Fungal/Bacterial DNA Kit (Zymo Research, California, USA). All buffers and reagents were supplied with the kit. For each sample, ground mycelia (0.1 g) were added to 750 µl DNA buffer in the ZR

Bashing tube. The tubes were vortexed vigorously for 5 min. The ZR Bashing tubes were centrifuged at 10,000 g for 1 min. The supernatants (400 µl) were transferred to the Zymo-Spin IV Spin filters in collection tubes and centrifuged at 7,000 g for 1 min. Fungal/Bacterial DNA Binding Buffer (1200 µl) was added to the filtrates in the collection tubes. Filtrates (800 µl) were transferred to the Zymo-Spin IIC columns in new collection tubes and centrifuged at 10,000 g for 1 min. The flow through was discarded. The remaining filtrates (800 µl) were added to the Zymo-Spin IIC columns in collection tubes and centrifuged at 10,000 g for 1 min. The flow through was discarded. DNA Pre-Wash Buffer (200 µl) was added to the Zymo-Spin IIC columns, in new collection tubes, and centrifuged at 10,000 g for 1 min. Fungal/Bacterial DNA Wash buffer (500 µl) was added to the Zymo-Spin IIC columns and centrifuged at 10,000 g for 1 min. The Zymo-Spin IIC columns were transferred to sterile 1.5 ml microcentrifuge tubes and DNA Elution Buffer (100 µl) was added to the columns. The columns were centrifuged at 10,000 g for 1 min to elute the DNA samples.

2.2.2.2 DNA Precipitation

2.5 X volume 100 % (v/v) ice cold ethanol (Section 2.1.14.1) and 0.1 X volume 3 M Sodium acetate (Section 2.1.14.3) were added to each DNA sample. The mixture was incubated at -20 °C for 30 min - 24 h. The mixtures were centrifuged at 17,900 g for 15 min at 4 °C. The supernatants were discarded and the pellets were resuspended in 100 µl 70 % (v/v) ice cold ethanol (Section 2.1.14.2). Samples were centrifuged at 13,000 g for 10 min. The supernatants were discarded

and the pellets were air-dried. Pellets were resuspended in 15 μ l sterile water. The precipitated DNA samples were stored at -20 °C until required.

2.2.2.3 Polymerase Chain Reaction (PCR)

Polymerase chain reaction (PCR) was used to amplify fragments of DNA for cloning, transformation constructs, probes, and to test for recombinant plasmid presence in *E. coli*. PCR was generally carried out using *Taq* polymerase (Sigma). PCR for the generation of constructs for gene disruption and the generation of DIG-labelled DNA probes was carried out using Expand Long Range Template PCR system (Roche). Annealing temperatures were estimated as *ca.* 4 °C below the melting temperature (T_m) of the primers used. Extension times used were *ca.* 1 min/kb of DNA to be synthesised. Reactions were carried out using either the Eppendorf PCR or G-Storm PCR (Roche) Systems.

The following reaction cycle was used unless otherwise stated:

95 °C (denaturing) 5 min

95 °C (denaturing) 1 min

56 °C (annealing) 1 min 30 s

72 °C (extending) 1 min

} x 35 cycles

72 °C (extending) 10 min

The general reaction constituents for each polymerase are:

Expand Long Range Template system

10 X reaction buffer	5 μ l
dNTP mix (20 μ M)	5 μ l
Primer F (100 pmol/ μ l)	2 μ l
Primer R (100 pmol/ μ l)	2 μ l
DNA Template	Up to 500 ng
Sterile Water	to a final volume of 50 μ l

Taq polymerase (Sigma)

10 X reaction buffer	2 μ l
dNTP mix (10 μ M)	2 μ l
Primer F (100 pmol/ μ l)	1 μ l
Primer R (100 pmol/ μ l)	1 μ l
DNA Template	10-100 ng
Sterile Water	to a final volume of 20 μ l

2.2.2.4 Agarose Gel Electrophoresis

Agarose gel electrophoresis was used to separate differently sized DNA fragments prior to purification, to visualise restriction digest reactions, to separate DNA fragments for Southern analysis and for estimation of DNA yield. Agarose gels were cast and run using Bio-Rad electrophoresis equipment. Agarose gels between 0.7 – 1.5 % (w/v) in 1 X TAE Buffer (Section 2.1.13.2) were used. For the majority of applications, a 0.7 % (w/v) agarose gel was suitable. Powered agarose was added to the appropriate volume of 1 X TAE Buffer (Section 2.1.13.2) in a 200 ml flask. This was then gently heated in a microwave, with frequent mixing, until the agarose had dissolved. While allowing the gel to cool, a mould was prepared by inserting the casting unit into the casting holder and sealed. After the gel had cooled to 40 -50 °C, the molten gel was poured into the prepared mould. Ethidium bromide (3 µl/100 ml) (Section 2.1.13.3) was added to the casting unit. A gel comb was inserted and the gel was allowed to set on a level surface. Once set, the gel comb was removed gently. The set gel, in the gel casting unit, was placed into the gel electrophoresis tank, with the wells nearer the negative (black) electrode. 1 X TAE Buffer (Section 2.1.13.2) was the poured into the tank to fully submerge the gel.

2.2.2.5 DNA Gel Electrophoresis

DNA samples were prepared by adding 5 volumes of DNA samples to 1 volume 6 X Loading Dye (Section 2.1.13.4). DNA fragment size was estimated by running molecular weight markers alongside the unknown samples. The different molecular weight markers used in this study were: DNA Molecular Weight Marker

VII (Roche), and DirectLoad™ Step Ladder, 50 bp (Sigma). Gels were electrophoresed at 50 – 100 V for 30 – 90 min and were visualised using an Alpha DigiDoc™ RT unit or a Syngene G:Box.

2.2.2.6 DNA Gel Extraction

DNA gel extraction was carried out using all the reagents and columns supplied with the QIA quick gel extraction kit (Qiagen, U.K) following the manufacturer's instructions. The DNA fragments of interest were excised from the agarose gel using a sterile scalpel, sliced into pieces which were then placed into sterile microcentrifuge tubes. For 1 volume of gel, 3 volumes of Buffer QG was added and they were heated at 50 °C in a heating block with vortexing every 2 min until completely dissolved. The solutions were transferred to QIA quick spin columns that were placed in 2 ml collection tubes and centrifuged at 12,000 g for 1 min. The flow through was discarded. Buffer PE (750 µl) was added to each column which were then centrifuged at 12,000 g for 1 min. The flow through was discarded and the columns centrifuged again at 12,000 g for 1 min to remove any residual traces of ethanol. The columns were placed in sterile microcentrifuge tubes and sterile water (30 µl) was added to each column to elute the DNA. The columns were allowed to stand for 2 min before being centrifuged at 12,000 g for 30 s. The DNA was stored at – 20 °C until required for use.

2.2.3 Cloning

2.2.3.1 TOPO TA Cloning

One step cloning of PCR products was carried out using the TOPO TA Cloning Kit from Invitrogen, according to the manufacturer's instructions. The principle behind one step cloning is based on the non-template dependant activity of *Taq* polymerase that results in the addition of a single deoxyadenosine (A) to the 3' ends of the PCR products. The linearised cloning vector has single 3' deoxythymidine (T) residues, therefore facilitating PCR inserts to ligate efficiently with the vector. The TOPO TA Cloning vector map is presented in Figure 2.1. The TOPO TA Cloning kit contains TOP 10 One Shot competent *E. coli* cells, Super Optimal Catabolite repression (SOC) media, TOPO vector and salt solution. Prior to cloning, TOP 10 cells were thawed on ice and LB agar plates (Section 2.1.8), containing 100 µg/ml ampicillin (Section 2.1.12) pre-warmed in a 37 °C incubator. Genomic DNA PCR product (4 µl), Salt solution (1 µl) and TOPO Vector (1 µl) were added to sterile 0.5 ml tube and left at room temperature for 30 min. A 2 µl aliquot of this reaction mixture was added to a vial of TOP 10 *E. coli* cells and placed on ice for 30 min. Cells were heat shocked in a water bath at 42 °C for 30 s. Pre-warmed SOC media (200 µl) was added to the vial. The vial was incubated at 37 °C for 45 min with constant agitation (200 rpm). During this incubation period, 32 µl of 5-bromo-4-chloro-3-indoyl-beta-D-galactopyranoside (X-gal) (Promega, Southampton, UK) (40 mg/ml) was spread over the pre-warmed LB agar plates (Section 2.1.8) using a sterile glass spreader. The plates were returned to the incubator. This reagent facilitated blue/white colony screening, which greatly aided

in the identification of desired clones. A 50 µl aliquot of the cell suspension was spread on the selection plates using a sterile disposable spreader and the plates were incubated overnight at 37 °C. White colonies were selected and sub-cultured onto LB agar plates (Section 2.1.8) with ampicillin (100 µg/ml) (Section 2.1.12). Colony PCR (Section 2.2.3.2) was carried out to verify the presence of the desired insert in the vector of the sample clones.

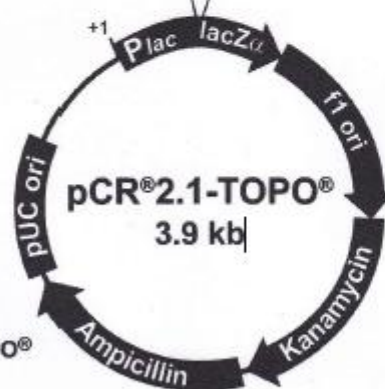
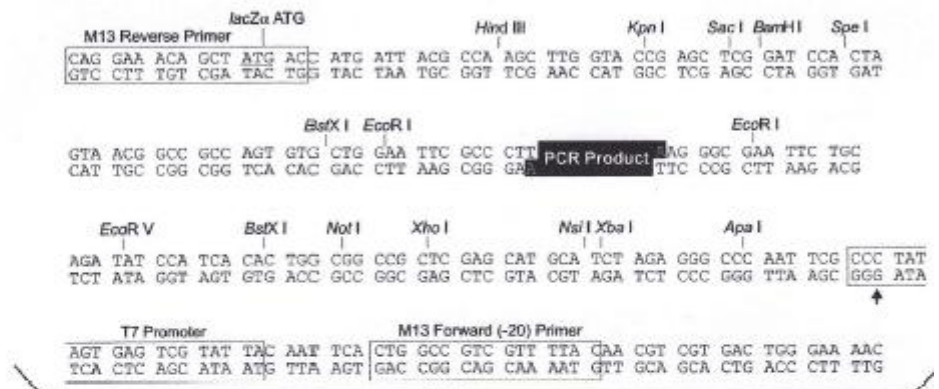
2.2.3.2 Colony PCR

Bacterial colonies observed following transformation could be directly screened for the presence of the desired plasmid by PCR. Using aseptic techniques, an isolated colony was removed using a sterile tip and placed in a sterile 0.2 ml microcentrifuge tube containing a PCR mastermix, having all the components necessary for PCR (Section 2.2.2.3) and also streaked onto a reference plate. Genomic DNA and DNA negative controls were included and PCR was carried out as described in Section 2.2.2.3, with the exception that the initial denaturing step was increased to 95 °C for 5 min to allow the bacterial cells to rupture and release DNA for the PCR reaction.

Map of pCR[®]2.1-TOPO[®]

pCR[®]2.1-TOPO[®] Map

The map below shows the features of pCR[®]2.1-TOPO[®] and the sequence surrounding the TOPO[®] Cloning site. Restriction sites are labeled to indicate the actual cleavage site. The arrow indicates the start of transcription for T7 polymerase. The complete sequence of pCR[®]2.1-TOPO[®] is available for downloading from our Web site (www.invitrogen.com) or by contacting Technical Service (page 24).



Comments for pCR[®]2.1-TOPO[®] 3931 nucleotides

LacZ α fragment: bases 1-547
M13 reverse priming site: bases 205-221
Multiple cloning site: bases 234-357
T7 promoter/priming site: bases 364-383
M13 Forward (-20) priming site: bases 391-406
f1 origin: bases 548-985
Kanamycin resistance ORF: bases 1319-2113
Ampicillin resistance ORF: bases 2131-2991
pUC origin: bases 3136-3809

Figure 2.1: Vector map of the TOPO[®] TA Cloning[®] vector (Invitrogen, The Netherlands).

2.2.3.3 Small Scale Plasmid Purification

Plasmid purification was carried out using the Qiagen QIA prep Mini-prep kit according to the Qiagen Plasmid Purification manual. All buffers (P1, P2, N3 and PE) and columns were supplied with the kit. Details of the buffer components are outlined in the Qiagen Plasmid Purification manual. Isolated colonies were picked aseptically and used to inoculate LB broth (4 ml) (Section 2.1.7) containing 100 µg/ml ampicillin (Section 2.1.12). They were cultured overnight at 37 °C with shaking at 200 rpm. The cells were harvested by centrifugation at 2,500 g for 5 min at 4 °C. The supernatants were discarded and the pellets were resuspended in ice cold Buffer P1 (250 µl) and transferred to sterile 1.5 ml microcentrifuge tubes. Buffer P2 (250 µl) and Buffer N3 (350 µl) were added and the tubes were inverted 5 times before centrifugation at 13,000 g for 10 min. The supernatants were transferred to the Qiaprep Spin Columns and centrifuged at 13,000 g for 1 min. The flow through was discarded and the columns were washed with Buffer PE (750 µl) and centrifuged at 13,000 g for 1 min. The flow through was again discarded and the columns were centrifuged again at 13,000 g for 1 min to remove residual buffer. The Qiaprep Spin columns were placed in sterile 1.5 ml microcentrifuge tubes. The DNA was eluted from the columns by the addition of sterile water (30 µl) followed by centrifugation at 13,000 g for 1 min. The purified plasmid was subsequently analysed by DNA Gel Electrophoresis (Section 2.2.2.5) and was stored at -20 °C until required for use.

2.2.3.4 DNA Sequencing

DNA Sequencing of plasmids was performed by LGC Genomics (Middlesex, UK) on a commercial basis.

2.2.4 RNA Analysis

2.2.4.1 RNA Isolation

A. fumigatus liquid cultures, which were inoculated at 37 °C at the required time, were filtered through autoclaved miracloth, washed with sterile water and the mycelia collected. The mycelial mat was rapid frozen in liquid Nitrogen and ground to a fine powder in a cold mortar and pestle. The RNA was isolated using the RNeasy Kit supplied by Qiagen, according to the manufacturer's instructions. β -mercaptoethanol (10 μ l) was added to Buffer RLC (1 ml) before RNA extraction. For each sample, mycelia (100 mg) were placed in sterile microcentrifuge tubes. Buffer RLC (450 μ l) was added to each sample which were then vortexed vigorously. The lysates were transferred to QIAshredder spin columns. The columns were centrifuged at 13,000 g for 2 min. The flow through was transferred to new microcentrifuge tubes, avoiding the cell debris pellet. Ethanol (100 %, 0.5 volume of the lysate) was added to the lysates and mixed immediately. Samples were then transferred to RNeasy spin columns, which were placed in 2 ml collection tubes. Columns were centrifuged at 10,000 g for 15 s. The flow through was discarded. Buffer RW1 (700 μ l) was added to the columns and then centrifuged at 10,000 g for 15 s. The flow through was discarded. Buffer RPE (500 μ l) was added to the columns and centrifuged at 10,000 g for 15 s. The flow through was discarded.

Buffer RPE (500 μ l) was added to the columns and centrifuged at 10,000 g for 2 min. The spin columns were removed and placed in new collection tubes and centrifuged for 2 min at 13,000 g, to remove residual buffer. The spin columns were placed in sterile 1.5 ml microcentrifuge tubes. RNase-free water (50 μ l) was added to the columns and the RNA was eluted by centrifuging at 10,000 g for 1 min. The RNA samples were stored at -70 °C until required.

2.2.4.2 RNA Gel Electrophoresis

1.2 % (w/v) agarose gels were prepared by adding agarose (1.2 g) to double-autoclaved water (80 ml). The agarose was melted and allowed to cool to 65 °C before 10 X Formaldehyde Agarose (FA) gel buffer (10 ml) (Section 2.1.15.3) was added in a fumehood. The final volume was adjusted to 100 ml using double-autoclaved water. The gel was poured into the casting unit and allowed to set. The gel was removed from the casting unit and placed in an electrophoresis rig, where it was completely submerged in 1 X FA running buffer (Section 2.1.15.4). The RNA samples were prepared as follows; RNA at desired concentration (4 μ l), 10 X FA Buffer (Section 2.1.15.3) (2.5 μ l), formaldehyde (37 %; 4 μ l), formamide (12 μ l) and ethidium bromide (1 mg/ml; 1 μ l). The prepared samples were heated to 65 °C for 15 min and allowed to cool before loading onto the gel and electrophoresis at 100 V for 60 min. The gel was visualised using an Alpha DigiDoc™ RT unit or a Syngene G:Box.

2.2.4.3 DNase Treatment of RNA

A DNase kit (Sigma) was used to DNase treat RNA samples. RNA samples (Section 2.2.4.1) (500 ng) were adjusted to a final volume of 8 μ l in Molecular Grade H₂O. 10 X Reaction Buffer (1 μ l) and DNase (1 μ l) were added to the RNA samples and the mixture was left to incubate at room temperature for 15 min. Stop Solution (1 μ l) was added to the reaction and they were then incubated at 70 °C for 10 min. The samples were chilled on ice and stored at – 70 °C if not for immediate use.

2.2.4.4 cDNA Synthesis

cDNA synthesis was performed using the Transcriptor First Strand cDNA Synthesis Kit (Roche Applied Science) using the supplied reagents in the kit and following the manufacturer's instructions. Anchored-oligo (dT)₁₈ Primer (1 μ l) was added to the DNase treated RNA (Section 2.2.4.3) and incubated at 65 °C for 10 min before cooling to 4 °C. A master-mix containing the remaining components needed was prepared according to Table 2.4. 8.6 μ l of the master-mix was added to each sample. The samples were heated to 55 °C for 30 min, increased to 85 °C for 5 min before cooling to 4 °C for up to 2 h.

Table 2.6: Table of the components making up the master-mix

Kit Component				1 reaction	10 reactions
Transcriptor	High	Fidelity	Reverse	4 μ l	40 μ l
Transcriptase Reaction Buffer, 5X					
Protector RNase Inhibitor				0.5 μ l	5 μ l
Deoxynucleotide Mix				2 μ l	20 μ l
DTT				1 μ l	10 μ l
Transcriptor	High	Fidelity	Reverse	1.1 μ l	11 μ l
Transcriptase					

2.2.4.5 Semi-quantitative RT-PCR

PCR was carried out on the cDNA samples (Section 2.2.4.4) as described in Section 2.2.2.3 using the primers 5' *elfA* RT-PCR and 3' *elfA* RT-PCR (Table 2.3). The *A. fumigatus calmodulin (calm)* gene (AFUA_4G10050) was used as a housekeeping gene (Burns *et al.*, 2005). The primers calmF and calmR (Table 2.3) span an intronic region in *calm*, resulting in an amplicon size of 617 bp from gDNA and an amplicon size of 314 bp from cDNA. This allows the detection of any contaminating gDNA in the cDNA samples. The RT-PCR amplicons were resolved on a 2 % (w/v) Agarose Gel (Section 2.2.2.5) and visualised using an Alpha DigiDoc™ RT unit or a Syngene G:Box.

2.2.5 Restriction Enzyme Digests

Restriction enzymes and 10 X reaction buffers were obtained from Fermentas (York, UK), Promega (Southampton, UK) and New England Biolabs (Ipswich, UK). Reactions were carried out according to the manufacturer's instructions, but a typical reaction was performed as follows:

DNA 1 µg

Enzyme 1 µl

10 X Buffer 1 µl

Sterile Water to final volume of 10 µl.

The total reaction volume was always > 10 X the volume of enzyme used in order to prevent high glycerol concentration, which could cause non-specific digestion (star activity). Reactions were typically carried out at 37 °C for 3 h, although some enzymes required different incubation temperatures, as per the manufacturer's instructions. Digestion reactions were visualised by DNA gel electrophoresis (Section 2.2.2.5) and if necessary gel purified using the Qiagen gel extraction kit (Section 2.2.2.6).

2.2.6 De-phosphorylation of blunt-end restriction digests

In order to prevent the re-annealing of a restriction digest resulting in blunt-ends, Calf Intestine Alkaline Phosphatase (CIAP) was used to de-phosphorylate the 5' ends in the following reaction:

DNA	1 pmol
10 X Alkaline phosphatase buffer	4 µl
CIAP	0.5 µl
Molecular grade H ₂ O	to final volume 40 µl

The reaction was incubated at 37 °C for 15 min and then at 56 °C for 15 min. A further 0.5 µl CIAP was added to the reaction and it was again incubated at 37 °C for 15 min and then at 56 °C for 15 min. The DNA was gel purified using the Qiagen gel extraction kit (Section 2.2.2.6) after being resolved on a 0.7 % agarose gel (Section 2.2.2.5).

2.2.7 Filling in overhangs from restriction digests

The 5' overhangs generated by a restriction digest were filled in using the DNA Polymerase I, Large (Klenow) Fragment to allow for the ligation of the DNA fragments to another DNA fragment with blunt-ends. The following reaction was used;

Digested DNA	1-4 μg in 20 μl
Klenow 10 X Buffer	4 μl
Klenow	4 μl
10 mM dNTPs	2 μl
Molecular grade water	10 μl

The reaction was incubated at 22 °C for 10 min before incubating at 75 °C for 10 min to stop the reaction. The DNA was gel purified using the Qiagen gel extraction kit (Section 2.2.2.6) after being resolved on a 0.7 % agarose gel (Section 2.2.2.5).

2.2.8 Ligation of DNA fragments

The ligation of DNA fragments was required for the generation of the *elfA* knockout constructs and the construct for complementation. DNA was digested (Section 2.2.5) to give compatible fragments. These fragments were separated by DNA electrophoresis (Section 2.2.2.5) and extracted from the gel (Section 2.2.2.6). The ligations were carried out using the Ligafast™ Rapid DNA Ligation System (Promega), which contains T4 DNA ligase, according to the manufacturer's

instructions. The molecular ratio for cohesive end ligation was usually 1:3 insert to backbone. For blunt ended ligation, the molecular ratio was usually 1:1 insert to backbone. The following formula is used to calculate the ligation reaction:

$$\frac{\text{ng Vector} \times \text{kb Insert} \times \text{Molar ratio Insert}}{\text{kb Vector} \times \text{Vector}} = \text{ng Insert}$$

A typical reaction consisted of the following:

Vector	100 ng
Insert	as per equation calculation
2X Fast Ligase Buffer	12.5 μ l
Fast Ligase	1 μ l
Sterile Water	to a final volume of 25 μ l

The reaction was incubated at 22 °C for 2 h.

2.2.9 Generation of *A. fumigatus elfA* deletion and complementation strains

2.2.9.1 Deletion of *elfA* in *A. fumigatus*

The strategy employed to generate the *elfA* deletion strain ($\Delta elfA$) in this study was the bipartite gene disruption strategy (Nielsen *et al.*, 2006), outlined in Figure 2.2. This strategy required the use of two constructs, each containing a partial fragment of a selection marker ligated to the 5' and 3' flanking regions of the gene of interest (GOI). When transformed into *A. fumigatus* protoplasts, homologous recombination of the overlapping fragments unifies the selection marker. Two

further homologous recombination events occur between the flanking regions of the GOI and the constructs. This results in the deletion of the GOI and its replacement with the selection marker. A single homologous integration of the selection marker is confirmed by Southern Blot Analysis.

The selection marker used in the deletion of *elfA* was the pyrithiamine resistance gene (*ptrA*) from *A. oryzae* (Kubodera *et al.*, 2002; Kubodera *et al.*, 2000). *ptrA* was present on the pSK275 plasmid (a kind gift from Prof. Sven Krappmann) and was released from the plasmid using appropriate restriction enzymes before its ligation to the GOI flanking regions. Pyrithiamine is lethal to *A. fumigatus*, however on the introduction of *ptrA*, this lethality is overcome.

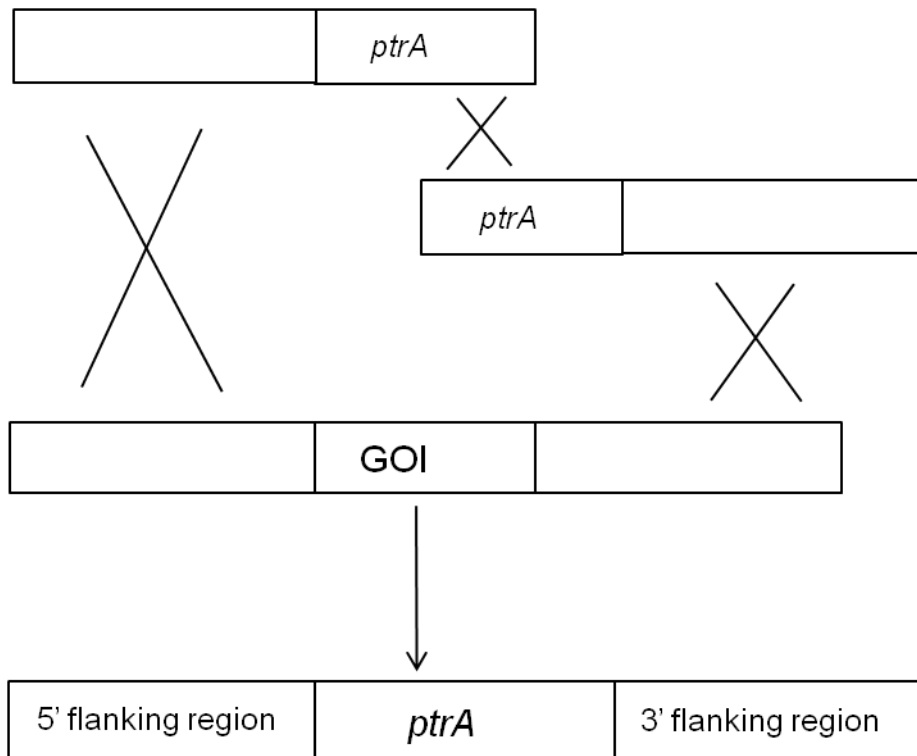


Figure 2.2: Schematic outlining the bipartite strategy for gene disruption. The 5' and 3' flanking regions of the gene of interest (GOI) are ligated to overlapping fragments of a selection marker (*ptrA*). Homologous recombination unifies *ptrA*, while homologous recombination between the flanking regions replaces the GOI with *ptrA*.

2.2.9.1.1 Generation of *A. fumigatus elfA* deletion constructs

The primers used in the PCR reactions are listed in Table 2.3. The strategy used for generation of the constructs for *elfA* deletion is outlined in Figure 2.3. The PCR reactions 1 and 2 amplified the flanking regions, approx. 1 – 1.5 kb in size, of *elfA*, while incorporating the restriction sites; *Pst*I and *Ase*I (Section 2.2.2.3). The *ptrA* gene was released from pSK275 by digesting with the restriction enzymes, *Pst*I and *Ase*I (Section 2.2.5). The amplified flanking regions were also digested with their respective enzyme, *Pst*I for the 5' flanking region, and *Ase*I for the 3' flanking region. The digestion of the flanking regions and the release of *ptrA* with the same restriction enzymes resulted in compatible ends allowing for the ligation of the flanking regions with *ptrA* (Section 2.2.8). PCR reactions 3 and 4 amplified the ligations, resulting in the final constructs; the 5' flanking region ligated to a partial region of *ptrA* and the 3' flanking region ligated to a partial region of *ptrA*.

All PCR reactions were carried out using Expand Long Range Template PCR System (Roche) (Section 2.2.2.3). All PCR reactions were resolved on 0.7 % (w/v) agarose gels (Section 2.2.2.5) from which they were extracted and purified using the Qiagen gel extraction Kit (Section 2.2.2.6)

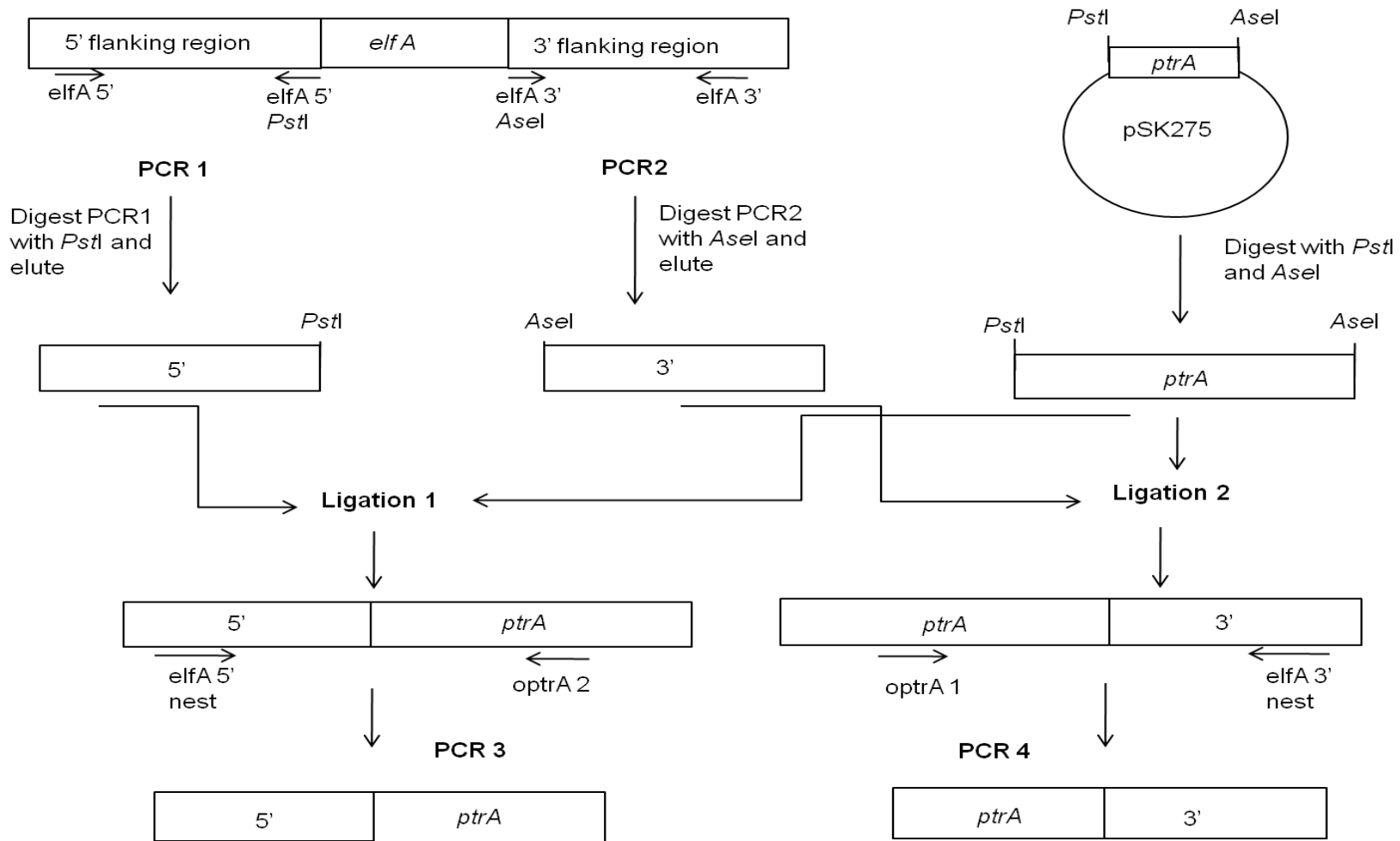


Figure 2.3: Schematic outlining the generation of the constructs for *elfA* deletion. The flanking regions of *elfA* were amplified to include specific restriction sites. *ptrA* was released from pSK275 using the same enzymes and was ligated to the flanking regions respectively. The ligated products were amplified to give the final constructs.

2.2.9.2 Complementation of *A. fumigatus* $\Delta elfA$

The deleted gene is re-inserted into the deletion strain to generate the complementation strain. A construct is generated by cloning the deleted gene and its flanking regions into the TOPO vector. If it is possible, the selection marker to be used is also inserted into the plasmid to give a single construct. In order for this to be achievable there must be at least two single restriction sites available on the plasmid. One of the restriction sites is used to linearise the plasmid to allow for the ligation of the selection marker. The second restriction site is used to linearise the plasmid before it is used to transform the deletion strain. If it is not possible to incorporate the selection marker into the plasmid, it is co-transformed along with the linearised plasmid where it inserts randomly. Transformation occurs with a single homologous recombination point.

The selection marker used to complement $\Delta elfA$ is the hygromycin resistance gene (*hph*). Hygromycin is also lethal to *A. fumigatus*, however with the insertion of *hph*, growth in the presence of hygromycin is possible. In this study it was possible to generate a complementation construct that contained both *elfA* and *hph*, allowing for the targeted insertion of *hph* with *elfA*.

2.2.9.2.1 Generation of the complementation construct

The primers used in the PCR reactions are listed in Table 2.3. The generation of the complementation construct is outlined in Figure 2.4. *elfA* and its flanking regions were amplified by PCR (Section 2.2.2.3), cloned into the TOPO vector (Section 2.2.3.1) and its orientation was determined, resulting in the *pelfA* plasmid. The *hph* gene was released from Pan 7.1 by digesting with *AvrII* and *XbaI*. The *pelfA* plasmid was digested with *EcoICR*, which had a single location in *pelfA*, allowing for the linearisation of *pelfA*. *EcoICR* digestion results in blunt ends, while *AvrII* and *XbaI* digestion result in overhangs. After digestion with *EcoICR*, *pelfA* was dephosphorylated with CIAP to prevent re-annealing (Section 2.2.6). The overhangs produced by digesting with *AvrII* and *XbaI* were filled in using DNA Pol I Klenow to give blunt ends (Section 2.2.7). *hph* was ligated to *pelfA* (Section 2.2.8) and cloned into the TOPO® vector, resulting in the plasmid *pelfA-hph*. *pelfA-hph* was linearised using the restriction enzyme *NruI*, which had a single location in the 3' flanking region of *elfA*, before transformation into $\Delta elfA$ protoplasts (Figure 2.5). Integration of the complementation construct was determined by Southern blot analysis.

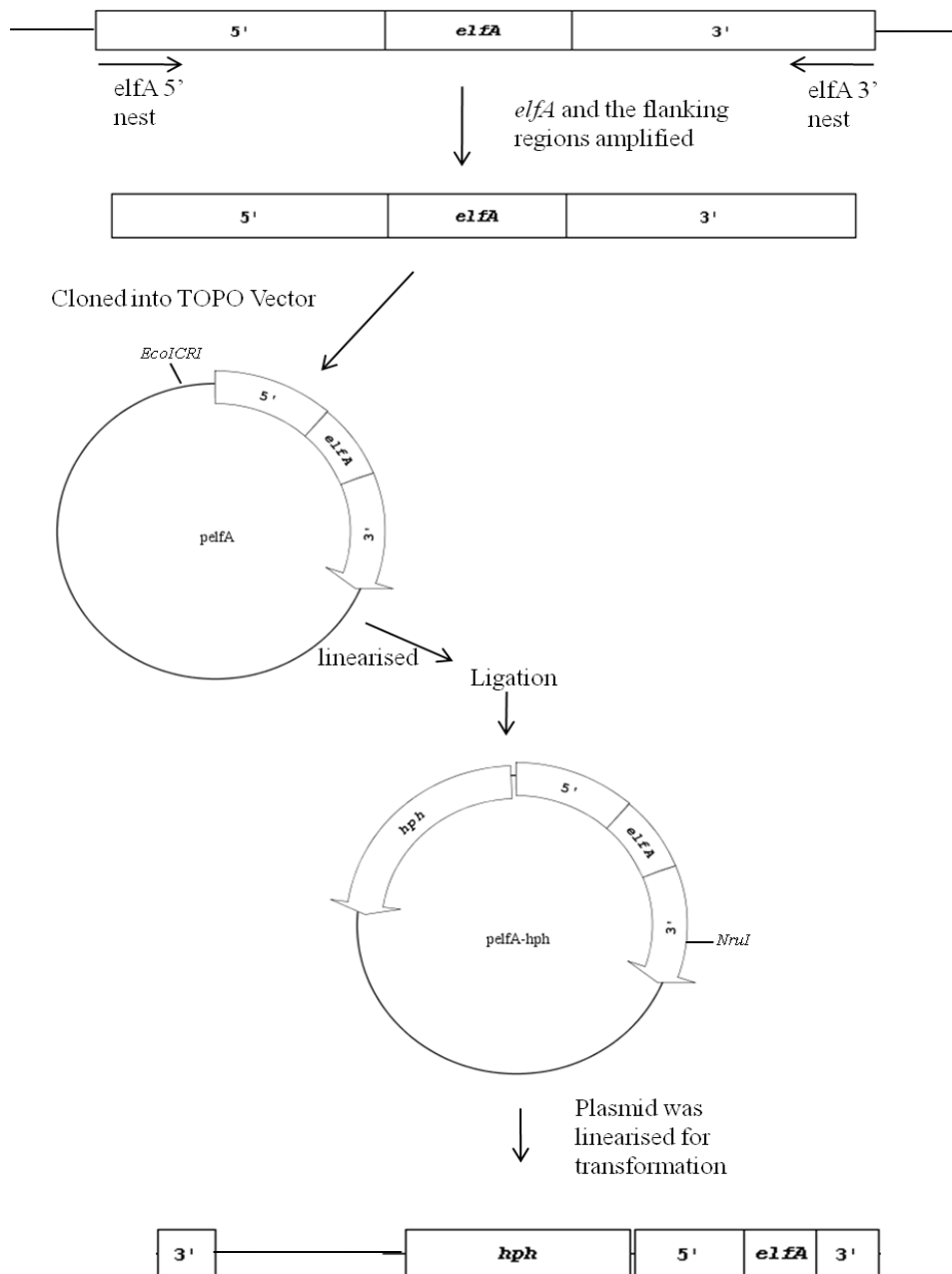


Figure 2.4: *elfA* and the 5' and 3' flanking regions were amplified and cloned into TOPO vector resulting in the plasmid; *pelfA*. *pelfA* was linearised and *hph*, which was released from Pan 7.1 by restriction digests, was ligated resulting in the plasmid; *pelfA-hph*. *pelfA-hph* was linearised before being used in transformation.

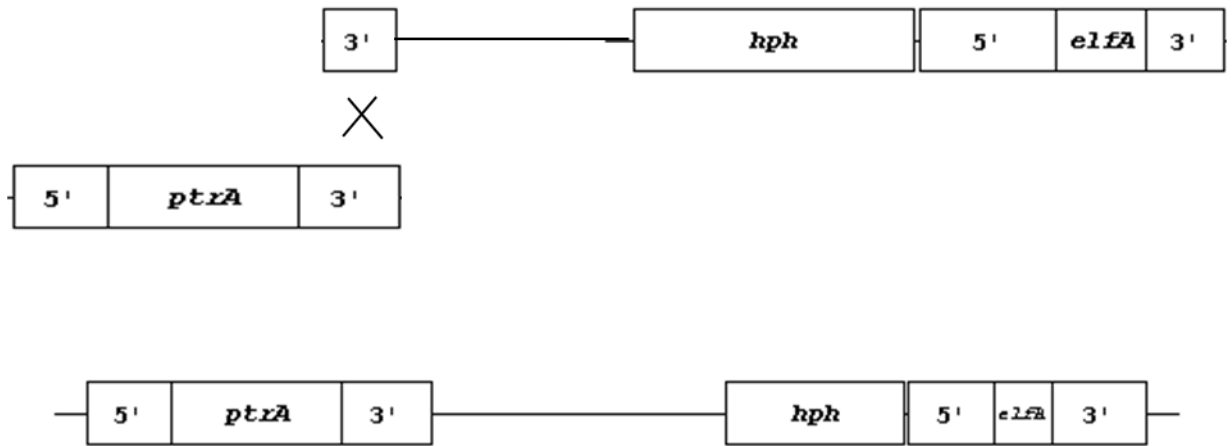


Figure 2.5: Schematic outlining the complementation of *A. fumigatus* $\Delta elfA$. A single homologous recombination between the 3' flanking region should result in the insertion of the construct into the 3' flanking region of $\Delta elfA$, directly after the selection marker used to generate *A. fumigatus* $\Delta elfA$.

2.2.9.3 *A. fumigatus* protoplast production and transformation

2.2.9.3.1 *A. fumigatus* protoplast production

AMM cultures (200 ml), inoculated with *A. fumigatus* were incubated overnight at 37 °C with shaking at 200 rpm. The mycelia were filtered through sterile miracloth and washed with sterile water. Excess liquid was removed from the mycelia by briefly drying them between sheets of sterile tissue. Mycelia (1.5 g) were weighed into a 50 ml sterile universal, in duplicate. Lysis Buffer containing Lytic enzymes (15 ml) (Section 2.1.16.5) was added to each tube and the mycelia were lysed by incubating them, horizontally, at 30 °C with shaking at 100 rpm. After incubating for 30 min, the tubes were removed from the incubator. A 1000 µl pipette tip, with a 200 µl pipette tip on top, were used to remove any mycelia clumps by pipetting continuously, up and down, for 10 min. The tubes were returned, horizontally, to the incubator at 30 °C with shaking at 100 rpm for a further 2.5 h. The samples were placed on ice for 5 min to terminate lysing enzyme action. The samples were centrifuged at 900 g for 18 min with no brake and the supernatants were filtered through sterile miracloth into sterile 50 ml universals. 0.7 M KCl (Section 2.1.16.1) was added to bring the final volume to 40 ml. The samples were centrifuged at 3,300 g for 12 min with no brake. The supernatant was discarded and 0.7 M KCl (10 ml) (Section 2.1.16.1) was used to resuspend the pellets. The samples were centrifuged again at 3,300 g for 12 min with no brake. The supernatant was again discarded and the tubes were placed upside-down on sterile tissue for 1 min. Buffer L6 (70 µl) (Section 2.1.16.6) was used to resuspend the pellets with gentle pipetting. The samples were centrifuged at 600 g with no brake for 1 min to gather

everything to the bottom of the tube. The duplicate samples were combined and stored on ice for no longer than 30 min before use. Protoplasts (5 µl) were checked for integrity under a light microscope.

2.2.9.3.2 *A. fumigatus* protoplast transformation with gene deletion constructs

For each transformation, 0.3 – 0.7 µg of gene construct DNA was used. The appropriate volume of DNA was added to a 50 ml sterile universal, and the final volume was adjusted to 50 µl with Buffer L6 (Section 2.1.16.6). Protoplasts (150 µl) (Section 2.2.9.3.1) were added to the DNA, which was gently shaken to mix them. A negative control was prepared by adding protoplasts (15 µl) (Section 2.2.9.3.1) to Buffer L6 (185 µl) (Section 2.1.16.6) in a sterile 50 ml universal. Buffer L7 (50 µl) (Section 2.1.16.7) was added to both tubes, gently shaken to mix, and incubated on ice for 20 min. Buffer L7 (1 ml) (Section 2.1.16.7) was added to each tube and they were incubated at room temperature for 5 min. Buffer L6 (5 ml) (Section 2.1.16.6) was added to each tube. The transformed protoplasts were then ready to be plated.

2.2.9.3.3 Plating transformed protoplasts on appropriate selection media.

The *Aspergillus* regeneration agar 1.8 % (Section 2.1.1.5.1) and *Aspergillus* regeneration agar 0.7 % (Section 2.1.1.5.2) were prepared freshly at the time transformation was undertaken. 2 x 25 ml plates of regeneration media 1.8 % were poured as positive control plates. To the remaining regeneration media 1.8 %, pyrithiamine or hygromycin at the appropriate concentration (Table 2.2) was added before pouring the remaining six plates, one negative control and 5 selection plates.

The negative control was prepared by adding 1.25 ml of the negative control protoplasts (Section 2.2.9.3.2) to a sterile 50 ml universal. This was adjusted to a final volume of 6 ml with regeneration media 0.7 % (Section 2.1.1.5.2) and poured onto the prepared negative control plate. The positive control plates were prepared by adding 12.5 μ l and 1.25 μ l of transformed protoplasts (Section 2.2.9.3.2) respectively to two 50 ml sterile universals. The final volume in these two tubes was adjusted to 6 ml with regeneration media 0.7 % (Section 2.1.1.5.2) and they were poured onto the 2 prepared positive control plates. The remaining transformed protoplasts (Section 2.2.9.3.2) were adjusted to a final volume of 30 ml with regeneration media 0.7 % (Section 2.1.1.5.2). 6 ml was poured on to each of the prepared selection plates. The plates were left upright at room temperature overnight. The following day, the selection plates and the negative control plates were overlaid with 6 ml of regeneration media 0.7 % (Section 2.1.1.5.2) containing either pyrithiamine or hygromycin at the appropriate concentration (Table 2.2). The plates were incubated at 37 °C for 5 – 7 days until colonies became visible. Colonies visible on the positive control plates after 2 – 3 days indicated that the protoplasts were viable and capable of regeneration.

2.2.9.3.4 Isolation of *A. fumigatus* transformed colonies

Colonies growing on the selection plates were deemed potential *A. fumigatus* transformants as they had resistance to either pyrithiamine or hygromycin. Spores from these colonies were sub-cultured, aseptically using a sterile P1000 pipette tip, onto fresh selective agar plates and incubated at 37 °C for 2-3 days. This was to verify resistance to the selection drug. Agar plugs from these colonies were taken,

aseptically, and transferred to sterile 1.5 ml microcentrifuge tubes. PBST 0.1% (750 µl) (Section 2.1.5) was added to each plug which were vortexed to dislodge the conidia into the PBST 0.1%. Sabourard Dextrose broth (20 ml) (Section 2.1.1.1) was inoculated with 500 µl of the conidia suspension from the plugs and incubated for 16 h at 37 °C with shaking at 200 rpm. These cultures were used to isolate genomic DNA (Section 2.2.2.1) to analyse by Southern Blotting (Section 2.2.10).

2.2.9.3.5 Single-spore isolation of *A. fumigatus* transformants

Colonies that demonstrated the desired insertion, as observed by Southern Blotting (Section 2.2.10), were single-spored in order to gain colonies of nuclear homogeneity. The conidial suspensions (Section 2.2.9.3.4) were diluted in PBST 0.1 % (Section 2.1.5), 10,000 fold. 50 µl of these dilutions was plated onto individual selection plates. The plates were incubated at 37 °C until individual colonies appeared. Agar plugs of these colonies were taken, as described earlier in Section 2.2.9.3.4. They were confirmed by Southern Blot analysis (Section 2.2.10)

2.2.10 Southern Blot Analysis

2.2.10.1 Transfer of Nucleic Acid

Southern Blot Analysis was carried out in order to confirm the deletion or replacement of a gene at a specific loci in *A. fumigatus* genomic DNA (gDNA). The gDNA was isolated from the transformants and wild-type strains (ATCC46645 and \DeltaakuB) (Section 2.2.2.1), and was digested with a relevant restriction enzyme as described earlier (Section 2.2.5). The restriction enzyme was chosen as one which

would cut the wild-type gDNA and mutants differentially resulting in different sized fragments (Figure 2.6 and Figure 2.7). The digested gDNA was subjected to electrophoresis on 0.7 % agarose gels (Section 2.2.2.5). Once the gDNA was resolved, the agarose gel was placed in a UV cross-linking machine and pulsed with 800 μ J to create nicks in the DNA, aiding its transfer onto the nylon membrane. A Southern tower was set up by pouring Southern Transfer Buffer (Section 2.1.17.1) into a large tank. Two sheets of Whatman filter paper (30 cm x 10 cm) were placed along the top of the tank, with both ends dipped into the Southern transfer buffer. The agarose gel was placed on top of the Whatman filter paper, load side facing down. A piece of H⁺ Nylon Membrane (Amersham), measuring the same size as the agarose gel, was placed on top of the agarose gel in one single movement. Three pieces of Whatman filter paper, measuring the same size as the agarose gel, were placed on top of the membrane, taking care not to move the membrane. Three packets of pocket-sized tissues were removed from their packaging and placed on top of the Whatman filter paper. This facilitated the absorbance of the Southern Transfer Buffer as it moved up through the layers of the Southern Tower. A glass plate was placed on top of this with a weight, weighing 400-500 g, on top on the glass plate. Southern Blotting was carried out overnight at room temperature.

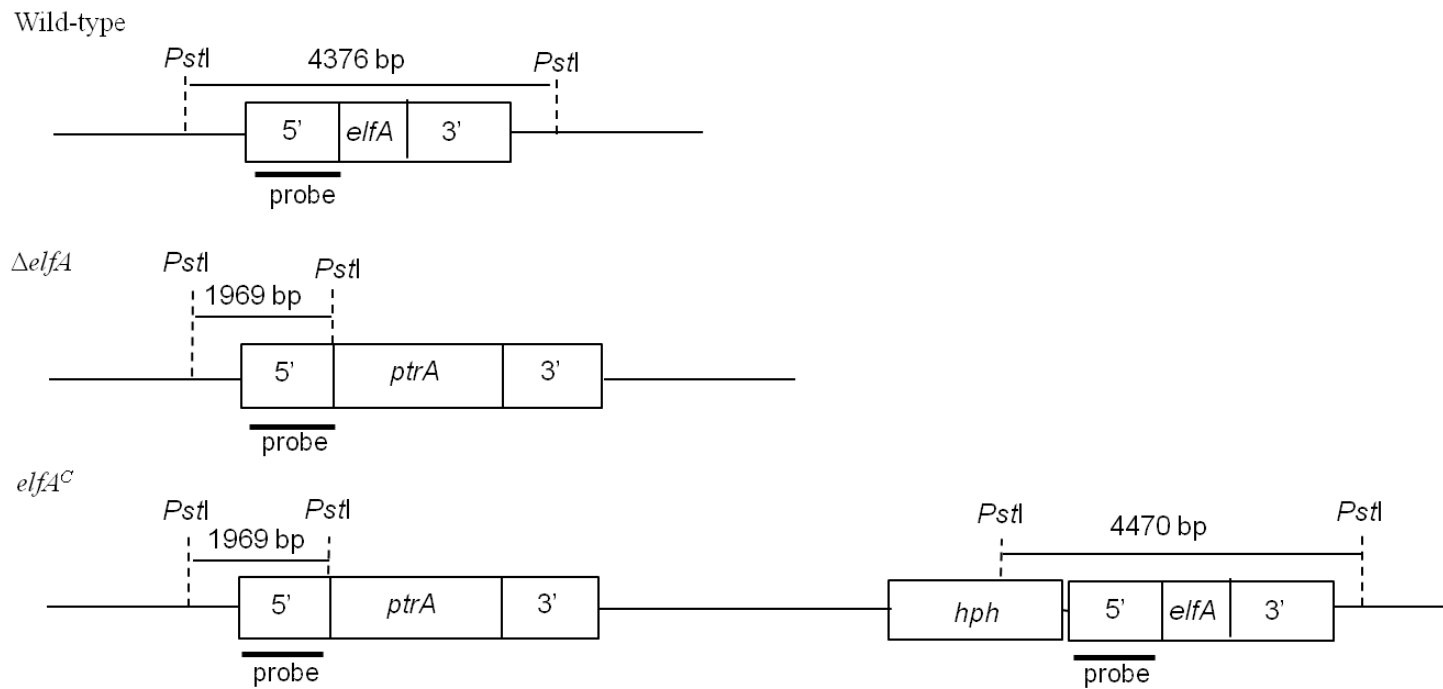


Figure 2.6: Schematic showing the probing strategy for Southern Blot analysis. *A. fumigatus* wild-type, $\Delta elfA$ and $elfA^C$ genomic DNA was digested with *Pst*I. When probed with a DIG-labelled probe for the 5' flanking region, *A. fumigatus* wild-type should have a fragment 4376 bp in size, *A. fumigatus* $\Delta elfA$ had a fragment size of 1969 bp, while *A. fumigatus* $elfA^C$ should contain two fragments; 1969 bp and 4470 bp in size. The probe was 1086 bp in size and its binding site is indicated by the black line.

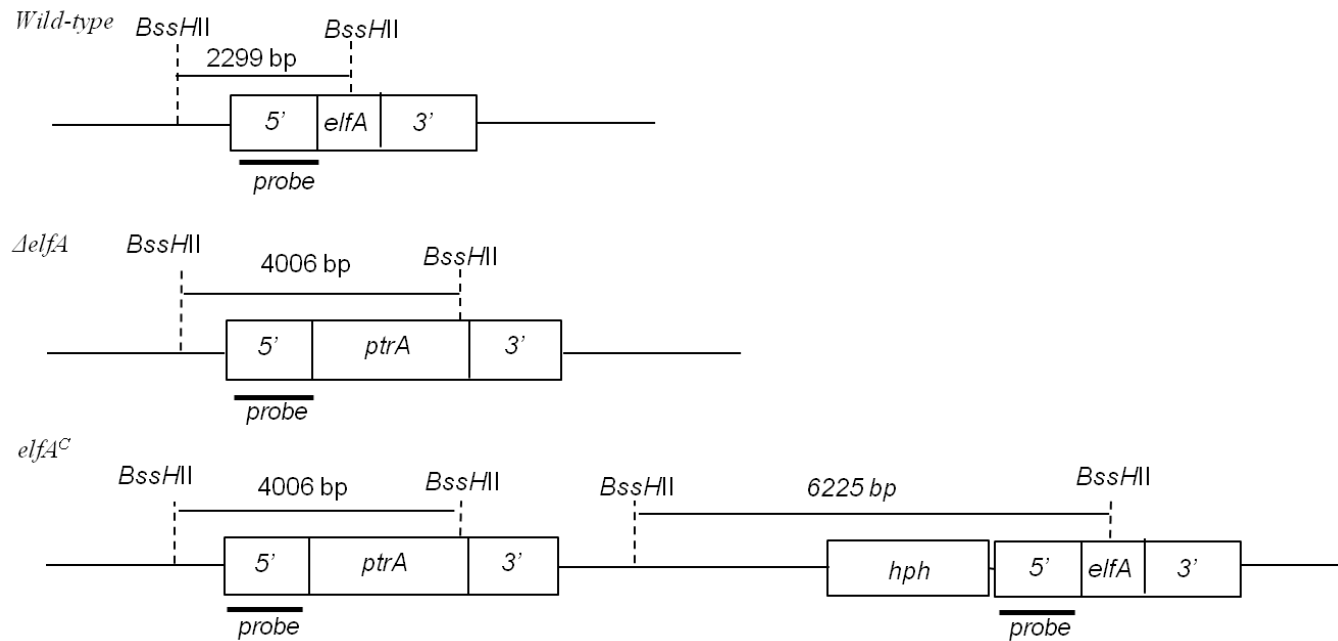


Figure 2.7: Schematic showing the probing strategy for Southern Blot analysis. *A. fumigatus* wild-type, *A. fumigatus* $\Delta elfA$ and *A. fumigatus* $elfA^C$ genomic DNA was digested with *BssHII*. When probed with a DIG-labelled probe for the 5' flanking region, *A. fumigatus* wild-type should have a fragment 2299 bp in size, *A. fumigatus* $\Delta elfA$ a fragment size of 4006 bp, while *A. fumigatus* $elfA^C$ should contain two fragments; 4006 bp and 6225 bp in size. The probe was 1086 bp in size and its binding site is indicated by the black line.

2.2.10.2 Disassembly of the Southern Tower

The tissue paper and Whatman filter paper was removed from the tower. Before the membrane was removed from the agarose gel, the position of the individual wells was marked onto the membrane using a pencil. The membrane was then removed from the agarose gel and washed in 2 X SSC Buffer (Section 2.1.17.3) for 20 min with gentle rocking at room temperature. The membrane was placed into a UV cross-linking machine and pulsed with 1,200 μ J. This cross-linked the nucleic acids onto the membrane, preventing them from removal by subsequent treatment steps.

2.2.10.3 Digoxigenin (DIG) – Detection of hybridised Nucleic Acids

2.2.10.3.1 Generation of DIG- labelled probes

The DIG-labelled probes were generated by PCR (Section 2.2.2.3). The primers used were specific to a gene or flanking region of the gene of interest (Table 2.3). DIG-labelled dNTPs (Section 2.1.17.14) were used to label the PCR products. The PCR product was resolved in a 0.7 % Agarose gel (Section 2.2.2.5) before extraction using the QIA Quick Gel extraction Kit (Section 2.2.2.6). The concentration was determined using a Nanodrop spectrophotometer (NanoDrop 1000 Spectrophotometer, Mason Technology). The PCR product was heated to 90 °C for 5 min in a heating block in order to denature it and it was placed on ice immediately. 400 ng of the PCR product was added to Membrane Pre-hybridisation Buffer (5 ml) (Section 2.1.17.7) that was preheated to 65 °C. This probe was stored at – 20 °C. Before use, it was heated to 65 °C for 30 min in a water bath.

2.2.10.3.2 Pre-hybridisation of Nylon membrane

The Nylon membrane was placed in a Hybridisation tube that was pre-heated to 42 °C. 10 ml of the Membrane Pre-hybridisation Buffer (Section 2.1.17.7), pre-heated to 65 °C, was added to the hybridisation tube. The tube was placed in a Hybaid oven and rotated at 42 °C for 4 -5 h to block the membrane.

2.2.10.3.3 Hybridisation of Nylon membrane with DIG-labelled probe

The DIG-labelled probe was pre-heated to 65 °C in a water bath. The membrane pre-hybridisation buffer was poured off, and the DIG-labelled probe solution (Section 2.2.10.3.1) was added to the tube. Care was taken not to pour the probe directly onto the blot. The tube was returned to the Hybaid oven at 42 °C and was incubated overnight while rotating. This allowed the probe to hybridise to specific regions of interest on the nylon membrane.

2.2.10.3.4 DIG Detection

The probe was removed from the hybridisation tube and stored at – 20 °C for further use. The membrane was removed from the hybridisation tube and was washed in 1 X SSC/0.1 % (w/v) SDS Buffer (Section 2.1.17.8) at room temperature for 15 min with gentle rocking. This buffer was poured off and the wash step repeated. The membrane was returned to the hybridisation tube. 1 X SSC/0.1 % (w/v) SDS Buffer (30 ml) (Section 2.1.17.8), pre-heated to 65 °C, was added to the hybridisation tube, which was rotated at 65 °C for 15 min. The buffer was removed; the tube was drained up-side-down on tissue paper before this step was repeated.

Between each addition of buffer, the tube was drained on tissue paper throughout the entire DIG-Detection procedure. DIG Wash Buffer (10 ml) (Section 2.1.17.9) was added to the tube and rotated at 25 °C for 5 min. DIG Buffer 2 (10 ml) (Section 2.1.17.10) was added to the hybridisation tube, which was then rotated at 25 °C for 30 min. This buffer was discarded and the Anti-DIG Fab Fragments – alkaline phosphatase (10 ml) (Section 2.1.17.12) was added and it was rotated at 25 °C for 30 min. This was discarded and DIG Wash Buffer (10 ml) (Section 2.1.17.9) was added and it was rotated at 25 °C for 15 min. The buffer was discarded and this wash step repeated. DIG Buffer 3 (10 ml) (Section 2.1.17.11) was added to the hybridisation tube and it was rotated at 25 °C for 5 min. This was poured off and the CSPD substrate (Section 2.1.17.13) was added to the hybridisation tube. This was rotated at 25 °C for 5 min. The CSPD was poured off and stored in a tinfoil covered tube at 4 °C for re-use within 1 week. The Nylon membrane was wrapped in cling-film and incubated at 37 °C for 15 min, allowing the Anti-DIG Fab alkaline - phosphatase to process the CSPD and thus increasing the intensity of the emitted signal.

2.2.11 Developing Blots that used a chemiluminescent substrate

The blot to be developed was placed in a Kodak exposure cassette. For Western blots treated with ECL, the blot was placed between two acetate sheets. Southern Blots were left in the cling film they were wrapped in during DIG-detection (Section 2.2.10.3.4). The blots were exposed to Kodak film in the dark. Southern Blots were usually exposed for 1 – 3 hr, and Western Blots were usually exposed for 2 – 15 min. The film was removed from the cassette and developed in

Developer Solution (Section 2.1.18.1). They were rinsed in water before being fixed in Fixer Solution (Section 2.1.18.2).

2.2.12 Bradford Protein Assay

A stock solution of BSA (1 mg/ml) was prepared and diluted in PBS (Section 2.1.3) to give solutions of known concentrations. These protein solutions, along with a PBS blank control were used to generate a standard curve. The sample to be assayed was diluted appropriately in PBS. 20 μ l of the blank, protein solutions or sample to be assayed was added to a 980 μ l of the Bradford solution (Section 2.1.22) and mixed. Following 5 min incubation, absorbances were measured using a spectrophotometer at $A_{595\text{nm}}$ (Eppendorf Biophotometer). A graph of $A_{595\text{nm}}$ versus BSA concentration was plotted and the protein concentration of the samples calculated using the curve. All samples were prepared and analysed in duplicate.

2.2.13 Sodium Dodecyl Sulphate Polyacrylamide Gel Electrophoresis (SDS-PAGE)

SDS-PAGE gels, both stacking and separating, were prepared according to Table 2.5. The gels were cast using the Mini-Protean II gel casting apparatus (BioRad, CA, USA) according to the manufacturer's guidelines. Samples were prepared by adding 1 volume 5 X Solubilisation Buffer (Section 2.1.19.6) to 4 volumes of sample. Samples were boiled for 5 min, centrifuged briefly, before loading onto the gel with a Hamilton syringe. Electrophoresis for 1D separation was carried out initially at 70 V for 20 min, increasing to 120 V until the sample reached the bottom of the separating gel, using 1 X Electrode Running Buffer (Section

2.1.19.9). Following electrophoresis, gels were stained with either (i) Coomassie Staining Solution (Section 2.1.19.10) for at least 1 h with gentle rocking and subsequent destaining with Destaining Solution (Section 2.1.19.11) for 30 min or (ii) Colloidal Coomassie Blue Staining (Section 2.2.14).

Table 2.7: Table of reagents for SDS-PAGE

Reagent (ml)	Separating Gel 12 %		Stacking Gel 4 %
	For small gel	For large gel	For small gel
30 % (w/v)	2.26 ml	25.35 ml	0.325 ml
Acrylamide/bis			
Tris-HCl; pH 8.3	1.4 ml	15.75 ml	-
Tris-HCL; pH 6.8	-	-	0.625 ml
Deionised Water	1.86 ml	20.85 ml	1.525 ml
10 % (w/v) SDS	56 µl	0.605 ml	25 µl
10 % (w/v)	20 µl	0.225 ml	50 µl
Ammonium persulphate			
TEMED	4.6 µl	52.5 µl	5 µl

2.2.14 Colloidal Coomassie Blue Staining

The gels were fixed for 3 h – overnight in Fixing Solution (Section 2.1.19.12.1) with gentle rocking. This was poured off and the gels were washed 3 X 20 min in deionised water. The gels were then pre-incubated in Incubation buffer (Section 2.1.19.12.2) for 1 h before being stained in Staining Solution (Section 2.1.19.12.3) for 4 – 5 days. Gels were destained with deionised water.

2.2.15 Western Blot Analysis; Semi-Dry

Nitrocellulose paper (NCP), and 6 sheets of filter paper, of appropriate size, were pre-soaked in Towbin Transfer Buffer (Section 2.1.20.1) for 15 min. The SDS-PAGE gels were removed carefully from the electrophoresis unit. They were assembled on the transfer unit as follows; 3 sheets of soaked filter paper, soaked NCP, SDS-Page gel, and 3 sheets of soaked filter paper. Transfer occurred at 18 V for 30 min. The NCP was blocked in Western Blocking Buffer (Section 2.1.20.2) for 1 h at room temperature with gentle rocking. The Western blocking buffer was poured off and the primary antibody, diluted in Antibody Buffer (Section 2.1.20.3), was added to the blots for 1 h at room temperature with gentle rocking. The antibody was removed and the blots were washed 3 X 5 min with PBST 0.05 % (Section 2.1.4). The secondary antibody, diluted in Antibody buffer, was added to the blots for 1 h at room temperature with gentle rocking. The secondary antibody was removed and the blots were washed 3 X 5 min in PBST 0.05 %. The blots were developed with Supersignal West Pico enhanced chemiluminescent (ECL) substrate (Section 2.1.20.4) according to the manufacturer's guidelines (Pierce).

2.2.16 Protein Extraction from *A. fumigatus*

2.2.16.1 Whole Cell Protein Extraction for 2D Analysis of *A. fumigatus*

The mycelia were harvested through miracloth and washed with cold deionised water. The mycelia were dried in tissue and snap frozen in liquid N₂. The mycelia were ground into a fine powder using a pestle and mortar under liquid N₂. The ground mycelia (250 mg) was added to 10 % (w/v) TCA (1.5 ml) (Section 2.1.23.2) and incubated on ice for 30 min. The samples were sonicated with a sonication probe (Bandelin Sonopuls, Bandelin electronic, Berlin) for 10 s at 10 % power on cycle 6. This was carried out 3 times in total with cooling on ice between each step. The lysed samples were incubated on ice for a further 30 min before centrifugation at 12,000 g for 10 min at 4 °C. The supernatants were discarded. 60 µl of H₂O was added to the samples and vortexed. Ice-cold acetone (1 ml) was added to each sample and the pellets were resuspended as much as possible by pipetting and vortexing. The samples were stored at – 20 °C and were vortexed every 10 min for 1 h. They were then stored overnight at – 20 °C. The samples were centrifuged at 12,000 g for 10 min. The supernatants were discarded and ice-cold acetone (500 µl) was added to each sample. The samples were vortexed before being centrifuged at 12,000 g for 10 min at 4 °C. The supernatants were discarded and the pellets were left to air-dry for 5 min. IEF Buffer (Section 2.1.23.3) (500 µl) was added to the pellets which were resuspended as much as possible by pipetting and vortexing. The samples were incubated at room temperature for 1 h before centrifuging at 13,000 rpm for 3 min in a benchtop microfuge. The supernatants were removed to clean microcentrifuge tubes and aliquots were stored at – 20 °C until required for use.

2.2.16.2 Whole Cell Protein extraction from *A. fumigatus*; Small scale

A. fumigatus mycelia were harvested using miracloth, washed with cold deionised water, dried in tissue paper and snap-frozen in liquid N₂. The mycelia were then lyophilised until completely dry. Lyophilised mycelia (100 mg) were weighed into a 2 ml eppendorf and a tungsten bead added. Samples were bead beaten at 30 Hz for 5 min in a bead beater (MM300, Retsch®). Ice-cold Lysis Buffer (500 µl) (Section 2.1.21.1) was added to each sample and they were bead beaten again at 30 Hz for 5 min. A further 100 µl of ice-cold Lysis buffer was added to the samples which were incubated on ice for 1 h. Samples were centrifuged at 12,000 g for 15 min at 4 °C. The supernatants were removed to clean microcentrifuge tubes. The samples were sonicated in a sonication bath (Fisher Scientific) for 5 min before being centrifuged again at 12,000 g for 5 min at 4 °C. The supernatants were removed to clean microcentrifuge tubes. Aliquots were stored at -20 °C until required for use.

2.2.16.3 Whole cell protein extraction from *A. fumigatus*; Large scale

Lyophilised mycelia were weighed into a 50 ml universal and Lysis Buffer (Section 2.1.21.1) (10 ml per g) was added. This suspension was incubated on ice for 1 h. The suspension was then sonicated using a sonication probe at 10 % power with 6 cycles for 1 min. The suspension was cooled on ice before repeating until lysis was complete. The lysate was incubated on ice for 30 min before centrifuging at 12,000 g at 4 °C for 20 min (Sorvall). The supernatant was removed and filtered through a 0.45 µm sterile filter to remove any small particulates.

2.2.16.4 Whole Cell Protein Extraction from *A. fumigatus* germlings

The *A. fumigatus* germlings were checked under the microscope after 9 h of growth, to ensure the conidia were now in the germling phase. The germlings were harvested by filtering through Whatman filter paper and were washed with distilled water. The germlings were scraped into a 50 ml universal and centrifuged at 2,000 g for 5 min to remove any excess liquid. The supernatant was carefully removed. The germling pellets were weighed and resuspended in Lysis Buffer (1 ml per g) (Section 2.1.21.1). The suspension was aliquoted into 1 ml aliquots, in 2 ml eppendorfs containing 0.1 mm Glass beads (0.4 g) and was bead-beaten at 30 Hz for 5 min (MM300, Retsch®) before cooling on ice. The germlings were bead-beaten 3 times in total, with cooling on ice between each cycle. The lysates were centrifuged at 12,000 g for 10 min at 4 °C. The supernatants were removed to microcentrifuge tubes. Aliquots were stored at – 20 °C until required for use.

2.2.17 TCA/Acetone precipitation before 2D-PAGE

100 % TCA (Section 2.1.23.1) was added to the samples to give a final TCA concentration of 10 %. They were incubated on ice for 3 h before centrifuging at 12,000 g for 10 min at 4 °C. The supernatants were removed and the pellets were resuspended in ice-cold Acetone (1 ml). The samples were incubated at – 20 °C for 1 hr before being centrifuged at 12,000 g for 10 min at 4 °C. The supernatants were removed and the pellets were washed once more with ice-cold Acetone. After the supernatant was removed, the pellets were air-dried for 5 min. The pellets were resuspended in IEF Buffer (Section 2.1.23.3). To aid in the resolubilisation of the

pellets into IEF Buffer, the samples were sonicated in a sonication bath for 5 min. The samples were left at room temperature for 1 h. The samples were centrifuged at 12,000 g for 2 min and the supernatants were removed to microcentrifuge tubes.

2.2.18 Isoelectric Focussing (IEF) and 2D-PAGE

The protein samples were prepared to the appropriate concentration and volume for the IPG strip size according to Table 2.6. Bromophenol blue was added to the protein samples, which were then centrifuged at 12,000 g for 5 min. Protein samples were loaded into the positive end of the ceramic IPG strip holders. The IPG strip was added, gel-side down, using a forceps, while the holder was tilted slightly to evenly distribute the sample along the holder. Care was taken to prevent the trapping of air bubbles. The strips were overlaid with Plus One Drystrip Coverfluid (Amersham) (1 - 1.5 ml) and subjected to IEF on an IPGphor II IEF Unit using the following programme;

Step	50 V	12 h
Step	250 V	0.15 h
Gradient	5000V	2 h
Step	5000 V	5 h
Gradient	8000 V	2 h
Step	8000 V	1 h
Step	250 V	1 h

Following IEF, the IPG strips were equilibrated in Reduction Buffer (Section 2.1.23.5) for 20 min, followed by equilibration in Alkylation Buffer (Section 2.1.23.6) for 20 min. The IPG strips were rinsed in 1 X Electrode Running Buffer (Section 2.1.19.9) and placed on top of 12 % SDS-PAGE gels using a forceps. The gels were overlaid with Agarose Sealing Solution (Section 2.1.23.7). Once set, the gels were placed in the PROTEAN Plus Dodeca Cell (BIO-RAD) as per manufacturer's instructions. The gels were electrophoresed in 1 X Electrode Running Buffer (Section 2.1.19.9) overnight at 1.5 W per gel. In the morning, the voltage was increased to 5 W per gel until the dye-front was 2 cm from the end of the gels. The gels were stained with Colloidal Coomassie Blue (Section 2.2.14).

Table 2.8: Protein amounts and volumes for different length IPG Strips

Strip Length	Protein amount	Volume of IEF Buffer
7 cm	125 µg	125 µl
13 cm	300 µg	250 µl

2.2.19 In-Gel Digestion of Protein Spots from 2D-PAGE Gels

In-Gel digestion was carried out according to Shevchenko *et al.* (2007). The samples were excised from the gel and placed in 1.5 ml microcentrifuge tubes. The gel pieces were destained by adding 100 mM ammonium bicarbonate/acetonitrile (1:1 (v/v)) (Section 2.1.24.2) (100 μ l) for 1 h at room temperature with vortexing at intervals. This liquid was removed and 500 μ l of acetonitrile was added to shrink the gel pieces. The liquid was removed before addition of trypsin solution (Section 2.1.24.4) (50 μ l) to each gel piece. The samples were incubated at 4 °C for 30 min, checked to ensure the gel piece was covered with trypsin solution, before incubation for a further 2.5 h at 4 °C. If required, 10 mM ammonium bicarbonate was added to cover the gel pieces. The gel pieces were incubated overnight at 37 °C. The gel pieces were sonicated in a sonication bath for 10 min. They were then centrifuged at 12,000 g for 10 min and supernatants were removed to clean microcentrifuge tubes.

2.2.20 MALDI-ToF Mass Spectrometry

2.2.20.1 Matrix (a-cyano-4-hydroxycinnamic acid) (4-HCCA) Preparation

0.1 % (v/v) TFA (350 μ l) (Section 2.1.24.7) was added to 4-HCCA (5 mg) and vortexed for 30 s. Acetonitrile (350 μ l) was added to the solution which was vortexed for a further 30 s before being centrifuged for 1 min at 13,000 rpm in a benchtop centrifuge. The supernatant was retained as the matrix sample to which the internal calibrants Angiotensin fragment III and human hATCH 19-39 were added.

2.2.20.2 Target preparation and MS analysis

The Trypsin digested samples (Section 2.2.19) were diluted 1:1 with the matrix sample (Section 2.2.20.1) in microcentrifuge tubes. The matrixed peptide sample (0.4 μ l) was transferred to an individual position on the MALDI target slide and allowed to dry fully. The samples were prepared in duplicate, and each MALDI target slide contained one spot of external calibration mix (LaserBio Labs, Proteomix C104). All samples were subjected to delayed extraction reflectron MALDI-ToF analysis with a nitrogen laser (337 nm) at 20 kV using an Ettan MALDI-ToF Pro mass spectrometer (Amersham Biosciences). Spectra were calibrated, before mass (m/z) lists were interrogated against (i) the NCBI nr database available as part of the mass spectrometer Evaluation Software Version 2.01 or (ii) a local FASTA version of the annotated *A. fumigatus* genome available at <http://www.cadre-genomes.org.uk>. All promising hits were compared to the NCBI nr database using MASCOT (www.matrixscience.com). For all database searches, criteria were set as monoisotopic peptide tolerance \pm 50 ppm and 1 missed cleavage with variable modifications set as oxidation of methionine and carbamidomethylation.

2.2.21 Liquid Chromatography Mass Spectrometry (LC-MS)

2.2.21.1 Sample Preparation

After trypsin digestion (Section 2.2.19), the peptides were dried down in a speedy vac (DNA Speedy Vac Concentrator, Thermo Scientific). The peptides were resuspended in 0.1 % formic acid (Section 2.1.24.5) (20 μ l). The samples were filtered through 0.22 μ m Cellulose Spin-filters (Costar) before being transferred to polypropylene vials. Care was taken to ensure there was no air trapped in the vials.

2.2.21.2 Sample Analysis

LC-MS Analysis was carried out on a 6340 Ion-trap LC Mass Spectrometer using electrospray ionisation (Agilent Technologies). Samples (5 μ l) (Section 2.2.21.1) were loaded onto a Zorbax 300 SB C-18 Nano-HPLC Chip (150 mm x 75 μ m) with 0.1 % (v/v) formic acid (Section 2.1.24.5) at a flow rate of 4 μ l/min. Peptides were eluted over a 15 min gradient of 5 – 100 % (v/v) Acetonitrile/formic acid (Section 2.1.24.6) with a post run of 5 min, using a flow rate of 0.6 μ l/min. The eluted peptides were ionised and analysed by the mass spectrometer. MSⁿ analysis was carried out on the 3 most abundant peptide precursor ions in each sample, as selected automatically by the mass spectrometer. The peptides from the MSⁿ spectra were compared to the NCBI nr database using MASCOT (www.matrixscience.com) for identification of the proteins. For the database search, the criteria were set as a peptide tolerance \pm 2 Da and peptide charge 1+, 2+, 3+, with a MS/MS tolerance \pm 1 Da and 2 missed cleavages. A fixed modification of Carboxymethyl (C) and a variable modification of oxidation of methionine were also set.

2.2.22 Biotinylation of Glutathione disulfide (Biotin-GSSG)

This protocol was adapted from Brennan *et al.* (2005). GSSG (61.2 mg) was dissolved in water (1.8 ml). To this, Sulfo-NHS-LC-Biotin (114.4 mg) (Section 2.1.27.1) was added and dissolved. The pH was adjusted to pH 7.2 using 5 M NaOH (Section 2.1.2.2) and pH indicator strips. It was left to react at room temperature for 1 h. The final volume was adjusted to 2 ml using 1 M Tris-HCl (pH 7.2) (Section 2.1.27.2) in order to stop the reaction. The solution was aliquoted and stored at – 70 °C until required for use. Confirmation of the successful biotinylation of GSSG was obtained using Reverse Phase – High Performance Liquid Chromatography (Section 2.2.23) and MALDI-ToF (Section 2.2.20).

2.2.23 Reverse Phase – High Performance Liquid Chromatography Analysis

The Biotin-GSSG, and the two controls; GSSG treated with Tris-HCl (1 M) and Sulfo-NHS-LC-Biotin treated with Tris-HCl (1 M) (Section 2.2.22) were diluted in DMSO to give a final concentration of 5 nmol/μl. The samples (50 μl) were transferred into glass vials. The samples were analysed by RP – HPLC with UV detection (Agilent 1200 system), using a C18 RP – HPLC column (Agilent Zorbax Eclipse XDB-C18; 5 mm particle size; 4.6 x 15 min) at a flow rate of 1 ml/min. A mobile phase of water with 0.1 % TFA (Section 2.1.25.1) and acetonitrile with 0.1 % TFA (Section 2.1.25.2) was used. Samples (20 μl) were injected onto the column.

2.2.24 Investigating protein glutathionylation using Biotin-GSSG

2.2.24.1 Western blot analysis of protein glutathionylation

Biotin-GSSG (Section 2.2.22) was incubated with whole protein lysate, extracted under non-reducing conditions, (Section 2.2.16.2) in a 1/10 ratio for 10 min at room temperature. Non-reducing 4 X Solubilisation Buffer (Section 2.1.19.7) was added to each sample and they were boiled for 5 min. The samples were separated by SDS-PAGE (Section 2.2.13), again under non-reducing conditions, and Western Blot was carried out as described in Section 2.2.15. Streptavidin-HRP and ECL (Section 2.1.20.4) were used to develop the blot.

2.2.25 Intracellular Glutathione Measurement

Intracellular glutathione was measured using a method adapted from the literature (Thön *et al.*, 2010; Rahman *et al.*, 2006). Total glutathione (glutathione (GSH) and glutathione disulfide (GSSG)) and GSSG only were measured independently, allowing for the calculation of GSH only.

Note: Care was taken throughout all steps in this procedure to avoid exposing the samples to light. All tubes were covered in tinfoil and a lid was kept on the ice box.

2.2.25.1 Sample Preparation

Mycelia from 24 h cultures in AMM were harvested through miracloth and dried on tissue paper, removing as much excess liquid as possible. Mycelia (500 mg) were weighed into a 2 ml Eppendorf tube and 5 % (w/v) SSA (Section 2.1.26.4) (500

µl) was added along with a tungsten bead. The samples were bead-beaten at 30 Hz for 5 min followed by centrifugation at 12,000 g for 10 min at 4 °C. The supernatants were removed to clean microcentrifuge tubes covered in tinfoil and neutralised using triethanolamine (Section 2.1.26.5). The samples were diluted (1/10 – 1/30) in GSH/GSSG Assay Buffer (Section 2.1.26.3) before centrifugation at 12,000 g for 10 min at 4 °C. The supernatants were removed to clean microcentrifuge tubes. Samples were stored at – 70 °C if not assayed immediately.

2.2.25.2 GSH Standard Preparation

GSH (1 mg/ml) (Section 2.1.26.11) was diluted 1/100 in GSH/GSSG Assay Buffer (Section 2.1.26.3) to give a stock of concentration 10 µg/ml. A 26.4 nmol/ml stock was prepared by adding 800 µl of the 10 µg/ml preparation to 200 µl of GSH/GSSG Assay Buffer (Section 2.1.26.3). A series of dilutions was carried out on the 26.4 nmol/ml preparation in order to generate a standard curve.

2.2.25.3 GSSG Standard Preparation

GSSG (2 mg/ml) (Section 2.1.26.12) was diluted 1/100 in GSH/GSSG Assay Buffer (Section 2.1.26.3) to give a stock of concentration 20 µg/ml. A 26.4 nmol/ml stock was prepared by adding 800 µl of the 10 µg/ml preparation to 200 µl of GSH/GSSG Assay Buffer (Section 2.1.26.3). A series of dilutions was carried out on the 26.4 nmol/ml preparation in order to generate a standard curve.

2.2.25.4 Pre-treatment of GSSG samples

GSSG standards and samples to be assayed for GSSG were pre-treated with 2-vinylpyridine, which covalently reacts with GSH, preventing its oxidation to GSSG, thereby allowing for the measurement of GSSG only. 2-vinylpyridine (Section 2.1.26.6) (2 μ l) was added to 100 μ l of a Blank sample, the GSSG standards (Section 2.2.25.3) and samples to be assayed for GSSG (Section 2.2.25.1). This was carried out in a fume hood. The samples were incubated at room temperature for 1 h before triethanolamine (Section 2.1.26.5) (6 μ l) was added to each sample to neutralise the 2-vinylpyridine. The samples were incubated for 10 min at room temperature before being assayed.

2.2.25.5 Glutathione Assay

All samples to be assayed for GSH or GSSG were assayed in the same manner. The blank/standard/sample (20 μ l) was added to a clear 96-well microtiter plate. To this, 10 mM DTNB + GR (Section 2.1.26.8) (44.2 μ l) was added and left for 30 sec. 5 mM NADPH (Section 2.1.26.10) (42 μ l) was added to each well and the plate was gently shaken to mix. The absorbance at 412 nm was measured after 1 min 30 sec.

2.2.26 Comparative Hydrophobicity Assay

Conidia were harvested from 7 day old AMM plates as described in Section 2.2.1.1. The conidia were washed by resuspending them in PBS (10 ml) (Section 2.1.3) followed by centrifugation at 2,000 g for 10 min. The supernatant was removed and the wash process repeated. The conidia were resuspended in 50 mM Sodium Phosphate (pH 7.4) containing 150 mM NaCl (Section 2.1.29) to an OD_{540nm} of 0.4. Xylene was added to the conidia suspension, 2.5:1 (v/v) and vortexed for 2 min. The suspension was allowed to settle for 20 min before the aqueous layer was removed and its absorbance measured at 540 nm.

2.2.27 *A. fumigatus* Germination Assay

Conidia were harvested from 5 day old MEA plates and AMM (20 ml) (Section 2.1.1.4.4) was inoculated with 1×10^7 /ml inoculum. The cultures were incubated at 37 °C static. The germination rate was measured by removing a 500 µl aliquot from each culture and transferring it to a 2 ml Eppendorf tube containing 0.1 mm glass beads (0.2 g). The cultures were returned to the incubator. The samples were vortexed briefly to disrupt any clumps of germinating conidia. 10 µl of each sample was loaded onto a haemocytometer and conidia and germlings were counted to 100. Swollen conidia were excluded from counting as germlings. Samples were counted in duplicate and the rate of germination was expressed as the percentage of germinated conidia in the total conidia counted. Germination was recorded after 6, 8 and 10 h.

2.2.28 MIC of Voriconazole

The MIC for voriconazole against *A. fumigatus* was measured following the European Committee on Antimicrobial Susceptibility Testing (EUCAST) guidelines (Pfaller et al., 2011). RPMI 1640 containing 2 % glucose (Section 2.1.1.6) and voriconazole (0 – 2 µg/ml) was inoculated with 3×10^5 conidia/ml in a flat bottom microdilution plate. The plate was incubated at 37 °C for 48 h. Growth was examined visually and the MIC was determined as the lowest concentration of voriconazole resulting in no growth of *A. fumigatus*.

2.2.29 Confocal Microscopy

9 h germlings were pelleted by centrifuging the cultures at 1,000 g for 5 min. The pellets were resuspended in 4 % (v/v) Formaldehyde (Section 2.1.28.4) to fix the germlings which were then centrifuged at 1,000 g for 5 min before the supernatants were discarded. The germlings were washed by resuspending in PBS (10 ml) (Section 2.1.3) centrifugation at 1,000 g for 5 min and discarding the supernatants. The wash step was repeated and the germlings were resuspended in PBS (10 ml) (Section 2.1.3). Aliquots (500 µl) of the germlings were centrifuged at 1,000 g for 2 min and the supernatants were discarded. The pellets were resuspended in Confocal Buffer (1 ml) (Section 2.1.28.5) to block the germlings overnight at 4 °C. The germlings were centrifuged at 1,000 g for 2 min and the supernatants were discarded. Mouse monoclonal antibody to linear-(1, 3)-β-glucan (Biosupplies, Australia) was added at 1 µg/ml in Confocal Buffer (Section 2.1.28.5) to the germlings which were incubated for 1 h at room temperature with gentle mixing. The germlings were

centrifuged at 1,000 g for 2 min and the supernatants were discarded. The germlings were washed by resuspending the pellets in Confocal buffer (1 ml) (Section 2.1.28.5) and incubating for 5 min with gentle mixing. The germlings were centrifuged at 1,000 g and the supernatants were discarded. This wash step was carried out 3 times in total. The germlings were stained with Alexa Fluor 488 goat anti-mouse IgG (H+L) (Invitrogen) at a 1/200 dilution in confocal Buffer (Section 2.1.28.5) for 1 h with gentle mixing. The germlings were again washed with Confocal Buffer as before. The pellets were resuspended in PBS (50 µl) (Section 2.1.3). 10 µl of this suspension was transferred onto a glass slides and covered with cover slips. The cover slips were sealed with nail varnish. The germlings were viewed under an Olympus FluoView 1000, and the images were processed using the software Olympus FluoView FV10-ASW Ver.01.07.

2.2.30 Statistical analysis

Data analysis was carried out using built-in GraphPad prism version 5.01 functions, as specified. Post hoc comparisons between groups were performed using the Bonferroni multiple comparisons test, unless otherwise stated. All graphs were compiled using Graphpad Prism version 5.01, unless otherwise stated.

2.2.31 Multiple Sequence Alignment

Amino acid sequences were obtained from the Ensembl genome browser (<http://www.ensembl.org/>) and were aligned using the ClustalW Multiple alignment tool in the BioEdit programme <http://www.mbio.ncsu.edu/bioedit/bioedit.html>.

3.1 Introduction

The eEF1 complex has been studied in many different organisms, including yeast, protozans and humans (Corbi *et al.*, 2010; Mateyak and Kinzy, 2010; Jonusiene *et al.*, 2005). The majority of the information available to date results from studies in *S. cerevisiae*, however little data about this complex in *A. fumigatus* has been forthcoming. In yeast, the majority of the studies focused on the eEF1A and eEF1B α subunits, which are involved in the transfer of aminoacyl-tRNA from the aminoacyl-tRNA synthetases to the elongating ribosome (Olawaju *et al.*, 2004). eEF1A is a G-protein and constituent nucleotide exchange activity derives from eEF1B α subunit which is a guanine nucleotide exchange factor. However, a function for the eEF1B γ subunit has yet to be conclusively elucidated, although recent studies indicate that eEF1B γ plays a role in protein metabolism, in particular protein transport and protein turnover in response to oxidative stress (Esposito and Kinzy, 2010).

The crystal structure of *S. cerevisiae* eEF1B γ has been characterised and the N-terminal domain contains sequence motifs that are found in the theta class of GSTs (Jeppesen *et al.*, 2003). Despite the presence of this domain, no GST activity has been demonstrated in eEF1B γ in *S. cerevisiae*. In *A. fumigatus*, Carberry *et al.* (2006) identified the eEF1B γ subunit; ElfA, by MALDI-ToF after selecting for GSH-binding proteins. They then demonstrated that ElfA exhibits GST activity using the substrates 1-chloro-2,4-dinitrobenzene (CDNB) and ethacrynic acid. The observation of GST activity in *A. fumigatus* ElfA raises many questions as to the role

it plays in the fungus, ranging from protection against oxidative stress, particularly at the elongating ribosome, to acting as a chaperone in protein folding.

In order to gain an insight into the function of *elfA* in *A. fumigatus*, a functional genomics and proteomics approach was employed. Central to this approach was the deletion of *A. fumigatus elfA* in order to allow for the investigation of phenotypes associated with the gene deletion. There are a number of different methods available to delete or disrupt genes in filamentous fungi; *Agrobacterium*-mediated transformation (AMT), protoplast-mediated transformation (PMT), electroporation and biolistic transformation (Meyer, 2008). Of these methods, some are more suitable to targeted gene disruption than others, namely AMT and PMT. AMT employs the use of the soil bacterium *Agrobacterium tumefaciens*, exploiting its ability to transfer DNA, known as T-DNA, to the host from the tumor-inducing (Ti) plasmid (Michielse *et al.*, 2008). This allows for the single targeted introduction of DNA into the host genome. The fungus to be transformed is co-cultivated with the bacterium containing a T-DNA plasmid with the DNA to be inserted. While the advantages of this method include targeted integration of DNA and the fact the different cell types can be transformed (protoplasts, conidia or hyphae), its disadvantages include the necessity to optimise co-cultivation parameters for the two species and the fact that this is a more time-consuming method than other methods (Meyer, 2008).

PMT involves the preparation of protoplasts by degrading the cell wall with enzymes (Meyer, 2008). The DNA is then incorporated by the addition of PEG and CaCl₂. PMT often results in the integration of multiple copies of DNA, resulting in

difficulties in trying to obtain targeted alterations of the genome with a single integration of DNA. Targeted gene deletions depend on homologous recombination events occurring between the deletion construct and the genome. However, the nonhomologous end-joining pathway (NHEJ) interferes with homologous recombination resulting in random integration of the construct (Nielsen *et al.*, 2008). The homologues of two genes involved in the NHEJ pathway, *ku70* and *ku80*, were identified in *A. fumigatus* (da Silva Ferreira *et al.*, 2006; Krappmann *et al.*, 2006a). The *ku70* and *ku80* homologues were deleted and the strains subsequently used for targeted gene deletions. The frequency of homologous recombination was increased significantly. However it must be noted that *ku70* or *ku80* needs to be replaced before phenotypic analysis can be carried out to ensure that any observed phenotypes are not as a consequence of the *ku70* or *ku80* deletion (Nielsen *et al.*, 2008).

The split bipartite method allows for targeted gene disruption using PMT and results in a higher frequency of successful gene disruptions when compared to the PMT method alone. Due to this increase in frequency of targeted gene disruption using the split bipartite method, it may be superior to using the NHEJ deletion strains as it does not require a pre-existing gene disruption. The split bipartite method involves the generation of two fragments by PCR that recombine by homologous recombination *in vivo* (Nielsen *et al.*, 2006). The two fragments contain a region homologous to the flanking region of the gene of interest. This homologous region is fused to a fragment of the selection marker. The two fragments of the selection marker overlap and therefore recombine *in vivo* to form a fully functional gene. At the same time, recombination events between the flanking regions of the gene of

interest with those in the construct also occur, deleting the gene and replacing it with the fully functional selection marker (Figure 3.1). This method has already proven successful in deleting genes in *A. fumigatus* (e.g., *gliG* (Davis *et al.*, 2011a), *gliT* (Schrettl *et al.*, 2010) and *pes3* (O'Hanlon *et al.*, 2011)).

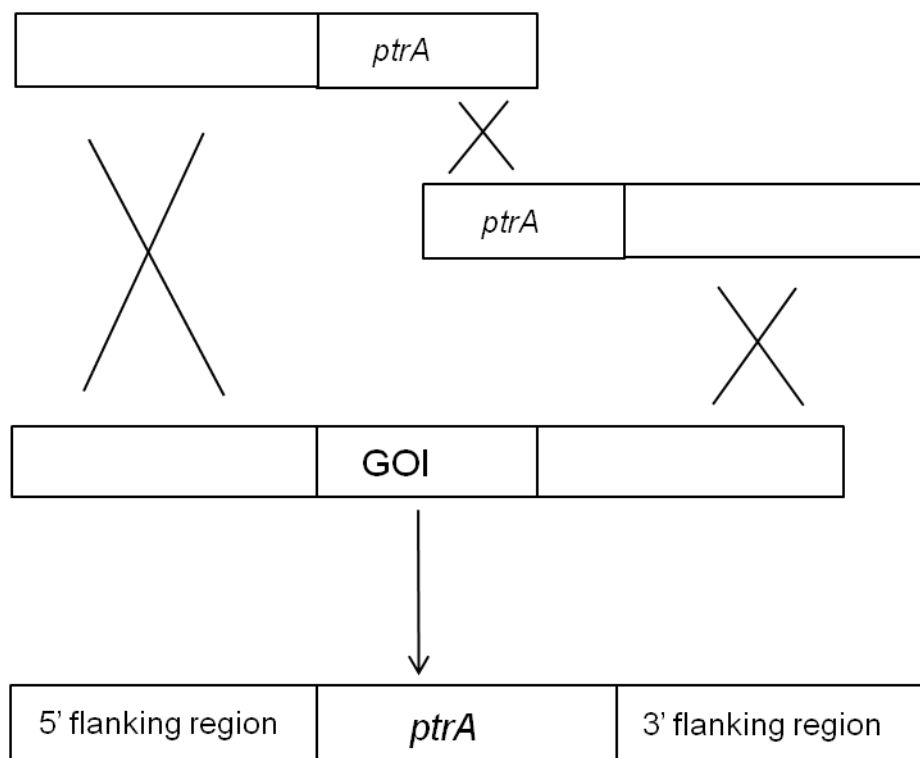


Figure 3.1: Schematic depicting the split bipartite method. Homologous recombination occurs between the overlapping *ptrA* fragments resulting in a functional *ptrA*. At the same time, two homologous recombination events occur between the flanking regions resulting in the deletion of the gene of interest (GOI).

Once the gene of interest has been successfully deleted, it must be complemented before phenotypic analysis can be undertaken to confirm any observed phenotypes associated with the deletion strain are as a direct result of the deletion and not the introduction of the resistance gene. Complementation of a deletion requires the use of an alternative resistance gene to the one used in carrying out the deletion.

The aims of the work presented in this chapter were (i) to generate the constructs required to delete *elfA* in *A. fumigatus* using the split bipartite method, (ii) to transform *A. fumigatus* protoplasts with the deletion constructs, (iii) to generate a construct to complement the deletion of *A. fumigatus elfA*, (iv) to complement *A. fumigatus Δ elfA*, (v) to analyse expression of *A. fumigatus elfA* in the ATCC46645 and complemented strains, as well as in *A. fumigatus Δ elfA*.

3.2 Results

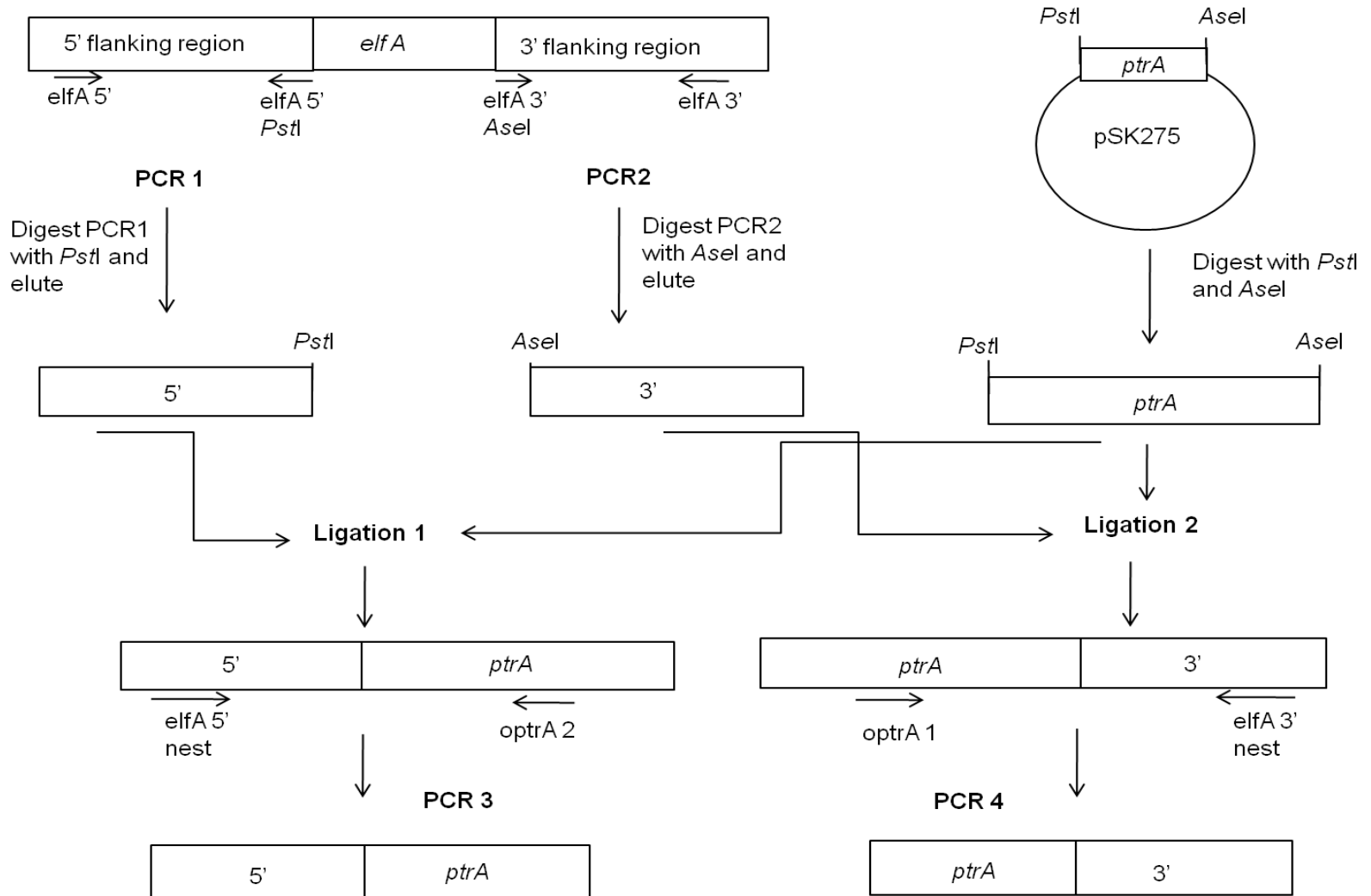
3.2.1 Generation of deletion constructs for the transformation of *A. fumigatus*

A gene deletion strategy was undertaken to generate the *A. fumigatus elfA* deletion strain; $\Delta elfA$ (Figure 3.2). $\Delta elfA$ was generated to facilitate the functional analysis of *A. fumigatus elfA*. Constructs were prepared in order to replace *elfA* with the pyrithiamine resistance gene (*ptrA*) (Kubodera *et al.*, 2000). These constructs were transformed into protoplasts from two *A. fumigatus* backgrounds, ATCC46645 and $\Delta akuB$ (Krappmann *et al.*, 2006b).

The 5' flanking region (1170 bp) of *A. fumigatus elfA* was amplified, introducing a *PstI* restriction site (Figure 3.3). The 3' flanking region (1247 bp) of *A. fumigatus elfA* was also amplified, introducing an *AseI* restriction site (Figure 3.3). The amplicons were digested with their respective restriction enzymes, allowing for their ligation to *ptrA*, which was released from pSK275 using the same restriction enzymes; *PstI* and *AseI*.

The ligation product between the 5' flanking region and *ptrA* was amplified, resulting in the 5' flanking region ligated to a partial fragment of *ptrA* (2615 bp) (Figure 3.4). The ligation product between the 3' flanking region and *ptrA* was amplified to produce another partial fragment of *ptrA* ligated to the 3' flanking region (2475 bp) (Figure 3.4). The two partial fragments of *ptrA* overlap by approximately 500 bp and should recombine by homologous recombination during transformation. The two constructs were gel purified to ensure removal of any contaminants, before use in protoplast transformation (Section 2.2.2.6).

A.



B.

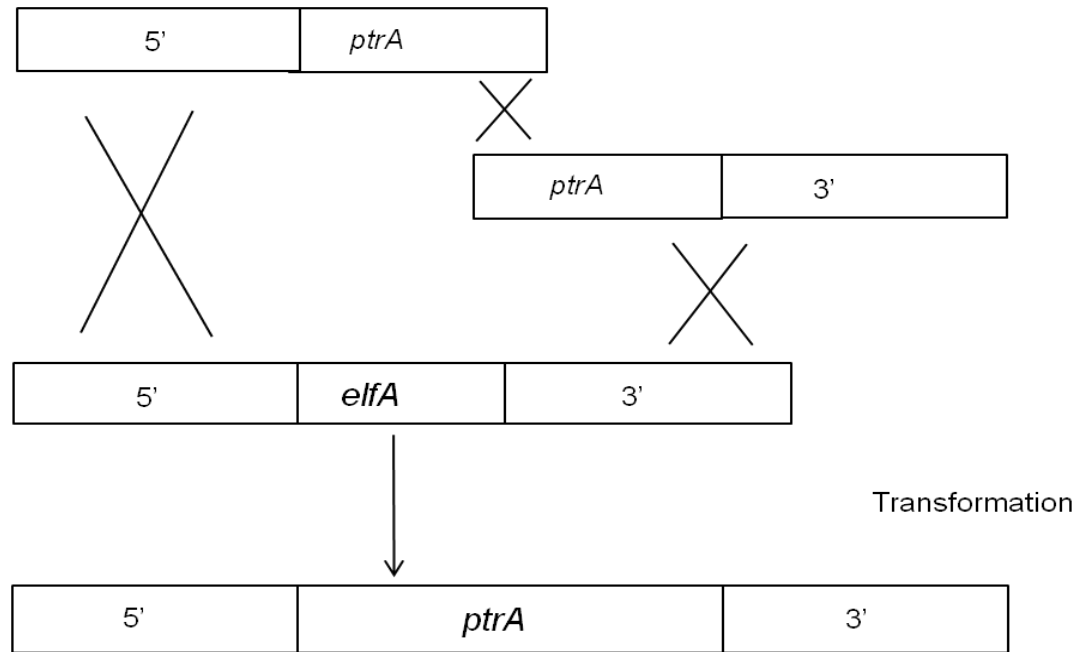


Figure 3.2: Schematic outlining the strategy used in the deletion of *elfA* in *A. fumigatus*

A. Outline of the steps involved in generating the deletion constructs for *A. fumigatus* $\Delta elfA$

B. Transformation of *A. fumigatus* with the deletion constructs in order to delete *A. fumigatus* *elfA*

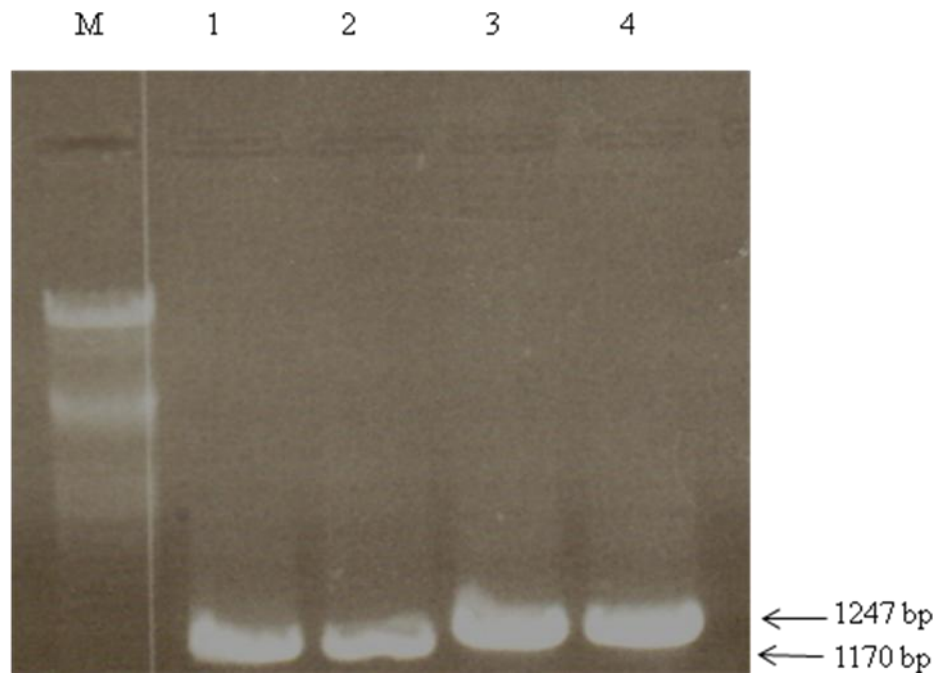


Figure 3.3: Generation of $\Delta elfA$ deletion constructs. PCR 1 for the 5' flanking region of *A. fumigatus elfA* (Lanes 1 and 2) and PCR 2 for the 3' flanking region of *A. fumigatus elfA* (Lanes 3 and 4) for the generation of *A. fumigatus elfA* deletion constructs. PCR 1 product; 1170 bp and PCR 2; 1247 bp. M: $\lambda PstI$ molecular weight marker.

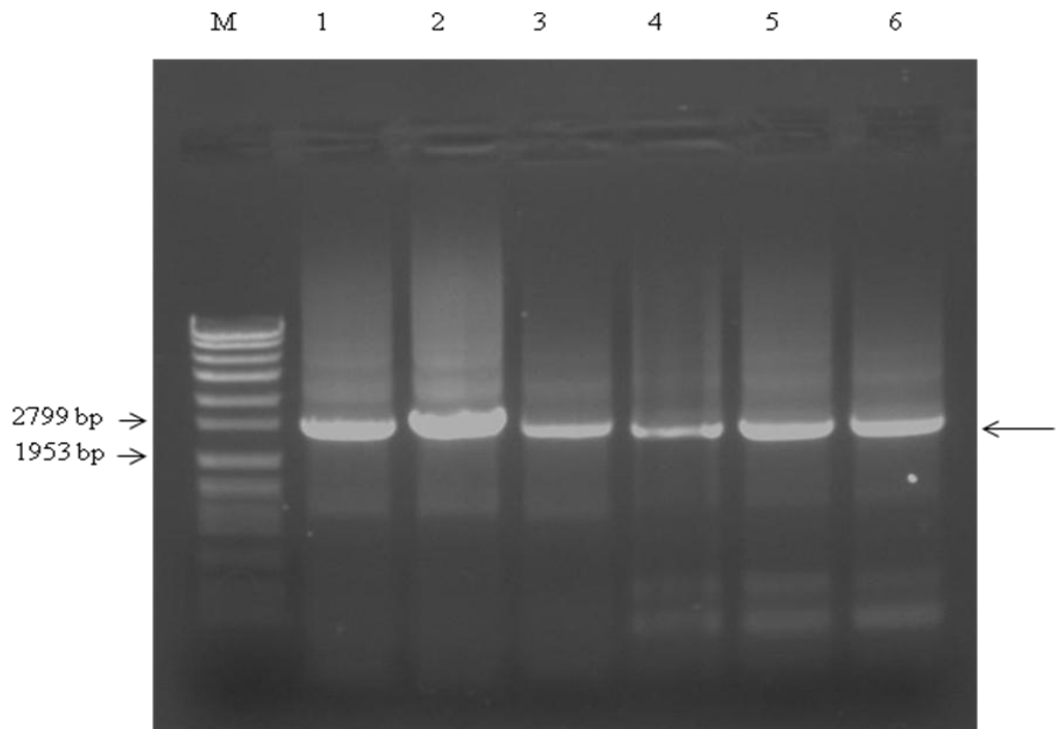


Figure 3.4: Generation of $\Delta elfA$ deletion constructs. PCR 3 (Lanes 1 – 3) and PCR 4 (Lanes 4 – 6) are the final constructs for the disruption of *A. fumigatus elfA*. PCR3 consists of the 5' flanking region of *A. fumigatus elfA* ligated to a partial fragment of *ptrA*. PCR4 consists of another partial fragment of *ptrA* ligated to the 3' flanking region of *A. fumigatus elfA*. The bands indicated by the arrow were excised from this gel and purified. M: Molecular weight marker (Roche VII).

3.2.2 Generation of Digoxigenin (DIG)-labelled probes for Southern blot analysis.

Two DIG-labelled probes were generated to identify $\Delta elfA$ transformants by Southern blot analysis. The probes were generated by PCR as described in Section 2.2.10.3.1 using DIG-labelled dNTPs. Probe 1, which hybridised to the 5' flanking region, was generated using the oligos; *elfA* 5' nest and *elfA* 5' *Pst*I (Table 2.3), and resulted in a probe 1087 bp in size (Figure 3.5). Probe 2, which hybridised to the *elfA* coding region was generated using the oligos; 5' *elfA* 02/10 DIG and 3' *elfA* 02/10 DIG (Table 2.3). This PCR resulted in a probe 707 bp in size (Figure 3.5). The PCRs were also carried out using unlabelled dNTPs and when resolved in an agarose gel, the probes were slightly larger than the unlabelled product due to the DIG label (Figure 3.5). The probes were gel purified to remove any contaminants and the concentration determined.

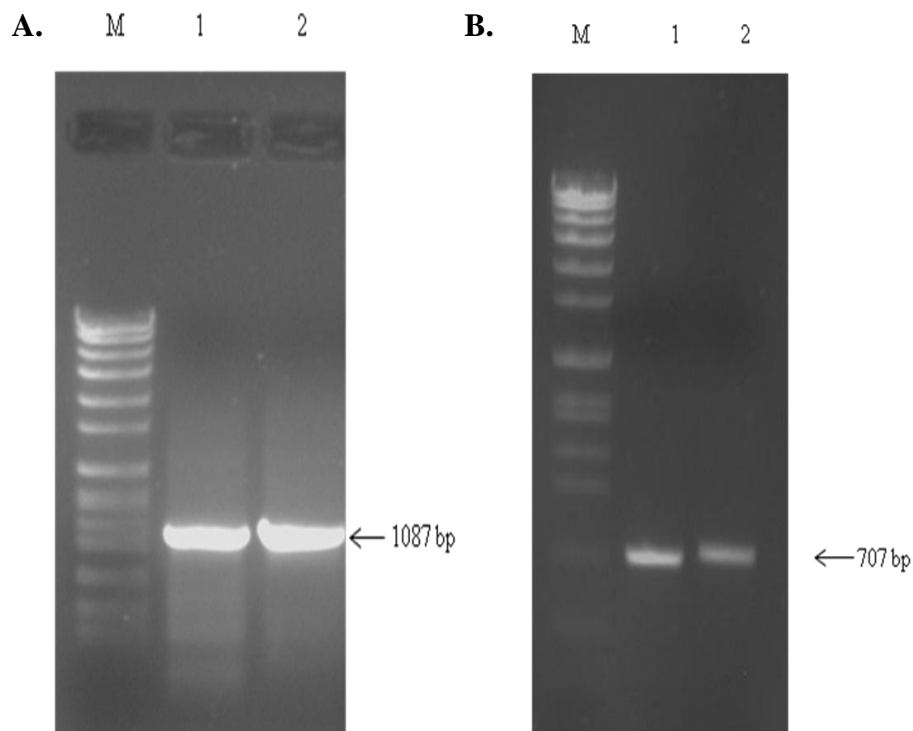


Figure 3.5: Generation of DIG-labelled probes for Southern analysis.

A. Probe 1: DIG-labelled probe for the 5' flanking region of *A. fumigatus elfA*, generated by PCR with the oligos; *elfA* 5' nest and *elfA* 5' *Pst*I. Lane 1 is the product of the PCR using regular dNTPs. Lane 2 is the DIG-labelled probe, generated by using DIG-labelled dNTPs in the PCR reaction. M: Molecular weight marker (Roche VII).

B. Probe 2: DIG-Labelled probe for the coding region of *A. fumigatus elfA*, generated by PCR with the oligos; 5' *elfA* 02/10 DIG and 3' *elfA* 02/10 DIG. Lane 1 is the product of the PCR using regular dNTPs. Lane 2 is the DIG-labelled probe, generated using DIG-labelled dNTPs in the PCR reaction. M: Molecular weight marker (Roche VII).

3.2.3 Transformation of *A. fumigatus* resulted in the deletion of *elfA* in ATCC46645 and \DeltaakuB

A. fumigatus ATCC46645 and \DeltaakuB protoplasts were transformed, independently, with the 5' and 3' constructs generated in Section 2.2.9.1.1 as described in Section 2.2.9.3, whereby 3 μ g of both the 5' and 3' constructs was used during the transformation of each strain. The protoplasts were regenerated on pyrithiamine plates to select for resistance. Transformants which demonstrated resistance to pyrithiamine were predicted to contain the reconstituted *ptrA* and were subjected to Southern blot analysis to check for the deletion of *A. fumigatus elfA*.

Transformation of ATCC46645 resulted in 17 transformants, while transformation of \DeltaakuB yielded 2 transformants. The transformed colonies were transferred onto fresh pyrithiamine plates to confirm resistance. Genomic DNA was extracted from all the transformants and digested with the restriction enzyme *PstI* (Figure 3.6). They were screened by Southern blot analysis using the probes for the *A. fumigatus elfA* coding region and the 5' flanking region (Figure 3.7). Two ATCC46645 transformants; 3 (Lane 4) and 11 (Lane 12), and one \DeltaakuB transformant; 1 (Lane 20) (Figure 3.7), contained a single integration of *ptrA*, as indicated by the presence of a band, 1969 bp in size.

It was decided to continue with $\DeltaelfA^{ATCC46645}$ in further studies, therefore colonies 3 and 11 were further confirmed by single spore isolation. Genomic DNA from the single spore isolates was digested with *PstI* and screened by Southern

analysis, again using the 5' probe (Figure 3.8). $\Delta elfA$ was confirmed by the presence of a band, 1969 bp in size.

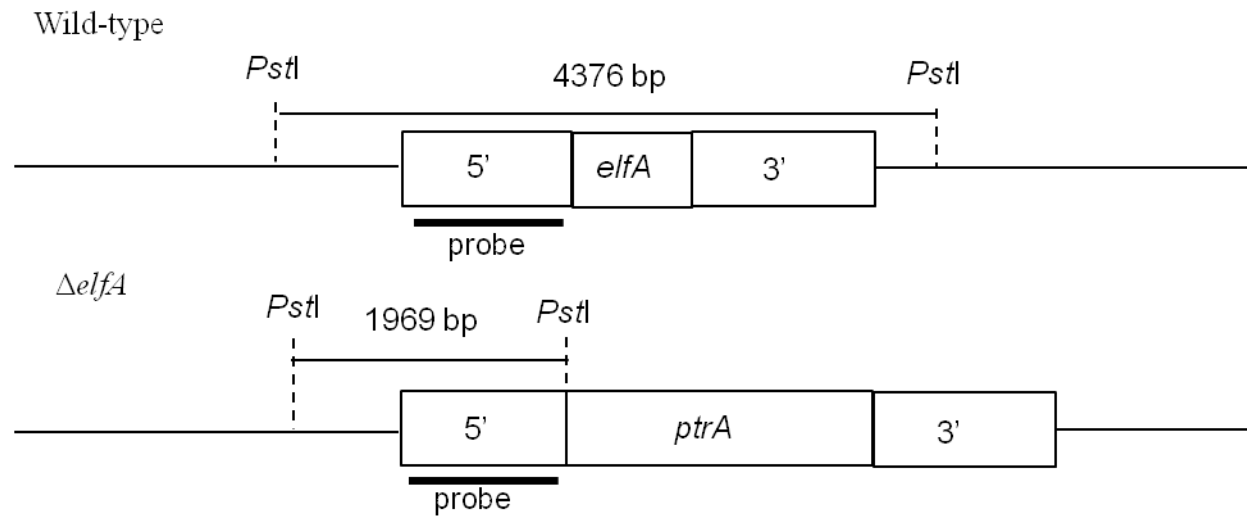
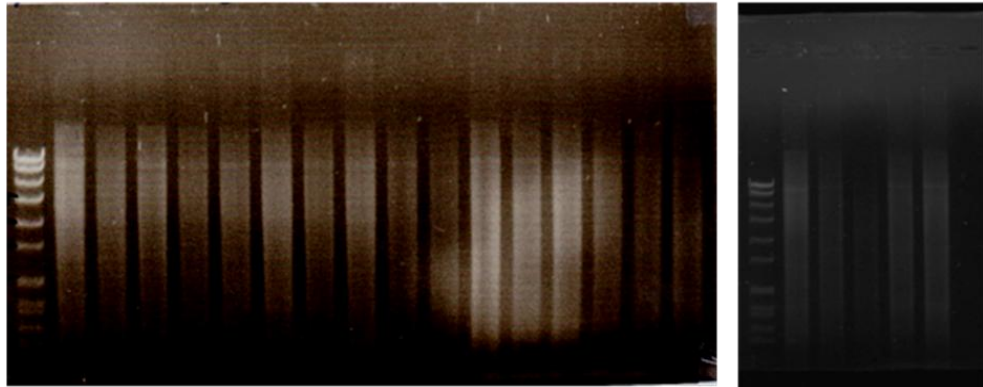
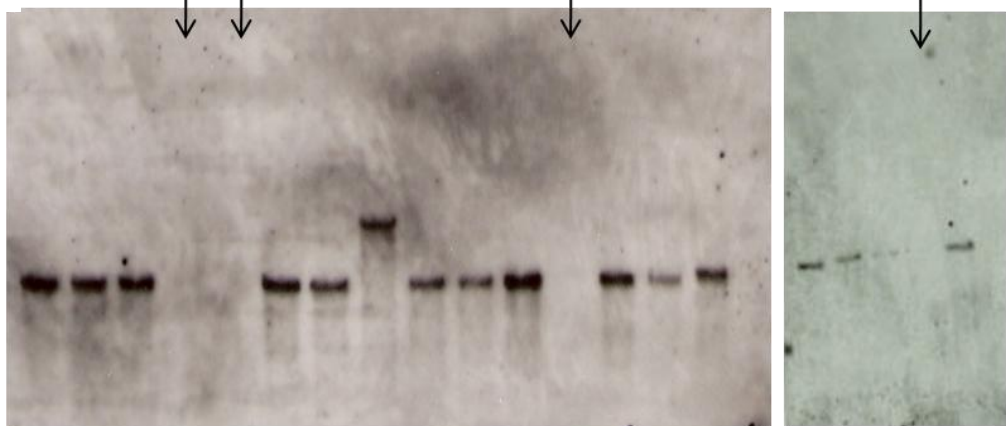


Figure 3.6: Schematic outlining the *PstI* restriction sites in both wild-type and $\Delta elfA$ genomic DNA for Southern analysis. Using a probe specific for the 5' region (indicated by the black line), wild-type was identified by a 4376 bp fragment, while $\Delta elfA$ was identified by a 1969 bp fragment. The *PstI* restriction sites generating the fragments for detection are indicated.

A. M 1 2 3 4 5 6 7 8 9 10 11 12 13 14 15 16 M 17 18 19 20 21



B. 1 2 3 4 5 6 7 8 9 10 11 12 13 14 15 16 17 18 19 20 21



C. 1 2 3 4 5 6 7 8 9 10 11 12 13 14 15 16 17 18 19 20 21

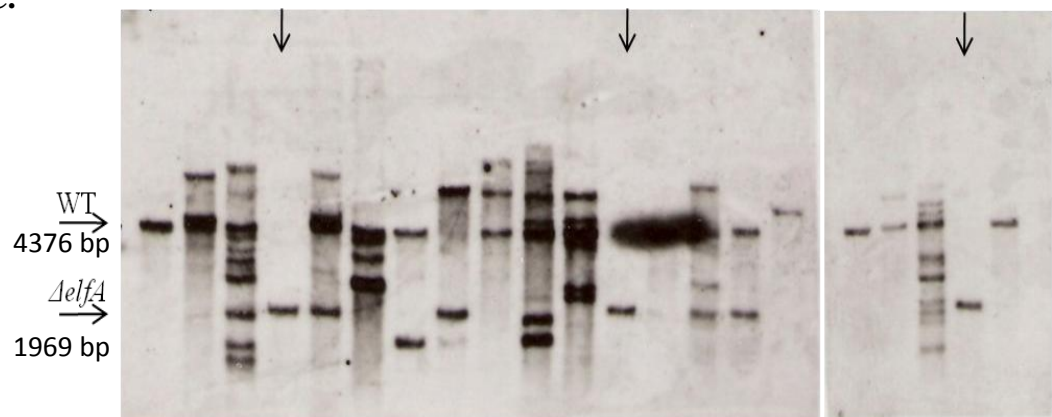


Figure 3.7: Southern analysis of ATCC46645 transformants and \DeltaakuB transformants.

A. Restriction digests (*Pst*I) of genomic DNA (1 μ g) from wild-type (Lanes 1 and 17), ATCC46645 transformants (Lanes 2 – 16) and \DeltaakuB transformants (Lanes 18 – 21). M: Molecular weight marker (Roche VII).

B. Southern analysis for the *A. fumigatus elfA* coding region. The bands indicate *A. fumigatus elfA* and transformants where *A. fumigatus elfA* has been deleted are indicated with arrows. Lanes 4, 5, and 12 are transformants in the ATCC46645 background and Lane 20 is a transformant in the \DeltaakuB background in which *A. fumigatus* has been deleted.

C. Southern blot probed for the *A. fumigatus elfA* 5' flanking region. The arrows indicate the transformants in which a single integration of *ptrA* was observed. Lanes 4 and 12 are transformants in the ATCC46645 background and Lane 20 is a transformant in the \DeltaakuB background where *A. fumigatus elfA* has been deleted. Wild-type fragment size: 4376 bp, \DeltaelfA fragment size: 1969 bp.

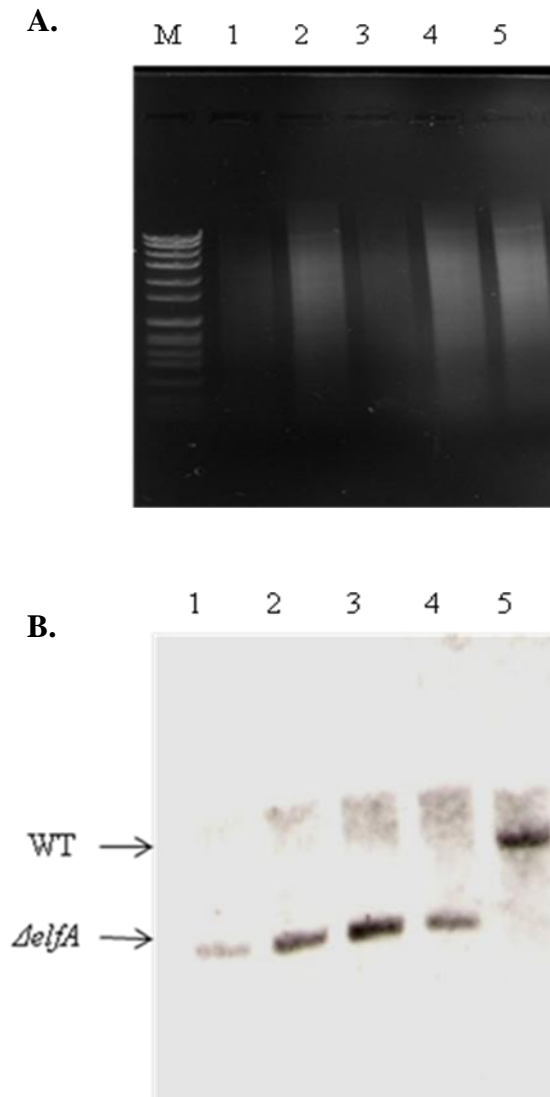


Figure 3.8: Southern analysis of *A. fumigatus* $\Delta elfA$ single spore isolates.

A. Restriction digest (*Pst*I) of genomic DNA (1 μ g) from wild-type (Lane 5) and single spore isolates (Lanes 1-4).

B. Southern blot of single spore isolates from colonies 3 (Lanes 1 and 2) and 11 (Lanes 4 and 5) probed with the 5' probe. Wild-type (Lane 5) is indicated by the band 4376 bp in size, while the band 1969 bp indicates $\Delta elfA$ (Lanes 1 – 4), confirming the deletion of *A. fumigatus* *elfA*.

3.2.4 Generation of construct for complementation of $\Delta elfA$

Once deletion of *A. fumigatus elfA* was confirmed, *A. fumigatus elfA* was re-introduced into $\Delta elfA$ in order to complement its deletion. A construct was generated as described in Section 2.2.9.2.1. This construct contained *A. fumigatus elfA* and the 5' and 3' flanking regions, and also a hygromycin resistance gene (*hph*) for selection (Woods *et al.*, 1998).

A. fumigatus elfA and the 5' and 3' flanking regions were amplified using the primers *elfA* 5' nest and *elfA* 3' nest (Table 2.3), resulting in a 3145 bp product (Figure 3.9). This product was cloned into TOPO® vector and the resulting plasmid was digested with the restriction enzyme *SpeI* to determine the orientation in which *elfA* integrated (Figure 3.10). Where *A. fumigatus elfA* had integrated in the 5' – 3' direction, two bands; 773 bp and 6295 bp were observed, as in Lane 1 (Figure 3.10). When *A. fumigatus elfA* integrated in the 3' – 5' direction the banding pattern observed was 2432 bp and 4636 bp, as in Lanes 2, 4 and 6 (Figure 3.10). The plasmid containing *A. fumigatus elfA* integrated in 5' – 3' direction was named *pelfA*. *pelfA* was linearised by restriction digestion with *EcoICRI* generating blunt ends. This was de-phosphorylated using CIAP (Section 2.2.6) to prevent re-annealing (Figure 3.11). *hph* was released from Pan 7.1 (Woods *et al.*, 1998) by restriction digestion with *AvrII* and *XbaI* (Figure 3.12). The 5' overhangs generated by these restriction enzymes were filled in using DNA Polymerase I, Large (Klenow) Fragment (Figure 3.11) (Section 2.2.7). *pelfA* and *hph* were ligated and cloned into TOPO® vector. Plasmids were checked by restriction digest with *BsgI* to determine

if the ligation was successful, and if so which orientation *hph* integrated (Figure 3.13). Determination of the orientation in which *A. fumigatus elfA* and *hph* integrated into *pelfA-hph* was important for designing the strategy for Southern analysis. One successful ligation of *hph* with *pelfA* was observed (Figure 3.13). The banding pattern; 1764 bp and 7649 bp indicated that *hph* is in the 3' – 5' direction. This plasmid was named *pelfA-hph*. As further confirmation of the integration of *hph* and its orientation, *pelfA-hph* was restriction digested with a second enzyme, *MfeI* (Figure 3.14). The observation of two bands, 1131 bp and 8278 bp in size confirmed the integration of *hph* in the 3' – 5' direction. Prior to its use in transforming *A. fumigatus* Δ *elfA* protoplasts, *pelfA-hph* was linearised by restriction digest with *NruI*, which had a single restriction site in the 3' flanking region of *A. fumigatus elfA*.

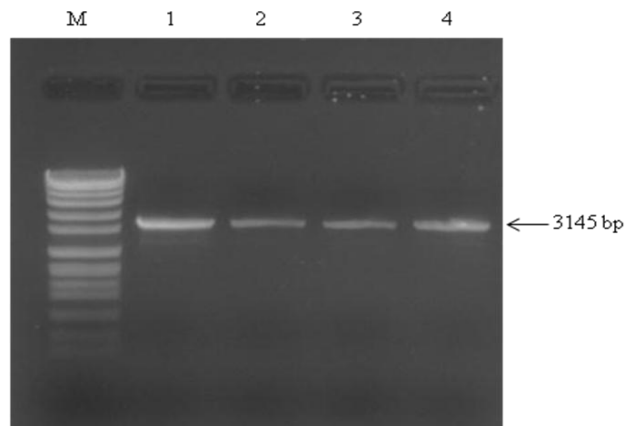


Figure 3.9: PCR of *A. fumigatus elfA* and flanking regions. The *A. fumigatus elfA* and flanking regions (3145 bp) were amplified using the primers *elfA* 5' nest and *elfA* 3' nest (Lanes 1 – 4) for the generation of the complementation construct. M: Molecular weight marker (Roche VII).

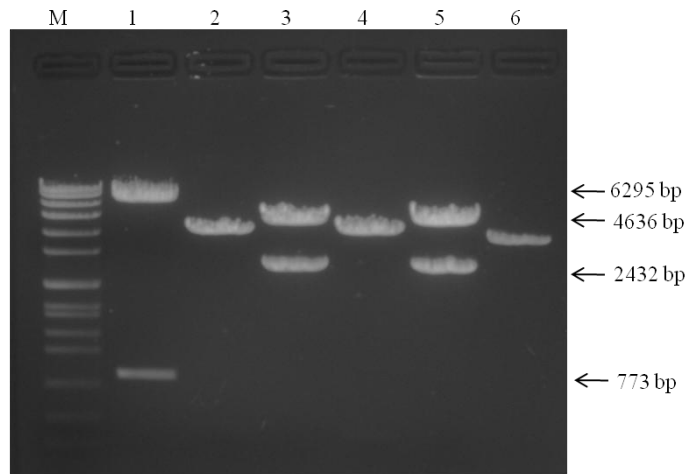


Figure 3.10: Restriction digest of *pelfA* with *SpeI*. The banding pattern in Lane 1 (773 bp and 6295 bp) indicated *A. fumigatus elfA* integration in the 5'- 3' orientation while the banding pattern in Lanes 3 and 5 indicated *A. fumigatus elfA* integration in the 3'- 5' orientation. Lanes 2 and 4 are undigested plasmid. M: Molecular weight marker (Roche VII).

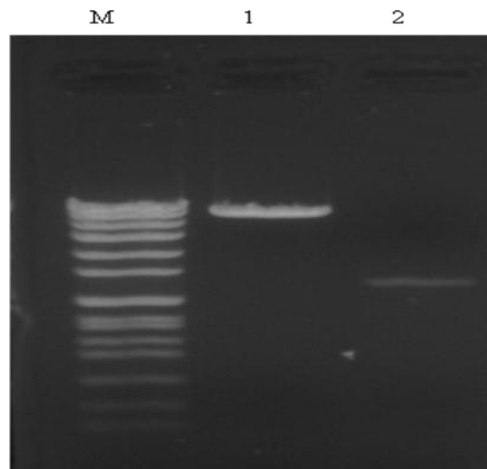


Figure 3.11: Dephosphorylation of *pelfA* and filling in the 5' overhangs of *hph*. Lane 1; *pelfA* which was linearised by restriction digestion with *EcoICR1* and dephosphorylated using CIAP. Lane 2; *hph* after filling in the 5' overhangs with DNA Polymerase I, Large (Klenow) Fragment. M: Molecular weight marker (Roche VII).

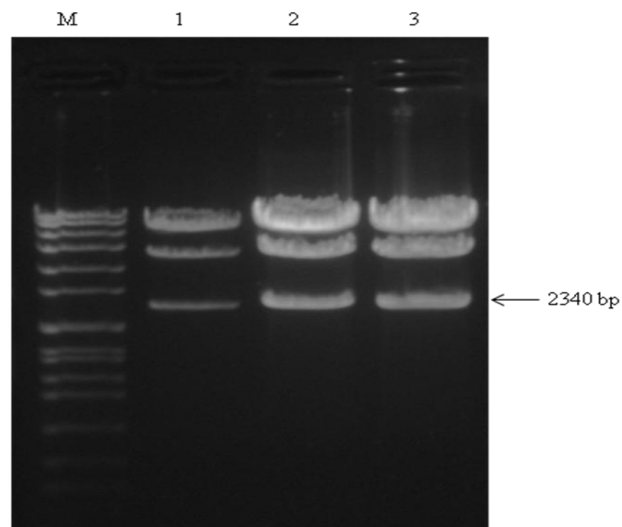


Figure 3.12: Restriction digest of Pan 7.1 with *AvrII* and *XbaI* to release *hph*. Lanes 1-3; a 2340 bp fragment, indicated by the arrow, which corresponds to *hph*. This was excised and gel purified.

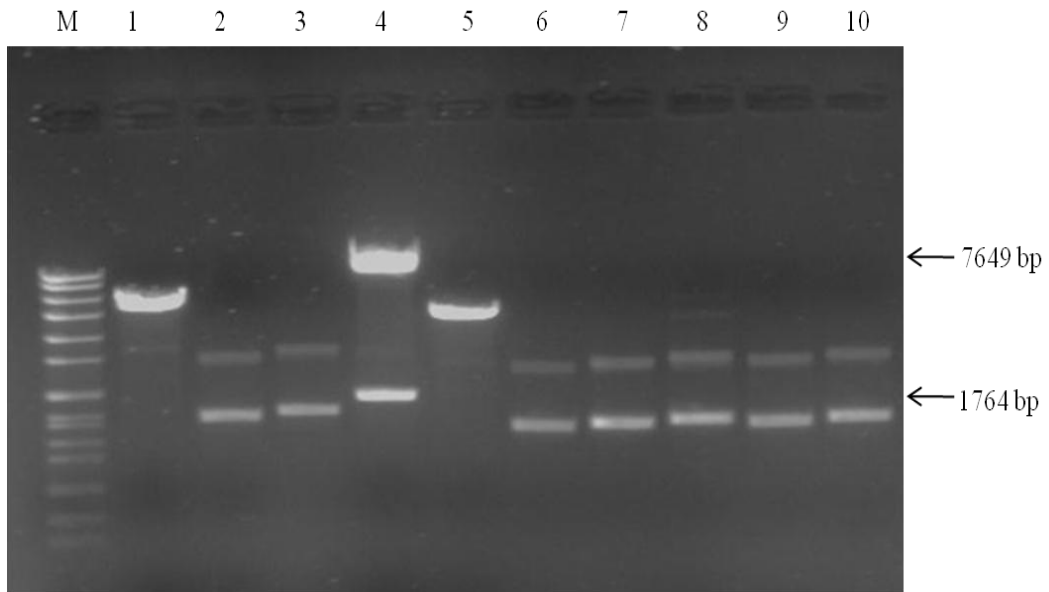


Figure 3.13: Restriction digest with *BsgI* of *pelfA* ligated with *hph*. Lane 4 contains 2 fragments, 7649 bp and 1764 bp, indicating the integration of *hph* into *pelfA* in the 3' – 5' orientation. Lanes 1 and 5; undigested plasmid. Lanes 2, 3, 6 – 10; plasmids in which *hph* ligated incorrectly with *pelfA*. M: Molecular weight marker (Roche VII).

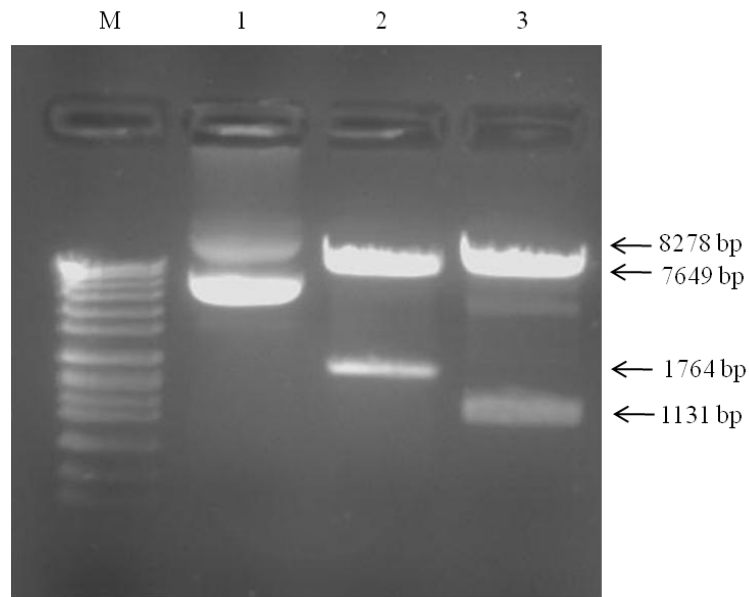


Figure 3.14: Digest of *pelfA-hph* with *BsgI* and *MfeI*. The plasmid was digested with *BsgI* and *MfeI* independently to check the integration of *hph* into *pelfA*. Lane 1 contained undigested plasmid. The *BsgI* digest resulted in 2 fragments, 7649 bp and 1764 bp (Lane 2) and the *MfeI* digest resulted in 2 fragments, 8278 bp and 1131 bp (Lane 3). This indicated that *hph* integrated into *pelfA* in the 3' – 5' orientation. M: Molecular weight marker (Roche VII).

3.2.5 Re-insertion of *elfA* into $\Delta elfA$ complements its deletion

A. fumigatus $\Delta elfA$ ⁴⁶⁶⁴⁵ protoplasts were transformed with the linearised *pelfA-hph* plasmid as described in Section 2.2.9.3. Transformants were selected on hygromycin plates, and any colonies growing were deemed likely to contain *hph*. Two transformants were obtained, and these were plated onto fresh hygromycin plates to confirm resistance. Genomic DNA from *A. fumigatus* ATCC46645, $\Delta elfA$ and the transformants was restriction-digested with *Pst*I and screened by Southern blot analysis, using the 5' probe (Figure 3.15). Transformant 1 contained two fragments, 1969 bp and 4470 bp, indicating the re-integration of *A. fumigatus elfA* (Figure 3.16).

As the Southern blot of the *Pst*I digests for the complementation contains two bands similar in size to those for *A. fumigatus* ATCC46645 and $\Delta elfA$, it was decided to do a second Southern screen, carrying out the restriction digests with *Bss*HII on single spore isolates (Figure 3.17). Use of this restriction enzyme results in the complemented strain exhibiting different bands to those found in *A. fumigatus* ATCC46645 or $\Delta elfA$. Transformant 1 was confirmed as having complemented the deletion of *elfA* as it contained the fragments; 4006 bp and 6225 bp (Figure 3.18).

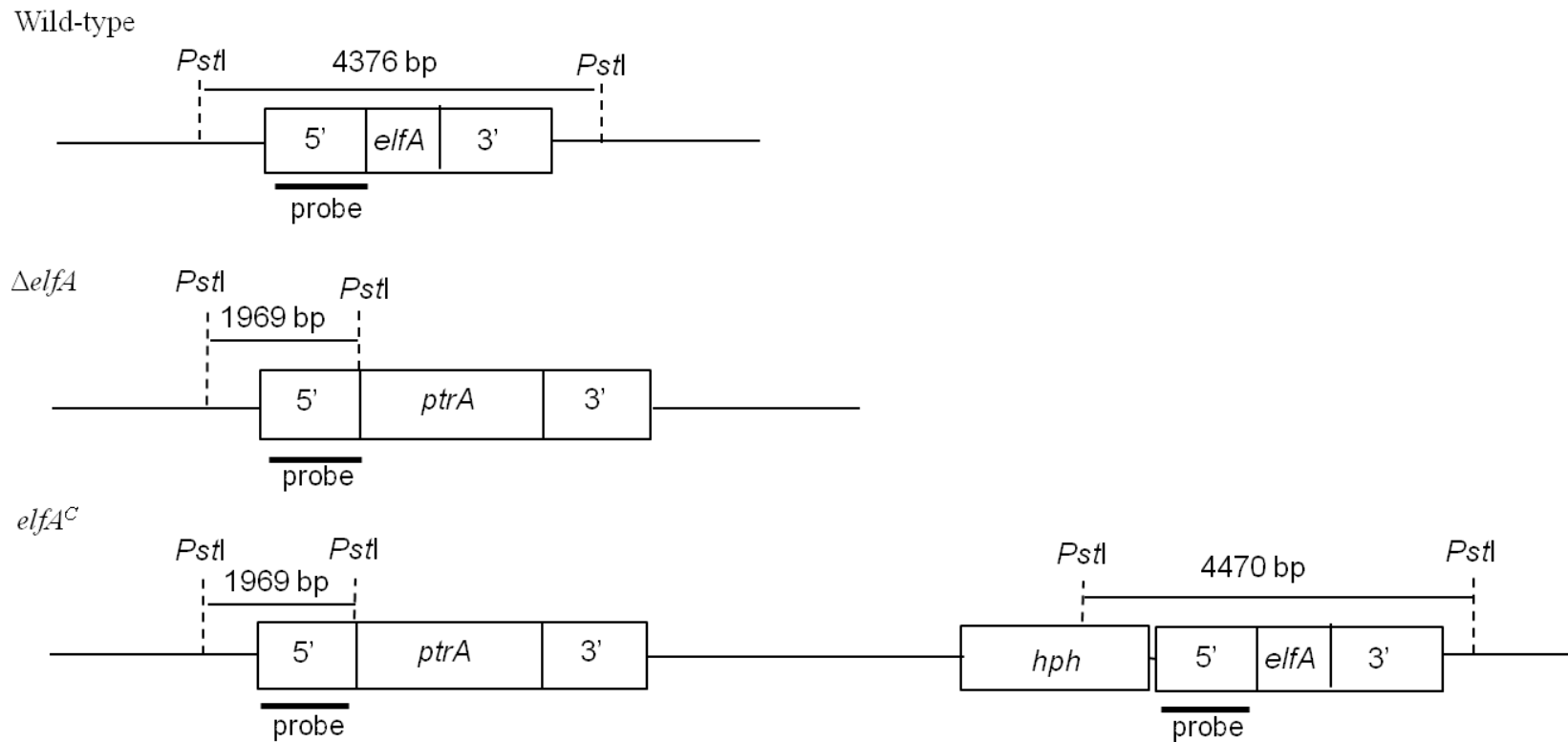


Figure 3.15: Schematic outlining the hybridisation pattern of the 5' probe (indicated by the black line) to wild-type, $\Delta elfA$ and $elfA^C$ genomic DNA digested with *PstI* for Southern blot analysis. In wild-type a fragment 4376 bp in size is observed, in $\Delta elfA$ a fragment 1969 bp in size is observed, while in $elfA^C$ two fragments should be observed, 1969 bp and 4470 bp.

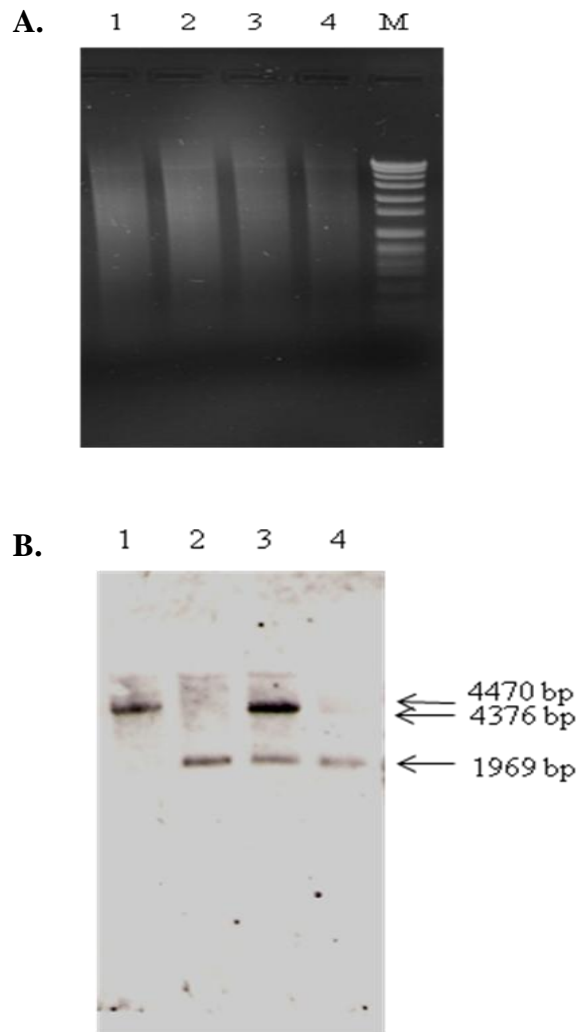


Figure 3.16: **A.** Restriction digest of genomic DNA (1 μ g) from *A. fumigatus* ATCC46645 wild-type (Lane 1), $\Delta elfA$ (Lane 2) and transformants (Lanes 3 and 4) with the restriction enzyme *Pst*I.

B. Southern blot probed with 5' probe. The *A. fumigatus* ATCC46645 wild-type exhibits a 4376 bp band (Lane 1), $\Delta elfA$ a 1969 bp band (Lane 2), while transformant 1 (Lane 3) exhibits the complemented pattern, two bands; 1969 bp and 4470 bp in size.

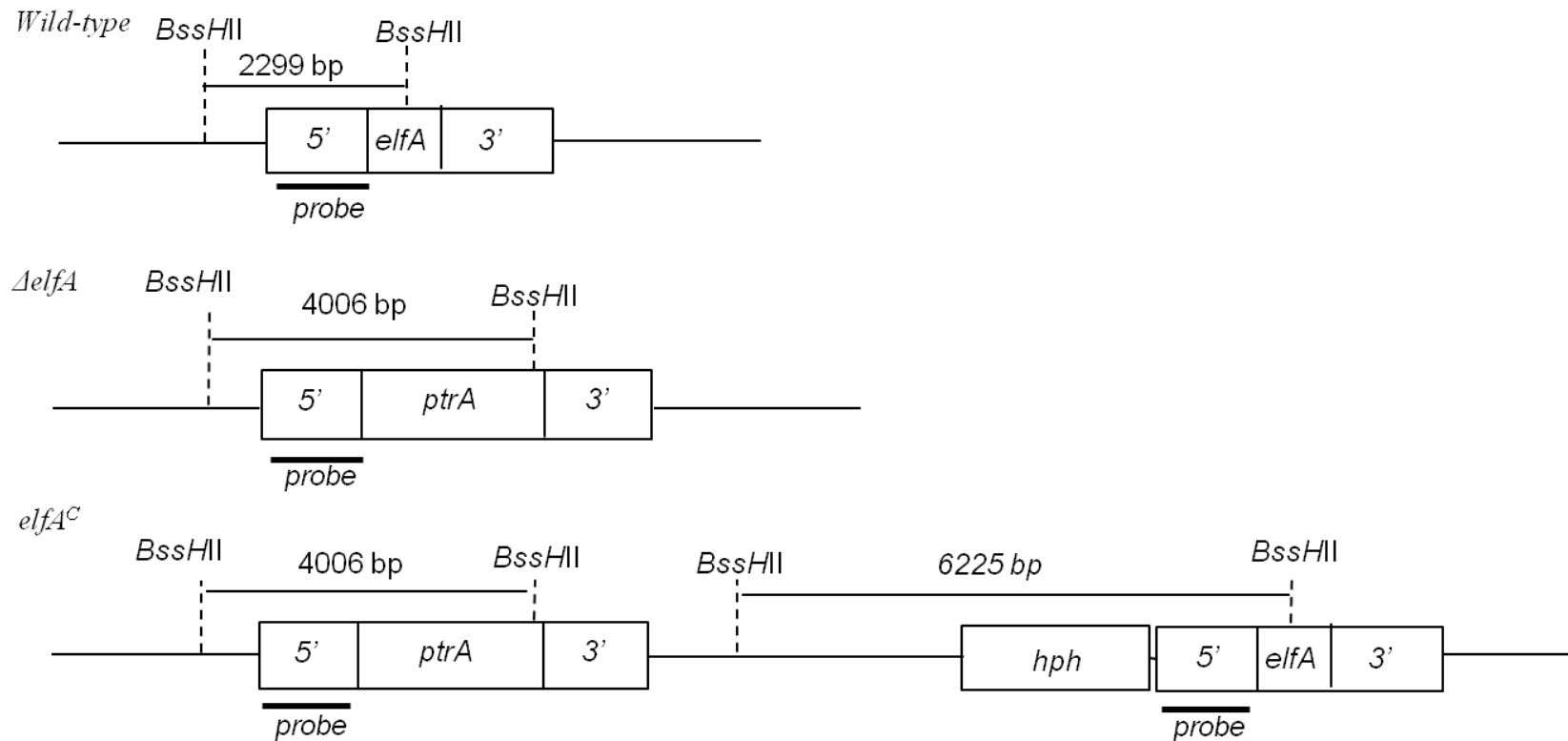


Figure 3.17: Schematic representation of the hybridisation pattern of the 5' probe (indicated by black line) after digestion with the restriction enzyme *BssHII*. The *A. fumigatus* ATCC46645 wild-type exhibits a 2299 bp band, $\Delta elfA$ has a band 4006 bp in size, while the complemented strain pattern contains two bands; 4006 bp and 6225 bp.

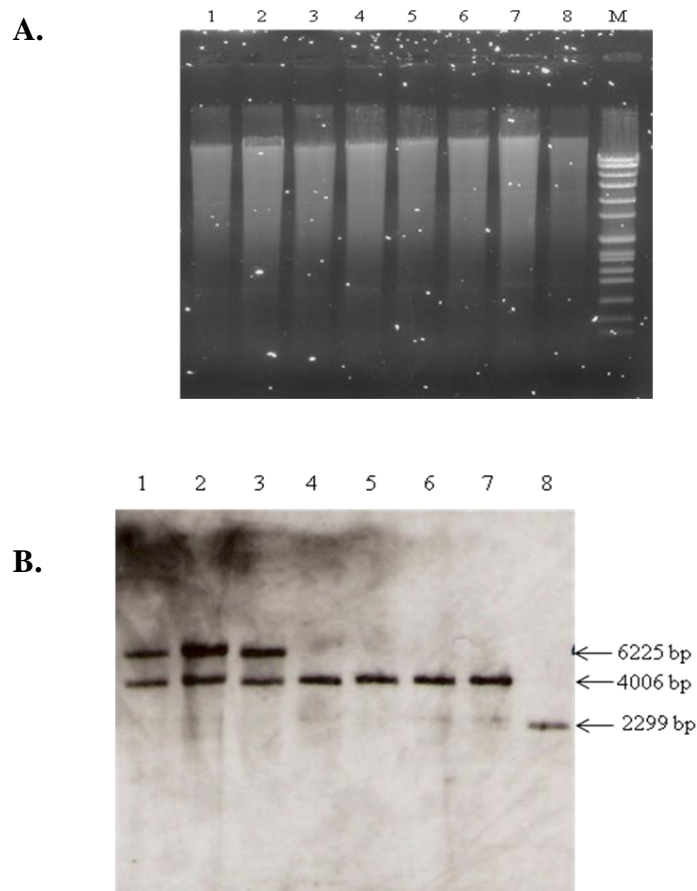


Figure 3.18: Southern analysis of single spore isolates to confirm complementation of *A. fumigatus* $\Delta elfA$.

A. Digest of genomic DNA from single spore isolates from the two transformants, $\Delta elfA$ and *A. fumigatus* ATCC46645 with the restriction enzyme *BssHIII* for Southern blot analysis.

B. Southern blot confirming the complementation of $\Delta elfA$ ($elfA^C$). When probed with the 5' probe, a 2299 bp band indicates *A. fumigatus* ATCC46645, a fragment size of 4006 bp indicated $\Delta elfA$, while two band, 4006 bp and 6225 bp in size confirms $elfA^C$.

3.2.6 RT-PCR confirms expression of *A. fumigatus elfA* in ATCC46645 and *elfA^C* and absence of expression in Δ *elfA*

Semi-quantitative RT-PCR of *A. fumigatus elfA* in ATCC46645, Δ *elfA* and *elfA^C* was carried out to confirm expression, or absence, in these strains. RNA was extracted as described in Section 2.2.4.1 from cultures grown for 24, 48 and 72 h. RNA was quantified using a Nanodrop (NanoDrop 1000 Spectrophotometer, Thermo Scientific) and its quality checked by running an RNA agarose gel (Section 2.2.4.2). cDNA was synthesised from the extracted RNA as described in Section 2.2.4.4.

The possibility of genomic DNA contaminating the cDNA was excluded using the *A. fumigatus calmodulin (calm)* gene (AFUA_4G10050) as a control gene (Burns *et al.*, 2005). The primers calmF and calmR were used (Table 2.3) and resulted in an amplicon 314 bp from cDNA, while the resulting amplicon from gDNA was 617 bp (Figure 3.19). When the cDNA was confirmed free from contaminating genomic DNA, the primers 5' *elfA* RT-PCR and 3' *elfA* RT-PCR (Table 2.3) were used in the PCR for *A. fumigatus elfA*, yielding a 529 bp amplicon (Figure 3.19).

The semi-quantitative RT-PCR for *A. fumigatus elfA* demonstrates that *A. fumigatus elfA* is expressed at 24, 48 and 72 h in both *A. fumigatus* ATCC46645 and *elfA^C*, while in Δ *elfA*, expression is absent. Although semi-quantitative RT-PCR was performed, it appears the expression across the 3 time points is equal.

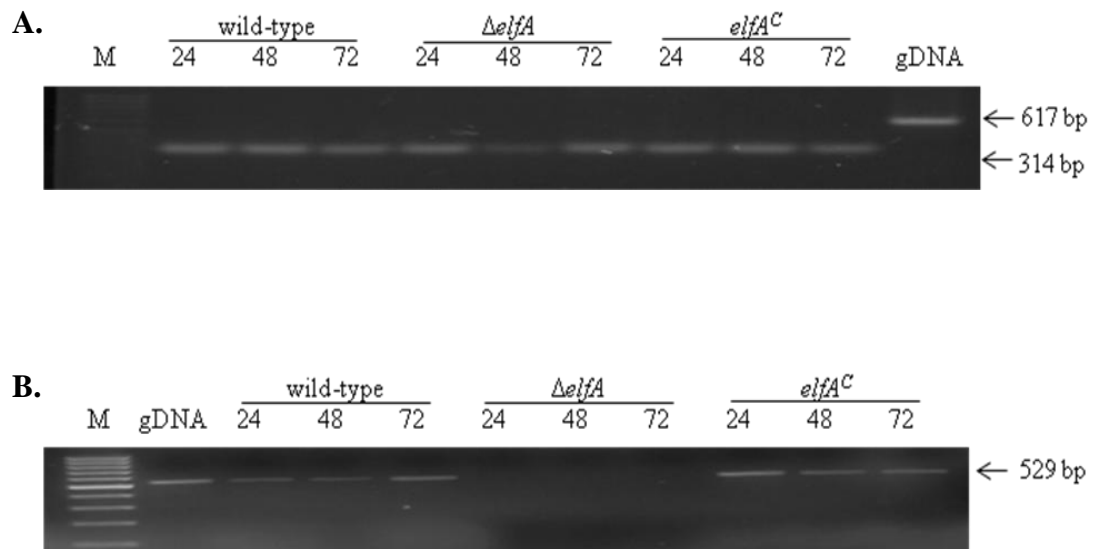


Figure 3.19: Expression analysis of *A. fumigatus* $\Delta elfA$ by semi-quantitative RT-PCR.

A. Semi-quantitative RT-PCR of the housekeeping gene *A. fumigatus calm*. Genomic DNA results in a 617 bp amplicon, while the amplicon for cDNA is 314 bp. M: Molecular Marker (Sigma 50 bp).

B. Semi-quantitative RT-PCR of *A. fumigatus elfA* in *A. fumigatus* ATCC46645, $\Delta elfA$ and $elfA^C$. The 529 bp amplicon observed, confirmed basal expression of *A. fumigatus elfA* in the ATCC46645 and $elfA^C$ strains, while the absence of the amplicon demonstrates absence of expression in $\Delta elfA$. M: Molecular Marker (Sigma 50 bp).

3.3 Discussion

The work presented in this Chapter describes the deletion of *A. fumigatus elfA* in two wild-type strain backgrounds; ATCC46645 and \DeltaakuB . *A. fumigatus* $\DeltaelfA^{ATCC46645}$ was complemented to restore *elfA* function. Semi-quantitative RT-PCR confirmed expression of *A. fumigatus elfA* in *A. fumigatus* ATCC46645 and *elfA^C*, while expression was absent in *A. fumigatus* \DeltaelfA after 24, 48 and 72 h growth.

The split bipartite method (Nielsen *et al.*, 2006) was employed in the deletion of *A. fumigatus elfA*, a putative translation elongation factor subunit 1B γ which has been shown previously to exhibit glutathione *s*-transferase activity (Carberry *et al.*, 2006). Two constructs were generated according to this method containing partial fragments of the pyrithiamine resistant gene, *ptrA*. The constructs were transformed into protoplasts from *A. fumigatus* ATCC46645 and \DeltaakuB independently.

In ATCC46645, 17 transformants were obtained, all of which were screened by Southern blot. After restriction digestion with *Pst*I, two transformants contained a 1969 bp fragment, corresponding to the successful integration of a fully functional *ptrA* in place of *A. fumigatus elfA*, resulting in *A. fumigatus* $\DeltaelfA^{ATCC46645}$. This represents a homologous integration frequency of 12 %, which is higher than that previously reported for wild-type strains (3 – 5 %) (da Silva Ferreira *et al.*, 2006). The homologous integration frequency reported here correlates with a homologous integration frequency of 20 % reported for the *A. fumigatus* $\Delta pes3$ strain (Dr. Karen O' Hanlon, personal communication). The *A. fumigatus* $\Delta pes3$ strain was also

generated using the split bipartite method with the pyrithiamine resistance gene in the wild-type strain *A. fumigatus* ATCC46645 (O'Hanlon *et al.*, 2011). A second round of Southern blot on single spore isolates of these two successful transformants confirmed the deletion of *A. fumigatus elfA*.

In *A. fumigatus* \DeltaakuB , two transformants were obtained, restriction digested with *PstI*, and screened by Southern blot. One transformant contained the 1969 bp fragment indicative of the successful deletion of *A. fumigatus elfA* and the generation of *A. fumigatus* \DeltaelfA^{\DeltaakuB} . A homologous integration frequency of 50 % is demonstrated here for *A. fumigatus* \DeltaakuB which is less than that previously reported by da Silva Ferreira *et al.* (2006), who reported at frequency of 80 %. However the sample size ($n = 2$) reduces the confidence of reporting this frequency.

A complementation construct was prepared, containing *elfA* and the selection marker *hph*, and transformed into $\DeltaelfA^{ATCC46645}$. Two transformants were obtained and screened by Southern blot after restriction digest with *PstI*. One of the transformants displayed the fragment pattern, 1969 bp and 4470 bp, indicating the generation of *elfA^C*. A second round of Southern Blot, following restriction digest with *BssHII*, confirmed the complementation when the fragment pattern; 4006 bp and 6225 bp, was observed in one of the transformants. The hygromycin resistance gene, *hph*, has been successfully used to complement other gene deletions in *A. fumigatus*, where it has been co-transformed as a plasmid along with the complementation construct (Blatzer *et al.*, 2011). The advantage of a single construct, containing the gene to be complemented and the resistance marker, rules out the situation whereby the resistance marker randomly integrates in the genome.

The targeted complementation of a gene deletion with a single construct has been successfully used to complement the deletion of *A. fumigatus glkA* (Fleck and Brock, 2010).

Semi-quantitative Real Time PCR (RT-PCR) was undertaken to assess *A. fumigatus elfA* expression in *elfA*^C and absence of expression in $\Delta elfA$. cDNA was prepared from RNA extracted from *A. fumigatus* ATCC46645, $\Delta elfA$, and *elfA*^C. Expression of *A. fumigatus elfA* was confirmed in ATCC46645 and *elfA*^C, while no expression was observed in $\Delta elfA$. This confirmed the successful deletion of *A. fumigatus elfA* in ATCC46645 and complementation of $\Delta elfA$.

The split bipartite method (Nielsen *et al.*, 2006) was employed in this study to delete *A. fumigatus elfA*. The two constructs were prepared by fusing partial fragments of *ptrA* to ~1.2 kb of the 5' and 3' flanking regions of *elfA*. The advantage this method has over other linear and PCR-based methods (e.g., the double-jointed method), is that only two rounds of PCR are required, reducing the possibilities of introducing mutations into the constructs (Nielsen *et al.*, 2006; Yu *et al.*, 2004). Three homologous recombination events are involved in this method. Firstly, the two overlapping fragments of the marker recombine to form a fully functioning *ptrA*. This recombination drives DNA recombination into homologous recombination and the 1.2 kb flanking regions on the constructs facilitate homologous recombination with those at the target site, resulting in the incorporation of the resistance marker at the target site. The ectopic integration of either the 5' or 3' construct alone will not confer resistance and therefore is selected against, and does not yield transformants (Nielsen *et al.*, 2006).

A. fumigatus elfA was successfully deleted in two wild-type background strains; ATCC46645 and \DeltaakuB . It was decided for the purpose of this study to continue with $\DeltaelfA^{ATCC46645}$ for the remainder of the work and therefore complementation of *elfA* deletion was undertaken in this strain only. The deletion was carried out in \DeltaakuB along with ATCC46645, because as \DeltaakuB is a NHEJ-deficient strain, it was hoped that transformation would be successful at least in this strain. *A. fumigatus* \DeltaakuB has been used as a background strain for the deletion of another GST in *A. fumigatus*, *gliG*, which is involved in gliotoxin biosynthesis (Davis *et al.*, 2011a). The frequency of homologous integrations is increased in \DeltaakuB because the NHEJ pathway is no longer active, thereby increasing the chances of successful targeted deletions (Nielsen *et al.*, 2008). While this strain has been reported to have the same characteristics as wild-type strains, regarding growth, virulence, sporulation and pigmentation, it has shown mild sensitivity towards DNA damaging agents (e.g., methyl methanesulphonate (MMS) and UV light (da Silva Ferreira *et al.*, 2006; Krappmann *et al.*, 2006a)). Therefore, ideally, the NHEJ activity needs to be restored before any phenotypic characterisation of the newly generated mutant can occur (Nielsen *et al.*, 2008). This removes any ambiguity regarding whether any observed phenotypes are due to the deletion of the gene of interest or the *aku* deletion. Strains have been developed in *A. nidulans* and *A. niger* in which *ku70* has been transiently disrupted enabling the restoration of *ku70* function once the desired gene deletion has been successful (Carvalho *et al.*, 2010; Nielsen *et al.*, 2008). As a targeted deletion of *A. fumigatus elfA* was successful in ATCC46645, this \DeltaelfA strain was used in the remainder of the work, as it did not

require any further manipulations, except complementation with *elfA*, before phenotypic characterisation could occur.

This Chapter describes the successful deletion of *A. fumigatus elfA* in the wild-type background strains; ATCC46645 and \DeltaakuB . The deletion was successfully complemented in the ATCC46645 background and is the first report of the deletion of a translation elongation factor in *A. fumigatus*. Phenotypic analysis was facilitated upon generation of the *A. fumigatus elfA* deletion and complementation strains, and will be described in Chapter 4.

4.1 Introduction

The availability of a fungal deletion strain accommodates phenotypic analysis with a view to elucidating possible functions of the gene of interest. Growing the deletion strain, along with the wild-type strain, in the presence of various stress-inducing agents can help identify altered phenotypes in the deletion strain. An altered phenotype in the presence of agents (e.g., H₂O₂, diamide, menadione) may indicate a possible role for the gene of interest in the response to oxidative stress. It is also important to test deletion strains for their sensitivity to antifungals to determine if the gene of interest could be a possible target to improve the efficacy of the antifungals, or alternatively if the absence of the gene affects the mode of action of the drug.

The three main classes of antifungals used in the treatment of *Aspergillus* infections are the triazoles, polyenes and echinocandins. The triazoles (e.g., voriconazole, itraconazole and posaconazole) target the ergosterol pathway and resistance is mediated in *A. fumigatus* by *cyp51A* (da Silva Ferreira *et al.*, 2005). The triazoles passively diffuse into the cell where they target the enzyme 14- α -demethylase, the product of *cyp51A*, inhibiting the synthesis of ergosterol (Sanglard and Odds, 2002). Resistance mechanisms to the triazoles have emerged that involve mutations in *cyp51A*, in both environmental and clinical isolates, which suggests a link between azole use as a fungicide and the emergence of resistant strains (Bueid *et al.*, 2010; Snelders *et al.*, 2009; Snelders *et al.*, 2008). However clinical isolates have been reported where resistance is not mediated by *cyp51A* mutations (Bueid *et al.*, 2010) indicating that other mechanisms of resistance exist. The upregulation of

cyp51A, of multidrug efflux transporters, namely the ATP-binding cassette (ABC) transporter and the major facilitator transporter, and alterations in ergosterol biosynthesis have also been implicated in azole resistance (da Silva Ferreira *et al.*, 2005; Sanglard and Odds, 2002)

The polyenes, namely amphotericin B, bind to ergosterol in the cell membrane, causing the formation of pores which results in leakage from the cell ultimately leading to cell death (Baginski *et al.*, 2006). The exact mechanism by which this occurs has not yet been fully elucidated. Oxidative stress has also been shown to be involved in the mode of action of amphotericin B (Blum *et al.*, 2008; Sokol-Anderson *et al.*, 1986). Sokol-Anderson *et al.* (1986) showed that oxidative stress was involved in the mode of action of amphotericin B in killing *C. albicans*. More recently, Blum *et al.* (2008) determined that increased catalase production in *A. terreus* plays a role in its increased resistance to amphotericin B.

The echinocandins are the newest class of antifungals and comprise caspofungin, anidulafungin and micafungin (Ostrosky-Zeichner *et al.*, 2010). The mode of action of the echinocandins is to inhibit the (1,3)- β -glucan synthase complex thereby preventing cell wall biosynthesis (Munro, 2010). (1,3)- β -glucan is synthesised by a protein complex consisting of Fks and Rho1 GTPase. Fks is the catalytic subunit of (1,3)- β -glucan synthase and studies on resistant strains have shown mutations in this protein are responsible for the acquired resistance (Munro, 2010; Douglas *et al.*, 1997). Increased chitin synthesis and the calcineurin signalling pathway have also been implicated in tolerance to the echinocandins (Walker *et al.*, 2008).

Oxidative stress occurs when the balance of reactive oxygen species (ROS) in the cell has been disturbed resulting in increased concentrations of ROS which leads to oxidative modification of cellular constituents and the disturbance of ROS-regulatory pathways (Lushchak, 2011). ROS are produced as side-products in many metabolic processes in aerobes and comprise superoxide anions ($O_2^{\cdot-}$), the hydroxyl radical ($\cdot OH$) and hydrogen peroxide (H_2O_2). The cell has both enzymatic and non-enzymatic systems to deal with increased ROS. Catalases convert H_2O_2 into H_2O and O_2 , superoxide dismutases accelerate dismutation of the superoxide anion into O_2 and H_2O_2 , while peroxidases are another enzymatic system involved in detoxifying ROS (Lushchak, 2011). The hydroxyl radical is depleted non-enzymatically and is detoxified by low molecular mass compounds such as glutathione (GSH) (López-Mirabal and Winther, 2008).

There are many different reagents which induce oxidative stress and are consequently used to study oxidative stress responses under different conditions (e.g., gene knockout strains). The most commonly used reagents are H_2O_2 , menadione, diamide and 4,4'-dipyridyl disulphide (DPS). H_2O_2 -induced oxidative stress increases the intracellular peroxide and superoxide levels and leads to the generation of $\cdot OH$ radicals (Lessing *et al.*, 2007). This results in the formation of oxidation products such as sulfinic-, sulfenic- and sulfonic-acids, and also methionine oxides (Thön *et al.*, 2010). Menadione induces the formation of superoxides, peroxides and $\cdot OH$ radicals, while it also chemically modifies cell components and enhances membrane fluidity (Pusztahelyi *et al.*, 2010). The oxidants, diamide and DPS, specifically target thiol-groups and do not result in the

formation of radicals (Pusztahelyi *et al.*, 2010; López-Mirabal and Winther, 2008; Lopez-Mirabal *et al.*, 2007). Diamide reacts with GSH and proteins leading to the formation of sulfenic acid which either generates a disulphide bond after reacting with another thiol (Scheme 1) or is oxidised to form sulfinic acid (Scheme 2) (López-Mirabal and Winther, 2008). This results in a change in the GSH/GSSG redox balance (Pusztahelyi *et al.*, 2010). DPS is also a thiol-oxidant and reacts specifically with thiol groups in thiol-disulphide reactions (López-Mirabal and Winther, 2008; Lopez-Mirabal *et al.*, 2007). These oxidised proteins can be reduced again by thioredoxins and glutaredoxins (López-Mirabal and Winther, 2008).

Glutathione is a tripeptide (γ -L-glutamyl-L-cysteinyl-L-glycine) which predominantly exists in the cell in a reduced form (GSH) but also as an oxidised form (GSSG) (Gao *et al.*, 2009). GSH plays an important role in the oxidative stress response as it directly scavenges free radicals, acts as a cofactor for anti-oxidant enzymes and is enzymatically conjugated to xenobiotics resulting in their removal from the cell (Wheeler and Grant, 2004). GSH is the most abundant low molecular mass thiol in many organisms and maintains the cytosol in a reduced state (Sato *et al.*, 2009). Under normal growth conditions, GSH is oxidised to GSSG which can then be reduced by glutathione reductase (GR) in a NADPH-dependant manner (Figure 4.1a) (López-Mirabal and Winther, 2008). The maintenance of the GSH/GSSG ratio in the cell is very important and any imbalance is an indicator as to the redox status of the cell.

Scheme 1:

Diamide reacts with a protein thiol to form a sulfenic acid derivative. This can react with another protein thiol to form a disulphide bond.

Scheme 2:

Alternatively, the sulfenic acid derivative can react with water resulting in the formation of sulfinic acid.

Under oxidative stress conditions, the levels of GSH drop while those of GSSG increase, resulting in a lower GSH/GSSG ratio (Rahman *et al.*, 2006). Once this occurs, glutathione reductase, glutaredoxins and glutathione peroxidases act to return the GSH/GSSG balance (Sato *et al.*, 2009). Glutathione also protects against oxidative stress by reversibly binding to the sulphhydryl groups of proteins in a process called glutathionylation (Wheeler and Grant, 2004). This protects the sulphhydryl groups from irreversible oxidation to sulfonic or sulfinic acid (Gao *et al.*, 2009). Deglutathionylation is catalysed by glutaredoxins (Gao *et al.*, 2009).

To investigate the GSH/GSSG ratio, total GSH and GSSG can be independently quantified using DTNB in the “recycling assay” (Figure 4.1b) (Rahman *et al.*, 2006). DTNB contains a disulphide bond which is reduced by GSH forming a TNB⁻ chromophore and an oxidised glutathione adduct. The TNB⁻ chromophore can be measured spectrophotometrically at 412 nm, while the oxidised glutathione-TNB adduct is reduced by glutathione reductase in the presence of NADPH, thereby recycling GSH back into the reaction (Figure 4.1b). GSSG is also reduced by glutathione reductase in the presence of NADPH so the total glutathione (GSH + GSSG) in a sample is measured. In order to measure GSSG only, the samples are first treated with 2-vinylpyridine, which covalently reacts with GSH only (Rahman *et al.*, 2006). GSSG is then reduced by glutathione reductase in the presence of NADPH to form 2GSH. To get the amount of GSH in a sample, the amount of GSSG is subtracted from the total GSH.

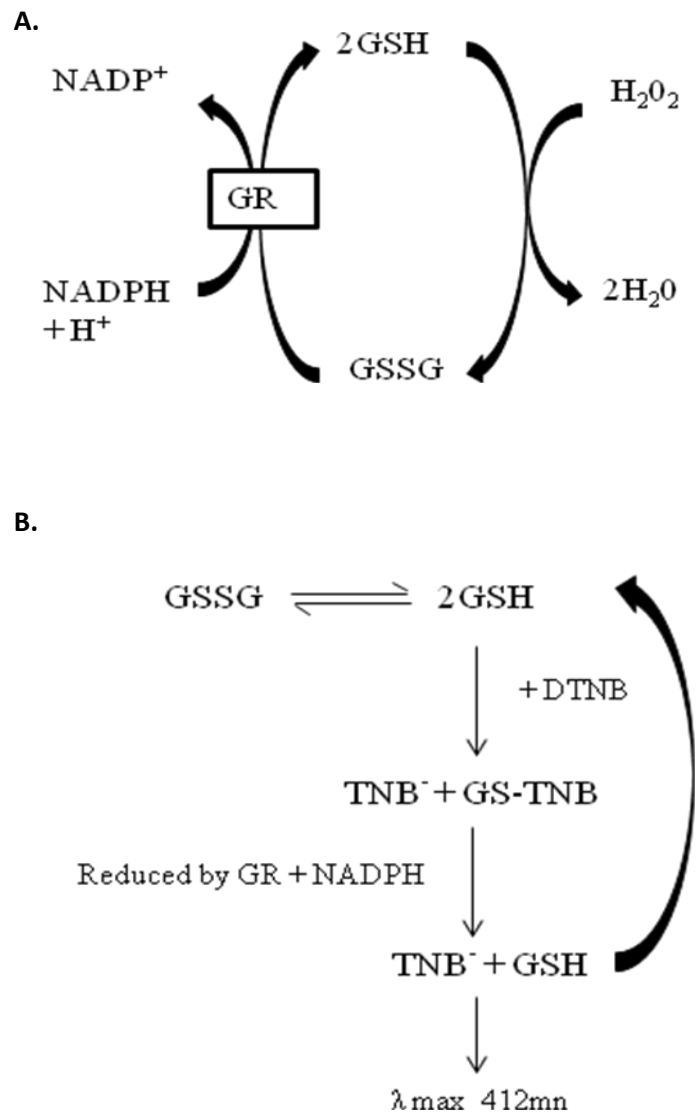


Figure 4.1: Glutathione in redox maintenance and in a quantitative assay.

- A.** The GSH/GSSG ratio is maintained through the oxidation of GSH and the subsequent reduction of GSSG by glutathione reductase (GR) in the presence of NADPH.
- B.** GSH and GSSG were quantified following the reduction of DTNB by GSH. This reaction produced a TNB^- chromophore which was measured at $A_{412\text{nm}}$.

The aims of the work presented in this chapter were (i) to carry out a phenotypic analysis of *A. fumigatus* $\Delta elfA$ in response to different conditions (e.g., oxidative stress and antifungal drug stress), (ii) to investigate the GSH/GSSG redox balance in *A. fumigatus* $\Delta elfA$ in the presence and absence of H₂O₂, (iii) to investigate any changes in the proteins susceptible to glutathionylation in *A. fumigatus* $\Delta elfA$.

4.2 Results

4.2.1 Multiple sequence alignment of *A. fumigatus elfA* and other eEF1B γ proteins

The amino acid sequences of *A. fumigatus elfA* and eEF1B γ proteins from other fungal species, plants and animals were aligned using ClustalW Multiple alignment (Section 2.2.31) (Figure 4.2). Alignment of the amino acid sequences reveals high similarity in the GST N-terminal domain between all the proteins, which was expected, as the N-terminal domain is quite conserved (Morel *et al.*, 2009; Frova *et al.*, 2006). Similarity was also observed in the GST C-terminal domain between all the proteins aligned. The eEF1B γ proteins from *S. cerevisiae*, *S. pombe* (SPAC29A4.02C only), and all the animal and plant species aligned are larger than those remaining fungal species. The extra amino acids in these proteins displayed a high level of sequence similarity and revealed that, with the exception of *S. cerevisiae* and *S. pombe*, the other fungal species used in this alignment do not contain these amino acids that appear conserved between animal and plants.

```

      10      20      30      40      50      60      70      80
AFUA_1G17120 MS-FGTIYSYPNN-PRVMKILAAANLNLSIST---PAFSFGTDNRTPPEFLAKFPFGKVPFAFEGTDG-TKLVESDAIAQ
AFUA_8G00580 -MVFGLTYTFPGDQCRTIAIKAVAKANGLDLDIR-----ETPRTPDHLISIKLQKVPFAFGADS-FKLFECMAIAL
ACLA_018390 MS-FGTIYSYPNN-PRVMKIQAAAFNNLTLTT---ADFTMGTTNRBPAFLAKFPFAKVPFAFEGADG-LTLTESDAIAQ
AFLA_109860 MSHPGTVTYTPNN-PRVMKIQAAAGNLSLSITTS---PDFQMGVTNRSEFLSKFPMGKAPAFEGADG-TLLFVESDAIAQ
AFUB_016510 MS-FGTIYSYPNN-PRVMKILAAANLNLSIST---PAFSFGTDNRTPPEFLAKFPFGKVPFAFEGTDG-TKLVESDAIAQ
ANIA_09304 MA-FGTIYSYPNN-PRVSKIQAVANLNGLTIES---GSFKLGVDNKSEEFLSKFPPLGKAPAFSTADG-VNIFESNAIAQ
AN01G09610 MS-FGTIYTPNN-PRVMKTQAAANFNNTLTLV---ADFRMGETNRDVFLSKFPPLGKVPFAFEGADG-TCLVESDAITQ
YKL081W MSQGTLYINRSPR-NYASEALISYFKLDVKIVDLE-----QSSSE-FASLFPPLKQAPAFPGPKG-LKLTEALAIQF
YPL048W MSQGTLYANFRIR-TWVPRGLVKALKLDVAVVTPD-----AAAEQFARDPFLKKVPAFVPGPKG-YKLTEAMAINY
SPAC29A4.02C -MSVGTIVYKIGS-PRVLCVSVAAVAVGVEVHVVDV-----QPHNFPADLAAKFPLQKMPFVFGKDG-FPLSETLAIAP
SPBC460.02C -MFLGTIYSFKTN-TRTPCLLELAKRLDLQVDLVET-----YHKKFPTDLAAKFPPLQKLPVFIADG-FELSEVIAIFK
SPCC1183.02 -MFLGTLYSFKTN-TRTVCLLELAKRLDLQVDLVET-----YHKKFPTDLAAKFPPLQKLPVFIADG-FELSEVIAIVK
FVEG_11084 MTSFGTLYTYMPN-ARVFKILAAAKLNLIIEI---PAYQHGVTKNSAEFLSKFPAGKVPFAFEGPDG-FCLVESDAIAQ
MG_12569 MVPPATTYSWPSD-FRASRVHALQGLGLEIVGA---PDFQMGVTNKSEEFLAKFPPLGKVPFAFETADG-FRLAESGAMAY
FBgn0029176 -MVKGLTYTYPEN-FRAYKALIAAQYSGAQVQVVA---DNFKFGETNKSAEFLSKFPAGKVPFAFEGPDG-QYLSEVIAIAY
gi | 31102 | emb | CAA45089.1 -MAAGTLYTYPEN-WRAFKALIAAQYSGAQVRLSAPPHFHFGQTNRTPEFLRKFPAKVPFAFEGDDG-FCVFEVSNAIAY
ENSMUSG00000071644 -MAAGTLYTYPEN-WRAFKALIAAQYSGAQVRLSAPPHFHFGQTNRTPEFLRKFPAKVPFAFEGDDG-FCVFEVSNAIAY
ENSOCUG00000020959 -MAAGTLYTYPEN-WRAFKALIAAQYSGAQVRLSAPPHFHFGQTNRTPEFLRKFPAKVPFAFEGDDG-FCVFEVSNAIAY
BGIBMGA008302 -MAAGVLYTYPEN-FRAYKALIAAQYSGTDVQVVA---PNFVFEGETNKSEEFLAKFPAGKVPFAFESADGKVLLETSNAIAY
F17C11.9 -----MLLQLTSS-HLELYVLVLYDT-----PAFE---GDALLFGAESIGL
AT1G09640.1 --MALVLHTYKGN-KSAEKALIAAEYVGVQIDVP---SDFQMGVTNKTPAFLKMNPIGKVPVLETPEG---SVFESNAIAR
AT1G09640.2 --MALVLHTYKGN-KSAEKALIAAEYVGVQIDVP---SDFQMGVTNKTPAFLKMNPIGKVPVLETPEG---SVFESNAIAR
LOC_Os02g12800.2 --MALVLHTFDGN-KNAFKALIAAEYSQVQVLELA---KNFQMGVSNKTPPEYLKMNPIGKVPVLETPDG---PVFESNAIAR
LOC_Os02g12800.3 -----
LOC_Os06g37440.1 --MALVLHCGSGN-KNAFKALIAAEYTVQVQVLELT---KNFEMGVSNTKPEFLKMNPLGKIPVLETPEG---AVFESNAIAR

```

```

      90      100     110     120     130     140     150     160
AFUA_1G17120 YVAESGPAQAQLLG----TKFVERAAIRQWIAFADGEIQS-PVIP-LVLPRIGLAAAFDEAVEKKNLEKLERSLAYLEGH
AFUA_8G00580 YITSONEQTTLLGK----DKKEVAEIIKMSFFNTBLIVI--LMTQQLLPQGLVPIYDRDQVEFFANMTQRSVDVVEEY
ACLA_018390 YVADSGPAQAQLLG----SSAVERAAVRQWVCFADGEVQC-PVIQ-LIPLRVGYKAFVSEVEKKSALGQLERALDYLEGH
AFLA_109860 YVAESGPAKQQLG----VSAAEERAHIRQWICFAEGDAMG-AVVP-PAIWQMLGRKRYTAEELBEEHLAKAERLGLVAEAB
AFUB_016510 YVAESGPAQAQLLG----TKFVERAAIRQWIAFADGEIQS-PVIP-LVLPRIGLAAAFDEAVEKKNLEKLERSLAYLEGH
ANIA_09304 YLAENGPAAKQQLG----STPAERATIQWVWMAETEAVAG-HVVT-CFLPRVGLVPPYNAETDNQALEKLERLGLALERH
AN01G09610 YVAESGPAQAQLVG----STPAERALLRQWICFAEGEVLG-AVTS-MVLRVGLVYKAYDEATEKESLEKLRALGALENR
YKL081W YLANQVADEKERARLLGS---DVIEKRSQILRWASLANSVMS--NIARPFLSFKGLIPYKNDVDAACFVKIDNLAAVFDAR
YPL048W YLVKLSQDDKMKTLQGLADDDLNAQQLIIRWQSLANSDLCI--QIANITIVLPKGGAPYKKSVDSAMDAVAIDKIVDFEINR
SPAC29A4.02C YLAS---LNKTRALN---GTTAEERAKVLYCSEFTNSELPG--AFRPIITAPRVFGAPYDEQAQEAATLIDFARFDEE
SPBC460.02C YFYEKGGKNDKEGLG---PINEIEEAEMLRKWCPIINFDIVTPQIVRPVWDMFRGVSVPYEDKAFKESAAARAIDSLKTIINEL
SPCC1183.02 YFYEKGGKNDKEGLG---PVINEVEEAEMLRKWCPIINFDIVTPQIVRPVWDMFRGNIPIYEEKPFKESATRAIDSLKIPNEL
FVEG_11084 YVAQSGPQASQLG----QDAMSSAKIRQWISFFAEEIYP-TVLD-LVMWRVGLGAFDETTEIKALAQLAYGLSVLEKH
MG_12569 YAAAAGNKADQLG----TDAQTKAKIMEWAFPADSELSA-NCMPIFVWCVMYKAPDENRYNSCITNIEBALGKIEAT
FBgn0029176 LLANEQLRGGK-----CFVQAQVQQWISFADNEIYP--ASCAMVFPPLGLLPQQKN--STAKQEAEAVALQQLNQK
gi | 31102 | emb | CAA45089.1 YVSNEELRGS-----TPEAAAQVQVWVSPADSDIVP--PASTWVFPPTLGMHNNKQATEENAKKEVRRILGLLDAY
ENSMUSG00000071644 YVSNEELRGS-----TPEAAAQVQVWVSPADSDIVP--PASTWVFPPTLGMHNNKQATEENAKKEVRRILGLLDTH
ENSOCUG00000020959 YVSNEELRGS-----TPEAAAQVQVWVSPADSDIVP--PASTWVFPPTLGMHNNKQATEENAKKEVRRILGLLDH
BGIBMGA008302 YVANESLRGG-----DLATQARVWQWASWSDSELLP--ASCAMVFPYGLTMQFNKQVBERAKSDLLAALGLVDGH
F17C11.9 HLTG-----TSANAEITVQWLQFAEGYLLP--AVLGVLPVSVSAANFDKKTVEYKNEVLENGQLQVLDV
AT1G09640.1 YVSRNLGDNLSL-----NGSSLIEYAQIEQWIDFSSLEIYA--SILRWFGPRMGFMPYSAPAEEGAISTLKRALDALNTH
AT1G09640.2 YVSRNLGDNLSL-----NGSSLIEYAQIEQWIDFSSLEIYA--SILRWFGPRMGFMPYSAPAEEGAISTLKRALDALNTH
LOC_Os02g12800.2 YVTRSKSDNPL-----YGSSLIEYAHIEQWIDFSATEVDA--NTGKWLFPRLGFAPYVAVSEEAATAALKRSLGALNTH
LOC_Os02g12800.3 -----
LOC_Os06g37440.1 YVARLKDNSL-----CGSSLIDYSHIEQWIDFSATEVDA--NIGRWLYPRLGFGPYVVPVLEEFAITSLKRSLGALNTH

```

```

      170     180     190     200     210     220     230     240
AFUA_1G17120 LS---GRNWIATEEKLSDADITVVSALYWFSTVIDREMRQRYPVVSWYERTIESEGVKQAFGKKKFEKREIPKA
AFUA_8G00580 LQD---RTFLVGDQLSLADLFCAGNLSLGFQFFYGKAWRQONPNVSRWYEMVCHQPIYAAVTDKQFLLEDEPKLTNNPEE
ACLA_018390 LR---GREWVAT-EKLSLADISVAALYWGFSMVIDQEMRQRYPVVSWYERTIESEGVKQAFGKKKFEKRETPKA---
AFLA_109860 LKTGGGRRLWATEEKLSDADISLVAALNWGFATVLDLAE LRARYPNVVAWYERTIESEGVKQAFGKKKFEKRPFAQ---
AFUB_016510 LS---GRNWIATEEKLSDADITVVSALYWFSTVIDREMRQRYPVVSWYERTIESEGVKQAFGKKKFEKREIPKA---
ANIA_09304 LA---GRTWLATPKQLSLADIAVAASLWGFTFVIDQEMRAKYPGVVDWFRDVTSSSEGKVEAFGKTKFIEKREVPK---
AN01G09610 LK---ERTWVAT-EKLSLADISVAALYWGFSMAIDAE MRKEYPGVVAWYERVIESEHVKEAFGPKVFEKREKPEEN---
YKL081W LRD---YTFVATENISLGLDHAAGSWAFGLATILGPEWRARHPHLMRWNTVAASPIVKTFFAEVVKLAEKALTYTPPKK
YPL048W LKN---YTYLATENISLADLVAASIFTRYPESELPGTEWRAGHPAIVRWFNTRASPEFLKDEYKDFKADKPLS--PPQK
SPAC29A4.02C LAS---RTYLVGSRRLTLADIFFTCFLEKFGATVLTLSYLAKYTHIYRYQTIYHQAKLDAITEPLKPIDQLPIIKAE
SPBC460.02C VKD---RTYLVGDRFTLADLFFGSMRLRRFFHSIIDEKTRKELPHLTRYYVTMFMHQAKLEYYP---LELPLTVTPNN
SPCC1183.02 VKD---RTYLVGDRFTLADLFFGSMRLRRFFHSIIDEKTRKELPHLTRYYVTMFMHQAKLEYYP---LELPLTVIVAKK
FVEG_11084 LN---PGILLTGDELTADLTCAGSTLLWAFMHIIDEPMRQQYPNVVAWYLVKVVQNEEVKVEVFKPNLIEKRRIGAK---
MG_12569 LAK---GNQKYLVDKRLTYADLMVFSPLFAGGSLVDAEMRKSAPTVMFSYLENLAAPLIEKTEFGLKVEKRVTL---
FBgn0029176 LQD---ATFLAGEKITLADIVVFSLLHLHYEYVLEPSVRSFAFGNVNWFVTILNQKQVAVVDKYLCEKALVDPKRY
gi | 31102 | emb | CAA45089.1 LKT---RTFLVGERVTLADITVVTCLLWLKYQVLEPSFRQAFPNTNRWFLTCINQPQFRAVLGVEVKLCERMAQFDKAKF
ENSMUSG00000071644 LKT---RTFLVGERVTLADITVVTCLLWLKYQVLEPSFRQAFPNTNRWFLTCINQPQFRAVLGVEVKLCERMAQFDKAKF

```



```

YPL048W          RGQDYV--PAFDVAPDWE SYDYAKLDPTNDDDK EFINNMWAWDKPVSVNGE--PKEIVDGRVLEK
SPAC29A4.02C    KGHDIY--PAFDVAPDWG SYTFTTKLDINKPEDKAFIEDAWAWDKPIEGR-----EVADGRVCK
SPBC460.02C    -----
SPCC1183.02    -----
FVEG_11084     -----
MGG_12569      -----
FBgn0029176    RGQDLAFTLSPDWQIDYEVYD WKKLDAKSEETKKLVLTQYFWSWG--TDKD---GRKFNQGGKIFK
gi|31102|emb|CAA45089.1  RGQELAFPLSPDWQVDYESTYWRKLDPGSEETQTLVREYFWSWEG-AFQHV--GKAFNQGKIFK
ENSMUSG00000071644  RGQELAFPLSPDWQVDYESTYWRKLDPGSEETQTLVREYFWSWEG-TFQHV--GKAVNQGKIFK
ENSOCUG00000020959  RGQELAFPLSPDWQVDYESTYWRKLD-----
BGIBMGA008302   RGKELVFPPLSSDWQVDYESTYD WKKLDPSSEETKKLVQDYFWSWG--TDKD---GRKFNQGGKIFK
F17C11.9        KGDKLAFELSPDWQVDYESTYWRKLD AKSDATKKEVNEYLWMEG--DFG---GKKNQGGKIFK
AT1G09640.1     RGPEIP-KFIMDEVYDMELYEWTKVDISDEA QKERVS--QMIEDAEPFE---GEALLDARCFK
AT1G09640.2     RGPEIP-KFIMDEVYDMELYEWTKVDISDEA QKERVS--QMIEDAEPFE---GEALLDARCFK
LOC_Os02g12800.2  RGPEIP-KFVMDEVYDMELYEWTKVDISDEA QKERVS--AMIEDLEPFE---GEALLDARCFK
LOC_Os02g12800.3  RGPEIP-KFVMDEVYDMELYEWTKVDISDEA QKERVS--AMIEDLEPFE---GEALLDARCFK
LOC_Os06g37440.1  RGQDIIP-KFVMDEVYDMELYEWTKVDLSDEA QKERVN--AMIEDQEPFE---GEDLLDARCFK

```

Figure 4.2: Multiple sequence alignment of amino acid sequences of *A. fumigatus* *elfA* and other eEF1 β proteins. The GST N-terminal domain is indicated by the black line, while the GST C-terminal domain is indicated by the red line. eEF1 β proteins were from the following fungi: *A. fumigatus* Af293 (AFUA_1G17120 (ElfA), AFUA_8G00580 (ElfB)); *A. clavatus* (ACLA_018390); *A. flavus* (AFLA_109860); *A. fumigatus* A1163 (AFUB_016510); *A. nidulans* (ANIA_09304); *A. niger* (An01g09610); *S. cerevisiae* (YKL881W (Tef4), YPL048W (Tef3)); *S. pombe* (SPAC29A4.02C, SPBC460.02C, SPCC1183.02); *Giberlla moniloformis* (FVEG_11804); *Magnaporthe oryzae* (MGG_12569), animals: *Drosophila melanogaster* (FBgn0029176); *Homo sapiens* (gi/31102/emb/CAA45089.1); Mouse (ENSMUSG00000071644); Rabbit (ENSOCUG00000020959); Silkworm (BGIBMGA008302); *C. elegans* (F17C11.9), and plants: *Arabidopsis thaliana* (ATIG09640.1, ATIG09640.2); *Oryza sativa* (LOC_Os02g12800.2, LOC_Os02g12800.3, LOC_Os06g37440.1).

4.2.2 Phenotypic analysis of *A. fumigatus* $\Delta elfA$

In order to identify any phenotypes associated with the deletion of *A. fumigatus* *elfA*, *A. fumigatus* ATCC46645, $\Delta elfA$ and *elfA*^C were grown in the presence of various stress-inducing compounds as outlined in Section 2.1.6. No difference in growth rate or sporulation was observed between *A. fumigatus* ATCC46645, $\Delta elfA$ and *elfA*^C when grown on AMM only (Figure 4.3).

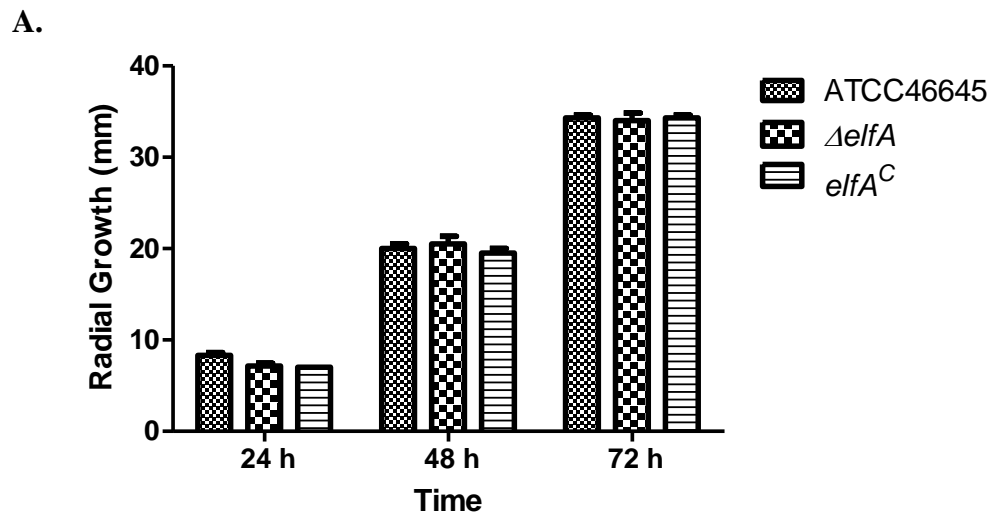


Figure 4.3: Growth of *A. fumigatus* ATCC46645, $\Delta elfA$ and $elfA^C$ on AMM only.

A. Radial growth of *A. fumigatus* ATCC46645, $\Delta elfA$ and $elfA^C$ on AMM for 24 – 72 h shows no significant difference in growth between these strains.

B. No difference in radial growth, sporulation or pigmentation was observed between ATCC46645 and $\Delta elfA$.

4.2.2.1 Phenotypic analysis of *A. fumigatus* Δ *elfA* in response to amphotericin B

A. fumigatus Δ *elfA* was investigated for an altered phenotype in the presence of the antifungal amphotericin B. *A. fumigatus* ATCC46645, Δ *elfA* and *elfA*^C were grown on AMM in the presence of amphotericin B (0 – 1 μ g/ml). No significant difference was observed between the three strains (Figure 4.4)

4.2.2.2 Phenotypic analysis of *A. fumigatus* Δ *elfA* in response to gliotoxin

Gliotoxin is produced by *A. fumigatus* and is involved in the virulence of the fungus (Gardiner *et al.*, 2005). Recently it has been shown that *A. fumigatus* is sensitive to gliotoxin in the absence of a gene involved in self-protection; *gliT* (Schrettl *et al.*, 2010). *A. fumigatus* ATCC46645 and Δ *elfA* were grown on AMM in the presence of gliotoxin (0 – 10 μ g/ml), concentrations previously shown to impair growth upon deletion of a gene involved in self-protection (Scharf *et al.*, 2010; Schrettl *et al.*, 2010). No difference was observed between the growth of these two strains (Figure 4.5), indicating that *A. fumigatus* *elfA* is not involved in self-protection against gliotoxin. Because *A. fumigatus* Δ *elfA* did not display an altered phenotype towards gliotoxin, it was unnecessary to repeat this using *A. fumigatus* *elfA*^C.

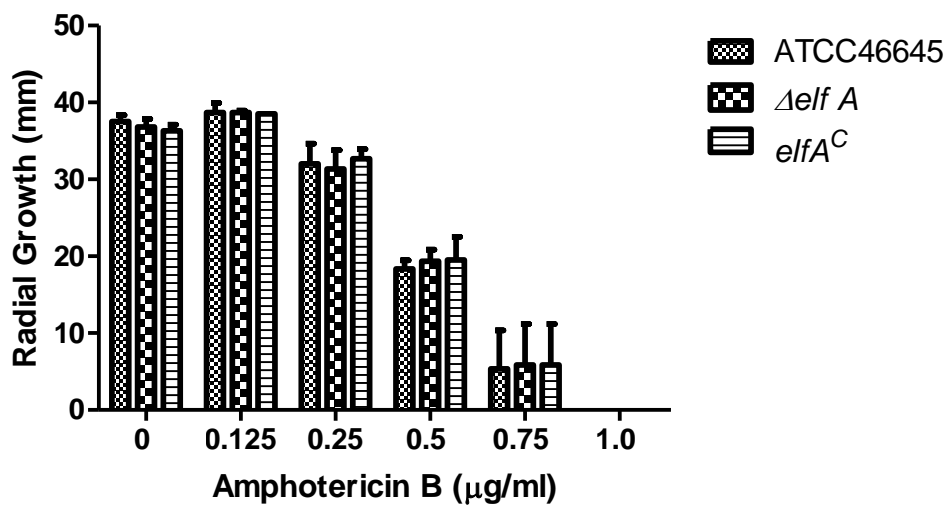


Figure 4.4: Growth of *A. fumigatus* ATCC46645, $\Delta elfA$ and $elfA^C$ on AMM containing amphotericin B (0 – 1 $\mu\text{g/ml}$). No differences were observed in growth of *A. fumigatus* ATCC46645, $\Delta elfA$ and $elfA^C$ in the presence of amphotericin B.

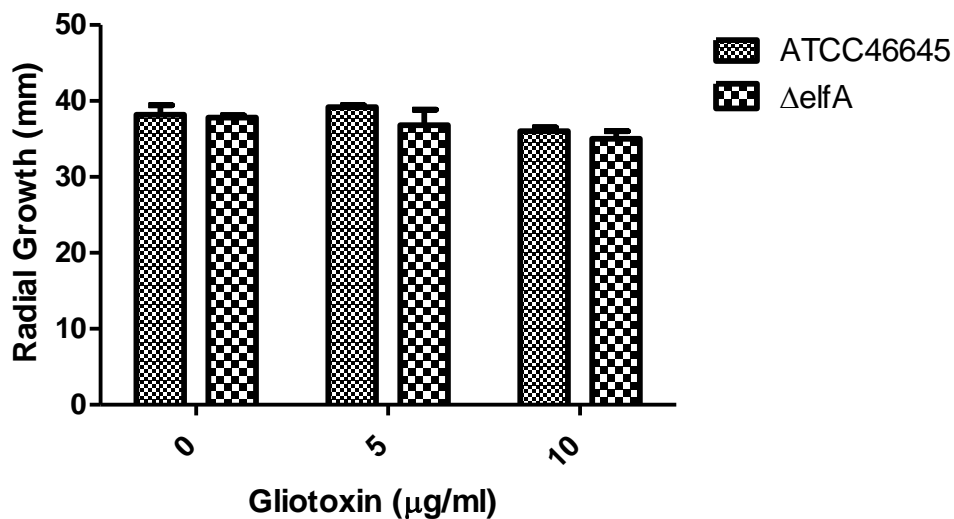


Figure 4.5: Growth of *A. fumigatus* ATCC46645 and $\Delta elfA$ on AMM containing gliotoxin (0 – 10 $\mu\text{g/ml}$). *A. fumigatus* $\Delta elfA$ did not exhibit an altered phenotype compared to *A. fumigatus* ATCC46645.

4.2.2.3 Phenotypic analysis of *A. fumigatus* Δ *elfA* in response to Glycerol-induced osmotic stress

A. fumigatus ATCC46645, Δ *elfA* and *elfA*^C were grown on AMM containing glycerol (0 – 10 % (v/v)) to determine if *A. fumigatus* Δ *elfA* had an altered phenotype as a result of osmotic stress. There were no differences observed in the growth of the three strains (Figure 4.6), indicating that *A. fumigatus* *elfA* is not involved in the response to osmotic stress.

4.2.2.4 Analysis of *A. fumigatus* Δ *elfA* protease secretion capacity

To investigate if *A. fumigatus* Δ *elfA* had an impaired protease secretory capacity, *A. fumigatus* ATCC46645, Δ *elfA* and *elfA*^C were grown on skimmed milk agar (0.5 % (w/v)) (Richie *et al.*, 2009). Skimmed milk is a complex lipoproteinaceous substrate and therefore any impairment in the secretory capacity of *A. fumigatus* Δ *elfA* would affect its ability to acquire nutrients from the complex substrate. The UPR affects the secretory pathway as it is involved in ER homeostasis (Richie *et al.*, 2009), and any differences observed in *A. fumigatus* Δ *elfA* may also be indicative of an altered UPR response. No differences in growth were observed between the three strains (Figure 4.7) indicating that *A. fumigatus* Δ *elfA* does not have an altered secretome compared to *A. fumigatus* ATCC46645.

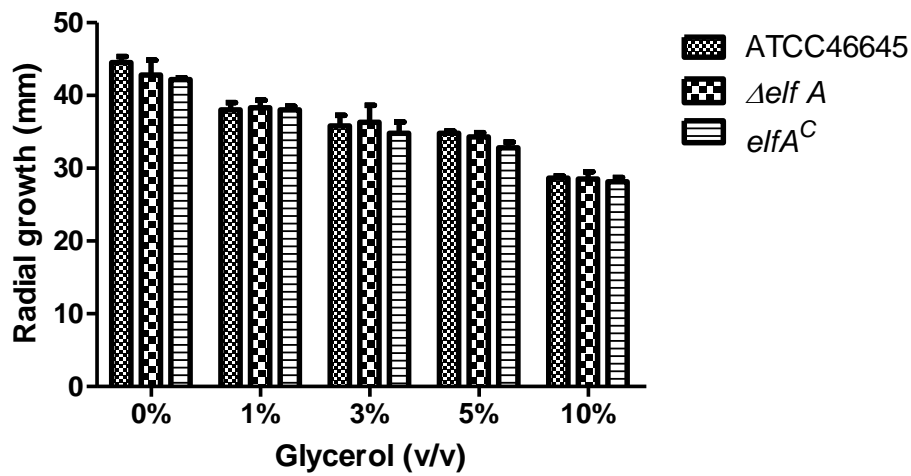


Figure 4.6: Growth of *A. fumigatus* ATCC46645, $\Delta elfA$ and $elfA^C$ on AMM containing glycerol (0 – 10 % (v/v)). *A. fumigatus* ATCC46645, $\Delta elfA$ and $elfA^C$ all displayed a similar phenotype.

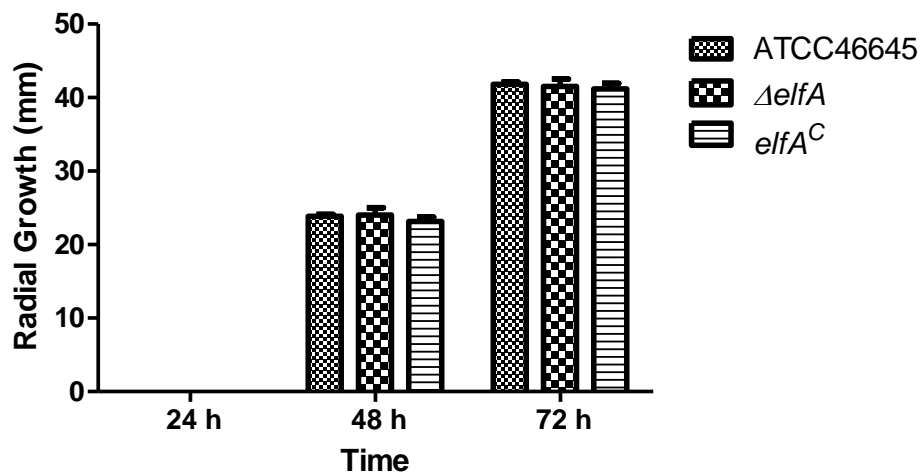


Figure 4.7: Growth of *A. fumigatus* ATCC46645, $\Delta elfA$ and $elfA^C$ on skimmed milk agar. There was no difference observed in growth of *A. fumigatus* $\Delta elfA$ when compared to *A. fumigatus* ATCC46645 and $elfA^C$ on skimmed milk (0.5 % (w/v)) indicating that there is no impairment of *A. fumigatus* $\Delta elfA$ secretory capacity.

4.2.2.5 Phenotypic analysis of *A. fumigatus* $\Delta elfA$ in response to DTT

Dithiothreitol (DTT) is a reducing agent and also induces endoplasmic reticulum (ER) stress (Back *et al.*, 2005). In the presence of ER stress, the UPR is activated in response to the increased levels of unfolded and misfolded proteins, and is involved in restoring ER homeostasis (Richie *et al.*, 2009). *A. fumigatus* ATCC46645, $\Delta elfA$ and *elfA*^C were grown in AMM liquid culture in the presence of DTT (0 – 5 mM) and the growth rate determined. There was no significant difference observed between the growth rates of any of the three strains (Figure 4.8).

4.2.2.6 Phenotypic analysis of *A. fumigatus* $\Delta elfA$ in response to voriconazole

To determine if *A. fumigatus* $\Delta elfA$ displayed a different phenotype to that of the wild-type to the antifungal voriconazole, *A. fumigatus* ATCC46645, $\Delta elfA$ and *elfA*^C were grown on AMM agar plates containing voriconazole (0 – 1 µg/ml). *A. fumigatus* $\Delta elfA$ was more resistant ($p = 0.0251$) to voriconazole (0.5 µg/ml) than *A. fumigatus* ATCC46645 and *elfA*^C after 72 h (Figure 4.9)

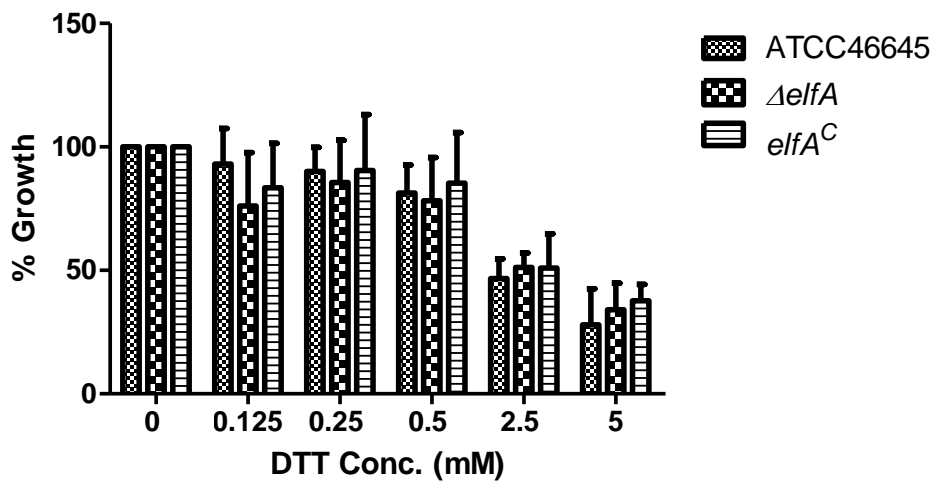


Figure 4.8: Growth of *A. fumigatus* ATCC46645, $\Delta elfA$ and $elfA^C$ in the presence of DTT. No significant difference in growth was observed between *A. fumigatus* ATCC46645, $\Delta elfA$ and $elfA^C$ when grown in the presence of DTT (0 – 5 mM).

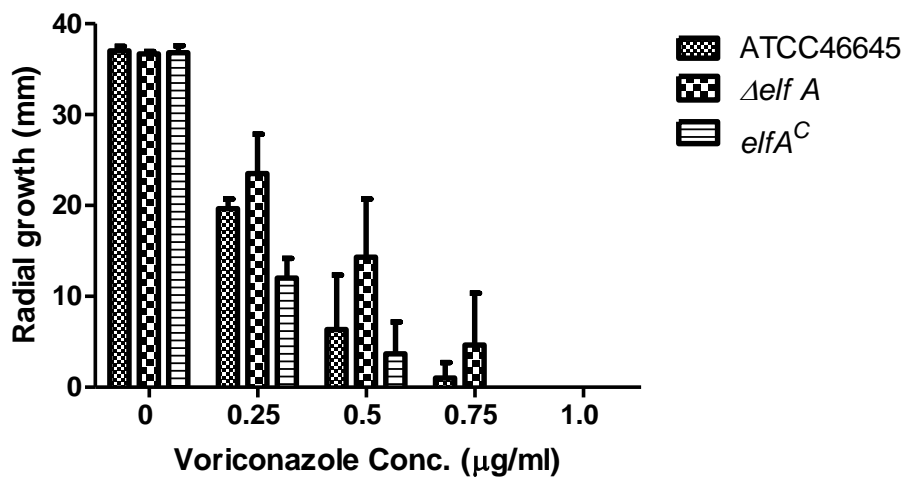


Figure 4.9: Effect of voriconazole (0 - 1 $\mu\text{g/ml}$) on the growth of *A. fumigatus* ATCC46645, $\Delta elfA$ and $elfA^C$ after 72 h. $\Delta elfA$ is significantly more resistant to voriconazole compared to ATCC46645 and $elfA^C$ at 0.5 $\mu\text{g/ml}$ ($p = 0.0251$). Data analysis by one-way ANOVA.

4.2.2.8 Phenotypic analysis of *A. fumigatus* Δ *elfA* in response to oxidative stress

As *A. fumigatus* *elfA* was previously observed to possess GST activity (Carberry *et al.*, 2006), one of its possible roles is an involvement in the oxidative stress response. *A. fumigatus* Δ *elfA* was investigated to ascertain if it displayed an altered phenotype in response to the oxidative stress-inducing agents, menadione, DPS, H₂O₂ and diamide. *A. fumigatus* ATCC46645, Δ *elfA* and *elfA*^C were grown on AMM agar plates containing menadione (0 – 50 μ M), DPS (0 – 7.5 μ M), H₂O₂ (0 – 5 mM) and diamide (0 – 4 mM). *A. fumigatus* Δ *elfA* did not display any significant growth differences in the presence of menadione when compared to *A. fumigatus* ATCC46645 and *elfA*^C (Figure 4.10). However *A. fumigatus* Δ *elfA* was found to be significantly more sensitive to DPS, H₂O₂ and diamide. After 96 h of growth, it was observed that *A. fumigatus* Δ *elfA* was significantly more sensitive to 7.5 μ M DPS ($p = 0.0007$) compared to *A. fumigatus* ATCC46645 or *elfA*^C (Figure 4.11). After 48 h of growth on AMM in the presence of H₂O₂, *A. fumigatus* Δ *elfA* was significantly more sensitive to 1 mM H₂O₂ ($p = 0.0026$) (Figure 4.12). After 72 h of growth, *A. fumigatus* Δ *elfA* was also significantly more sensitive to 1 mM H₂O₂ ($p = 0.0006$) (Figure 4.12). *A. fumigatus* Δ *elfA* was significantly more sensitive to 0.5 mM diamide after both 48 ($p = 0.0041$) and 72 h ($p = 0.0001$) of growth (Figure 4.13). It was observed that the wild-type phenotype was not fully restored to *A. fumigatus* *elfA*^C upon exposure to H₂O₂ and diamide.

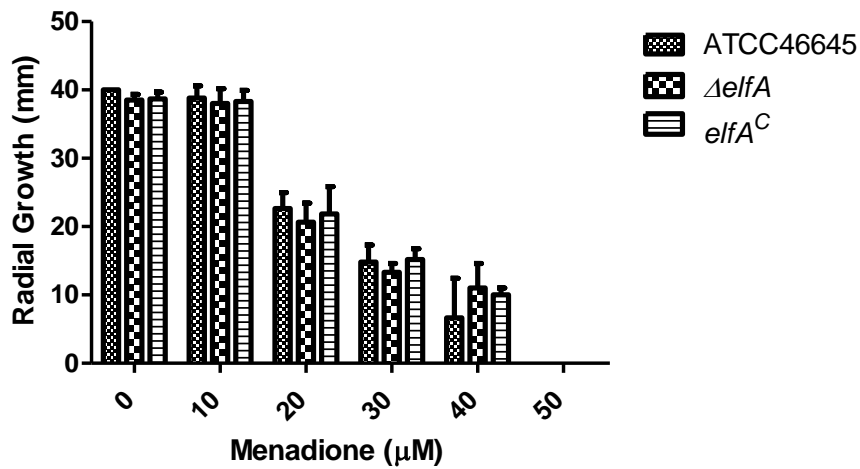


Figure 4.10: Growth of *A. fumigatus* ATCC46645, $\Delta elfA$ and $elfA^C$ on AMM containing menadione. *A. fumigatus* ATCC46645, $\Delta elfA$ and $elfA^C$ displayed the same radial growth in the presence of menadione (0 – 50 μM).

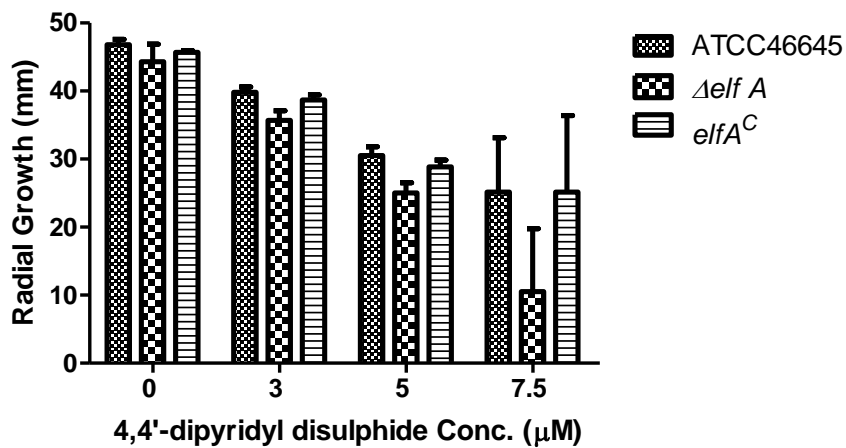


Figure 4.11: Effect of 4,4'-dipyridyl disulphide (0 – 7.5 μM) on the growth of *A. fumigatus* ATCC46645, $\Delta elfA$ and $elfA^C$. There is significant growth inhibition of $\Delta elfA$ compared to ATCC46645 and $elfA^C$ at 7.5 μM 4,4'-dipyridyl disulphide ($p = 0.0007$). Data analysis by one-way ANOVA.

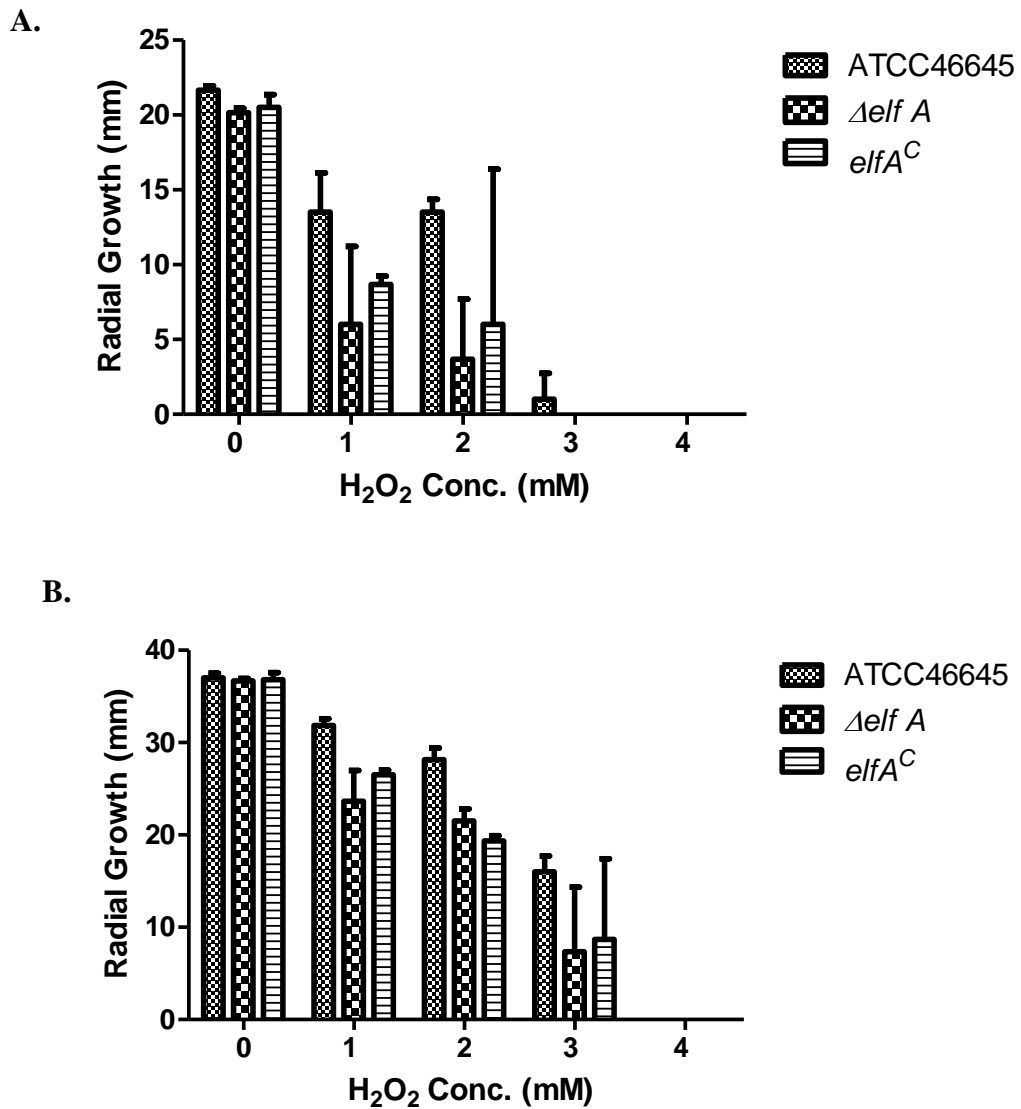


Figure 4.12: Growth of *A. fumigatus* ATCC46645, $\Delta elfA$ and $elfA^C$ on AMM containing H₂O₂.

A. Effect of H₂O₂ (0 - 4 mM) on the growth of *A. fumigatus* ATCC46645, $\Delta elfA$ and $elfA^C$, respectively after 48 h. There is significant growth inhibition of $\Delta elfA$ compared to ATCC46645 ($p = 0.0026$).

B. Effect of H₂O₂ (0 - 4 mM) on the growth of *A. fumigatus* ATCC46645, $\Delta elfA$ and *elfA*^C, respectively after 72 h. There is significant growth inhibition of $\Delta elfA$ compared to ATCC46645 (p = 0.0006). Data analysis by one-way ANOVA.

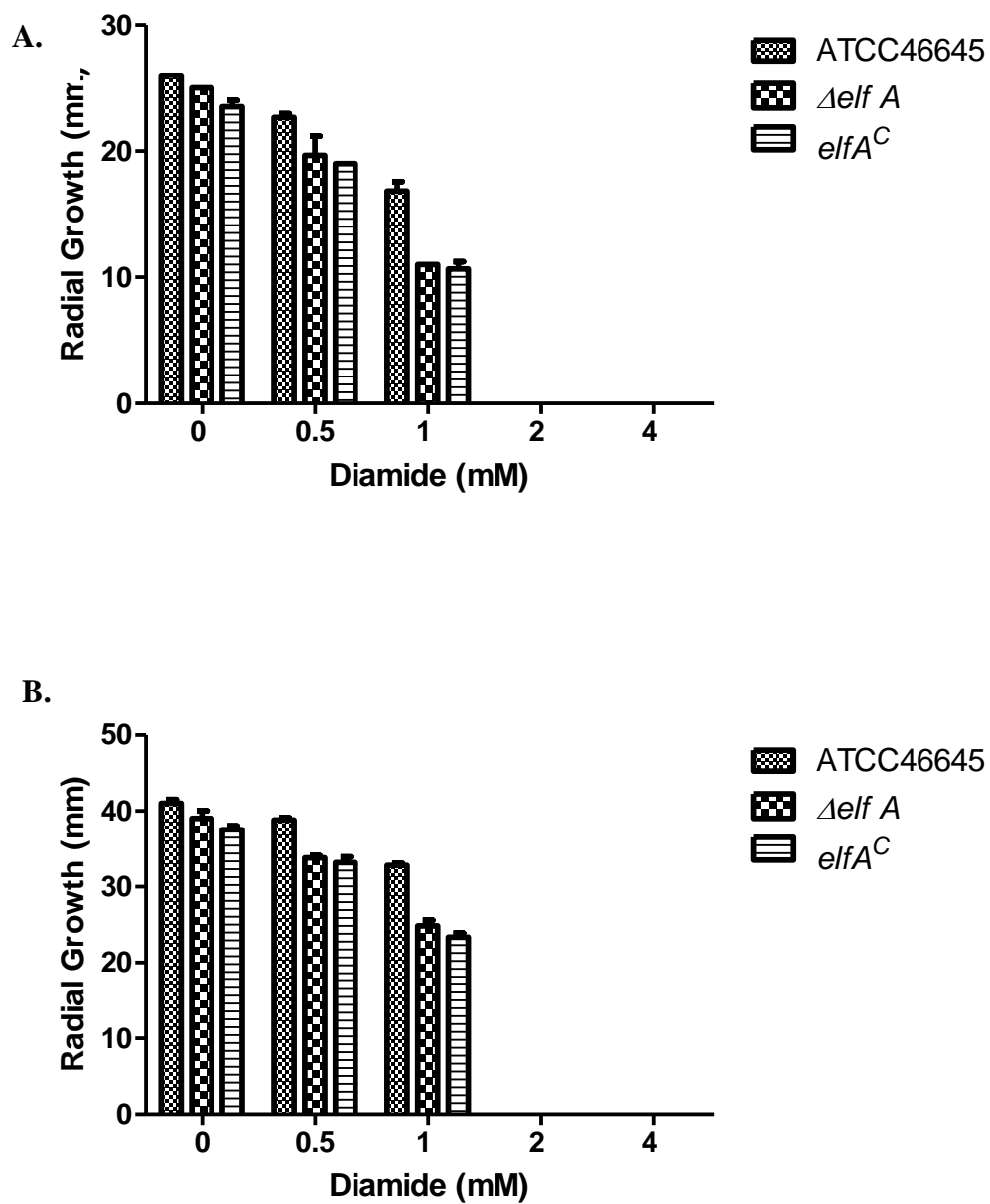


Figure 4.13: Effect of diamide (0 – 4 mM) on the growth of *A. fumigatus* ATCC46645, $\Delta elfA$ and $elfA^C$. After 48 h (A.) and 72 h (B.) growth there was significant growth inhibition of $\Delta elfA$ compared to ATCC46645 (48 h: $p = 0.0041$; 72 h: $p = 0.0001$) Diamide. Data analysis by one-way ANOVA.

4.2.3 Intracellular glutathione measurement

4.2.3.1 GSH and GSSG determination

In order to measure the intracellular total GSH and GSSG levels, standard curves for GSH and GSSG were constructed as described in Section 2.2.25 following independent assays and optimisation of the reaction time (data not shown). The standards were prepared at a concentration range of 26.4 – 0.4125 nmol/ml and assayed as described in Section 2.2.25.5. A linear relationship occurs between the concentration of glutathione and the absorbance. The standard curves (Figure 4.14) were used in subsequent assays to calculate the amount of intracellular GSH and GSSG in fungal extracts.

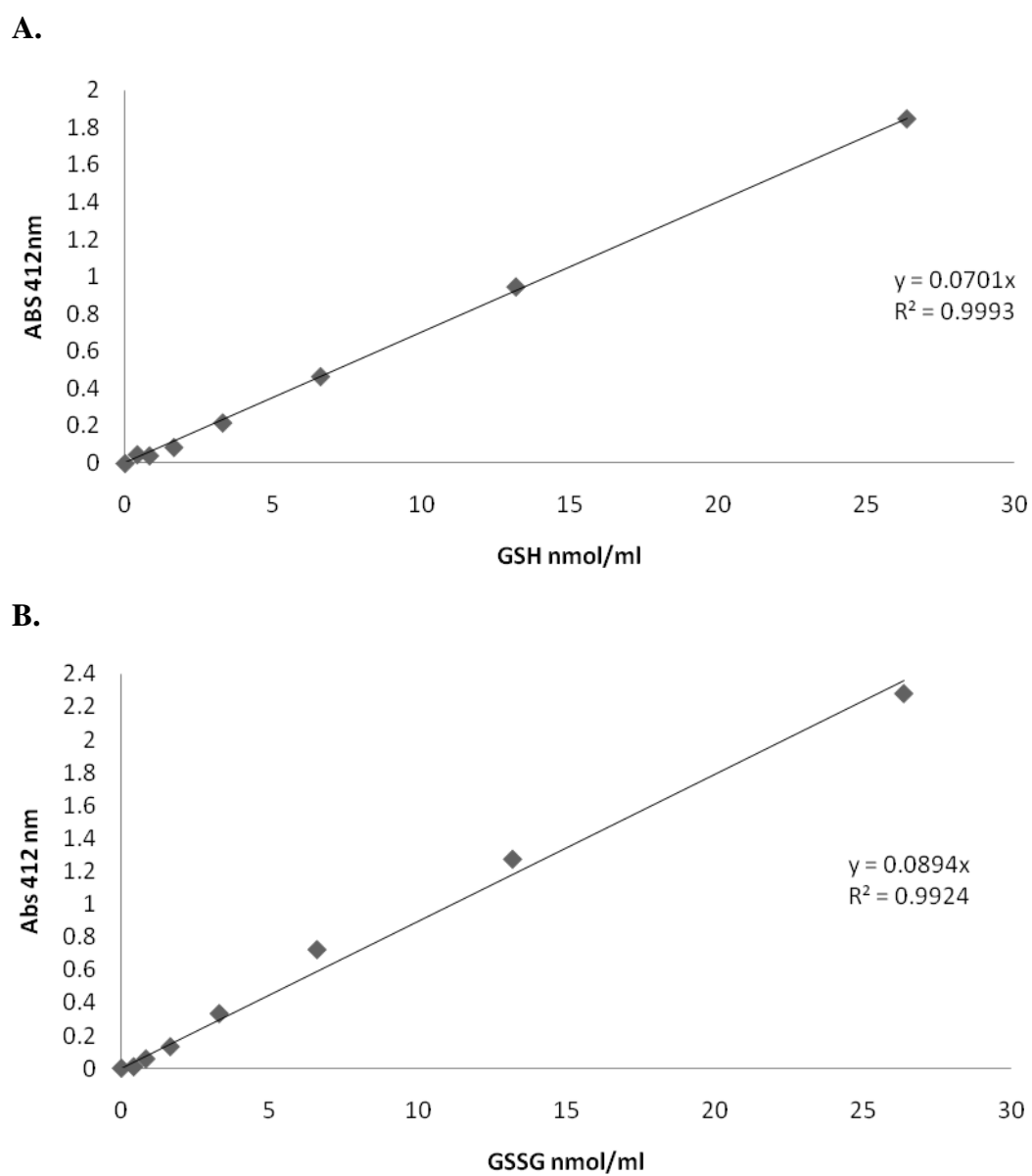


Figure 4.14: GSH and GSSG standard curves.

A. Standard curve prepared for the measurement of GSH

B. Standard curve prepared for the measurement of GSSG

4.2.3.2 Measurement of the intracellular GSH and GSSG levels in *A. fumigatus* strains under normal growth conditions

The intracellular levels of GSH and GSSG, respectively, were determined in *A. fumigatus* $\Delta elfA$ and compared to those in *A. fumigatus* ATCC46645 and *elfA*^C. Preparations for glutathione measurement and for protein quantification were extracted from mycelia harvested from 24 h cultures in AMM as described in Sections 2.2.25.1 and 2.2.16.2 respectively. Those for GSSG measurement were pre-treated with 2-vinylpyridine (Section 2.2.25.4) before analysis as described in Section 2.2.25.5. The optimum amount of 2-vinylpyridine required to react with the GSH in fungal extracts was experimentally determined (Data not shown). The concentration of total GSH or GSSG was calculated from the standard curves. The GSH concentration was calculated by subtracting the GSSG concentration from the total GSH concentration, and both were expressed as per mg protein.

Under normal growth conditions (AMM 24 h cultures), the level of GSH in *A. fumigatus* $\Delta elfA$ was lower than that in *A. fumigatus* ATCC46645, while the amount of GSSG in *A. fumigatus* $\Delta elfA$ is higher than that measured in *A. fumigatus* ATCC46645 or *elfA*^C (Figure 4.15). While these changes in GSH and GSSG between the two strains was not determined as significant, the same trend was observed over many experiments. The observation of lower GSH and higher GSSG levels in *A. fumigatus* $\Delta elfA$ is indicative of cells under oxidative stress. The GSH/GSSG ratio for *A. fumigatus* $\Delta elfA$ is lower than the ratios observed for *A. fumigatus* ATCC46645 or *elfA*^C (wild-type; 5.6, $\Delta elfA$; 3.3, *elfA*^C; 6.0).

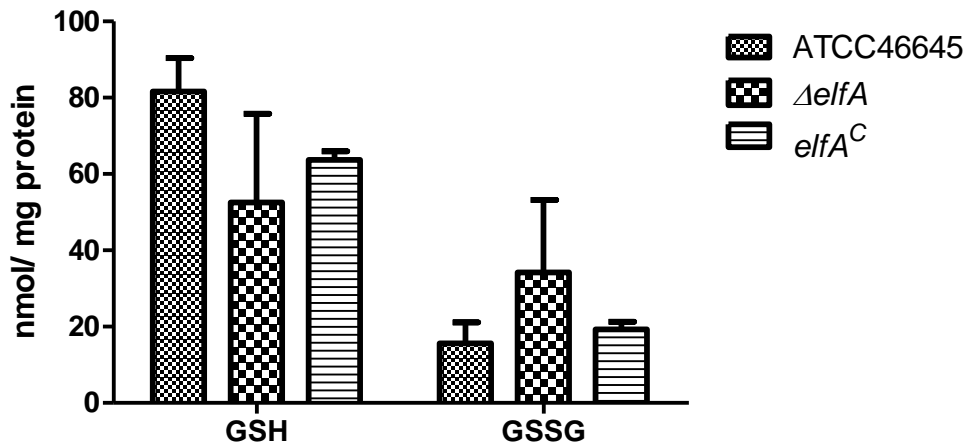


Figure 4.15: GSH and GSSG determination in *A. fumigatus* ATCC46645, $\Delta elfA$ and $elfA^C$ under normal growth conditions. A reduction in the amount of GSH and an increase in GSSG amounts in *A. fumigatus* $\Delta elfA$ compared to the other two strains was observed. This indicates that *A. fumigatus* $\Delta elfA$ is undergoing oxidative stress.

4.2.3.3 Investigation of intracellular GSH and GSSG levels in *A. fumigatus* $\Delta elfA$ after exposure to H₂O₂

As the GSH/GSSG ratio of *A. fumigatus* $\Delta elfA$ indicates that it is undergoing oxidative stress under normal growth conditions, and also since it was sensitive to oxidative stress induced by H₂O₂, DPS and diamide, the GSH/GSSG ratio was determined when subjected to stress from H₂O₂ in *A. fumigatus* ATCC46645, $\Delta elfA$ and $elfA^C$. *A. fumigatus* ATCC46645, $\Delta elfA$ and $elfA^C$ were cultured in AMM for 24 h before 2 mM H₂O₂ final was added. Mycelia were harvested after 15 and 30 min and the samples for GSH/GSSG and protein measurement were extracted, treated and quantified as described earlier in Section 4.2.3.2.

Following exposure to H₂O₂ for 15 and 30 min, the GSH/GSSG ratios in *A. fumigatus* ATCC46645 decreased as a result of decreased GSH and increased GSSG, indicating a response to oxidative stress (Table 4.1). However, in *A. fumigatus* $\Delta elfA$, exposure to H₂O₂ for 15 min resulted in an increased GSH/GSSG ratio, while there was a decrease in the GSH/GSSG ratio following 30 min exposure to H₂O₂ (Tables 4.1 and 4.2). The increased GSH/GSSG ratio following 15 min exposure of *A. fumigatus* $\Delta elfA$ to H₂O₂ resulted from decreased GSH and GSSG levels (Figure 4.16). While after 30 min exposure to H₂O₂, an increase in the amount of GSH in *A. fumigatus* $\Delta elfA$ and a slight decrease in the amount of GSSG resulted in the decreased GSH/GSSG ratio (Figure 4.17). A significant difference ($p < 0.05$) between the amounts of GSH in *A. fumigatus* ATCC46645 and $\Delta elfA$ following 30 min exposure to H₂O₂ was observed. While significant differences were not noted for the other conditions investigated, the same trend in GSH/GSSG ratios was

observed over repeated experiments and the lack of significance may be attributed to the robustness of the assay.

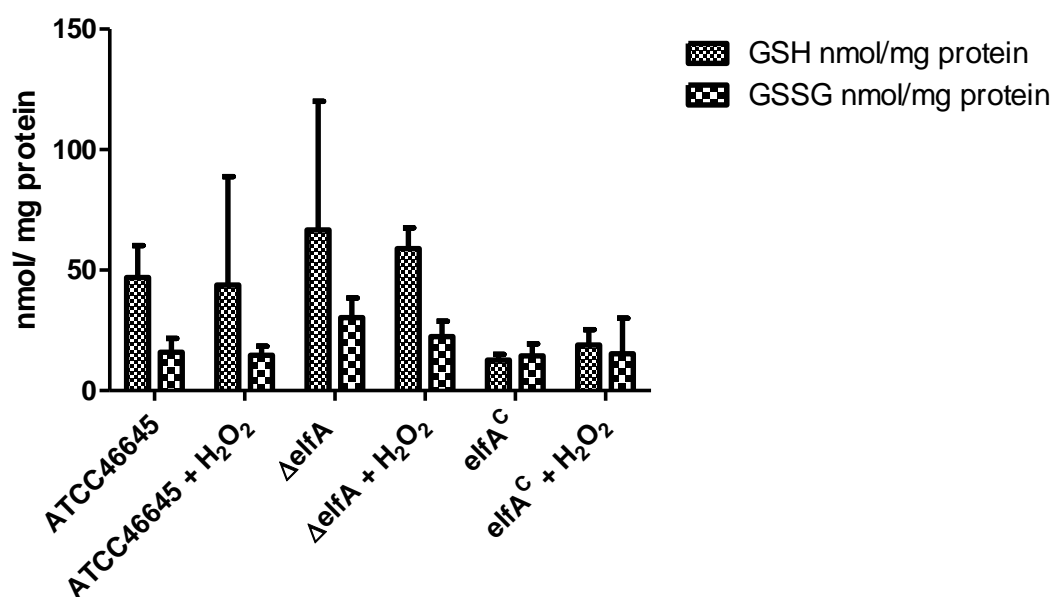


Figure 4.16: The amount of GSH and GSSG in *A. fumigatus* ATCC46645, $\Delta elfA$ and $elfA^C$ in the absence and presence of 2 mM H₂O₂ for 15 min. There is a slight decrease in the level of GSH in *A. fumigatus* ATCC46645 in the presence of H₂O₂ while the level of GSSG slightly increases. There is a slight decrease in the amounts of GSH and GSSG in *A. fumigatus* $\Delta elfA$ following exposure to H₂O₂.

Table 4.1: GSH/GSSG ratios for *A. fumigatus* ATCC46645, $\Delta elfA$ and $elfA^C$

<i>A. fumigatus</i> strain	AMM	AMM + 2 mM H ₂ O ₂ ^a	
		<u>GSH/GSSG</u>	
ATCC46645	3.35	2.7	
$\Delta elfA$	2.01	2.78	
$elfA^C$	0.9	1.92	

^a 15 min incubation

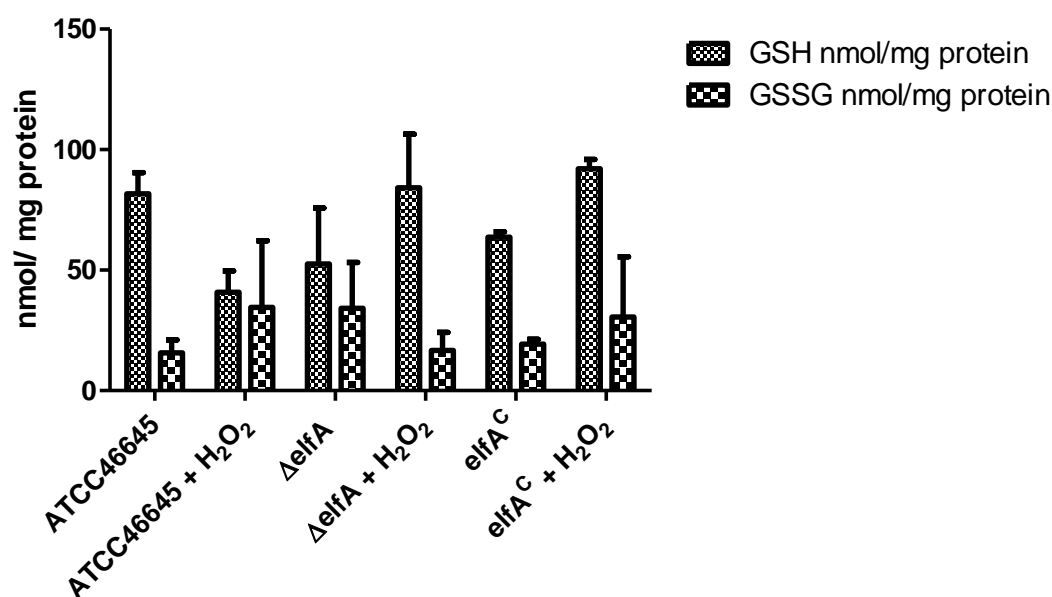


Figure 4.17: The amount of GSH and GSSG in *A. fumigatus* ATCC46645, $\Delta elfA$ and $elfA^C$ in the absence and presence of 2 mM H₂O₂ for 30 min. In *A. fumigatus* ATCC46645 there is a decrease in the amount of GSH and an increase in GSSG levels upon exposure to H₂O₂. However, in *A. fumigatus* $\Delta elfA$ there is an increase in GSH levels and a decrease in the amount of GSSG present after being exposed to H₂O₂.

Table 4.2: GSH/GSSG ratios for *A. fumigatus* ATCC46645, $\Delta elfA$ and $elfA^C$

<i>A. fumigatus</i> strain	AMM	AMM + 2 mM H ₂ O ₂ ^a	
		<u>GSH/GSSG</u>	
ATCC46645	5.66		2.05
$\Delta elfA$	3.33		1.90
$elfA^C$	5.96		4.44

^a 30 min incubation

4.2.3.4 Determination of an altered redox status in *A. fumigatus* $\Delta gliT$

The GSH/GSSG ratio was also measured in another *A. fumigatus* deletion strain; *A. fumigatus* $\Delta gliT$ (Schrettl *et al.*, 2010). *A. fumigatus* $\Delta gliT$ was transformed with the resistance marker *ptrA*, as was *A. fumigatus* $\Delta elfA$; thereby serving as a control to ensure that the results observed were as a consequence of the deletion of *A. fumigatus* $\Delta elfA$ and not the introduction of *ptrA*. While *A. fumigatus* *elfA*^C acts as a control for the wild-type phenotype, it contains *ptrA* along with a second resistance marker *hph*, and therefore is not a control for the consequences of the introduction of *ptrA*. The GSH/GSSG ratio was measured in *A. fumigatus* ATCC26933 and *A. fumigatus* $\Delta gliT$ under normal growth conditions and in the presence of gliotoxin (5 $\mu\text{g/ml}$), to which it has been shown by Schrettl *et al.* (2010) to be sensitive. *A. fumigatus* ATCC26933 and $\Delta gliT$ were cultured for 21 h in AMM before the addition of gliotoxin at a final concentration of 5 $\mu\text{g/ml}$ for 3 h. The mycelia were harvested and the samples for GSH/GSSG and protein measurement were extracted, treated and quantified as described earlier in Section 4.2.3.2.

The GSH/GSSG ratio in *A. fumigatus* ATCC26933 was 8.15, while it was increased to 47.5 in *A. fumigatus* $\Delta gliT$ (Table 4.3). This dramatic increase in ratio in *A. fumigatus* $\Delta gliT$ can be attributed to a significant increase ($p < 0.05$) in GSH levels as there was no observed difference in the GSSG levels (Figure 4.18). Upon exposure of both *A. fumigatus* ATCC26933 and $\Delta gliT$ to gliotoxin, the GSH/GSSG ratios in both strains decreased (Table 4.3). This drop in ratios was due to a decrease in GSH in both strains while the levels of GSSG were unchanged following exposure to gliotoxin (Figure 4.18). Even following exposure to gliotoxin, there remained a

significant difference ($p < 0.05$) in the amount of GSH in *A. fumigatus* ATCC26933 and $\Delta gliT$.

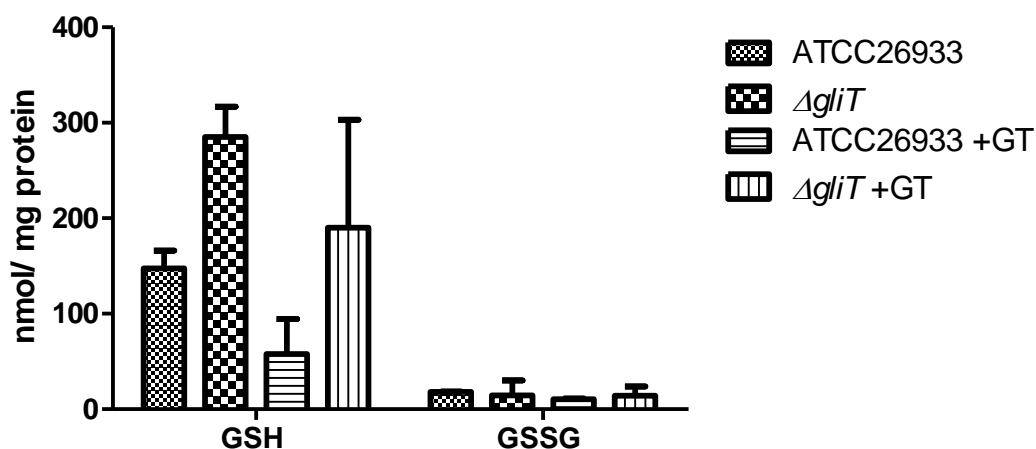


Figure 4.18: The amount of GSH and GSSG present in *A. fumigatus* ATCC26933 and $\Delta gliT$ in the absence and presence of gliotoxin (GT) for 3 h. There is a significant ($p < 0.05$) 1.9 fold increase in GSH levels in *A. fumigatus* $\Delta gliT$ compared to *A. fumigatus* ATCC26933 under normal growth conditions. However, upon exposure to gliotoxin (5 $\mu\text{g/ml}$), the levels of GSH in both strains decrease, while there is little change in GSSG levels in both strains. There still remained a significant difference ($p < 0.05$) in the GSH levels between *A. fumigatus* ATCC26933 and $\Delta gliT$ following exposure to gliotoxin.

Table 4.3: The GSH/GSSG ratios for *A. fumigatus* ATCC26933 and $\Delta gliT$

<i>A. fumigatus</i> strain	AMM	AMM + gliotoxin ^a
		<u>GSH/GSSG</u>
ATCC26933	8.15	5.6
$\Delta gliT$	47.5	13.8

^a 3 h incubation with 5 $\mu\text{g/ml}$ gliotoxin

4.2.4 Protein glutathionylation investigation

4.2.4.1 Synthesis of biotin-GSSG

To allow for the detection of proteins susceptible to glutathionylation, biotin was coupled to the primary amine groups of GSSG using a water soluble biotin reagent, sulfo-NHS-LC-biotin, as described in Section 2.2.22 (Brennan *et al.*, 2005). Sulfo-NHS-LC-biotin consists of a long chain spacer arm containing sodium sulfonate groups that is attached to the biotin (Figure 4.19). The long spacer arm increases the accessibility of biotin to avidin, increases the accessibility of the disulphide to protein thiols, and also increases the water solubility of the compound. When incubated with protein lysates, the GSSG of biotin-GSSG will react with protein thiol groups resulting in the proteins not only becoming glutathionylated, but also carrying a biotin tag which can then be detected by Western blot.

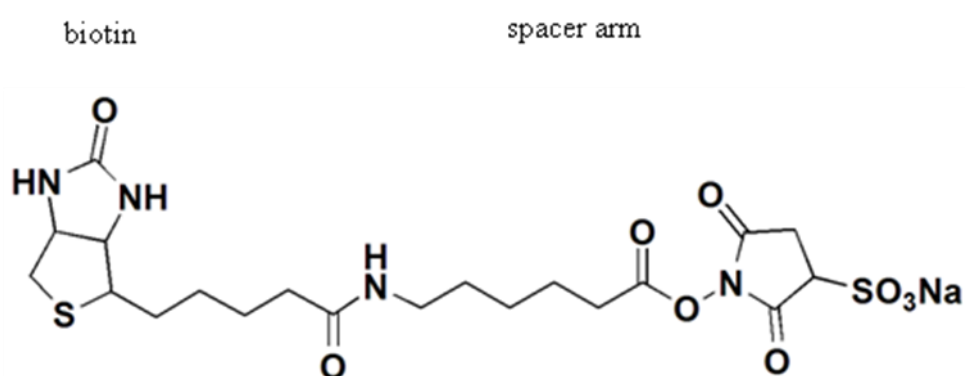


Figure 4.19: Chemical structure of sulfo-NHS-LC-biotin. A long chain “spacer arm” containing sodium sulfonate groups is attached to a biotin moiety.

HPLC (Section 2.2.23) and MALDI-ToF MS (Section 2.2.20) analysis was carried out to confirm the successful biotinylation of GSSG. HPLC analysis of biotin-GSSG detected a unique molecular species that eluted after 10.5 min which was not present in either the Sulfo-NHS-LC-Biotin or GSSG controls (Figure 4.20) and therefore indicated the presence of biotin-GSSG. MALDI-ToF analysis was also carried out as further confirmation of the synthesis of biotin-GSSG (Figure 4.21).

Biotin-GSSG has a mass of 1290.85, as two biotin moieties are added to each GSSG. A mass of 1312.042 was detected which is the equivalent of biotin-GSSG containing a sodium adduct. Furthermore, biotin-GSSG was also detected containing up to 4 sodium adducts (Figure 4.21).

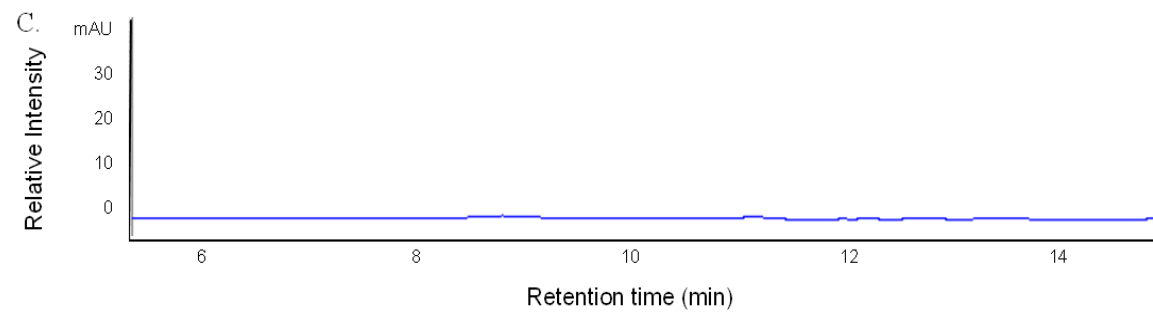
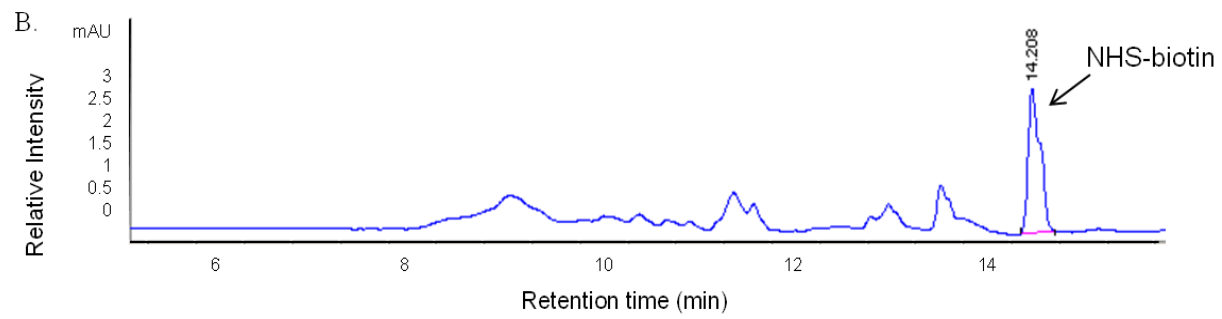
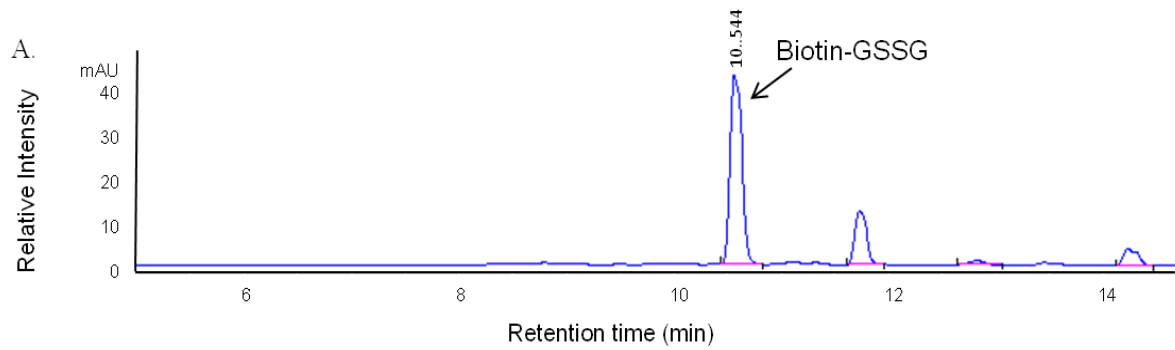
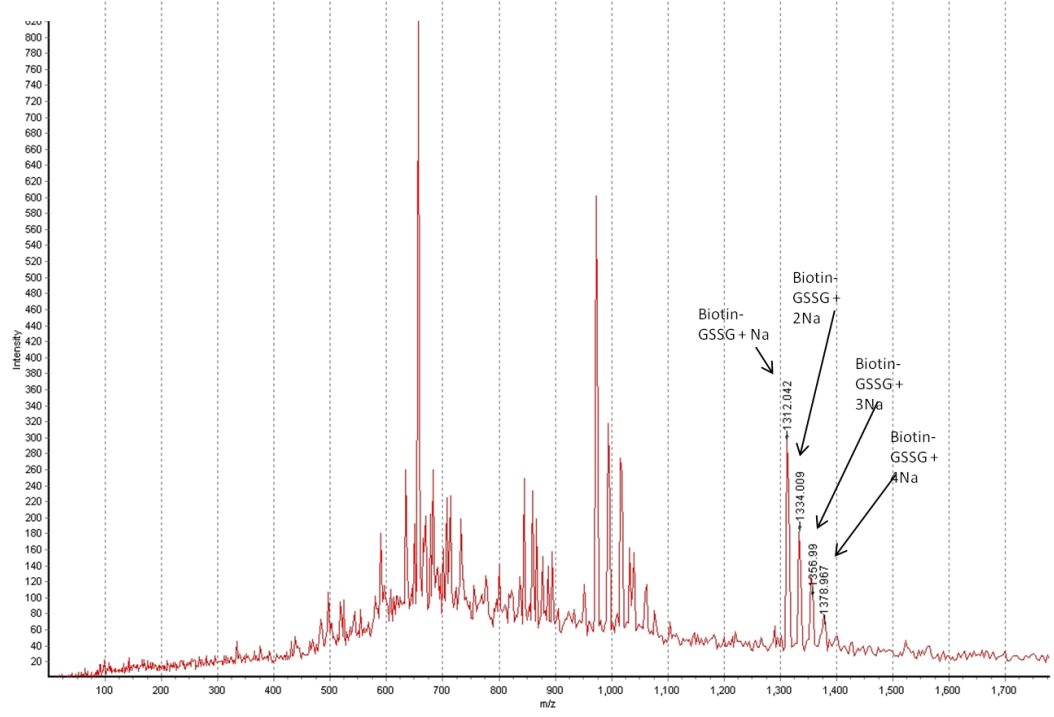


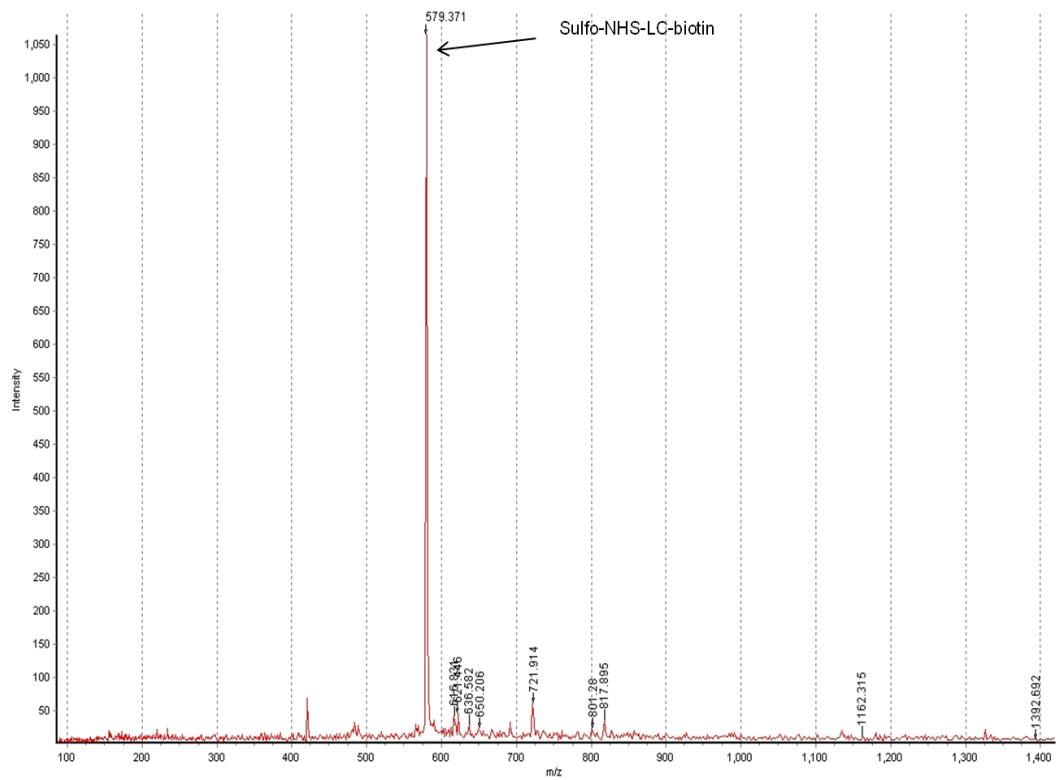
Figure 4.20: HPLC analysis of biotin-GSSG detected at absorbance 280nm

- A.** Biotin-GSSG was observed at the retention time of 10.5 min as a dominant peak.
- B.** Sulfo-NHS-LC-biotin was present at the retention time of 14.2 min as a single peak. No molecular species eluted from the column at the 10.5 retention time.
- C.** GSSG eluted off the column prior to 2.5 min as there were no other molecular species detected after that time.

A.



B.



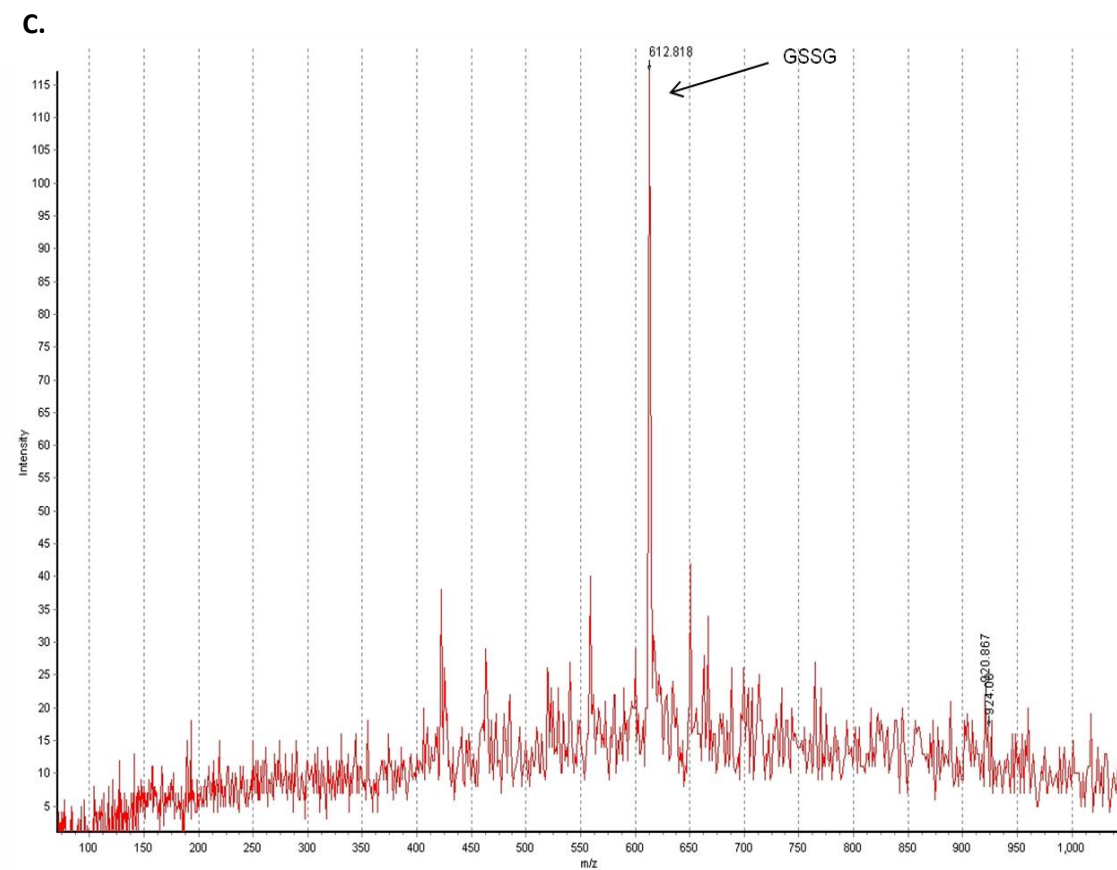


Figure 4.21: MALDI-ToF mass spectra of biotin-GSSG, sulfo-NHS-LC-biotin and GSSG.

- A.** MALDI-ToF mass spectrum confirming the biotinylation of GSSG. The expected mass of biotin-GSSG is 1290.85. MALDI-ToF analysis identified a product with mass 1312.042, which is the Na^+ adduct of biotin-GSSG. Biotin-GSSG with 2, 3 and 4 sodium adducts were also detected.
- B.** MALDI-ToF MS analysis identified sulfo-NHS-LC-biotin with a mass of 573.31.
- C.** MALDI-ToF analysis identified GSSG with a mass of 612.818.

4.2.4.2 Investigating protein glutathionylation in *A. fumigatus* ATCC46645 and Δ *elfA*

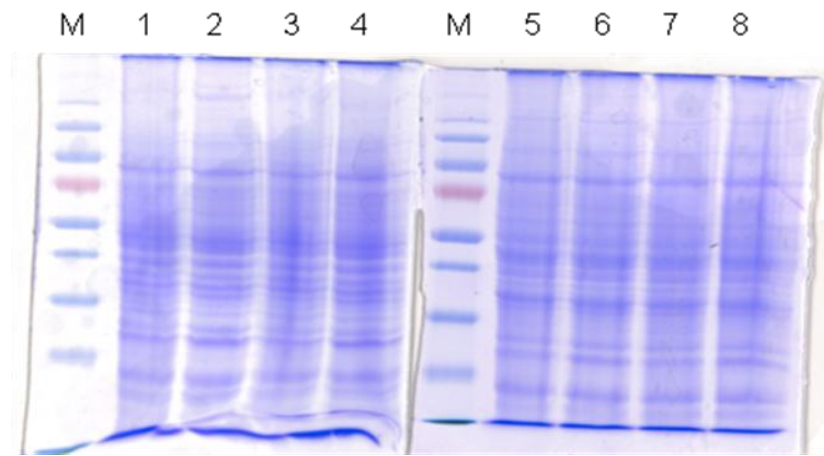
Protein glutathionylation in *A. fumigatus* ATCC46645 and Δ *elfA* was investigated. Biotin-GSSG was used as a probe to detect proteins susceptible to glutathionylation as the addition of GSSG leads to thiol-disulphide exchange reactions with these proteins, while the biotin moiety allows for their detection by Western blot (Brennan *et al.*, 2005).

Whole cell lysate from *A. fumigatus* ATCC46645 and Δ *elfA*, respectively, were treated with biotin-GSSG and separated by SDS-PAGE under non-reducing conditions before Western blotting and streptavidin-HRP detection (Section 2.2.24). It appeared that there was increased protein glutathionylation in *A. fumigatus* Δ *elfA* compared to *A. fumigatus* ATCC46645 (Figure 4.22). This was supported by image analysis which determined a 24 % increase in pixel intensity in *A. fumigatus* Δ *elfA* compared to wild-type signals (Figure 4.22). The experiment was also carried out under reducing conditions and whole cell lysates were also treated with water as controls to ensure that any proteins detected were as a direct result of glutathionylation by biotin-GSSG (Figure 4.22).

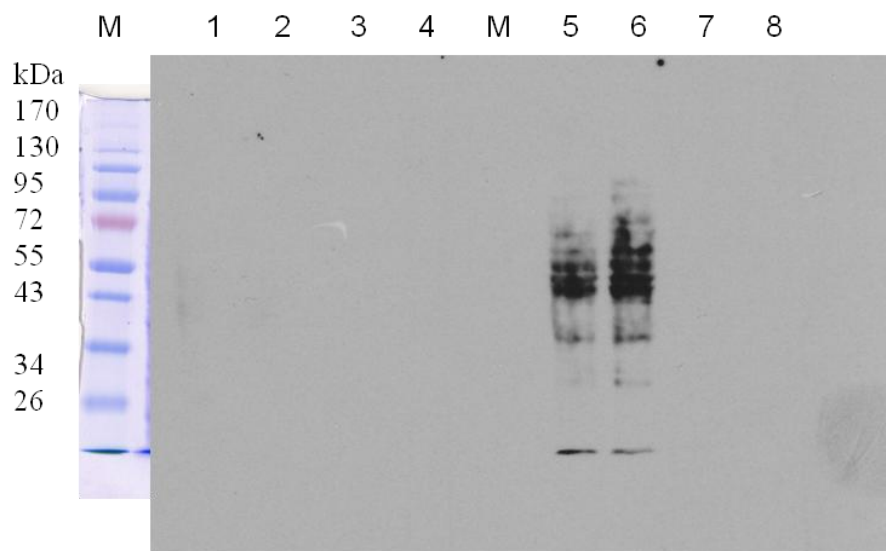
Attempts to identify the proteins susceptible to glutathionylation were unsuccessful. 2D-PAGE and pull-down experiments using streptavidin coated magnetic particles were employed to isolate the proteins glutathionylated with biotin-GSSG. The removal of any reducing agents from the buffers used in 2D-PAGE resulted in poor separation of the proteins and therefore 2D-PAGE was

unsuitable. Non-specific interference in the pull-down assays with streptavidin coated magnetic particles deemed this method unsuitable also. Despite this, the observation of a higher level of proteins susceptible to glutathionylation in *A. fumigatus* $\Delta elfA$ compared to *A. fumigatus* ATCC46645 indicates that *A. fumigatus* *elfA* is either directly or indirectly involved in protein glutathionylation in *A. fumigatus*.

A.



B.



C.

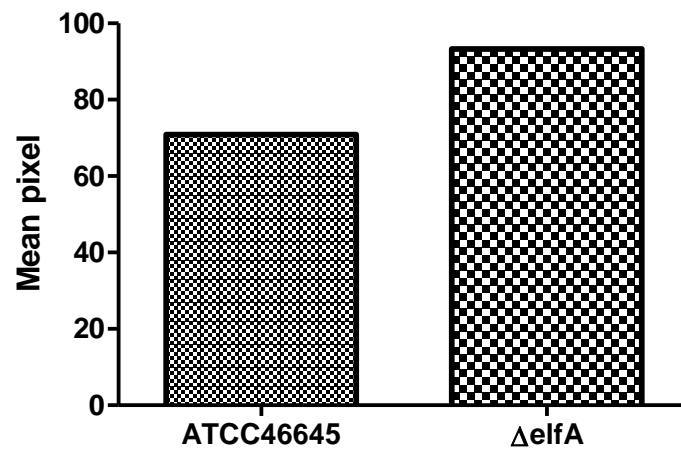


Figure 4.22: Western Blot analysis of protein glutathionylation in *A. fumigatus* ATCC46645 and $\Delta elfA$.

- A.** SDS-PAGE of *A. fumigatus* ATCC46645 (Lanes 1, 3, 5, 7) and $\Delta elfA$ (Lanes 2, 4, 6, 8) whole cell lysates (50 μ g) under reducing (Lanes 1 – 4) and non-reducing conditions (Lanes 5 – 8). The samples in Lanes 1, 2, 5 and 6 were incubated with biotin-GSSG, while the samples in Lanes 3, 4, 7 and 8 were incubated with water as a control.
- B.** Western blot probed with streptavidin-HRP. Proteins glutathionylated upon addition of biotin-GSSG were detected in *A. fumigatus* ATCC46645 (Lane 5) and $\Delta elfA$ (Lane 6). There appeared to be more glutathionylated proteins detected in *A. fumigatus* $\Delta elfA$ (Lane 6) than in *A. fumigatus* ATCC46645 (Lane 5). No glutathionylated proteins were detected on the reduced blot (Lanes 1 - 4) or in the samples treated with water (Lanes 7 – 8), indicating that the glutathionylated proteins are as a direct result of the addition of biotin-GSSG.
- C.** Image analysis indicates a 24 % increase in pixel intensity in *A. fumigatus* $\Delta elfA$ compared to *A. fumigatus* ATCC46645 supporting the observation that there appeared to be a higher level of protein glutathionylation in *A. fumigatus* $\Delta elfA$.

4.3 Discussion

The work described in this Chapter investigated possible functions of *A. fumigatus elfA*. Phenotypic analysis of *A. fumigatus ΔelfA* in response to different reagents determined that *A. fumigatus ΔelfA* had an increased resistance to voriconazole and was more sensitive to oxidative stress induced by H₂O₂, diamide and DPS when compared to the wild-type, *A. fumigatus* ATCC46645 (summarised in Table 4.4). Under normal growth conditions, measurement of the GSH/GSSG ratios indicated that *A. fumigatus ΔelfA* had a lower ratio and therefore was under stress when compared to *A. fumigatus* ATCC46645. Upon exposure to H₂O₂, the GSH/GSSG ratio in *A. fumigatus* ATCC46645 decreased across all the timepoints, while the GSH/GSSG ratio in *A. fumigatus ΔelfA* increased after 15 min but decreased after 30 min. It was also observed that there were more proteins glutathionylated in *A. fumigatus ΔelfA* compared to the wild-type.

A. fumigatus ΔelfA was investigated for any altered phenotypes in response to the antifungals amphotericin B and voriconazole. *A. fumigatus* ATCC46645, *ΔelfA* and *elfA^C* were grown in the presence of amphotericin B (0 – 1 µg/ml) and no differences was observed in growth between the three strains. However, in the presence of voriconazole (0 – 1 µg/ml) *A. fumigatus ΔelfA* was more resistant to voriconazole (0.5 µg/ml, $p = 0.0251$) than *A. fumigatus* ATCC46645 and *elfA^C*. Therefore *elfA* may be involved in the sensitisation of *A. fumigatus* to voriconazole. Both amphotericin B and voriconazole target ergosterol, with amphotericin B targeting the membrane itself, while voriconazole targets ergosterol biosynthesis (Sanglard and Odds, 2002). Azole resistance has been identified in clinical and

Table 4.4: Overall phenotypes associated with the loss of *A. fumigatus elfA*^a.

Treatment	Concentration	Phenotype Observed
Voriconazole	0 – 1 µg/ml	<i>ΔelfA</i> was less sensitive to voriconazole (p = 0.0251) than ATCC46645 or <i>elfA</i> ^C . <i>elfA</i> ^C exhibited the same phenotype as the wild-type
4,4'-dipyridyl disulphide (DPS)	0 – 7.5 µM	<i>ΔelfA</i> was more sensitive to 4,4'-dipyridyl disulphide (p = 0.0007) than ATCC46645. The wild-type phenotype in <i>elfA</i> ^C was partially restored
H₂O₂	0 – 5 mM	<i>ΔelfA</i> was more sensitive to H ₂ O ₂ (p = 0.0006) than ATCC46645. The wild-type phenotype was not fully restored in <i>elfA</i> ^C .
Diamide	0 – 4 mM	<i>ΔelfA</i> was more sensitive to diamide (p = 0.0001) than ATCC46645. The wild-type phenotype was not fully restored to <i>elfA</i> ^C .

^a agents that resulted in no phenotypes are not included.

environmental isolates (Bueid *et al.*, 2010; Snelders *et al.*, 2009). Decreased susceptibility to voriconazole was also observed in an *A. fumigatus* strain expressing a truncated *Afyap1* gene, while the *Afyap1* deletion strain did not exhibit increased resistance (Qiao *et al.*, 2010). *A. fumigatus elfA* was identified as being either directly or indirectly under the control of *Afyap1* (Lessing *et al.*, 2007). However, a search of the upstream region of *A. fumigatus elfA* in this study found no *yap1* binding site (data not shown). Consequently, *A. fumigatus elfA* may be indirectly controlled by *Afyap1*. Voriconazole inhibits ergosterol biosynthesis, however, it does not appear that the resistance to voriconazole is due to a change in or lack of ergosterol in *A. fumigatus ΔelfA* as this should also have resulted in an altered phenotype to amphotericin B. *A. fumigatus elfA* may directly or indirectly mediate voriconazole sensitivity in *A. fumigatus*.

A. fumigatus elfA was identified as a GSH-binding protein following GSH-Sepharose chromatography and was then shown to exhibit GST activity for the substrates CDNB and ethacrynic acid (Carberry *et al.*, 2006). As GSTs respond to oxidative stress, *A. fumigatus ΔelfA* was subjected to oxidative stress from menadione, H₂O₂, diamide and DPS to determine whether *A. fumigatus elfA* was involved in the oxidative stress response. In the presence of menadione (0 – 50 μM), *A. fumigatus ΔelfA* showed no growth differences when compared to *A. fumigatus* ATCC46645 and *elfA^C*. However *A. fumigatus ΔelfA* did show increased susceptibility to oxidative stress induced by H₂O₂, diamide and DPS. *A. fumigatus ΔelfA* was more sensitive to H₂O₂ (p = 0.0006) after 72 h when compared to *A. fumigatus* ATCC46645. *A. fumigatus ΔelfA* was significantly more sensitive (p <

0.0001) to diamide after 48 and 72 h growth compared to *A. fumigatus* ATCC46645. Following 96 h of growth in the presence of 7.5 μ M DPS, there was a significant decrease ($p = 0.0007$) in the growth of *A. fumigatus* Δ *elfA* when compared to *A. fumigatus* ATCC46645. Therefore *A. fumigatus* *elfA* is involved in the oxidative stress response in *A. fumigatus*. The involvement of GSTs in response to H₂O₂ induced oxidative stress has been previously described whereby two GSTs, *A. fumigatus* *gstA* and *gstC*, were shown to be up-regulated in the presence of H₂O₂ (Burns *et al.*, 2005). Meanwhile, GSTs have been implicated in the response to H₂O₂ induced oxidative stress in other fungi (e.g., *Aspergillus nidulans* and *Schizosaccharomyces pombe* (Sato *et al.*, 2009; Veal *et al.*, 2002)). Interestingly, in *S. cerevisiae* loss of eEF1B γ resulted in an increased resistance to oxidative stress induced by H₂O₂ (Olarewaju *et al.*, 2004), however in *S. cerevisiae*, eEF1B γ did not show any GST activity despite the presence of a GST domain (Jeppesen *et al.*, 2003). In addition to this, multiple sequence alignment determined that eEF1B γ from *S. cerevisiae* contains a domain not found in *A. fumigatus* *elfA*, which may account for the different phenotype observed to oxidative stress. Deletion of glutathione reductase (*glrA*) in *A. nidulans* increased sensitivity to diamide (Sato *et al.*, 2009), while in *A. fumigatus* deletion of *yap1* increased its sensitivity to diamide also (Qiao *et al.*, 2008; Lessing *et al.*, 2007). *A. fumigatus* *yap1* and *A. nidulans* *glrA* are involved in the oxidative stress response as a transcription factor and the enzyme glutathione reductase, respectively (López-Mirabal and Winther, 2008). In *S. cerevisiae* deletion of *yap1* renders yeast sensitive to DPS (Lopez-Mirabal *et al.*, 2007). Lopez-Mirabal *et al.* (2007) carried out a screen of redox-impaired *S.*

cerevisiae strains and identified the importance of genes involved in redox balance (e.g., *gsh1*, *trx2*, *sod1* and *glr1*) in mediating resistance to DPS.

It is interesting that *A. fumigatus* Δ *elfA* is sensitive to oxidative stress induced by H₂O₂, diamide and DPS but not by menadione. A study of gene expression in *A. nidulans* in response to diamide, H₂O₂ and menadione revealed that not only was there a set of genes commonly responsive to all three oxidants, there was a set of genes uniquely responsive to menadione (Pocsi *et al.*, 2005). In response to menadione, 32.6% of the gene probes were uniquely responsive compared to 6.3 % for H₂O₂ and 8.4 % for diamide. One of the genes uniquely responsive to menadione was superoxide dismutase which was required to deal with the increased levels of superoxide anions generated by menadione. If the same occurs in *A. fumigatus* it may provide some explanation for the fact that *A. fumigatus* Δ *elfA* is not sensitive to menadione, but sensitive to H₂O₂, diamide and DPS. Also it must be noted that the wild-type phenotype was not fully restored to *A. fumigatus* *elfA*^C in response to H₂O₂ or diamide but was restored in response to DPS and voriconazole. Semi-quantitative RT-PCR for *elfA* in *A. fumigatus* *elfA*^C showed expression of *elfA*. Also the GSH/GSSG ratio in *A. fumigatus* *elfA*^C is comparable to that in *A. fumigatus* ATCC46645. As *A. fumigatus* *elfA* expression was not quantified, a different amount of ElfA may be present in *A. fumigatus* *elfA*^C compared to the wild-type which may have contributed to the non-restoration of the wild-type phenotype in response to oxidants H₂O₂ and diamide.

The GSH/GSSG redox status of *A. fumigatus* ATCC46645 and Δ *elfA* was investigated and it was found that there was a reduced level of GSH in *A. fumigatus*

$\Delta elfA$ compared to ATCC46645, while *A. fumigatus* $\Delta elfA$ exhibited an increase in GSSG levels compared to those in ATCC46645. This resulted in a decreased GSH/GSSG ratio and implies that *A. fumigatus* $\Delta elfA$ is undergoing stress when grown under normal conditions (Rahman *et al.*, 2006). In *A. nidulans*, the deletion of *napA*, the ortholog of *A. fumigatus yap1*, also resulted in a decreased GSH/GSSG ratio when grown under normal conditions (Thön *et al.*, 2010). The decrease in GSH levels in *A. fumigatus* $\Delta elfA$ also partly explains the sensitivity to diamide and DPS observed in this strain. Diamide and DPS are thiol-specific oxidants and react with GSH directly (López-Mirabal and Winther, 2008; Lopez-Mirabal *et al.*, 2007). With an already decreased amount of GSH in *A. fumigatus* $\Delta elfA$, addition of diamide and DPS could result in the depletion of GSH to a greater extent than in *A. fumigatus* ATCC46645 and result in increased sensitivity to the thiol-oxidants.

The effect of H₂O₂ on the GSH/GSSG ratio in *A. fumigatus* ATCC46645, $\Delta elfA$ and *elfA*^C was investigated. The behaviour of the GSH/GSSG ratios in response to 2 mM H₂O₂ in *A. fumigatus* ATCC46645 resulted in decreased ratios. This is the expected response to oxidative stress (Rahman *et al.*, 2006) and was also the observed response in *A. nidulans* (Pócsi *et al.*, 2005). Pócsi *et al.* (2005) measured the GSH/GSSG ratio in *A. nidulans* in response to H₂O₂ over 10 h and observed a sharp decrease in the ratio immediately after exposure with a gradual recovery of the GSH/GSSG ratio. However, in *A. fumigatus* $\Delta elfA$ in the presence of 2 mM H₂O₂, after 15 min the GSH/GSSG ratio increases but decreases following 30 min exposure. At 15 min, both the GSH and GSSG amounts decreased compared to non-exposed cultures. GSH decreases in response to oxidative stress, while the

decreased levels of GSSG may indicate an increase in glutathione reductase activity reducing GSSG to GSH or that GSSG was removed from the cell by members of the multidrug resistance associated protein (MRP) family (Hayes and McLellan, 1999). Following 30 min exposure to H₂O₂, the GSH levels in *A. fumigatus* $\Delta elfA$ increased significantly compared to non-exposed cultures, while the levels of GSSG was decreased. The increase in GSH may indicate an up-regulation of GSH synthesis in order to deal with the oxidative stress conditions. In *A. nidulans*, an increased GSH/GSSG ratio in response to H₂O₂ was also observed in a *napA* deletion strain (Thön *et al.*, 2010).

The GSH/GSSG ratio was investigated in another *A. fumigatus* deletion strain, $\Delta gliT$ (Schrettl *et al.*, 2010), transformed with the *ptrA* resistance gene to confirm that the change in GSH/GSSG ratios in *A. fumigatus* $\Delta elfA$ were as a result of the deletion of *elfA* and not due to the introduction of *ptrA*. Under normal growth conditions, the GSH/GSSG ratio for *A. fumigatus* $\Delta gliT$ was increased 5.8 fold when compared to *A. fumigatus* ATCC26933. This is different to the GSH/GSSG ratio in *A. fumigatus* $\Delta elfA$, where there was a decrease in the GSH/GSSG ratio. This confirms that the observed GSH/GSSG ratio in *A. fumigatus* $\Delta elfA$ was as a result of the deletion of *elfA* and not due to the introduction of *ptrA*, as *A. fumigatus* $\Delta gliT$ was also transformed using *ptrA* as the selection marker (Schrettl *et al.*, 2010; Kubodera *et al.*, 2000). Moreover when exposed to gliotoxin (5 μ g/ml), the GSH/GSSG ratios in both *A. fumigatus* ATCC26933 and $\Delta gliT$ decreased, indicative of cells undergoing a stress response. The GSH levels in both *A. fumigatus* ATCC26933 and $\Delta gliT$ dropped upon exposure to gliotoxin, while the GSSG levels

remained the same. Interestingly, the increased levels of GSH observed in *A. fumigatus* $\Delta gliT$ compared to *A. fumigatus* ATCC26933 may implicate GSH in the sensitivity of *A. fumigatus* $\Delta gliT$ to gliotoxin. *A. fumigatus* *gliT* has been shown to be involved in self-protection against gliotoxin in *A. fumigatus*, and the levels of glutathione present in the cells may play a role in this self-protection (Schrettl *et al.*, 2010). As there was no increase in the GSSG levels in *A. fumigatus* ATCC26933 and $\Delta gliT$ upon exposure to gliotoxin, it appears that the decrease in GSH is not due to oxidation to GSSG. Therefore, GSH may be reacting with gliotoxin directly.

Protein glutathionylation in *A. fumigatus* $\Delta elfA$ was investigated and it was found that there was increased protein glutathionylation in *A. fumigatus* $\Delta elfA$ when compared to *A. fumigatus* ATCC46645. The loss of *A. fumigatus* *elfA* may result in the necessity for increased protein glutathionylation as a protective measure since the GSH/GSSG status of *A. fumigatus* $\Delta elfA$ also revealed stress conditions. To fully understand the increased protein glutathionylation in *A. fumigatus* $\Delta elfA$, identifying the proteins detected as glutathionylated is necessary. However, extensive attempts to identify the glutathionylated proteins by 2D-PAGE or pull down using magnetic streptavidin-coated particles were unsuccessful.

This work describes the investigation of phenotypes associated with *A. fumigatus* $\Delta elfA$. *A. fumigatus* $\Delta elfA$ displayed an increased resistance to voriconazole compared to *A. fumigatus* ATCC46645, implicating *A. fumigatus* *elfA* in mediating the effects of voriconazole. In response to oxidative stress-inducing agents, *A. fumigatus* $\Delta elfA$ exhibited increased sensitivity to H₂O₂, diamide and DPS when compared to *A. fumigatus* ATCC46645. This points to an involvement of *A.*

fumigatus elfA in the oxidative stress response and was further supported by the decreased GSH/GSSG ratio in *A. fumigatus ΔelfA* compared to *A. fumigatus* ATCC46645 which indicated that under basal conditions, *A. fumigatus ΔelfA* is under stress. In the presence of H₂O₂, the GSH/GSSG ratio increased, which is the opposite of the decreased GSH/GSSG ratios usually observed in response to stress, and implies that the synthesis of GSH and the reduction and/or removal of GSSG are a response to the increased levels of stress in *A. fumigatus ΔelfA*. Finally, it was determined that there were more proteins glutathionylated in *A. fumigatus ΔelfA* when compared to *A. fumigatus* ATCC46645, which is also indicative of an altered redox environment. The effect of the altered redox balance on the proteome of *A. fumigatus ΔelfA*, under both normal growth conditions and in response to H₂O₂, will be described in Chapter 5.

5.1 Introduction

The “classical” proteomics strategy involves protein separation by 2D-PAGE followed by protein identification by mass spectrometry (MS) (Carberry and Doyle, 2007). 2D-PAGE involves the separation of proteins on the basis of charge (pI) in the first dimension. This is usually carried out with IPG strips of different pH ranges (Gorg *et al.*, 2009). The second dimension involves the separation of the proteins by SDS-PAGE. The gels are usually stained with high sensitivity dyes or stains (e.g., colloidal Coomassie blue, silver stain or fluorescent stains) to allow the visualisation of the protein spots. These spots are then excised, digested with trypsin, and the peptides subjected to MS for identification (Kniemeyer, 2011).

One important aspect is the extraction of proteins before separation. In fungi, this usually involves mechanical lysing of the cells, by sonication, bead beating or grinding in liquid N₂, due to the presence of a robust cell wall (Carberry *et al.*, 2006; Kniemeyer *et al.*, 2006). TCA/Acetone is the most commonly used method to remove contaminants before resuspension of the protein in a buffer suitable for isoelectric focusing (Carberry *et al.*, 2006; Kniemeyer *et al.*, 2006). Another important aspect is the use of a highly sensitive dye or stain to visualise the proteins on the gel. When choosing a dye or stain, its sensitivity as well as its compatibility with MS must be taken into consideration as not all stains are MS compatible and therefore can lead to problems with protein identification (Carberry and Doyle, 2007). For example, silver stain is highly sensitive but generally not MS compatible however silver stains are now available that are compatible with MS (Jin *et al.*, 2008).

Prior to 2005, proteomics studies of *A. fumigatus* were few and far between, however, the availability of the sequenced genome along with mass spectrometry methods has allowed for the routine identification of proteins (Kniemeyer *et al.*, 2009). Matrix Assisted Laser Desorption Ionisation-Time of Flight Mass Spectrometry (MALDI-ToF-MS) and Liquid Chromatography Mass Spectrometry (LC-MS) are the most commonly used mass spectrometric methods for protein identification (Griffiths and Wang, 2009). In general, mass spectrometers consist of an ionisation source to ionise the peptides, a mass analyser to separate them and a detector to record the ions of different mass/charge ratio (m/z) (Han *et al.*, 2008). In MALDI-ToF-MS, the peptides are mixed with a matrix, loaded onto the sample plate and allowed to dry forming a heterogenous crystalline surface (Duncan *et al.*, 2008). The matrix is then pulsed with a laser which frees the peptides and ionises them at the same time (Albrethsen, 2007). The ionised peptides then travel along the time of flight tube, the smallest peptides travelling fastest and the m/z ratios for each ion detected (Duncan *et al.*, 2008; Albrethsen, 2007). With LC-MS the sample is first separated on a reversed phase C₁₈ column and peptides directly eluted into the mass spectrometer before being ionised and finally the m/z ratio is measured (Winnik and Kitchin, 2008). Tandem mass spectrometry (MS/MS) involves another separation stage whereby peptide precursor ions are targeted and fragmented before m/z ratio detection (Griffiths and Wang, 2009).

In recent years, great progress has been made in studying the proteome of *A. fumigatus*. Reliable protein extraction methods for whole cell protein and sub-proteomes (e.g., mitochondria), have enabled the study of the *A. fumigatus* proteome

and sub-proteomes in response to different conditions (Carberry *et al.*, 2006; Kniemeyer *et al.*, 2006). Proteome maps for the whole proteome and sub-proteomes; mitochondria, GSH-binding proteins, have been established for *A. fumigatus* (Vodisch *et al.*, 2009; Carberry *et al.*, 2006; Kniemeyer *et al.*, 2006). Studies have also been carried out to investigate any effects on the *A. fumigatus* proteome in response to different stresses (e.g., oxidative stress (Lessing *et al.*, 2007), hypoxia (Vodisch *et al.*, 2011), heat shock (Albrecht *et al.*, 2010b) and gliotoxin (Schrettl *et al.*, 2010)). Lessing *et al.* (2007) investigated the effect of H₂O₂ on the proteome of *A. fumigatus* and identified differences in expression of proteins involved in oxidative stress as well as metabolism, protein translocation, cytoskeletal elements and a protease. Lessing *et al.* (2007) also investigated differences in the proteome of *A. fumigatus* wild-type and *A. fumigatus* $\Delta yap1$, a deletion strain for the transcription factor Yap1. This resulted in the identification of possible Yap1 targets in *A. fumigatus*. Studies have also been carried out to investigate changes in the proteome in response to antifungals in an attempt to identify possible targets to improve drug efficacy (Cagas *et al.*, 2011; Gautam *et al.*, 2011; Gautam *et al.*, 2008). In *A. nidulans* investigation of the proteome of glutathione reductase (*glrA*) deletion strain resulted in the identification of a GST (Sato *et al.*, 2009). These studies emphasise the potential for proteomics to improve our understanding of the global changes within an organism in response to a gene deletion, environmental stress or antifungal exposure.

The hypothesis is that comparative proteomics of *A. fumigatus* ATCC46645 and $\Delta elfA$ will uncover changes in the proteome in response to the absence of ElfA

which will provide insights into possible functions. From the observation that *A. fumigatus* $\Delta elfA$ was sensitive to H₂O₂ (Chapter 4), investigation of the effect of H₂O₂ on the proteome of *A. fumigatus* $\Delta elfA$ compared to that of *A. fumigatus* ATCC46645 may also aid in the elucidation of *A. fumigatus* *elfA* function. The aims of the work described in this Chapter were i) to investigate any changes in the proteome of *A. fumigatus* $\Delta elfA$ compared to that of *A. fumigatus* and ii) to investigate the proteomes of *A. fumigatus* ATCC46645 and $\Delta elfA$ following exposure to hydrogen peroxide.

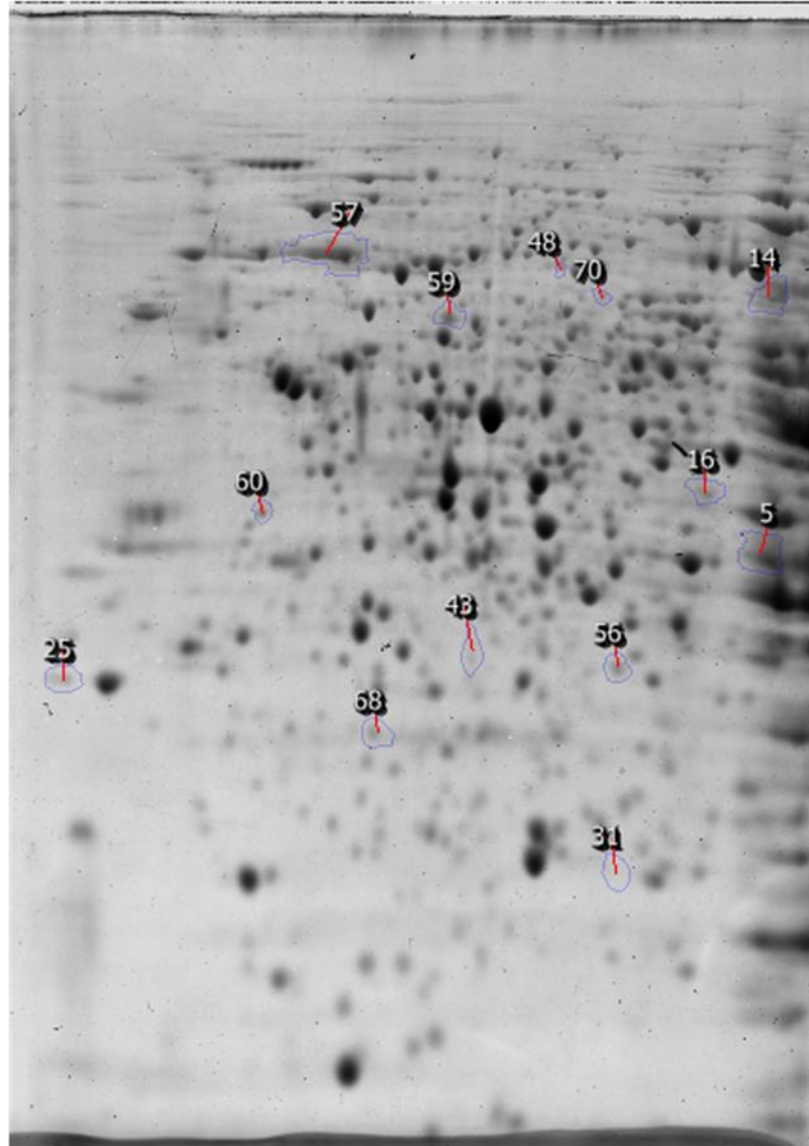
5.2 Results

5.2.1 2D-PAGE of *A. fumigatus* ATCC46645 and $\Delta elfA$ under normal growth conditions

A. fumigatus ATCC46645 and $\Delta elfA$ were cultured ($n = 5$, respectively) for 24 h in AMM before the mycelia were harvested and protein was extracted as described in Section 2.2.16.1. The protein lysates were TCA/Acetone precipitated and resuspended in IEF Buffer (Section 2.2.17) before separation on pH 4 - 7 strips (Section 2.2.18). Following separation by SDS-PAGE on 12 % gels, staining with Colloidal Coomassie (Section 2.2.14) was performed and analysed using Progenesis™ SameSpot Software (Nonlinear Dynamics Ltd. UK) (Figure 5.1).

Thirteen proteins were found to be differentially expressed; eight proteins had a fold increase ≥ 1.5 ($p < 0.05$) in *A. fumigatus* $\Delta elfA$ while five proteins had a fold decrease ≥ 1.5 ($p < 0.05$) when compared to *A. fumigatus* ATCC46645. These spots were excised from the gels, trypsin digested as described in Section 2.2.19 and analysed by LC-MS/MS (Section 2.2.21).

A. pH 4 _____ 7



B. pH 4 ————— 7

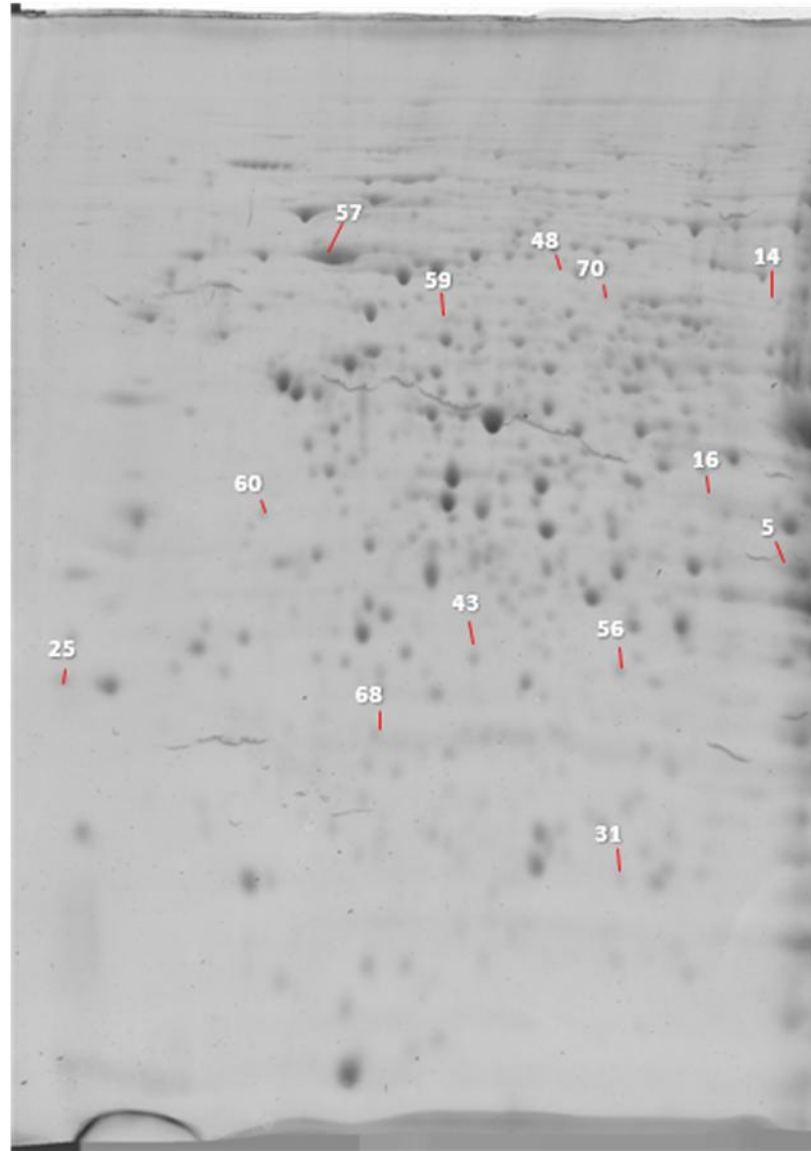


Figure 5.1: 2D-PAGE analysis of *A. fumigatus* ATCC46645 (A) and $\Delta elfA$ (B) under normal growth conditions. The proteins were first separated on pH 4 – 7 strips followed by SDS-PAGE on 12 % gels. The proteins found to be differentially expressed after analysis using Progenesis™ SameSpot software are numbered.

5.2.2 Mass spectrometry analysis of differentially expressed proteins

Thirteen proteins were identified from the excised spots by LC-MS/MS (Tables 5.1 and 5.2). The protein identified as having the highest fold increase in *A. fumigatus* Δ *elfA* compared to *A. fumigatus* ATCC46645 was tyrosyl-tRNA synthetase (AFUA_5G10640) (Figure 5.2). While the protein with the highest fold decrease in *A. fumigatus* Δ *elfA* compared to *A. fumigatus* ATCC46645 was ketol-acid reductoisomerase (AFUA_3G14490).

Of the proteins identified, some are involved in the oxidative stress response, others in translation, while others are associated with the cytoskeleton, the mitochondria or the endoplasmic reticulum (ER). Mitochondrial peroxiredoxin Prx1 (AFUA_4G08580) (Figure 5.2), molecular chaperone Hsp70 (AFUA_1G07440) and Hsc70 co-chaperone (SGT) (AFUA_1G09830) are all involved in the oxidative stress response (Henderson, 2010; Greetham and Grant, 2009). Tyrosyl-tRNA synthetase (AFUA_5G10640) and phosphoribosylaminoimidazole carboxamide formyltransferase/IMP cyclohydrolase (AFUA_4G07690) are involved in translation and purine biosynthesis, respectively (Boccalatte *et al.*, 2009; Paukstelis and Lambowitz, 2008). Actin-bundling protein Sac6 (AFUA_2G07420) (Figure 5.2) and polysaccharide deacetylase family protein (AFUA_5G09130) are associated with the cytoskeleton (Cheng *et al.*, 1999). The nuclear pore complex subunit Sec13 (AFUA_4G06090) is associated with the ER (Nielsen, 2009). Proteins identified that are associated with the mitochondria include the mitochondrial peroxiredoxin Prx1 (AFUA_4G08580), the regulatory protein SUAPRGA1 (AFUA_3G09030) and the MRS7 family protein (AFUA_3G08230). Short chain dehydrogenase showed a

1.6 fold decreased expression in *A. fumigatus* $\Delta elfA$ but was identified as up-regulated in *A. fumigatus* exposed to gliotoxin (Carberry, 2008). Interestingly, the transcription factor RfeF (AFUA_4G10200) which was identified as down-regulated in *A. fumigatus* $\Delta elfA$, has no known functions.

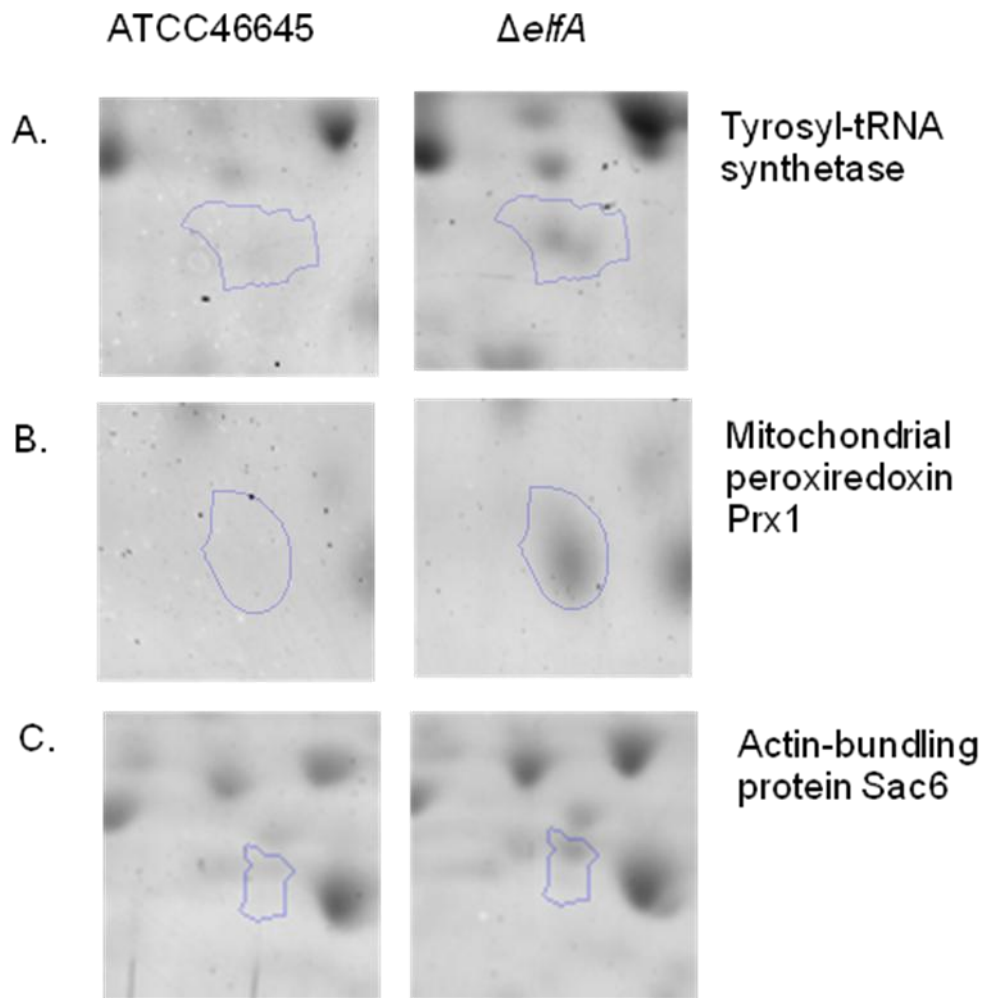


Figure 5.2: Differential expression of tyrosyl-tRNA synthetase, mitochondrial peroxiredoxin Prx1 and actin-bundling protein Sac6 in *A. fumigatus* ATCC46645 and $\Delta elfA$. Tyrosyl-tRNA synthetase was increased 2.7 fold, mitochondrial peroxiredoxin Prx1 was increased 2.2 fold and actin-bundling protein Sac6 was increased 1.9 fold in expression in *A. fumigatus* $\Delta elfA$ compared to *A. fumigatus* ATCC46645.

Table 5.1: Proteins ($n = 8$) with a fold increase in *A. fumigatus* $\Delta elfA$ compared to *A. fumigatus* under normal growth conditions following identification by 2D-PAGE and LC-MS/MS.

Spot No.	Annotation name	CADRE ID	Fold change	tpI	tMW	% Sequence coverage
16	Tyrosyl-tRNA synthetase	AFUA_5G10640	2.7	6.18	43588	20
25	Regulatory protein SUAPRGA1	AFUA_3G09030	2.4	4.88	40070	32
31	Mitochondrial peroxiredoxin Prx1	AFUA_4G08580	2.2	5.38	23378	33
43	Polysaccharide deacetylase family protein	AFUA_5G09130	2.0	5.39	35188	42
48	Actin-bundling protein Sac6	AFUA_2G07420	1.9	5.78	72434	12
56	Nuclear pore complex subunit SEC13	AFUA_4G06090	1.7	6.17	33856	28
57	Molecular chaperone Hsp70	AFUA_1G07440	1.7	5.09	69618	56
70	MRS7 family protein	AFUA_3G08230	1.5	6.42	68745	18

CADRE I.D.: *A. fumigatus* gene annotation nomenclature according to Nierman *et al.* (2005) and Mabey *et al.* (2004).

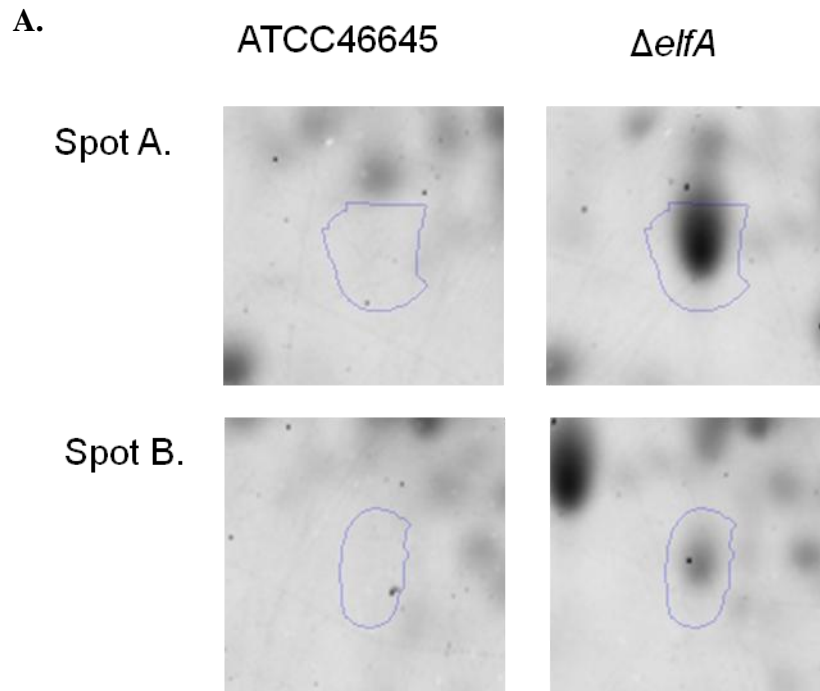
Table 5.2: Proteins ($n = 5$) with a fold decrease in *A. fumigatus* $\Delta elfA$ compared to *A. fumigatus* under normal growth conditions following identification by 2D-PAGE and LC-MS/MS.

Spot No.	Annotation name	CADRE ID	Fold change	tpI	tMW	% Sequence coverage
5	Ketol-acid reductoisomerase	AFUA_3G14490	4.9	9.32	56318	21
14	Phosphoribosylaminoimidazole carboxamide formyltransferase/ IMP cyclohydrolase	AFUA_4G07690	3.0	6.39	64987	33
59	Transcription factor RfeF	AFUA_4G10200	1.7	4.91	71649	18
60	Hsc70 cochaperone (SGT)	AFUA_1G09830	1.7	4.74	35721	38
68	Short chain dehydrogenase	AFUA_4G08710	1.6	5.28	30909	38

CADRE I.D.: *A. fumigatus* gene annotation nomenclature according to Nierman *et al.* (2005) and Mabey *et al.* (2004).

5.2.3 Identification of a unique protein in *A. fumigatus* Δ *elfA* corresponding to the selection marker *ptrA*.

Two unique protein spots were present following 2D-PAGE and image analysis of *A. fumigatus* Δ *elfA* that were not observed in *A. fumigatus* ATCC46645 (Figure 5.3). These spots were also excised and subjected to LC-MS/MS. Both spots were identified as a thiazole synthase from *A. oryzae* with sequence coverage of 36 % and 19 %, respectively. This is the protein encoded by the pyrithiamine resistance gene (*ptrA*) used in the generation of *A. fumigatus* Δ *elfA*. This thiazole synthase was identified from two individual spots, indicating two different isoforms of the protein present in the gel. The two protein spots differed in both pI and molecular mass. The molecular mass of Spot A was ~ 35300 kDa and the pI was 5.29 while for Spot B, the molecular mass was ~ 32000 kDa and the pI was ~ 5.4 (Figure 5.3). Investigation of peptides identified by LC-MS/MS does not indicate the identification of different subunits as the peptides map over the same region of the protein sequence (Figure 5.3). A post-translational modification may account for the presence of the two isoforms of the thiazole synthase.



B.

Spot A

```

1  MSPPAAIYEP  TVAATGLKGK VVVSETVPVE GASQTKLLDH  FGGKWDEFKF
51  APIRESQVSR  AMTRRYFEDL DKYAESDVVI VGAGSCGLST AYVLAKARPD
101 LKIAIVEASV  SPGGGAWLGG QLFSAMVMRR PAEVFLNELG VPYEEDANPN
151 YVVVKHASLF TSTLMSKVLS FPNVKLFNAT  AVEDLITRPT  ENGNPQIAGV
201 VVNWTLVTLH  HDDHSCMDPN  TINAPVIIST  TGHDGPFGAF  CAKRLVSMGS
251 VDKLGGMRGL  DMNSAEDAIV  KNTREVTKGL  IIGGMELSEI  DGFNRMGPTF
301 GAMVLSGVKA  AEEALKVFDE  RQRECAE

```

Spot B

```

1  MSPPAAIYEP  TVAATGLKGK VVVSETVPVE GASQTKLLDH  FGGKWDEFKF
51  APIRESQVSR  AMTRRYFEDL DKYAESDVVI VGAGSCGLST AYVLAKARPD
101 LKIAIVEASV  SPGGGAWLGG QLFSAMVMRR PAEVFLNELG VPYEEDANPN
151 YVVVKHASLF TSTLMSKVLS FPNVKLFNAT  AVEDLITRPT  ENGNPQIAGV
201 VVNWTLVTLH  HDDHSCMDPN  TINAPVIIST  TGHDGPFGAF  CAKRLVSMGS
251 VDKLGGMRGL  DMNSAEDAIV  KNTREVTKGL  IIGGMELSEI  DGFNRMGPTF
301 GAMVLSGVKA  AEEALKVFDE  RQRECAE

```

Figure 5.3: The observation and identification of the thiazole synthase encoded by *A. oryzae ptrA*.

- A.** This protein was identified from two spots (Spot A and Spot B) in *A. fumigatus* $\Delta elfA$ and was not present in *A. fumigatus* ATCC46645. This protein is encoded by the pyrithiamine resistance gene, *ptrA*, from *A. oryzae* that was used as a selection marker in the deletion of *A. fumigatus elfA* (Chapter 3).

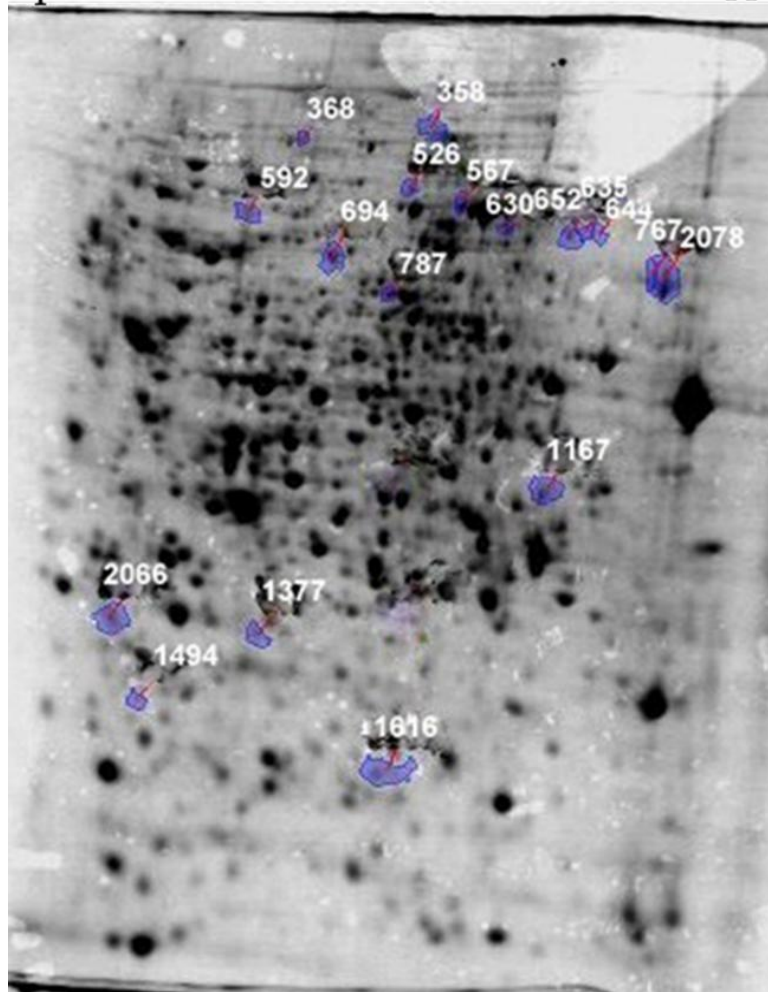
- B.** The protein sequence of thiazole synthase with the peptides identified by LC-MS/MS (in red) show that the same area of the protein was identified from both Spot A and Spot B.

5.2.4 2D-PAGE of *A. fumigatus* ATCC46645 and Δ elfA following exposure to H₂O₂

A. fumigatus ATCC46645 and Δ elfA were cultured ($n = 5$, respectively) for 24 h in AMM before H₂O₂ was added at a final concentration of 2 mM. After 1 h the mycelia were harvested and protein was extracted as described in Section 2.2.16.1. The protein lysates were TCA/Acetone precipitated and resuspended in IEF Buffer (Section 2.2.17) before separation on pH 3 - 11 strips (Section 2.2.18). Following separation by SDS-PAGE, the gels were stained with Colloidal Coomassie (Section 2.2.14) and analysed using Progenesis™ SameSpot Software (Figure 5.4).

Eighteen protein spots were found to be differentially expressed; thirteen of these protein spots had a fold increase ≥ 1.5 ($p < 0.05$) in *A. fumigatus* Δ elfA while five protein spots had a fold decrease ≥ 1.5 ($p < 0.05$) when compared to *A. fumigatus* ATCC46645 in response to 2 mM H₂O₂ exposure for 1 h. These protein spots were excised from the gels, trypsin digested as described in Section 2.2.19 and analysed by LC-MS/MS (Section 2.2.21).

A. pH 3 _____ 11



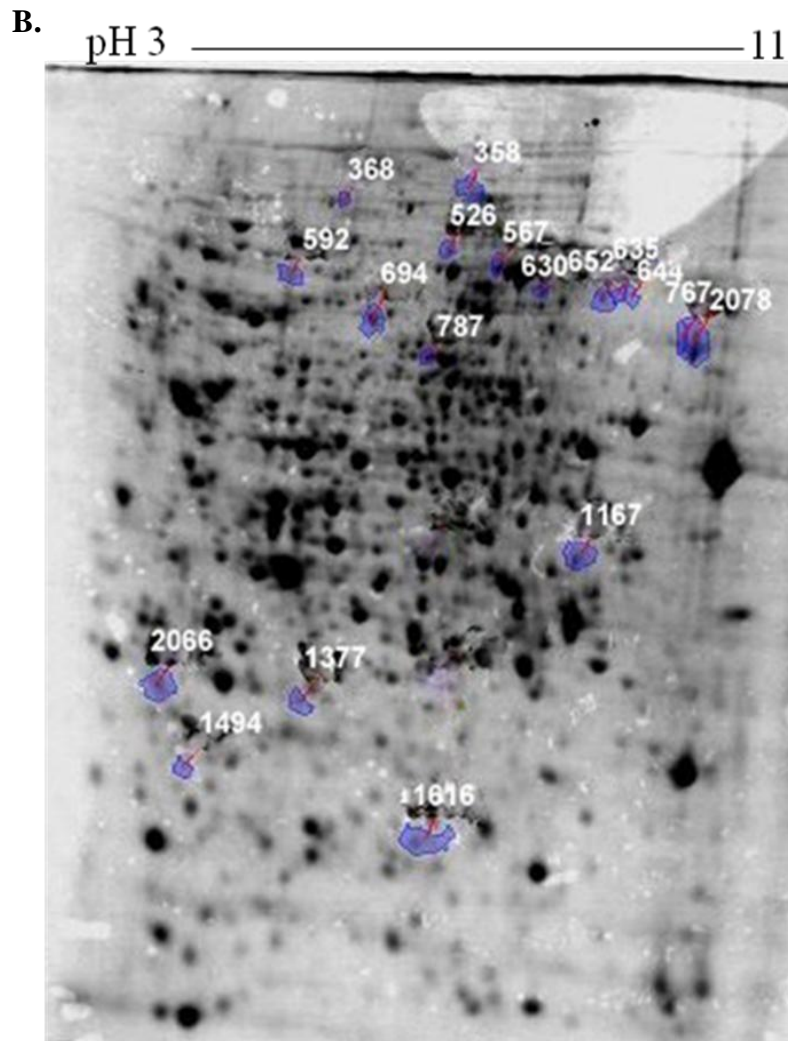


Figure 5.4: 2D-PAGE analysis of *A. fumigatus* ATCC46645 (A) and $\Delta elfA$ (B) following exposure to 2 mM H₂O₂ for 1 h. The proteins were first separated on pH 3 – 11 strips followed by SDS-PAGE on 12 % gels. The proteins found to be differentially expressed after analysis using Progenesis™ SameSpot software are numbered.

5.2.5 LC-MS/MS analysis of differentially expressed proteins

LC-MS/MS was carried out on the thirteen up-regulated protein spots and the five down-regulated protein spots in *A. fumigatus* Δ *elfA* compared to *A. fumigatus* ATCC46645 (Table 5.3 and 5.4). Vacuolar dynamin-like GTPase VpsA (AFUA_5G02360) showed the highest fold-increase in *A. fumigatus* Δ *elfA* compared to *A. fumigatus* ATCC46645, while RAS small monomeric GTPase RasA showed the highest fold-decrease.

Ten of the up-regulated proteins were identified from thirteen excised spots. Vacuolar dynamin-like GTPase VpsA (AFUA_5G02360), was identified from three different spots, while ATP Citrate lyase, subunit 1 (AFUA_6G10650) was identified from two spots. The molecular mass for all isoforms of vascular dynamin-like GTPase was the same; however there was a slight change in pI resulting in the three protein spots lying side by side in the gel (Figure 5.5). This was also observed for ATP Citrate lyase, where the molecular mass was the same for both protein spots but the pI changed slightly, again resulting in the protein spots being close together on the gel (Figure 5.5). These slight changes in pI may have resulted from post-translational modifications.

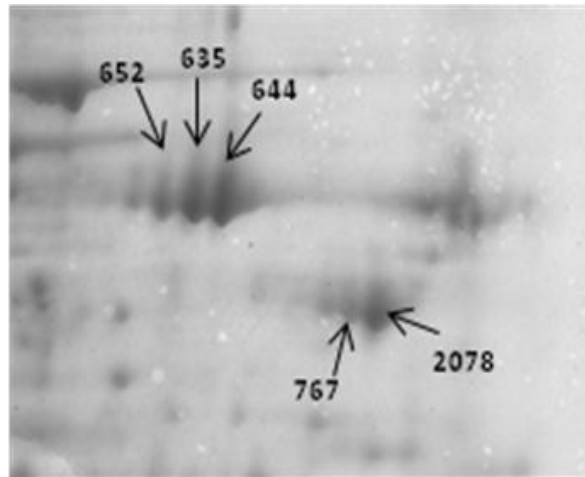


Figure 5.5: The positions of the protein spots corresponding to the isoforms of vascular dynamin-like GTPase and ATP Citrate lyase. Three isoforms of vascular dynamin-like GTPase (652, 635, 644) were observed as having the same molecular mass but slightly different pIs. Two isoforms of ATP Citrate lyase (767, 2078) had slightly different pIs but the same molecular mass.

As expected, proteins involved in the oxidative stress response were identified. Also identified were proteins involved in translation, metabolism and proteins associated with the mitochondria and the cytoskeleton. Cobalamin-independent methionine synthase Met H/D (AFUA_4G07360), glycerol-3-phosphate dehydrogenase (AFUA_1G08810) and Ras small monomeric GTPase RasA (AFUA_5G11230) are all involved in the oxidative stress response (Maeng *et al.*, 2010; Lessing *et al.*, 2007; Pahlman *et al.*, 2001). Cysteinyl-tRNA synthetase (AFUA_5G09610) and carbamyl-phosphate synthase (AFUA_2G10070), large subunit are involved in translation and purine biosynthesis, respectively (Pittman *et al.*, 2009). The proteins pyruvate decarboxylase PdcA (AFUA_3G11070) and pyruvate carboxylase (AFUA_4G07710) are involved in pyruvate metabolism (Hynes and Murray, 2010; Huet *et al.*, 2000). Proteins associated with the mitochondria include Mitochondrial outer membrane translocase receptor (TOM70) (AFUA_2G01660), ATP Citrate lyase subunit 1 (AFUA_6G10650) and glycerol-3-phosphate dehydrogenase (AFUA_1G08810), while Vacuolar dynamin-like GTPase VpsA (AFUA_5G02360) is associated with the cytoskeleton (Yu and Cai, 2004).

Table 5.3: Proteins ($n = 13$) with a fold increase in *A. fumigatus* Δ *elfA* compared to *A. fumigatus* after exposure to 2 mM H₂O₂ following identification by 2D-PAGE and LC-MS/MS.

Spot No.	Annotation name	CADRE ID	Fold Change	tpI	tMW	% Sequence coverage
644	Vacuolar dynamin-like GTPase VpsA	AFUA_5G02360	7.8	8.30	78425	18
635	Vacuolar dynamin-like GTPase VpsA	AFUA_5G02360	4.3	8.30	78425	3
652	Vacuolar dynamin-like GTPase VpsA	AFUA_5G02360	3.0	8.30	78425	19
592	Mitochondrial outer membrane translocase receptor (TOM70) putative	AFUA_2G01660	1.9	5.40	70009	10
767	ATP Citrate lyase, subunit 1, putative	AFUA_6G10650	1.9	8.60	78828	33
368	Carbamoyl-phosphate synthase, large subunit (A1163)	AFUA_2G10070	1.7	6.10	129214	25
567	Cobalamin-independent methionine synthase Met H/D	AFUA_4G07360	1.7	6.33	87072	31
1377	Metallo-beta-lactamase family protein	AFUA_5G12770	1.6	5.60	34197	30
526	Cysteinyl-tRNA synthetase	AFUA_5G09610	1.5	5.95	91041	25

continued

Table 5.3 continued.

630	Glycerol-3-phosphate dehydrogenase, mitochondrial	AFUA_1G08810	1.5	6.71	76899	31
694	Vacuolar ATP synthase catalytic subunit A	AFUA_5G02370	1.5	5.83	75329	43
787	Pyruvate decarboxylase PdcA	AFUA_3G11070	1.5	6.08	63307	33
2078	ATP Citrate lyase, subunit 1	AFUA_6G10650	1.5	8.66	79359	42

CADRE I.D.: *A. fumigatus* gene annotation nomenclature according to Nierman *et al.* (2005) and Mabey *et al.* (2004).

Table 5.4: Proteins ($n = 5$) with a fold decrease in *A. fumigatus* $\Delta elfA$ compared to *A. fumigatus* after exposure to 2 mM H₂O₂ following identification by 2D-PAGE and LC-MS/MS.

No.	Annotation name	CADRE ID	Fold Change	tpI	tMW	% Sequence coverage
1494	RAS small monomeric GTPase RasA	AFUA_5G11230	2.2	4.97	24292	61
1167	Nuclear pore complex protein (SonA)	AFUA_1G09020	2.1	7.61	40220	32
2066	Proteasome Regulatory Particle Subunit (RpnL)	AFUA_3G08940	1.8	4.9	31201	55
358	Pyruvate carboxylase	AFUA_4G07710	1.6	6.23	132003	27
1616	Haloalkanoic acid dehalogenase	AFUA_6G14460	1.6	6.19	26716	39

CADRE I.D.: *A. fumigatus* gene annotation nomenclature according to Nierman *et al.* (2005) and Mabey *et al.* (2004).

5.3 Discussion

The proteome of *A. fumigatus* $\Delta elfA$ was investigated and compared to the proteome of *A. fumigatus* ATCC46645 under both normal growth conditions and when exposed to H_2O_2 . Under normal growth conditions (24 h cultures in AMM), thirteen proteins were found to be differentially expressed in *A. fumigatus* $\Delta elfA$, eight proteins had an increase in expression, while five proteins exhibited a decrease in expression when compared to *A. fumigatus* ATCC46645. When exposed to H_2O_2 (2 mM for 1 h), eighteen spots, which corresponded to 15 proteins, were found to be differentially expressed in *A. fumigatus* $\Delta elfA$ when compared to *A. fumigatus* ATCC46645. Ten proteins showed increased expression in *A. fumigatus* $\Delta elfA$, while five proteins underwent a decrease in expression. Of particular interest was the increased expression of two aminoacyl-tRNA synthetases in *A. fumigatus* $\Delta elfA$; tyrosyl-tRNA was up-regulated under basal conditions, while cysteinyl-tRNA expression was increased upon exposure to H_2O_2 . Two proteins were identified from multiple spots, vacuolar dynamin-like GTPase VpsA was identified from three individual spots, while ATP Citrate lyase, subunit 1, was identified from two individual spots, indicating the presence of isoforms of these proteins, possibly as a result of posttranslational modifications. The proteins identified in both investigations were involved in different processes within the cell including the oxidative stress response, translation, cytoskeleton and metabolism.

A. fumigatus *elfA* is annotated as a translation elongation factor 1B gamma subunit (www.cadre-genomes.org.uk) therefore it was interesting to observe that in *A. fumigatus* $\Delta elfA$ tyrosyl-tRNA synthetase levels were increased 2.7 fold when

compared to *A. fumigatus* ATCC46645. Aminoacyl-tRNA synthetases catalyse the aminoacylation of tRNA, and so tyrosyl-tRNA synthetase tyrosylates tRNA^{Tyr} (Paukstelis and Lambowitz, 2008). In *S. cerevisiae*, it has been shown that eEF1A is involved in transferring the aminoacyl-tRNA from the tRNA synthetase to the elongating ribosome (Pittman *et al.*, 2009; Liu *et al.*, 1996). eEF1A is also involved in binding and bundling actin, a process which is conserved from yeast to mammals (Pittman *et al.*, 2009). In the presence of aminoacyl-tRNA, the actin bundling properties of eEF1A are reduced, and conversely, if eEF1A is binding actin it is not in a complex with aminoacyl-tRNA (Liu *et al.*, 1996). With the presence of an actin binding and bundling protein, Sac6, up-regulated in *A. fumigatus* $\Delta elfA$, eEF1A may be predominantly involved in binding and bundling actin as a response to the stress conditions observed with the deletion of *elfA* in *A. fumigatus*.

A. fumigatus possesses different mechanisms to respond to oxidative stress. Under basal growth conditions, the proteins mitochondrial peroxiredoxin Prx1, molecular chaperone Hsp70 and the Hsc70 co-chaperone, which were differentially expressed in *A. fumigatus* $\Delta elfA$, are involved in the oxidative stress response. Mitochondrial peroxiredoxin Prx1 had a fold-increase of 2.2 in *A. fumigatus* $\Delta elfA$ compared to *A. fumigatus* ATCC46645. Peroxiredoxins are ubiquitous thiol-specific proteins that function as antioxidants. In *S. cerevisiae*, a *prx1* deletion strain was sensitive to H₂O₂ and oxidative stress induced by cadmium (Greetham and Grant, 2009). Interestingly, in the same study it was found that mitochondrial peroxiredoxin Prx1 requires GSH for its antioxidant activity as both GSH and a thioredoxin were

required to maintain the mitochondrial peroxiredoxin Prx1 in a reduced active state. In *A. fumigatus*, mitochondrial peroxiredoxin Prx1 was up-regulated in response to H₂O₂ indicating a role in the oxidative stress response in *A. fumigatus* (Lessing *et al.*, 2007). In the same study mitochondrial peroxiredoxin Prx1 and ElfA were both down-regulated in an *A. fumigatus yap1* deletion strain leading the authors to suspect that they may be Yap1 targets, either directly or indirectly. In *A. nidulans*, orthologs of both ElfA and mitochondrial peroxiredoxin Prx1 were up-regulated in a glutathione reductase (*glrA*) deletion strain indicating a possible role for these two proteins in the oxidative stress response in *A. nidulans* (Sato *et al.*, 2009). The increased expression of mitochondrial peroxiredoxin Prx1 in *A. fumigatus* Δ *elfA* suggests that in the absence of ElfA, a stressed environment requires increased levels of Prx1 in the cell.

The molecular chaperone Hsp70 exhibited a 1.7 fold expression increase in *A. fumigatus* Δ *elfA* while the Hsc70 co-chaperone had a fold decrease of 1.7 when compared to *A. fumigatus* ATCC46645. Heat shock proteins (Hsps) are induced under different stress conditions as they are essential proteins involved in maintaining cellular homeostasis and increased levels can result in stress tolerance (Henderson, 2010; Guo *et al.*, 2007). Hsps are involved in many cellular processes including folding of newly synthesised proteins, degradation of misfolded proteins, disassembly of protein complexes, protein translocation and control of the activity of regulatory proteins (Bursac and Lithgow, 2009; Mayer and Bukau, 2005). During stress, (e.g., oxidative stress), the presence of oxygen radicals leads to the proteins in the cell becoming damaged or misfolded resulting in formation of protein aggregates

which are toxic to the cell (Goldberg, 2003). This results in the increased expression of molecular Hsp70 chaperones, among other proteins, in order to prevent the aggregation of misfolded proteins and promote normal protein folding and the refolding of denatured proteins (Goldberg, 2003). The Hsc70 co-chaperone is involved in recruiting Hsp70 to protein complexes and co-chaperones also play a role in determining whether Hsp70 will be involved in protein folding or protein degradation, thereby regulating their activity (Bursac and Lithgow, 2009; Tobaben *et al.*, 2003). Interestingly, in an eEF1B γ deletion strain in *S. cerevisiae*, the molecular Hsp70 chaperone ortholog, Ssa2p, was up-regulated when compared to the wild-type strain, and appeared in the wild-type strain once subjected with stress from CdSO₄ (Esposito and Kinzy, 2010). In *A. fumigatus*, molecular chaperone Hsp70 was up-regulated in response to heat shock, which increases the rate of respiration resulting in increased levels of ROS (Albrecht *et al.*, 2010b). The molecular chaperone Hsp70 was also found to be present at higher levels in *A. fumigatus* conidia compared to the mycelia (Teutschbein *et al.*, 2010). Conidia require the presence of proteins to confer tolerance and resistance to stress when they are in their dormant form but also to protect against host defence mechanisms, which includes ROS. In canine kidney cells, it was found that increased Hsp70 levels resulted in the increased activity of the GSH utilising enzymes glutathione reductase and glutathione peroxidase and in doing so, regulated the cellular redox status (Guo *et al.*, 2007).

The nuclear pore complex subunit Sec13 showed a 1.7 fold increase in expression in *A. fumigatus* Δ *elfA* compared to *A. fumigatus* ATCC46645. Sec13 is involved in coat protein complex II (COPII), vesicular trafficking, nuclear pore

function, and ER-directed protein sequestration and degradation control (Nielsen, 2009). Sec13 is involved in the final step in COPII vesicle formation (Gaspar *et al.*, 2008). The COPII complex is involved in transporting vesicles, usually containing secretory proteins and lipids, from the ER (Nielsen, 2009). COPII has also been shown to transport misfolded proteins to the endoplasmic reticulum associated degradation pathway (ERAD) (Fu and Sztul, 2003). The Sec13 ortholog in *S. cerevisiae* was up-regulated by the unfolded protein response (UPR) (Travers *et al.*, 2000). The observed Sec13 increased expression in *A. fumigatus* Δ *elfA* may indicate the need to deal with protein synthesis and secretion deficiencies which may have resulted in increased levels of misfolded proteins. Sec13 along with molecular chaperone Hsp70 may be up-regulated as they are both involved in dealing with increased levels of misfolded proteins, which may have arisen due to the presence of stress conditions.

There was a 1.9 fold increase in actin-bundling protein Sac6 in *A. fumigatus* Δ *elfA* compared to *A. fumigatus* ATCC46645. In *S. cerevisiae* the Sac6 ortholog, Sac6p, co-localises with actin and is involved in bundling actin filaments (Cheng *et al.*, 1999). Actin is a conserved cytoskeleton protein and is involved in many processes including growth, differentiation, endocytosis and exocytosis (Kummasook *et al.*, 2011). Actin also plays a role in response to stresses including heat stress, hyperosmotic stress and oxidative stress (Farah *et al.*, 2011). During oxidative stress, protection is conferred by the collapse of the cytoskeleton and the formation of actin bundles that sequester actin and its associated proteins into immobile and non-dynamic structures (Farah *et al.*, 2011; Zhu *et al.*, 2005). Farah *et*

al. (2011) observed the co-localisation of Sac6-GFP with these actin bundles in *S. cerevisiae* upon treatment with H₂O₂, menadione and diamide. This actin bundling prevents the cell from growing during oxidative stress conditions and also provides a source of cytoskeletal precursors for the reassembly of the actin cytoskeleton once the oxidative stress conditions have ceased. The increased expression of Sac6 in *A. fumigatus* Δ *elfA* points to an important role in protection against the stress conditions present under normal growth conditions in *A. fumigatus* Δ *elfA*. In *A. fumigatus* an increased expression of Sac6 was observed when subjected to heat shock, along with the molecular chaperone Hsp70, which may be in response to the increased ROS levels associated with heat stress, as well as the actual heat stress itself (Albrecht *et al.*, 2010b). Sac6 was present at higher levels in *A. fumigatus* conidia compared to mycelia, as was molecular chaperone Hsp70 also, again possibly to protect against the stresses encountered by conidia in the host (Teutschbein *et al.*, 2010).

Ketol-acid reductoisomerase displayed a 4.9 fold decrease in expression and phosphoribosylaminoimidazole carboxamide formyltransferase /IMP cyclohydrolase showed a 3 fold decrease in expression in *A. fumigatus* Δ *elfA* compared to *A. fumigatus* ATCC46645. These enzymes are involved in amino acid and nucleotide biosynthesis. Specifically, ketol-acid reductoisomerase is involved in the biosynthesis of branched-chain amino acids (Tyagi *et al.*, 2005; Dumas *et al.*, 2001), while phosphoribosylaminoimidazole carboxamide formyltransferase /IMP cyclohydrolase is involved in the *de novo* biosynthesis of purines (Boccalatte *et al.*, 2009; Wang *et al.*, 2009). The reduced expression of these enzymes indicates a

reduced requirement for protein synthesis and transcription and may be a response to the presence of the stress environment of *A. fumigatus* $\Delta elfA$.

Two unique spots in *A. fumigatus* $\Delta elfA$, not present in *A. fumigatus* ATCC46645, were identified as a thiazole synthase from *A. oryzae*. This protein is encoded by the pyrithiamine resistance gene, *ptrA*, used as the selection marker for deleting *A. fumigatus* *elfA* (Kubodera *et al.*, 2000). The identification of this protein confers confidence in both the comparative proteomics strategy and the identification of which protein spots are differently expressed between *A. fumigatus* ATCC46645 and $\Delta elfA$. The ability to identify the selection marker could also be exploited in other applications such as shotgun proteomics or quantitative label-free LC-MS (Neilson *et al.*, 2011), as it can act as a control between two different strains.

In the presence of H₂O₂, of the proteins differentially expressed in *A. fumigatus* $\Delta elfA$ compared to *A. fumigatus* ATCC46645, Vacuolar dynamin-like GTPase VpsA, Cobalamin-independent methionine synthase Met H/D and RAS small monomeric GTPase RasA have been linked to stress responses (Maeng *et al.*, 2010; Lessing *et al.*, 2007; Vizeacoumar *et al.*, 2006; Yu and Cai, 2004). Vacuolar dynamin-like GTPase VpsA was up-regulated in *A. fumigatus* $\Delta elfA$ compared to *A. fumigatus* ATCC46645 upon exposure to H₂O₂. Three isoforms of VpsA were identified in *A. fumigatus* $\Delta elfA$, which had fold increases of 7.8, 4.3 and 3.0. The three isoforms were of the same molecular mass but had a slight change in pI, most likely as a result of post-translational modification. In *S. cerevisiae*, the VpsA ortholog; Vps1, which it shares 60% sequence identity with, functions in membrane fusion and fission events within the Golgi, vacuole, endosome and peroxisome, and

also actin cytoskeleton organisation (Rooij *et al.*, 2010; Vizeacoumar *et al.*, 2006; Yu and Cai, 2004). Yu and Cai (2004) demonstrated that Vps1 is required for the normal organisation of the actin cytoskeleton and that over-expression of Vps1 led to actin defects. The reorganisation of actin has been shown in response to stress (Farah *et al.*, 2011) and may explain the increased expression of VpsA in *A. fumigatus* Δ elfA. With the absence of *A. fumigatus* ElfA, VpsA expression may be increased to allow for actin reorganisation in response to the oxidative stress induced by H₂O₂. Vps1 is also required for vacuole fission, a process that along with vacuole fusion, is required for the adaptation of vacuoles to changing environmental conditions (Baars *et al.*, 2007; Peters *et al.*, 2004). Fungal vacuoles are acidic organelles that have functions in both degradation and storage (Li and Kane, 2009). Vacuolar ATP synthase catalytic subunit A, which had a 1.5 - fold increase in expression in *A. fumigatus* Δ elfA, has been shown to be involved in both vacuole fusion and fission in *S. cerevisiae* (Baars *et al.*, 2007). Vacuolar ATPases work as proton pumps and regulate the pH of fungal vacuoles (Melin *et al.*, 2004). Baars *et al.* (2007) found that the acidification of the vacuole was necessary for vacuolar fission. The up-regulation of both VpsA and Vacuolar ATP synthase catalytic subunit A indicates that in the absence of *A. fumigatus* ElfA, VpsA expression is increased as a compensatory mechanism possibly resulting in increased vacuole fission in *A. fumigatus* Δ elfA. VpsA has also been implicated in peroxisome fission (Vizeacoumar *et al.*, 2006). Peroxisomes are involved in lipid metabolism and also in the detoxification of free radicals (Schluter *et al.*, 2006). We speculate that the increased levels of free radicals in *A. fumigatus* Δ elfA, upon exposure to H₂O₂, may have resulted in increased

peroxisomal activity and consequent VpsA up-regulation in order to increase the rate of peroxisome fission.

Cobalamin-independent methionine synthase Met H/D was up-regulated 1.7-fold in *A. fumigatus* $\Delta elfA$ compared to *A. fumigatus* ATCC46645 following exposure to H₂O₂. Cobalamin-independent methionine synthase is involved in the final step of methionine synthesis where it converts L-homocysteine to methionine (Suliman *et al.*, 2007). In *A. fumigatus*, cobalamin-independent methionine synthase was induced in response to heat shock (Albrecht *et al.*, 2010b) and was also identified as a possible *A. fumigatus yap1* target, suggesting a role in the oxidative stress response (Lessing *et al.*, 2007). The observed up-regulation of cobalamin-independent methionine synthase in *A. fumigatus* $\Delta elfA$ indicates an increased requirement for methionine in response to the stress induced by H₂O₂. Cobalamin-independent synthase is one of the enzymes in the S-adenosylmethionine (SAM) cycle (Figure 5.6) (Fontecave *et al.*, 2004). One of the intermediates of this pathway, homocysteine, can be converted to glutathione, resulting in increased glutathione levels in the cell (Fontecave *et al.*, 2004). In *Penicillium chrysogenum*, addition of methionine to the culture medium resulted in increased intracellular GSH levels (Emri *et al.*, 1998). Interestingly, in Chapter 4 increased intracellular GSH levels were observed in *A. fumigatus* $\Delta elfA$ following exposure to H₂O₂ and this will be discussed in more detail in Chapter 7. In *E. coli*, oxidative stress results in methionine auxotrophy, however cobalamin-independent methionine synthase was inactivated by glutathionylation under these conditions (Hondorp and Matthews, 2009; Hondorp and Matthews, 2004). The inactivation of cobalamin-independent

methionine synthase in *E. coli* may be a protective measure by preventing growth until stress conditions had abated (Hondorp and Matthews, 2009). In *A. fumigatus*, in the absence of ElfA, cobalamin-independent methionine synthase is up-regulated and may contribute to the oxidative stress response by participating in increasing intracellular GSH levels.

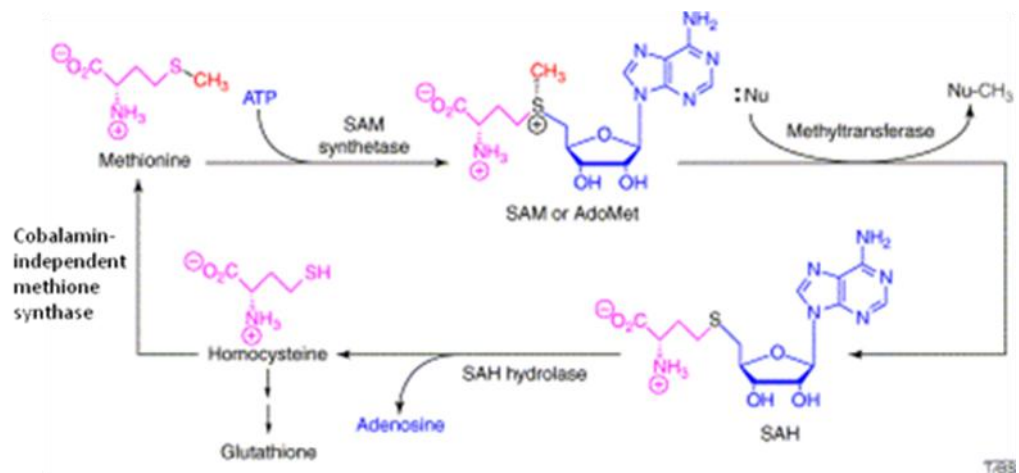


Figure 5.6: The *S*-adenosylmethionine (SAM) cycle. Cobalamin-independent methionine synthase catalyses the methylation of homocysteine to methionine. Figure adapted from Fontecave *et al.* (2004).

Mitochondrial glycerol-3-phosphate dehydrogenase was up-regulated in *A. fumigatus* Δ *elfA* 1.5 fold compared to *A. fumigatus* ATCC46645. Mitochondrial glycerol-3-phosphate dehydrogenase is a member of the glycerol-3-phosphate shuttle which is involved in transporting excess NADH to the mitochondrial electron transport chain (Saliola *et al.*, 2008; Pahlman *et al.*, 2001). In doing so, the cellular redox balance is maintained. Mitochondrial glycerol-3-phosphate dehydrogenase may be up-regulated in *A. fumigatus* Δ *elfA* in order to restore the redox balance, disrupted by the addition of H₂O₂.

Expression of RAS small monomeric GTPase RasA was decreased 2.2 fold in *A. fumigatus* Δ *elfA* compared to *A. fumigatus* ATCC46645 following exposure to 2 mM H₂O₂. In *A. fumigatus*, RasA regulates hyphal morphogenesis and is involved in multiple cellular processes including maintenance of polarity, cell wall integrity and vacuolar expansion (Fortwendel *et al.*, 2011). In *C. albicans* the Ras-cAMP cascade represses the expression of oxidative stress response conditions and mutants in this cascade have shown increased resistance to oxidative stress (Deveau *et al.*, 2010; Bahn *et al.*, 2007). The down-regulation or deletion of Ras genes in *S. cerevisiae* and *C. neoformans* have also resulted in increased resistance to oxidative stress (Maeng *et al.*, 2010; Longo and Fabrizio, 2002). There are two orthologs of *A. fumigatus* *rasA* in *S. cerevisiae*; *ras1* and *ras2* sharing 41 % and 42 % sequence identity to *A. fumigatus* *rasA*. Deletion of *S. cerevisiae* *ras2* resulted in increased stress resistance, particularly to superoxide toxicity (Longo and Fabrizio, 2002; Longo, 1999). In *C. neoformans*, the deletion of *ras1* resulted in a strain that demonstrated increased resistance to oxidative stress exerted by H₂O₂ or menadione

compared to the wild-type (Maeng et al., 2010). The down-regulation of RasA in *A. fumigatus* Δ *elfA* may therefore be a response to the oxidative stress induced by H₂O₂.

The 26S proteasome is a protease complex functioning in the degradation of misfolded proteins and short-lived regulatory proteins (Tone *et al.*, 2000). The 26S proteasome is composed of the 19S regulatory particle and the 20S proteasome (Goldberg, 2003; Tone *et al.*, 2000). The 20S proteasome is the catalytic core responsible for protein degradation of oxidised proteins, while the 19S regulatory particle is required for the degradation of ubiquitinated proteins (Shringarpure *et al.*, 2003; Tone *et al.*, 2000). The Proteasome regulatory particle subunit (RpnL) had a fold decrease of 1.8 in *A. fumigatus* Δ *elfA*. The ortholog of RpnL in *S. cerevisiae*, Rpn12, along with other proteins, forms the lid of the 19S regulatory particle (Tone *et al.*, 2000). Shringarpure *et al.* (2003) reported that the 26S proteasome is sensitive to oxidative stress while the 20S proteasome is resistant. In fact, in oxidative stress conditions, the 20S proteasome dissociates from the 19S regulatory particle (Wang *et al.*, 2010). Yeast mutants in which this dissociation has been blocked, and consequently contain 26S proteasomes, are more sensitive to H₂O₂ than wild-type yeast cells in which the dissociation occurs (Wang *et al.*, 2010). We speculate that as the 19S regulatory subunit inhibits degradation of oxidised proteins upon exposure to H₂O₂, it exhibits decreased expression in *A. fumigatus* Δ *elfA*.

As was the case under basal growth conditions, an aminoacyl-tRNA synthetase was found to be up-regulated in *A. fumigatus* Δ *elfA* following exposure to H₂O₂. Under basal conditions, expression of tyrosyl-tRNA synthetase was increased, however following H₂O₂ exposure, cysteinyl-tRNA synthetase expression was

elevated 1.5 fold in *A. fumigatus* $\Delta elfA$ compared to *A. fumigatus* ATCC46645. Cysteine-containing proteins are required in redox homeostasis in reactions (e.g., glutathionylation and sulfenic acid formation), and are very important for signalling processes in response to environmental stress, including oxidative stress (Jones and Go, 2011; Meyer and Hell, 2005a). In *A. fumigatus* $\Delta elfA$, in the presence of H_2O_2 , increased synthesis of cysteine-containing proteins may be required, resulting in the increased expression of cysteinyl-tRNA synthetase.

ATP Citrate lyase, subunit 1, was identified from two spots, which were up-regulated 1.9 and 1.5 fold, respectively, in *A. fumigatus* $\Delta elfA$ compared to *A. fumigatus* ATCC46645. ATP Citrate lyase cleaves citrate into oxaloacetate and cytosolic acetyl coenzyme A (CoA) (Son *et al.*, 2011; Hynes and Murray, 2010). Acetyl-CoA is required for carbon and energy metabolism, many biosynthetic processes including the synthesis of polyketides and fatty acids, acetylation of histones, and is essential for normal growth and development (Hynes and Murray, 2010). In particular cytoplasmic acetyl-CoA is required for fatty acid biosynthesis (Hynes and Murray, 2010). In *A. fumigatus*, ATP Citrate lyase was up-regulated in response to heat shock (Albrecht *et al.*, 2010b). Pyruvate carboxylase was decreased 1.6 fold in expression in *A. fumigatus* $\Delta elfA$ compared to *A. fumigatus* ATCC46645. Pyruvate carboxylase converts pyruvate into oxaloacetate which then enters the TCA cycle (Huet *et al.*, 2000). This would suggest that there is decreased aerobic respiration in *A. fumigatus* $\Delta elfA$ upon exposure to H_2O_2 . This is supported by the observation of increased expression of pyruvate decarboxylase PdcA, which had a fold increase of 1.5 in *A. fumigatus* $\Delta elfA$. Pyruvate decarboxylase decarboxylates

pyruvate to form acetaldehyde which can then be converted to acetate or is metabolised to ethanol by anaerobic respiration (Hynes and Murray, 2010). The decreased expression of pyruvate carboxylase and the increased expression of pyruvate decarboxylase suggest a switch from aerobic respiration to anaerobic respiration following exposure to H₂O₂ in *A. fumigatus* $\Delta elfA$, while the increased expression of ATP Citrate lyase indicates a requirement for increased levels of cytosolic acetyl-CoA possibly for fatty acid biosynthesis (Figure 5.7).

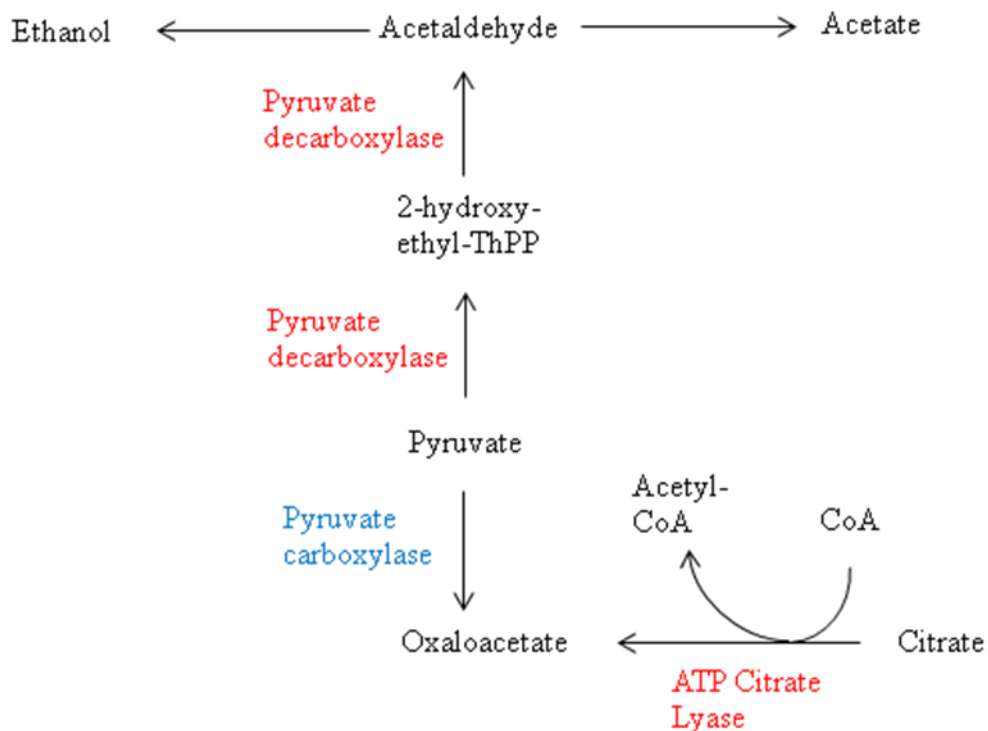


Figure 5.7: Pyruvate metabolism in *A. fumigatus* $\Delta elfA$ following exposure to H_2O_2 . ATP Citrate lyase (red) cleaves citrate into oxaloacetate and Acetyl-CoA. Acetyl-CoA may be required for fatty acid synthesis. At the same time pyruvate carboxylase (blue), which converts pyruvate into oxaloacetate which enters the TCA cycle, was down-regulated. Pyruvate decarboxylase (red) expression was increased in *A. fumigatus* $\Delta elfA$. Pyruvate decarboxylase converts pyruvate into acetaldehyde which is then converted into either ethanol or acetate. The increased expression of pyruvate decarboxylase and the decreased expression of pyruvate carboxylase suggest a shift from aerobic to anaerobic respiration. (Figure adapted from www.genome.jp/kegg/pathway).

In summary, the work in this chapter describes changes in the proteome of *A. fumigatus* Δ *elfA* compared to that of *A. fumigatus* ATCC46645, under basal growth conditions and following exposure to H₂O₂. Under basal growth conditions proteins ($n = 8$) had a fold increase in *A. fumigatus* Δ *elfA*, while proteins ($n = 5$) had a fold decrease when compared to *A. fumigatus* ATCC46645. Upon exposure to H₂O₂ ten proteins had a fold increase in *A. fumigatus* Δ *elfA* while there was a fold decrease for five proteins when compared to *A. fumigatus* ATCC46645. All of the proteins were identified by LC-MS/MS and had functions ranging from stress response, translation, actin cytoskeleton and metabolism. Proteins involved in stress response (e.g., mitochondrial peroxiredoxin Prx1 and molecular chaperone Hsp70) were identified with increased expression in *A. fumigatus* Δ *elfA* grown under basal conditions, indicating the induction of cellular stress possibly due to the absence of ElfA. This supports the phenotypes and altered GSH/GSSG ratios observed in Chapter 4, and will be discussed in detail in Chapter 7. Proteins involved with the actin cytoskeleton were also identified as undergoing differential expression in *A. fumigatus* Δ *elfA* revealing previously unknown changes in the actin cytoskeleton, upon deletion of *A. fumigatus* *elfA*. From the proteins identified in *A. fumigatus* Δ *elfA*, following exposure to H₂O₂, possible changes in vacuole and peroxisome numbers along with changes in metabolism were different to the *A. fumigatus* ATCC46645 response to H₂O₂. Investigating the proteome of *A. fumigatus* Δ *elfA* has provided an insight into the systems changes within the fungus as a result of the loss of ElfA, and not only complements the phenotypic studies carried out, but also provides evidence of other possible roles of ElfA in *A. fumigatus*. In Chapter 6, a

study of the proteome of germlings from an NRPS deletion strain, *A. fumigatus* $\Delta pes3$, will be described to determine if this proteomic approach can offer insight into additional gene function in another *A. fumigatus* deletion strain.

6.1 Introduction

Comparative proteomics of *A. fumigatus* ATCC46645 and $\Delta elfA$, described in Chapter 5 extended the information gained from phenotypic analysis and also provided further insight into possible roles of *A. fumigatus elfA*. 2D-PAGE proteome maps of *A. fumigatus* contain proteins which are annotated as unknown function proteins (Vodisch *et al.*, 2009). One of the challenges facing fungal proteomics is in assigning functions to these unknown function proteins (Doyle, 2011). Comparative proteomics is one strategy employed to elucidate protein function. In conjunction with the gene deletion of an unknown function protein, comparative proteomics can determine the effects of the loss of the unknown function protein on the systems within the cell, as was observed with *A. fumigatus* ElfA in Chapter 5. *A. fumigatus pes3* is a nonribosomal peptide synthetase (NRPS) that encodes a protein of unknown function. Comparative proteomics was applied to a *pes3* disrupted strain, *A. fumigatus* $\Delta pes3$, to determine if comparative proteomics could aid the elucidation of the function of this enzyme in *A. fumigatus*.

Nonribosomal peptides (NRPs) are synthesised independently of the ribosome during secondary metabolism in bacteria and fungi (Stack *et al.*, 2007; Cramer *et al.*, 2006a) and include many secondary metabolites such as gliotoxin in *A. fumigatus* (Cramer *et al.*, 2006b), and the iron-chelating siderophores (Schrettl *et al.*, 2007). NRPs are derived not only from the twenty proteinogenic amino acids but also non-proteinogenic amino acids, fatty acids, and α -hydroxy acids (Strieker *et al.*, 2010). NRP synthesis is carried out by multimodular enzymes called nonribosomal peptide synthetases (NRPSs) (Stack *et al.*, 2007). Each module in an NRPS is

composed of an adenylation domain (A), a thiolation (T) (also known as a peptidyl carrier protein (PCP)) domain, and a condensation domain (C) (Figure 6.1) (Mootz *et al.*, 2002). The adenylation domain is responsible for the recognition and activation of amino acid substrates by adenylation by ATP hydrolysis. The peptidyl carrier protein covalently binds the substrate, which was transferred from the adenylation domain, to the enzyme via a thioester linkage. Finally, the condensation domain catalyses the formation of a peptide bond between the bound aminoacyl and peptidyl intermediates (Stack *et al.*, 2007; Cramer *et al.*, 2006a). The final product is released by a thioesterase domain, which is found at the most downstream module of the NRPS. The three domains are in the order adenylation, thiolation and condensation in a linear NRPS, forming an elongation module that adds one amino acid to the growing chain. The order of modules within an NRPS dictates the order of the amino acids in the peptide product (Neville *et al.*, 2005). Iterative NRPSs and nonlinear NRPSs deviate from this A-T-C organisation of domains in the modules (Stack *et al.*, 2007).

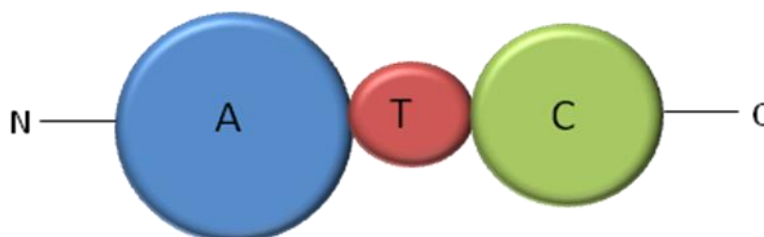


Figure 6.1: Schematic representation of a module in an NRPS. Each module contains an adenylation domain (A), a thiolation domain (T) and a condensation domain (C) in this order.

NRPSs are activated when 4'-phosphopantetheine is transferred from coenzyme A to a conserved serine residue within the thiolation domain by the enzyme 4'-phosphopantetheinyl transferase (4'-PPTase) (Stack *et al.*, 2009; Neville *et al.*, 2005). The phosphopantetheinylation of the thiolation domain converts the inactive apo-enzyme to the active holo-enzyme. The 4'-phosphopantetheine prosthetic groups anchor the activated aminoacyl intermediates, via a thioester linkage (Stack *et al.*, 2007). This anchorage allows for the movement of intermediates between the active sites of the NRPS during NRP synthesis (Neville *et al.*, 2005).

A. fumigatus contains fourteen genes encoding putative NRPSs (Cramer *et al.*, 2006a). *A. fumigatus gliP* is a bimodular NRPS and is required for the biosynthesis of gliotoxin (Cramer *et al.*, 2006b). Siderophores are involved in the acquisition of iron, and two siderophores in *A. fumigatus*; SidC and SidD, are synthesised by NRPSs (Schrettl *et al.*, 2007). The NRPS brevianamide F synthetase (FtmA) produces the precursor of the fumitremorgin family of secondary metabolites, brevianamide F which is the diketopiperazine scaffold (Maiya *et al.*, 2006). Pes1, a multimodular NRPS, has roles in the protection against oxidative stress and also virulence in *A. fumigatus* (Reeves *et al.*, 2006).

A. fumigatus pes3 is encoded by the largest gene (25 kb) in the *A. fumigatus* genome (O'Hanlon, 2010; Stack *et al.*, 2009). *A. fumigatus pes3* is predicted to synthesise a peptide containing six amino acids as it contains six adenylation domains, provided each adenylation domain is specific for a unique substrate (Figure 6.2) (Cramer *et al.*, 2006a). Stack *et al.* (2009) demonstrated that a

recombinant Pes3 module was a target for 4'-phosphopantetheinylation by 4'-PPTase, and therefore it is likely that Pes3 is activated *in vivo* by this process. *A. fumigatus pes3* expression was highest in ungerminated spores when the expression of all the NRPS genes in *A. fumigatus* was analysed, leading to a hypothesis that *A. fumigatus pes3* may be involved in germination (Cramer *et al.*, 2006a). Despite extensive metabolite profiling, no intracellular or secreted Pes3 produced product was identified (O'Hanlon, 2010). However, in the same study, a *pes3* disrupted strain; *A. fumigatus Δpes3*, exhibited increased sensitivity to voriconazole and increased resistance to diamide. In both a *G. mellonella* and a murine model of pulmonary aspergillosis, *A. fumigatus Δpes3* displayed increased virulence. Finally, comparative SEM analysis of *A. fumigatus* ATCC46645 and *Δpes3* germlings revealed smoother hyphal surfaces on *A. fumigatus Δpes3* compared to wild-type and the loss of rod-like strands that were present in the wild-type. While these phenotypes are very informative regarding cellular processes affected by the loss of *A. fumigatus* Pes3, there is no molecular explanation for these phenotypes. It was hypothesised that the use of comparative proteomics would provide further insight into *A. fumigatus* Pes3 function.

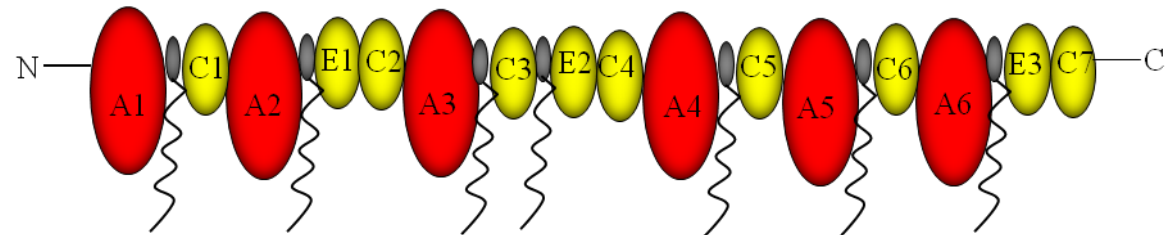


Figure 6.2: Schematic representation of the domain structure of *A. fumigatus* Pes3 (Stack *et al.*, 2009). *A. fumigatus* Pes3 consists of six adenylation domains (A1 - A6), seven thiolation domains (in grey), seven condensation domains (C1 - C7), and three epimerisation domains (E1 - E3). The black helices that extend from the thiolation domains represent the 4'-phosphopantetheine groups that are added post-translationally.

Consequently, the aims of the work described in this chapter were to (i) investigate differences in the proteome of *A. fumigatus* ATCC46645 and $\Delta pes3$ germlings, (ii) to image and compare the surface (1,3)- β -glucan of *A. fumigatus* ATCC46645 and $\Delta pes3$ germlings using confocal microscopy (iii) to determine the germination rate of *A. fumigatus* ATCC46645 and $\Delta pes3$ conidia under static conditions and (iv) to determine the MIC of voriconazole for *A. fumigatus* ATCC46645 and $\Delta pes3$. This analysis of *A. fumigatus pes3* was carried out to further the elucidation of its function.

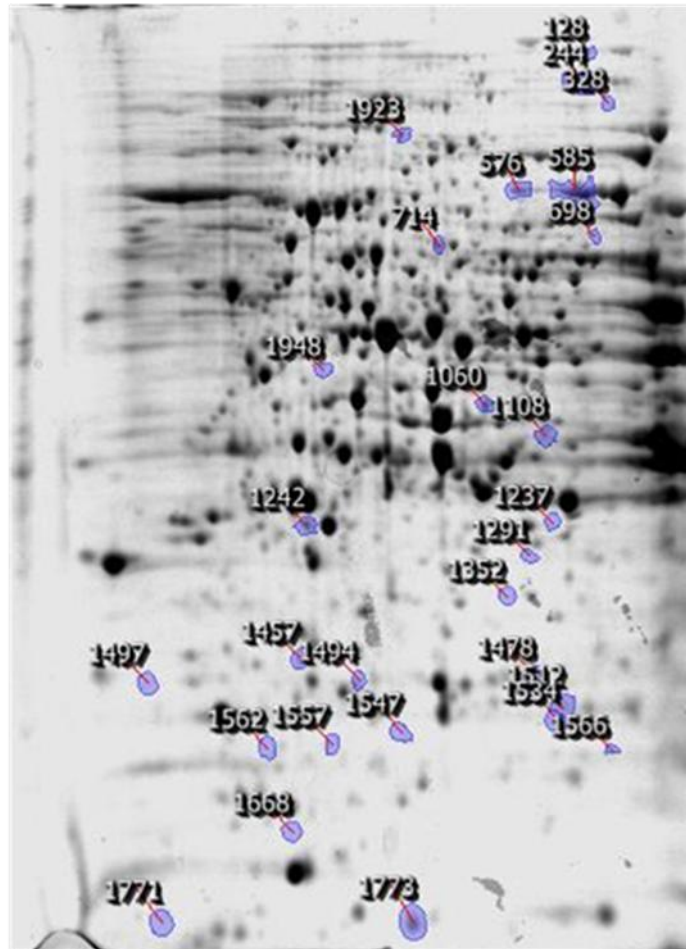
6.2 Results

6.2.1 Comparative proteomic analysis of *A. fumigatus* ATCC46645 and *A. fumigatus* $\Delta pes3$

A. fumigatus ATCC46645 and $\Delta pes3$ were cultured for 9 h in AMM before the germlings were harvested and protein was extracted as described in Section 2.2.16.4. The protein lysates were TCA/Acetone precipitated and resuspended in IEF Buffer (Section 2.2.17) before separation on pH 4 - 7 strips (300 μ g protein/ strip) (Section 2.2.18). Following separation by SDS-PAGE on a 12 % gel, the gels were stained with Colloidal Coomassie (Section 2.2.14) and analysed using ProgenesisTM SameSpot Software (Figure 6.3).

Twenty six protein spots were found to be differentially expressed; fifteen protein spots had a fold increase ≥ 1.5 in *A. fumigatus* $\Delta pes3$ germlings while eleven protein spots had a fold decrease ≥ 1.5 when compared to *A. fumigatus* ATCC46645 germlings. These spots were excised from the gels, trypsin digested as described in Section 2.2.19 and analysed by LC-MS/MS (Section 2.2.21).

A. pH 4 _____ 7



B. pH 4 _____ 7

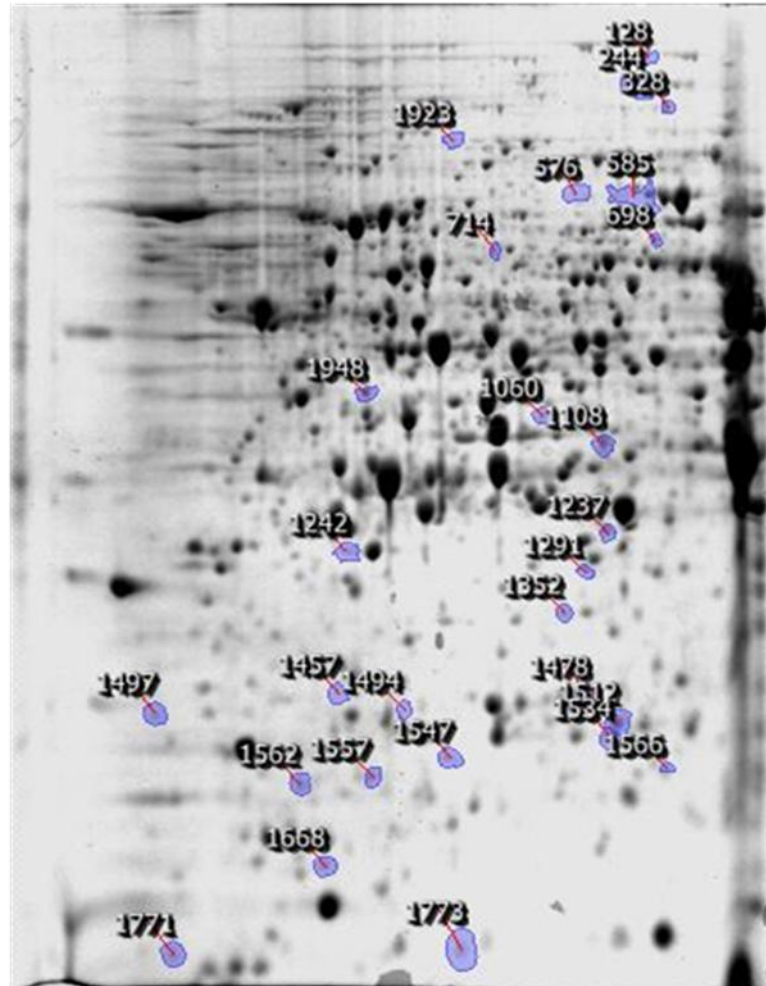


Figure 6.3: 2D-PAGE analysis of *A. fumigatus* ATCC46645 (A) and $\Delta pes3$ 9 h germlings (B). The proteins were first separated on pH 4 – 7 strips followed by SDS-PAGE on 12 % gels. The proteins found to be differentially expressed after analysis using Progenesis™ SameSpot software are numbered.

6.2.2 LC-MS/MS analysis of differentially expressed proteins

Twenty five proteins were identified from the twenty six excised spots by LC-MS/MS (Tables 6.1 and 6.2). The protein identified as having the highest fold increase in *A. fumigatus* $\Delta pes3$ germlings compared to *A. fumigatus* ATCC46645 was 60S ribosomal protein L5 (AFUA_1G12890). Whereas, the protein exhibiting the highest fold decrease in *A. fumigatus* $\Delta pes3$ germlings compared to *A. fumigatus* ATCC46645 was transketolase TktA (AFUA_1G13500).

Transketolase TktA was identified from two different spots which were decreased 3.1 and 2.5 fold, respectively. Both protein spots exhibited the same molecular mass however they differed in pI. The pI for protein spot 576 was 6.12 but was higher for protein spot 585 at pI 6.3. This increased pI may have resulted from post-translational modification.

Among the proteins with increased expression in *A. fumigatus* $\Delta pes3$ were proteins involved in heat shock, the electron transport chain and proteins associated with the ribosome. Three heat shock proteins; Hsp70 (AFUA_1G07440), Hsp30/Hsp42 (AFUA_3G14540) and molecular chaperone Hsp70 (AFUA_1G07440) (Albrecht *et al.*, 2010b) were all up-regulated 2.6, 1.6 and 2.1 fold respectively. The 40S ribosomal protein S5 and the 60S ribosomal protein L5 were increased 3.2 and 4.1 fold in expression in *A. fumigatus* $\Delta pes3$. Proteins involved in germination and morphology were among the proteins with decreased expression in *A. fumigatus* $\Delta pes3$ compared to *A. fumigatus* ATCC46645. These proteins comprise of pentafunctional polypeptide AroM (AFUA_1G13740) (Lamb *et*

al., 1991), spermidine synthase (AFUA_1G13490) (Jin *et al.*, 2002) and actin (AFUA_6G04740) which had fold decreases of 2.9, 1.8 and 2.1, respectively.

Table 6.1: *A. fumigatus* proteins ($n = 15$) with a fold increase in *A. fumigatus* $\Delta pes3$ germlings compared to *A. fumigatus* germlings following identification by 2D-PAGE and LC-MS/MS.

Spot No.	Annotation name	CADRE ID	Fold Change	tpI	tMW	% Sequence coverage
328	Glycine dehydrogenase	AFUA_4G03760	1.8	6.71	116116	12
698	t-complex protein 1, zeta subunit	AFUA_3G09590	2.2	6.31	59081	6
1108	NGG1 interacting factor Nif3	AFUA_6G12480	1.7	6.08	42126	23
1291	ATP Synthase gamma chain, mitochondrial precursor	AFUA_1G03510	1.8	8.31	32530	47
1352	Glucosamine-6-phosphate deaminase	AFUA_1G00480	3.2	8.35	40181	4
1478	GTP-Binding nuclear protein Ran	AFUA_6G13300	1.9	7.50	24077	23
1497	Heat Shock Protein 70	AFUA_1G07440	2.6	5.09	69792	2
1512	Heat Shock Protein Hsp30/Hsp42	AFUA_3G14540	1.6	6.09	20450	46
1534	Ubiquinol-cytochrome C reductase iron-sulfur subunit precursor	AFUA_5G10610	1.8	9.20	33111	33
1557	Ras GTPase Rab11	AFUA_1G02190	3.6	5.95	22568	43

Continued

Table 6.1: continued

1562	40S Ribosomal protein S5	AFUA_1G15020	3.2	9.35	25886	6
1566	Mitochondrial ATPase subunit ATP4	AFUA_8G05440	2.0	9.36	29767	33
1668	60S Ribosomal protein L5	AFUA_1G12890	4.1	8.59	35519	14
1771	Molecular Chaperone Hsp70	AFUA_1G07440	2.1	5.09	69792	7
1948	Enolase/Allergen Asp F 22	AFUA_6G06770	2.1	5.39	47392	42

CADRE I.D.: *A. fumigatus* gene annotation nomenclature according to Nierman *et al.* (2005) and Mabey *et al.* (2004).

Table 6.2: *A. fumigatus* proteins ($n = 10$) with a fold decrease in *A. fumigatus* $\Delta pes3$ germlings compared to *A. fumigatus* germlings following identification by 2D-PAGE and LC-MS/MS.

Spot No.	Annotation name	Gene ID	Fold Change	tpI	tMW	% Sequence coverage
128	Pentafunctional polypeptide (AroM)	AFUA_1G13740	2.9	6.15	175521	12
244	Pyruvate Carboxylase	AFUA_4G07710	2.2	6.23	132003	16
576	Transketolase TktA	AFUA_1G13500	3.1	6.12	75245	24
585	Transketolase TktA	AFUA_1G13500	2.5	6.12	75245	31
714	Phosphoglucomutase	AFUA_3G03020	2.2	5.78	56680	18
1060	Actin	AFUA_6G04740	2.1	5.37	43397	52
1242	Spermidine synthase	AFUA_1G13490	1.8	5.24	33444	28
1457	Phosphoserine phosphatase	AFUA_4G12730	1.6	5.67	33442	26
1494	Glycerol-3-phosphate phosphatase	AFUA_1G10570	2.5	5.48	25765	34
1773	Nascent polypeptide-associated complex (NAC) subunit	AFUA_6G02750	2.0	5.32	20591	27
1923	Aminopeptidase	AFUA_5G04330	2.0	6.26	109277	22

CADRE I.D.: *A. fumigatus* gene annotation nomenclature according to Nierman *et al.* (2005) and Mabey *et al.* (2004).

6.2.3 Identification of thiazole synthase, which is encoded by the selection marker *ptrA*, in *A. fumigatus* $\Delta pes3$ germlings only.

Two unique spots, observed in *A. fumigatus* $\Delta pes3$ germlings only following 2D-PAGE and image analysis, were excised and subjected to LC-MS/MS (Figure 6.4). Both spots were identified as a thiazole synthase from *A. oryzae*. As mentioned in Chapter 5, this protein is encoded for by the pyrthiamine gene, which was used as the selection marker in the transformation of *A. fumigatus* $\Delta pes3$ (O'Hanlon *et al.*, 2011). As was the case with *A. fumigatus* $\Delta elfA$, two isoforms of thiazole synthase were also identified in *A. fumigatus* $\Delta pes3$. The observation of two isoforms of this protein was discussed in Chapter 5.

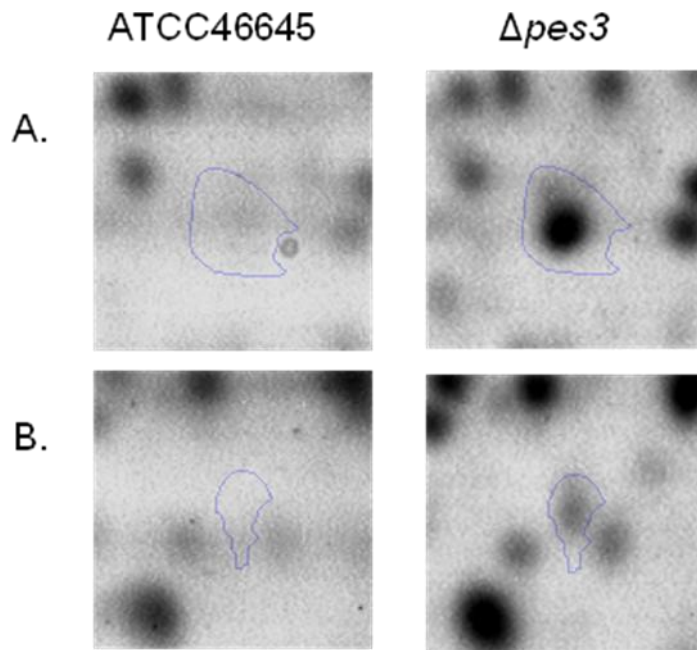


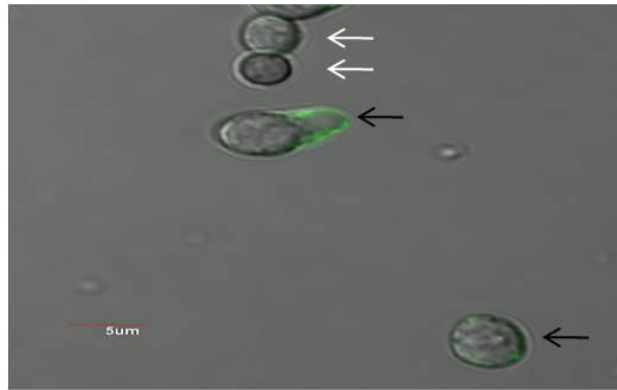
Figure 6.4: The observation and identification of the thiazole synthase encoded by *A. oryzae ptrA*. This protein was identified from two spots (A. and B.) in *A. fumigatus* $\Delta pes3$ and was not present in *A. fumigatus* ATCC46645. This protein is encoded by the pyrithiamine resistance gene, *ptrA*, from *A. oryzae* that was used as a selection marker in the deletion of *A. fumigatus pes3* (O'Hanlon *et al.*, 2011).

6.2.4 Confocal Imaging of (1,3)- β -glucan in *A. fumigatus* ATCC46645 and *A. fumigatus* $\Delta pes3$

A. fumigatus ATCC46645 and $\Delta pes3$ were cultured for 9 h in AMM before the germlings were harvested and fixed in 4 % (v/v) formaldehyde, followed by staining for confocal microscopy as described in Section 2.2.29. (1,3)- β -glucan in the cell wall was stained by first incubating the germlings with a mouse antibody IgG [anti-linear-(1,3)- β -glucan], followed by staining with Alexa Fluor 488 goat anti-mouse antibody. The germlings were then imaged by confocal microscopy.

(1,3)- β -glucan was successfully stained and was visible in the cell walls of both *A. fumigatus* ATCC46645 and $\Delta pes3$ germlings (Figure 6.5). Interestingly, (1,3)- β -glucan was only visible in germinating conidia and germ tubes, and not in resting conidia (Figure 6.5a). Differences in germling length between *A. fumigatus* ATCC46645 and $\Delta pes3$ was observed whereby the *A. fumigatus* $\Delta pes3$ germlings were shorter in length than those of *A. fumigatus* ATCC46645 (Figure 6.5b). The expression of (1,3)- β -glucan on the surface of the cell walls of the germlings from the two strains was compared by measuring the intensity of the stained (1,3)- β -glucan. The pixel intensity of a fixed area on each germling was measured to determine the (1,3)- β -glucan content. A fixed area on each germling was measured to ensure that germling size did not affect the measurement. There were significantly ($p = 0.0325$) reduced levels of (1,3)- β -glucan present on the cell surface of *A. fumigatus* $\Delta pes3$ compared to that in *A. fumigatus* ATCC46645 (Figure 6.5c).

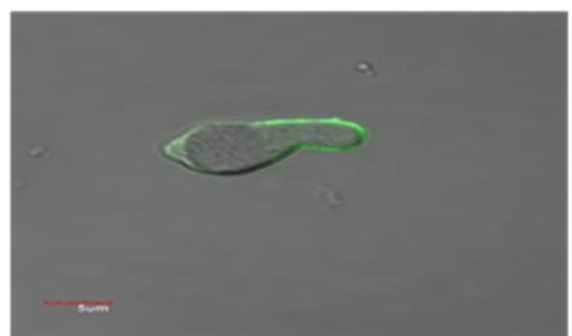
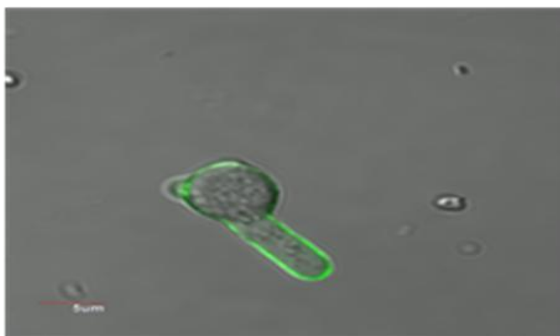
A.



B.

ATCC46645

$\Delta pes3$



C.

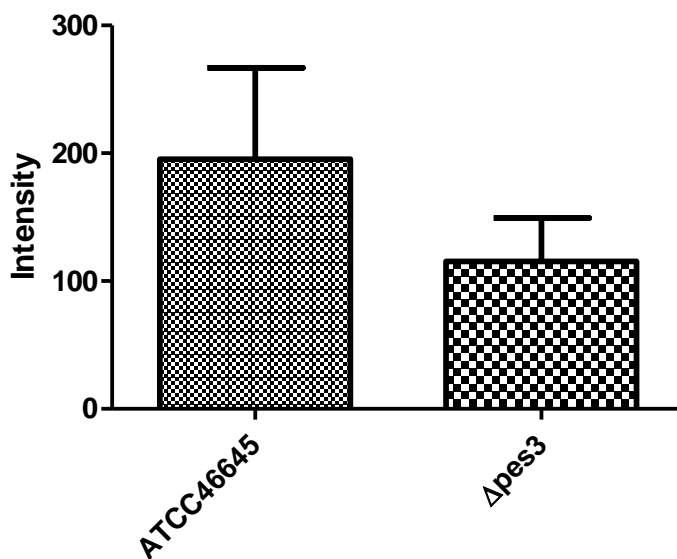


Figure 6.5: Confocal microscopy analysis of (1,3)- β -glucan in *A. fumigatus* ATCC46645 and $\Delta pes3$ germlings.

- A.** Representative confocal image of a germling and conidia. (1,3)- β -glucan was detected on the surface of the cell wall in the germling and the swollen conidia (indicated by black arrows), while no (1,3)- β -glucan was detected in resting conidia (indicated by white arrow).
- B.** Confocal images of *A. fumigatus* ATCC46645 and $\Delta pes3$ germlings show the stained (1,3)- β -glucan on the cell wall surface and also the difference in length of the germ tubes. *A. fumigatus* $\Delta pes3$ exhibits shorter germ tubes than *A. fumigatus* ATCC46645.
- C.** There was significantly less ($p = 0.0325$) (1,3)- β -glucan on the surface of *A. fumigatus* $\Delta pes3$ germlings when compared to those of *A. fumigatus* ATCC46645.

6.2.5 *A. fumigatus* $\Delta pes3$ germinated at a slower rate than *A. fumigatus* ATCC46645 under static conditions

When cultured under shaking conditions, both *A. fumigatus* ATCC46645 and $\Delta pes3$ conidia germinated at the same rate (O'Hanlon *et al.*, 2011). Proteins involved in germination were down-regulated in expression in *A. fumigatus* $\Delta pes3$ 9 h germlings, so the rate of germination under static conditions was determined for both *A. fumigatus* ATCC46645 and $\Delta pes3$ (Section 2.2.27). Germination was first recorded in both strains at 6 h. The germination rate of *A. fumigatus* $\Delta pes3$ was significantly slower ($p < 0.01$) than that of *A. fumigatus* ATCC46645 after 8 h and 10 h (Figure 6.6). After 8 - 10 h, the percentage of *A. fumigatus* $\Delta pes3$ conidia that had germinated was 10 – 20 %, whereas 20 – 35 % of *A. fumigatus* ATCC46645 conidia had germinated.

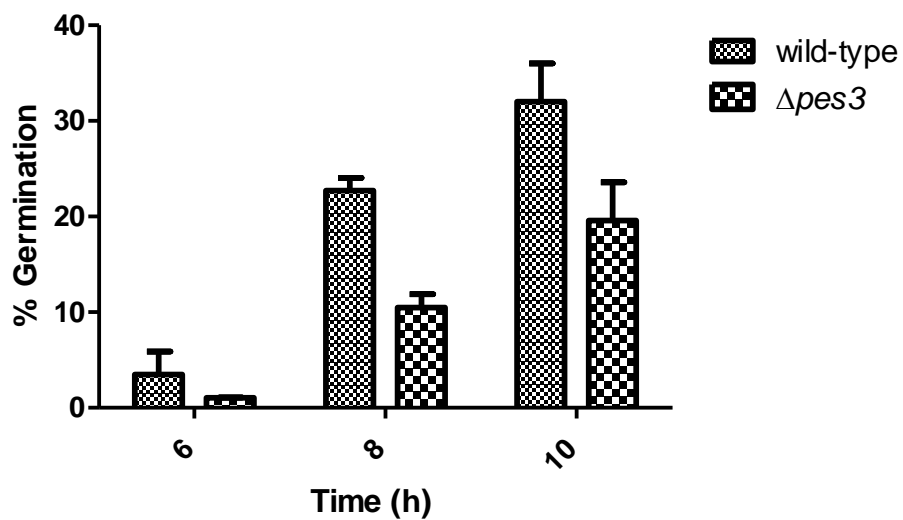


Figure 6.6: Germination rate of *A. fumigatus* ATCC46645 and $\Delta pes3$ conidia under static conditions. Germination was first recorded in both strains after 6 h and the rate of germination of *A. fumigatus* $\Delta pes3$ was significantly slower ($p < 0.01$) than that in *A. fumigatus* ATCC46645.

6.2.6 Investigation of hydrophobicity of *A. fumigatus* $\Delta pes3$ conidia

Scanning electron microscopy (SEM) analysis of *A. fumigatus* ATCC46645 and $\Delta pes3$ revealed that the surface of *A. fumigatus* $\Delta pes3$ germlings appeared smoother than that of *A. fumigatus* ATCC46645 and did not have distinctive rod-like strands that were present on *A. fumigatus* ATCC46645 (O'Hanlon *et al.*, 2011). The hydrophobicity of *A. fumigatus* ATCC46645 and $\Delta pes3$ conidia was determined (Section 2.2.26) and no difference between the two strains was observed (Figure 6.7).

6.2.7 Determining the MIC of voriconazole for *A. fumigatus* $\Delta pes3$

A. fumigatus $\Delta pes3$ was more sensitive to voriconazole than *A. fumigatus* ATCC46645 in plate assays (O'Hanlon *et al.*, 2011). The antifungal MIC of voriconazole was determined for both *A. fumigatus* ATCC46645 and $\Delta pes3$ following EUCAST guidelines (Pfaller *et al.*, 2011). The MIC for voriconazole was 0.125 $\mu\text{g/ml}$ for *A. fumigatus* ATCC46645, while it was 0.0625 $\mu\text{g/ml}$ for *A. fumigatus* $\Delta pes3$.

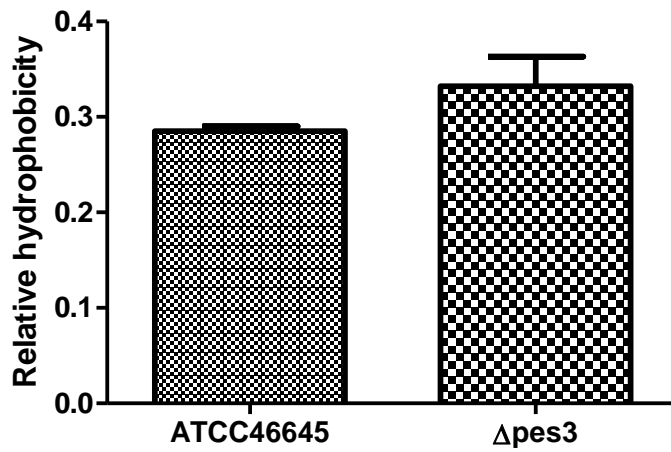


Figure 6.7: Hydrophobicity of *A. fumigatus* ATCC46645 and $\Delta pes3$. There was no difference in the hydrophobicity of the conidia from the two strains.

6.3 Discussion

The work described in this chapter details the application of comparative proteomics to another deletion strain; *A. fumigatus* $\Delta pes3$. Comparative proteomics of *A. fumigatus* ATCC46645 and $\Delta pes3$ germlings revealed the differential expression of a number of proteins. Fifteen proteins were up-regulated in *A. fumigatus* $\Delta pes3$ germlings, while ten proteins were down-regulated when compared to *A. fumigatus* ATCC46645 germlings. Confocal microscopy of (1,3)- β -glucan not only determined a decrease in surface (1,3)- β -glucan in *A. fumigatus* $\Delta pes3$ germlings, but also illustrated decreased germ tube length in the *A. fumigatus* $\Delta pes3$ germlings compared to those of *A. fumigatus* ATCC46645. The germination rate for *A. fumigatus* $\Delta pes3$ was significantly ($p < 0.01$) lower than *A. fumigatus* ATCC46645 under static conditions. The hydrophobicity of both *A. fumigatus* ATCC46645 and $\Delta pes3$ conidia was the same. The MIC of voriconazole for *A. fumigatus* $\Delta pes3$ was measured as 0.0625 $\mu\text{g/ml}$, and 0.125 $\mu\text{g/ml}$ for *A. fumigatus* ATCC46645. These results point to the involvement of *A. fumigatus* *pes3* in germination and cell wall composition, particularly with respect to (1,3)- β -glucan content, which has consequences regarding resistance to azoles, in particular voriconazole.

Three heat shock proteins were up-regulated in *A. fumigatus* $\Delta pes3$ germlings. Hsp70 had a 2.6 fold increase, Hsp30/Hsp42 had a 1.6 fold increase and molecular chaperone Hsp70 showed a fold increase of 2.1. Heat shock proteins are involved in many cellular processes maintaining cellular homeostasis and promoting stress tolerance (Henderson, 2010). In *A. fumigatus* $\Delta elfA$, molecular chaperone

Hsp70 was up-regulated under basal growth conditions. Heat shock proteins are induced under stress conditions and have been identified in numerous studies in which *A. fumigatus* has been subjected to stress (e.g., exposure to heat shock (Albrecht *et al.*, 2010b), H₂O₂ (Lessing *et al.*, 2007) and amphotericin B (Gautam *et al.*, 2008)). Teutschbein *et al.* (2010) identified Hsp70 and Hsp30/Hsp42 to be more abundant in conidia than mycelia. In the study where *A. fumigatus* was subjected to heat shock, the heat shock proteins that were up-regulated in *A. fumigatus* $\Delta pes3$ were also increased in expression (Albrecht *et al.*, 2010a). Interestingly, the nascent polypeptide-associated complex (NAC), which was down-regulated 2 fold in *A. fumigatus* $\Delta pes3$, was also down-regulated upon exposure to heat shock (Albrecht *et al.*, 2010a). This protein complex is involved in protein biosynthesis and translation (Panasenko *et al.*, 2009). The differential expression of these heat shock proteins and the NAC protein in *A. fumigatus* $\Delta pes3$ indicates a generalised stress environment in *A. fumigatus* $\Delta pes3$.

Ras GTPase Rab11 expression was increased 3.6 fold in *A. fumigatus* $\Delta pes3$. Rab proteins belong to a subfamily of Ras-related small GTPases and are involved in vesicle trafficking and transport (Inaba *et al.*, 2002). Rab11 has been implicated in regulating plasma membrane-endosome trafficking in *Drosophila melanogaster*, specifically transport through the recycling endosome (Assaker *et al.*, 2010). Possible alterations in endocytic trafficking may play a role in the increased sensitivity of *A. fumigatus* $\Delta pes3$ to voriconazole. The increased expression of Rab11 in *A. fumigatus* $\Delta pes3$ may point to Pes3 playing a role in membrane-cell wall interactions.

The 60S ribosomal protein L5 and the 40S ribosomal protein S5 were both up-regulated 4.1 and 3.2 fold respectively in *A. fumigatus* $\Delta pes3$. The 60S ribosomal protein had the highest fold increase of all the up-regulated proteins in *A. fumigatus* $\Delta pes3$. The increased expression of the ribosomal subunits is possibly indicative of a need for increased protein synthesis in *A. fumigatus* $\Delta pes3$, perhaps to overcome the slower germination rate observed under static conditions. Ribosome biogenesis is usually increased in germinating spores as the ribosome content in ungerminated spores is insufficient for polarised hyphal growth (Bhabhra *et al.*, 2008; Mirkes, 1974).

The increased expression of proteins involved in ATP synthesis, ATP hydrolysis and oxidative phosphorylation suggest increased energy requirements in *A. fumigatus* $\Delta pes3$. ATP synthase expression, which was up-regulated 1.8 fold, in *A. fumigatus* $\Delta pes3$ is involved in ATP synthesis (Davies *et al.*, 2011), while mitochondrial ATPase, which was up-regulated 2 fold, is involved in ATP hydrolysis (Senior *et al.*, 2002). Ubiquinol-cytochrome C reductase iron-sulphur subunit precursor was up-regulated 1.8 fold and is proposed to have a role in oxidative phosphorylation (Schrettl *et al.*, 2008).

Spermidine synthase was down-regulated 1.8 fold in *A. fumigatus* $\Delta pes3$ germlings compared to *A. fumigatus* ATCC46645. Spermidine, along with spermine and putrescine, are the most common naturally occurring polyamines in fungi. In *Ustilago maydis*, spermidine synthase is required for both morphogenesis (i.e., the yeast to mycelium transition) and fungal survival during infection of plants (Valdes-Santiago *et al.*, 2009). In *A. nidulans*, deletion of spermidine synthase resulted in

morphological defects and altered germination (Jin *et al.*, 2002). Delayed spore germination and mycelial formation as well as enlarged conidia were also observed in the spermidine synthase deletion strain (Jin *et al.*, 2002). SEM revealed the absence of rod-like strands on *A. fumigatus* $\Delta pes3$ germlings that were present on *A. fumigatus* ATCC46645 germlings while confocal microscopy revealed shorter germ tubes in *A. fumigatus* $\Delta pes3$ compared to the wild-type (O'Hanlon *et al.*, 2011). These morphological defects observed in *A. fumigatus* $\Delta pes3$ may partly result from the decreased spermidine synthase levels, because in *A. nidulans*, absence of spermidine synthase resulted in morphological defects (Jin *et al.*, 2002).

Also down-regulated in *A. fumigatus* $\Delta pes3$ was the pentafunctional polypeptide AroM, which was decreased 2.9 fold compared to *A. fumigatus* ATCC46645. AroM is essential for viability in *A. fumigatus* (Carr *et al.*, 2010), and produces aromatic amino acids by catalysing the conversion of 3-deoxy-D-arabino-heptalsonate 7-phosphate, a metabolite of quinic acid, to 5-enolpyruvylshikimate 3-phosphate by the shikimate pathway (Hawkins *et al.*, 1993). The overexpression of AroM in *A. nidulans* inhibited conidial germination (Lamb *et al.*, 1991), thus AroM may negatively regulate conidial germination. It is plausible that, in an attempt to remove inhibition of germination, *A. fumigatus* $\Delta pes3$ decreased the expression of AroM to reduce the negative affect it has on germination.

Actin expression exhibited a 2.1 fold decrease in *A. fumigatus* $\Delta pes3$. This decrease in actin may have been a factor affecting the germ tube length in *A. fumigatus* $\Delta pes3$ which was shorter than that in *A. fumigatus* ATCC46645, since the integrity of the actin cytoskeleton is required for normal germ tube emergence in *A.*

nidulans (Harris *et al.*, 1999). Actin was identified as one of the most abundant proteins present in *A. fumigatus* conidia (Teutschbein *et al.*, 2010).

The down-regulation of spermidine synthase, pentafunctional polypeptide AroM and actin, which have been shown to affect morphology and germination, is in complete accordance with the reduced germination rate under static conditions observed for *A. fumigatus* $\Delta pes3$, as well as the morphological differences observed by both SEM and confocal microscopy (O'Hanlon *et al.*, 2011).

Transketolase TktA was identified from two individual spots which had fold decreases of 3.1 and 2.5, respectively. Transketolase links the pentose phosphate pathway and glycolysis by catalysing the transfer of a two-carbon residue from a ketose to an aldose (Figure 6.7) (Kochetov and Sevostyanova, 2005; Esakova *et al.*, 2004). The pentose phosphate pathway and glycolysis are central pathways in metabolism and so the down-regulation of transketolase may indicate reduced activity of these pathways in *A. fumigatus* $\Delta pes3$. In addition to transketolase, expression of two other proteins involved in glycolysis, phosphoglucomutase and pyruvate carboxylase, was also downregulated, 2.2 fold for both, in *A. fumigatus* $\Delta pes3$ (Figure 6.7) (Teutschbein *et al.*, 2010). Transketolase also provides erythrose 4-phosphate, a precursor for aromatic amino acid biosynthesis (Sundstrom *et al.*, 1993). The decreased expression of transketolase and AroM in *A. fumigatus* $\Delta pes3$, which are both involved in aromatic amino acid biosynthesis, possibly results from the decreased requirement for aromatic amino acids in *A. fumigatus* $\Delta pes3$.



Figure 6.7: Interconnectivity between the glycolytic pathway and the pentose phosphate pathway. The enzymes; phosphoglucomutase and pyruvate carboxylase, which are involved in the glycolysis, exhibited decreased expression in *A. fumigatus* $\Delta pes3$. Transketolase, which was also decreased in expression in *A. fumigatus* $\Delta pes3$, connects the two pathways. Figure adapted from Teutschbein *et al.* (2010).

Interestingly, both transketolase and phosphoglucomutase were identified as antigens which reacted with rabbit immunosera that was exposed to *A. fumigatus* conidia (Asif *et al.*, 2010). *A. fumigatus* $\Delta pes3$ cytokine induction (TNF- α , IL-6, RANTES and IL-10) was reduced compared to that in *A. fumigatus* ATCC46645 leading to the possibility that *A. fumigatus* $\Delta pes3$ is immunologically silenced, which is supported by the increased virulence of *A. fumigatus* $\Delta pes3$ in both *G. mellonella* and a hydrocortisone acetate (HCA) immunosuppressed murine model of invasive aspergillosis (O'Hanlon *et al.*, 2011). The decreased expression of transketolase and phosphoglucomutase in *A. fumigatus* $\Delta pes3$ may contribute to the reduced cytokine induction and, along with the absence of Pes3 may result in the immunological silenced phenotype.

Thiazole synthase from *A. oryzae*, encoded by the pyrithiamine resistance gene *ptrA* (Kubodera *et al.*, 2000), which was used as the selection marker in the deletion of *A. fumigatus* $\Delta pes3$ (O'Hanlon *et al.*, 2011), was identified from two unique spots in *A. fumigatus* $\Delta pes3$. As described in Chapter 5, this protein was also identified from two unique spots in *A. fumigatus* $\Delta elfA$. The identification of thiazole synthase in both *A. fumigatus* $\Delta elfA$ and $\Delta pes3$ strengthens the case whereby this selection marker could be used as a control between two different strains in applications such as shotgun proteomics or quantitative label-free LC-MS (Neilson *et al.*, 2011).

(1,3)- β -glucan on the cell surface was significantly ($p = 0.0325$) reduced in *A. fumigatus* $\Delta pes3$ germlings compared to *A. fumigatus* ATCC46645. This reduction in surface (1,3)- β -glucan is relevant with respect to the increased sensitivity of *A.*

fumigatus $\Delta pes3$ to voriconazole, and the lowered MIC of voriconazole compared to that for *A. fumigatus* ATCC46645 (O'Hanlon *et al.*, 2011). In *C. albicans*, it has been shown that extracellular (1,3)- β -glucan contributes to azole resistance as it sequesters the antifungal preventing its entry into the cell and consequently its intracellular action (Nett *et al.*, 2010). *C. albicans fks1* is responsible for cell wall (1,3)- β -glucan synthesis and is proposed to be an essential gene as construction of a *FKS1* null mutant was unsuccessful (Nett *et al.*, 2010). In a heterozygous deletion mutant, *FKS1*/ $\Delta fks1$, biofilm cell wall (1,3)- β -glucan was reduced 30% and *FKS1*/ $\Delta fks1$ biofilms were reduced 80 % following treatment with fluconazole compared to the wild-type strain (Nett *et al.*, 2010). By using radio-labelled fluconazole, Nett *et al.* (2010) observed that the (1,3)- β -glucan matrix sequesters fluconazole, and that the *FKS1*/ $\Delta fks1$ biofilm matrix contained 50 % less fluconazole than the wild-type. As further confirmation of the azole sequestering ability of the (1,3)- β -glucan matrix, treatment of wild-type with glucanase reduced the amount of radio-labelled fluconazole detected in the matrix. In *A. fumigatus* $\Delta pes3$, reduced surface (1,3)- β -glucan was observed by confocal microscopy. As a consequence of the absence of Pes3, we hypothesise that the reduced surface (1,3)- β -glucan may sensitise *A. fumigatus* $\Delta pes3$ to voriconazole by facilitating greater intracellular accumulation.

In summary, this work describes the comparative proteomic investigation of *A. fumigatus* ATCC46645 and $\Delta pes3$ germlings. Proteins ($n = 25$) were differentially expressed and comprised fifteen proteins with increased expression and ten proteins with decreased expression in *A. fumigatus* $\Delta pes3$ germlings. The functions of the proteins with increased expression included heat shock, membrane trafficking,

ribosomal and electron transport, whereas proteins with decreased expression had functions in morphogenesis and germination. Confocal microscopy identified reduced (1,3)- β -glucan on the surface of *A. fumigatus* $\Delta pes3$ germlings and also shorter germ tube length in *A. fumigatus* $\Delta pes3$. The decreased expression of proteins related to morphogenesis and germination supports the observed differences in SEM and also the reduced germination rate of *A. fumigatus* $\Delta pes3$ germlings. The reduced surface (1,3)- β -glucan in *A. fumigatus* $\Delta pes3$ provides an explanation as to the lower MIC of *A. fumigatus* $\Delta pes3$ to voriconazole than that of *A. fumigatus* ATCC46645 as surface (1,3)- β -glucan sequesters azoles and prevents entry into the cell. While comparative proteomics, in conjunction with the confocal microscopy and previous SEM analysis (O'Hanlon *et al.*, 2011) has illuminated a structural role for Pes3 in *A. fumigatus* with respect to the cell wall, the actual molecular function of this NRP still remains to be elucidated. Future studies to isolate the *A. fumigatus* *pes3* encoded peptide need to be carried out along with studies to investigate the exact nature of the structural role of Pes3. However, the work presented here, in addition to the work described in Chapter 5, illustrates the significant utility of comparative proteomics in identifying possible gene functions while supporting phenotypes already identified. *A. fumigatus pes3* will not be discussed further in Chapter 7, which will focus solely on *A. fumigatus elfA*.

7.1 Discussion and conclusion

The detailed systems biology of filamentous fungi has, until recently, proven refractory to detailed analysis. However, the advent of fungal genome sequencing, targeted gene deletion technologies, comparative proteomics and allied phenotypic analyses have coalesced to provide the tools necessary to tackle hitherto impossible challenges (Carberry *et al.*, 2006; Knimeyer *et al.*, 2006; Nielsen *et al.*, 2006; Nierman *et al.*, 2005). Thus, this thesis primarily describes the detailed functional characterisation of a translation elongation factor 1B subunit gamma (eEF1B γ) from the opportunistic pathogen, *Aspergillus fumigatus*. Resultant data has revealed significant new insights into fungal systems biology, specifically with respect to protein synthesis, oxidative stress responses, protein degradation control and cytoskeletal organisation- in addition to demonstrating the power of comparative proteomics to reveal much about inter-related systems within the organism.

The work presented in this thesis describes the functional characterisation of ElfA, an eEF1B γ from *A. fumigatus*. eEF1B γ is a member of the eEF1 complex required for protein synthesis and, along with eEF1B α , forms the eEF1B component of the eEF1 complex which provides nucleotide exchange factor activity to the eEF1A subunit (Pittman *et al.*, 2009; Ozturk and Kinzy, 2008). Studies in *S. cerevisiae* have determined that eEF1B γ does not act as a nucleotide exchange factor but may act to stimulate the nucleotide exchange activity of eEF1B α , moreover it lacks any GST activity (Esposito and Kinzy, 2010; Le Sourd *et al.*, 2006; Jeppesen *et al.*, 2003; Janssen and Moller, 1988). However, *A. fumigatus* ElfA has previously been shown to contain a catalytically active GST domain (Carberry *et al.*, 2006) and

so, we initially hypothesised that in addition to intimate involvement in protein synthesis, ElfA may play a role in the oxidative stress response in *A. fumigatus*. Moreover, we considered that it may function as a redox “sensor” or modulator to either detect or prevent oxidative damage to newly synthesised polypeptides. Therefore, absence of ElfA would not only result in aberrant protein synthesis, but also in disruption of the cellular redox status, consequent oxidative stress and protein misfolding. The successful deletion of *A. fumigatus elfA* facilitated both comparative proteomic and phenotypic investigation against the wild-type strain. Indeed, this comparative proteomic investigation of *A. fumigatus* ATCC46645 and $\Delta elfA$ revealed unexpected insights into the effect that the loss of *A. fumigatus elfA* had on the proteome of the mutant (Figure 7.1).

Firstly, the increased expression of aminoacyl-tRNA synthetases in *A. fumigatus* $\Delta elfA$ under both normal growth conditions and following exposure to H_2O_2 strongly indicates that eEF1B γ is required for protein synthesis in *A. fumigatus*. Specifically, tyrosyl-tRNA synthetase exhibited increased expression in *A. fumigatus* $\Delta elfA$ under normal growth conditions, while cysteinyl-tRNA synthetase exhibited increased expression upon exposure to H_2O_2 . We conclude that the increased expression of these aminoacyl-tRNA synthetases is indicative of altered protein synthesis in *A. fumigatus* $\Delta elfA$ which reveals a role for ElfA in either the delivery or binding of the cognate aminoacyl adenylated tRNAs to the ribosome. In particular, the increased expression of cysteinyl-tRNA strongly suggests an increased requirement for cysteine-containing proteins, such as peroxiredoxins,

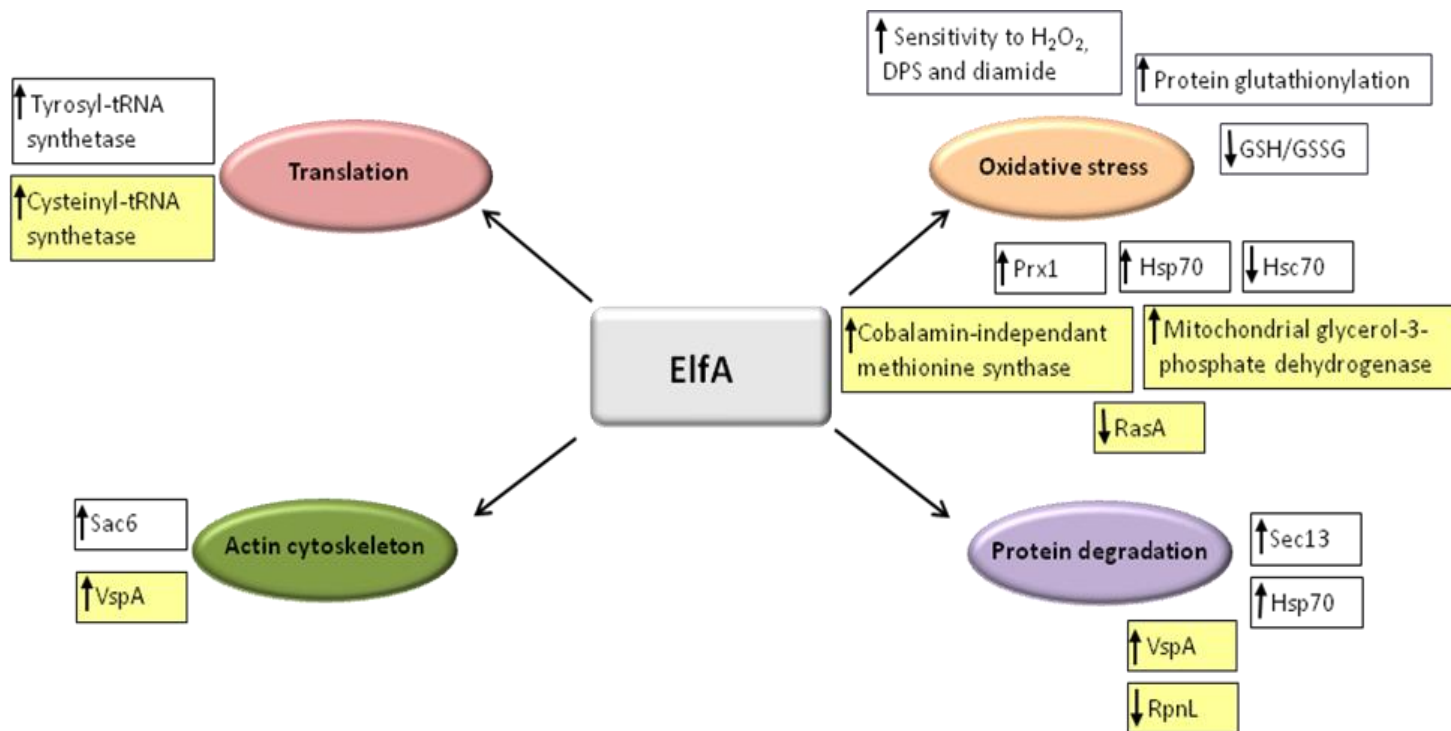


Figure 7.1: Putative systems biology of ElfA functionality in *A. fumigatus*. The loss of ElfA on translation, oxidative stress response, protein degradation and actin cytoskeleton is illustrated. The proteins in white had altered expression under normal growth conditions, while those in yellow were altered following H₂O₂ exposure. Prx1: Mitochondrial peroxiredoxin Prx1, RasA: RAS small monomeric GTPase RasA, Sec13: Nuclear pore complex subunit Sec13, VspA; Vacuolar dynamin-like GTPase VspA, RpnL: Proteasome regulatory particle subunit RpnL Sac6; Actin-bundling protein Sac6.

which are essential for attenuation of oxidative stress within the cell (Jones and Go, 2011; Meyer and Hell, 2005b).

Secondly, comparative proteomics highlighted that under normal growth conditions proteins involved in stress responses (e.g., mitochondrial peroxiredoxin Prx1, molecular chaperone Hsp70 and Hsc70 co-chaperone) were differentially expressed, with Prx1 and Hsp70 expression increased while the expression of Hsc70 was decreased. The observation of these differentially expressed proteins indicates that in the absence of *A. fumigatus elfA*, a stressed cellular environment exists. This is mirrored by redox alterations in *A. fumigatus ΔelfA* where, under normal growth conditions the GSH/GSSG ratio of *A. fumigatus ΔelfA* was decreased compared to that of *A. fumigatus* ATCC46645. This decreased GSH/GSSG ratio is indicative of oxidative stress conditions (Rahman *et al.*, 2006). Combined, these data suggest that in the absence of ElfA, protein synthesis is partially disrupted, either resulting in- or consequent to- oxidative stress, and a resultant dysregulation of the GSH/GSSG ratio occurs in *A. fumigatus* (Figure 7.2).

The increased expression of mitochondrial peroxiredoxin Prx1 in *A. fumigatus ΔelfA* was especially interesting because in *S. cerevisiae*, mitochondrial peroxiredoxin Prx1 requires GSH-mediated reduction for antioxidant activity (Greetham and Grant, 2009). Indeed, both GSH and a thioredoxin were required to maintain the mitochondrial peroxiredoxin Prx1 in its reduced, active state. Specifically, the catalytic cysteine of peroxiredoxin is reactivated by glutathionylation and subsequent reduction by thioredoxin reductase coupled with GSH (Greetham and Grant, 2009). If this is also the case in *A. fumigatus*, then the

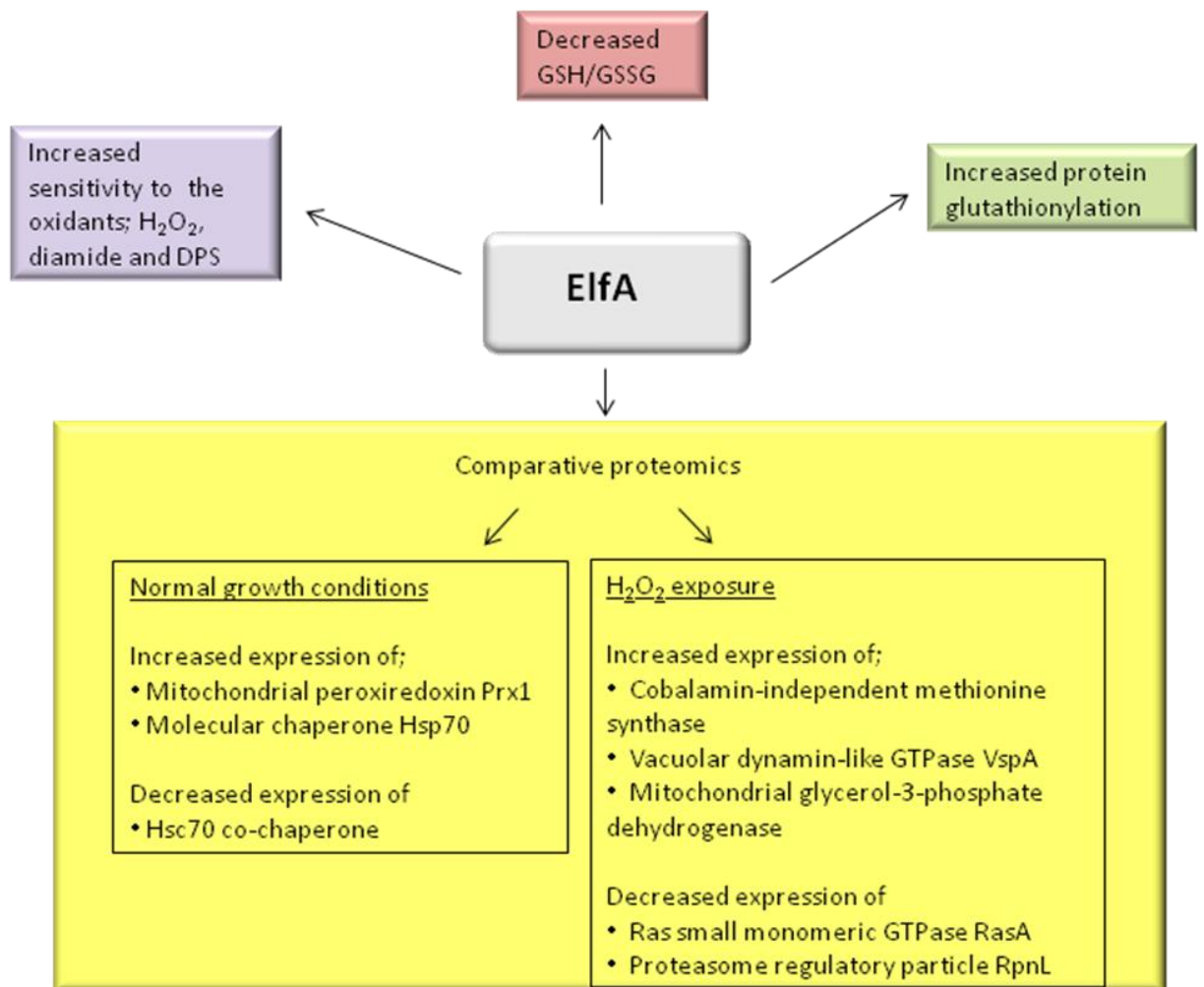


Figure 7.2: Summary of the results which support the hypothesis that *A. fumigatus* E1fA is a component of the oxidative stress response.

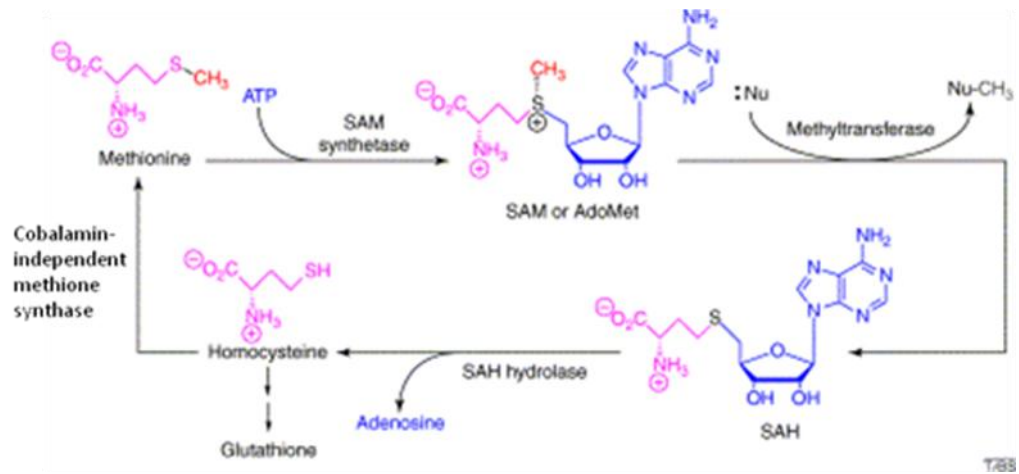
increased expression of Prx1 observed in *A. fumigatus* Δ elfA can be explained as follows: Due to decreased GSH levels in *A. fumigatus* Δ elfA, mitochondrial peroxiredoxin Prx1 may not be able to return to its reduced active state and its expression is consequently up-regulated to compensate for this molecular bottleneck. Alternatively, Prx1 expression may be up-regulated in response to the oxidative stress conditions in *A. fumigatus* Δ elfA directly as a result of increased GSSG levels within the cell.

Consolidating the hypothesis that *A. fumigatus* elfA is involved in the oxidative stress response, *A. fumigatus* Δ elfA was found to be significantly more sensitive than wild-type to the oxidants; H₂O₂, diamide and DPS. Both diamide and DPS are thiol-specific oxidants which react directly with GSH (López-Mirabal and Winther, 2008). The reduced GSH levels in *A. fumigatus* Δ elfA compared to those in *A. fumigatus* ATCC46645 confirm that GSH levels are depleted to a greater extent in *A. fumigatus* Δ elfA in the presence of these oxidants resulting in the increased sensitivity of *A. fumigatus* Δ elfA. Conversely, in *S. cerevisiae*, an eEF1B γ deletion strain was more resistant to the oxidants; H₂O₂, menadione and CdSO₄ (Olarewaju *et al.*, 2004). However, in *S. cerevisiae*, the GST domain of eEF1B γ is not active (Jeppesen *et al.*, 2003), whereas in *A. fumigatus*, Carberry *et al.* (2006) demonstrated GST activity in ElfA. Thus, the data presented in this thesis lead to the conclusion that the eEF1B γ proteins in *A. fumigatus* and *S. cerevisiae*, respectively, mediate differential responses consequent to oxidative stress, and that this may be due to the presence of a functionally active GST domain in ElfA. Targeted inactivation of the GST activity within ElfA would conclusively resolve this hypothesis.

The effects of H₂O₂-induced oxidative stress on the proteome of *A. fumigatus* Δ *elfA* was investigated and compared to that of *A. fumigatus* ATCC46645 (Figure 7.2). Proteins which participate in the oxidative stress response such as cobalamin-independent methionine synthase, vacuolar dynamin-like GTPase VpsA, and mitochondrial glycerol-3-phosphate dehydrogenase exhibited increased expression, while Ras small monomeric GTPase RasA and the proteasome regulatory particle were decreased in expression.

Cobalamin-independent methionine synthase, which exhibited increased expression in *A. fumigatus* Δ *elfA*, is essential for SAM cycle occurrence (Fontecave *et al.*, 2004) and homocysteine, an intermediate of the SAM cycle, can be converted to glutathione (Figure 7.3) (Fontecave *et al.*, 2004). This is particularly relevant since GSH/GSSG determination in *A. fumigatus* Δ *elfA*, following exposure to H₂O₂, revealed an increase in GSH levels. Thus, a clear cross-supporting link is established between the proteomic and phenotypic analyses. Oxidative stress generally results in a decreased GSH/GSSG ratio as GSH levels decrease as a result of its utilisation in protein glutathionylation reactions, scavenging ROS, and in antioxidant enzyme-mediated reactions (López-Mirabal and Winther, 2008; Rahman *et al.*, 2006). Consequently, GSH is oxidised to GSSG thereby increasing the GSSG levels in the cell during oxidative stress (López-Mirabal and Winther, 2008; Rahman *et al.*, 2006). However, because GSH levels in *A. fumigatus* Δ *elfA* were already lower than those in the wild-type due to the stressed environment upon deletion of *elfA*, we speculate that cobalamin-independent methionine synthase expression was up-regulated to increase the GSH levels following exposure to H₂O₂ (Figure 7.3).

A.



B.

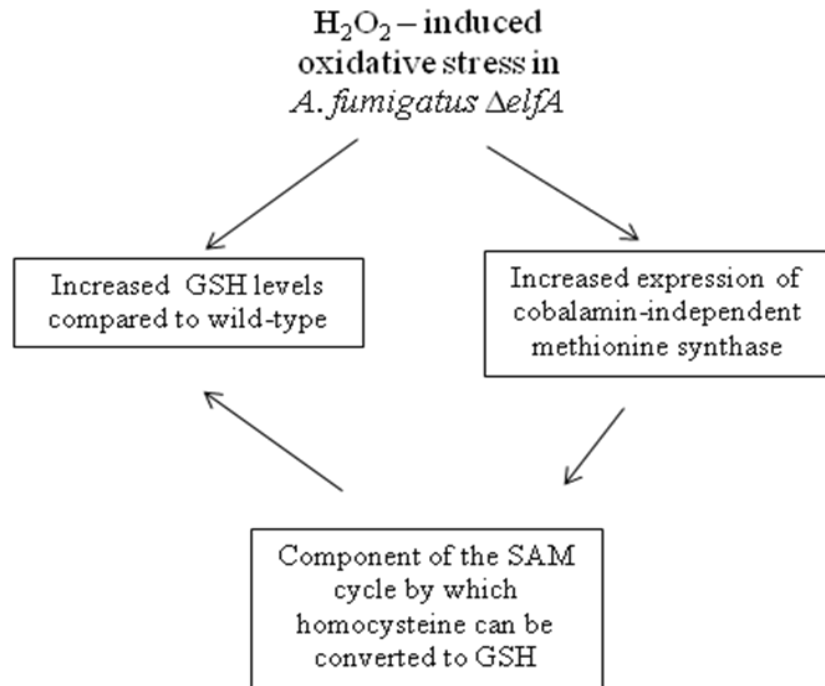


Figure 7.3: Proposed relationship between GSH and cobalamin-independent methionine synthase. **A.** Cobalamin-independent methionine synthase is a component of the *S*-adenosylmethionine (SAM) cycle from which the intermediate homocysteine can be converted into cysteine and then subsequently into glutathione. Figure adapted from Fontecave *et al.* 2004. **B.** Schematic outline of the proposed relationship between the increased GSH levels in *A. fumigatus* $\Delta elfA$ and cobalamin-independent methionine synthase increased expression following exposure to H₂O₂. Since homocysteine can be converted into GSH, consequently the increased expression of cobalamin-independent methionine synthase may account for the increased GSH levels in *A. fumigatus* $\Delta elfA$ after H₂O₂ addition.

Interestingly, it has been observed that addition of methionine to *Penicillium chrysogenum* cultures also resulted in increased intracellular GSH levels (Emri *et al.*, 1998), and if this is also the case in *A. fumigatus*, it may represent a universal response to GSH depletion consequent to oxidative stress in filamentous fungi.

Thirdly, further analysis of the differentially expressed proteins identified in *A. fumigatus* Δ *elfA* under both normal growth conditions and following exposure to H₂O₂, revealed that a number of proteins involved in protein folding and protein degradation were differentially expressed. Under normal growth conditions, molecular chaperone Hsp70 and nuclear pore complex Sec13 exhibited increased expression in *A. fumigatus* Δ *elfA*. The Hsp protein family is required for the disassembly of protein aggregates, protein folding and the degradation of misfolded proteins (Bursac and Lithgow, 2009; Mayer and Bukau, 2005), while Sec13 functions in the coat protein complex II (COPII), vesicular trafficking, nuclear pore function and ERAD (Nielsen, 2009). The COPII complex also transports misfolded proteins to the ERAD (Fu and Sztul, 2003), which in turn is involved in the retrotranslocation of misfolded proteins from the ER to the cytosol for degradation by proteasomes (Goeckeler and Brodsky, 2010). Previously, Sec13 was found to be up-regulated in *S. cerevisiae* by the UPR (Travers *et al.*, 2000), which has been shown to target genes involved in the ERAD (Malhotra and Kaufman, 2007; Ron and Walter, 2007). The increased expression of these proteins under normal growth conditions is indicative of a greater requirement for protein degradation in *A.*

fumigatus Δ elfA which is in accordance with the stressed environment evident due to aberrant protein synthesis and decreased GSH/GSSG ratio.

One of the consequences of oxidative stress is an increase in misfolded and irreversibly damaged proteins which, unless removed from the cell, are highly toxic (López-Mirabal and Winther, 2008; Hayes and McLellan, 1999). Following exposure to H₂O₂, the increased expression of vacuolar dynamin-like GTPase VpsA and the decreased expression of the proteasome regulatory particle subunit (RpnL) pointed towards an increased requirement for protein degradation in *A. fumigatus* Δ elfA. One of the functions of vacuolar dynamin-like GTPase VpsA is in vacuole fission (Baars *et al.*, 2007). Vacuoles, along with proteasomes, degrade proteins exported from the ER by the ERAD (Esposito and Kinzy, 2010; Goeckeler and Brodsky, 2010; Li and Kane, 2009). The proteasome regulatory particle subunit forms the lid of the 19S regulatory subunit which is required for degradation of ubiquitinated proteins but inhibits degradation of oxidised proteins (Wang *et al.*, 2010; Tone *et al.*, 2000). This decreased expression of the proteasome regulatory particle subunit in *A. fumigatus* Δ elfA is strongly indicative of an attenuation of proteasome regulation to facilitate degradation of the increased levels of misfolded or oxidised proteins present in the cell, consequent to loss of ElfA. We speculate that the increased protein glutathionylation observed in *A. fumigatus* Δ elfA, compared to wild-type, indicates a parallel attempt to confer protection against oxidative stress, in particular to prevent protein oxidation, following altered redox homeostasis. Interestingly, in *S. cerevisiae*, increased accumulation of oxidised proteins was observed in an eEF1 β deletion strain which also exhibited altered vacuole

morphology and altered expression of Hsp proteins (Esposito and Kinzy, 2010). Thus, the identification of a number of proteins involved in protein folding and degradation of misfolded proteins in *A. fumigatus* Δ *elfA*, under both normal growth conditions and following exposure to H₂O₂, suggests that in the absence of ElfA, the cellular protein degradation systems are activated. We hypothesise that in the absence of this key component of the cellular translational machinery, a stressed environment ensues resulting in increased levels of misfolded and irreversibly damaged proteins, which must be removed from the cell to prevent manifestation of toxic effects.

Fourthly, comparative proteomics enabled the identification of an additional function of *A. fumigatus* *elfA* that could not have been elucidated through phenotypic analysis alone. Here, increased expression of additional proteins (i.e., actin-bundling protein Sac6 and vacuolar dynamin-like GTPase VpsA), in *A. fumigatus* Δ *elfA* under both normal growth conditions and following oxidative stress, involved in cytoskeletal transformation, highlighted the involvement of ElfA with the cytoskeleton.

Under normal growth conditions, actin-bundling protein Sac6 exhibited increased expression in *A. fumigatus* Δ *elfA*. Moreover, following exposure to H₂O₂, increased expression of vacuolar dynamin-like GTPase VpsA, which in addition to its function in vacuole fission is also required for normal actin cytoskeleton organisation in *S. cerevisiae* (Yu and Cai, 2004), was observed. The cytoskeleton plays a role in the oxidative stress response whereby it confers protection by collapsing into actin bundles that sequester actin and its associated proteins into

immobile structures (Farah *et al.*, 2011). In *S. cerevisiae*, Sac6 was observed to co-localise with these actin bundles during oxidative stress induced by H₂O₂, menadione and diamide (Farah *et al.*, 2011). Translation elongation and actin cytoskeleton modulation are linked, because eEF1A in addition to its canonical role of delivering aminoacyl-tRNA to the elongating ribosome, is also an actin binding and bundling protein (Gross and Kinzy, 2005). In *S. cerevisiae*, eEF1Ba regulates the actin binding and bundling activities of eEF1A and has been proposed to direct eEF1A towards binding aminoacyl-tRNA (Pittman *et al.*, 2009). In mammalian epithelial cells, eEF1B γ increased the formation of keratin intermediate filament bundles *in vivo* (Kim *et al.*, 2007). Moreover, over-expression of eEF1B γ in epithelial cells resulted in a disrupted interaction between eEF1B γ and keratin, and also reduced protein synthesis suggesting a functional link between the cytoskeletal structure and translation in epithelial cells (Kim and Coulombe, 2010; Kim *et al.*, 2007). The observation of increased expression of Sac6 in *A. fumigatus* Δ elfA under normal growth conditions strongly suggests that ElfA (an EF1B γ) also links the actin cytoskeleton with the translational apparatus, an interaction that warrants further investigation in future work.

Finally, the findings presented herein have revealed a diverse role for ElfA with respect to translation, the oxidative stress response, GSH/GSSG redox homeostasis, regulation of protein degradation, the actin cytoskeleton, and antifungal resistance in *A. fumigatus*. More globally, this study has also demonstrated the effectiveness of using targeted gene deletion approaches to studying gene function in filamentous fungi. In addition to this, the advantages of comparative proteomics

investigations to reveal protein systems are clearly evident. Indeed, in the two proteomic studies presented here (*A. fumigatus elfA* and *pes3*), the comparative approach adopted, highlighted previously unknown functions for both of these biochemically unannotated proteins. However, there still remain questions regarding the function of ElfA in *A. fumigatus* (Figure 7.4). Although phenotypic analysis revealed that *A. fumigatus ΔelfA* was significantly more resistant to voriconazole than the wild-type strain, no mechanism was detectable. However, this increased resistance requires further investigation to improve understanding of azole resistance in *A. fumigatus*, a phenomenon that has become more prevalent in clinical isolates (Bueid *et al.*, 2010). The interaction between ElfA and the actin cytoskeleton also warrants further investigation to determine the precise molecular mechanism linking translation and cytoskeletal organisation. The order of events leading to increased misfolded proteins and the activation of the oxidative stress response following loss of ElfA remains to be fully elucidated. We hypothesise that the ensuing alteration in protein synthesis, after loss of ElfA, results in increased levels of misfolded proteins which may in turn generate a stressed environment activating the oxidative stress response. Alternatively, loss of ElfA and the subsequent deficit in translation results in a stressed environment, which not only activates the oxidative stress response, but also results in increased levels of misfolded and irreversibly damaged proteins. The result of either hypothesis put forward here is an increase in protein degradation mechanisms and oxidative stress response mechanisms. These hypotheses require further investigation to fully elucidate the molecular mechanism of ElfA in *A. fumigatus*.

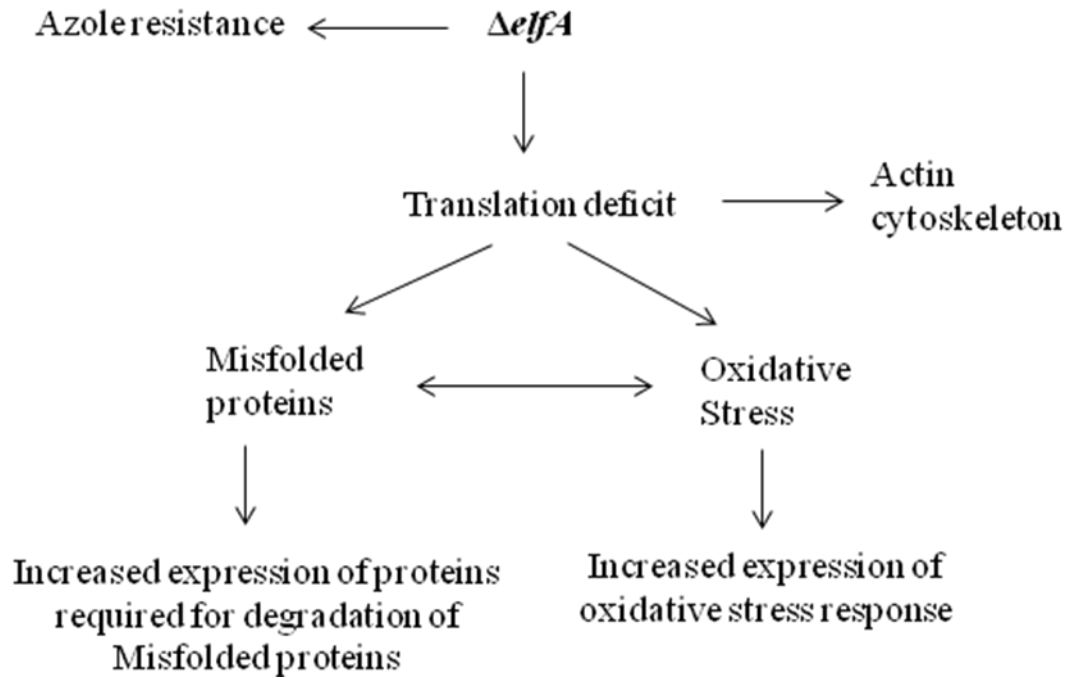


Figure 7.4: Schematic outlining the responses in *A. fumigatus* following the loss of ElfA and proposed interactions warranting further investigation.

To conclude, this study represents the first functional characterisation of ElfA in *A. fumigatus*, a translation elongation factor 1B gamma subunit with a catalytically active GST domain, and has provided significant new information to inform our thoughts on the complexity of protein systems operating within this opportunistic pathogen.

8.1 Bibliography

Abad, A., Fernandez-Molina, V., Bikandi, J., Ramirez, A., Margareto, J., Sendino, J., *et al* (2010) What makes *Aspergillus fumigatus* a successful pathogen? Genes and molecules involved in invasive aspergillosis. *Revista Iberoamericana de Micologia*. **27**: 155-182.

Albrecht, D., Guthke, R., Brakhage, A.A. and Kniemeyer, O. (2010a) Integrative analysis of the heat shock response in *Aspergillus fumigatus*. *BMC Genomics*. **11**: 32.

Albrecht, D., Guthke, R., Brakhage, A.A. and Kniemeyer, O. (2010b) Integrative analysis of the heat shock response in *Aspergillus fumigatus*. *BMC Genomics*. **11**.

Albrecht, D., Kniemeyer, O., Mech, F., Gunzer, M., Brakhage, A. and Guthke, R. (2011) On the way toward systems biology of *Aspergillus fumigatus* infection. *International Journal of Medical Microbiology Colonisation and infection by human-pathogenic fungi*. **301**: 453-459.

Albrechtsen, J. (2007) Reproducibility in Protein Profiling by MALDI-TOF Mass Spectrometry. *Clinical Chemistry*. **53**: 852-858.

Alkalaeva, E.Z., Pisarev, A.V., Frolova, L.Y., Kisselev, L.L. and Pestova, T.V. (2006) In Vitro Reconstitution of Eukaryotic Translation Reveals Cooperativity between Release Factors eRF1 and eRF3. *Cell*. **125**: 1125-1136.

Andersen, G.R., Valente, L., Pedersen, L., Kinzy, T.G. and Nyborg, J. (2001) Crystal structures of nucleotide exchange intermediates in the eEF1A-eEF1B α complex. *Nature Structural Biology*. **8**: 531-534.

Andersen, M.R. and Nielsen, J. (2009) Current status of systems biology in *Aspergilli*. *Fungal Genetics and Biology Thematic Issue: Aspergillus Genomics and Beyond*. **46**: S180-S190.

Andersen, M.R., Nielsen, M.L. and Nielsen, J. (2008) Metabolic model integration of the bibliome, genome, metabolome and reactome of *Aspergillus niger*. *Molecular Systems Biology*. **4**.

Anderson, M.T., Trudell, J.R., Voehringer, D.W., Tjioe, I.M., Herzenberg, L.A. and Herzenberg, L.A. (1999) An Improved Monobromobimane Assay for Glutathione Utilizing Tris- (2-carboxyethyl)phosphine as the Reductant. *Analytical Biochemistry*. **272**: 107-109.

Arnaud, M.B., Chibucos, M.C., Costanzo, M.C., Crabtree, J., Inglis, D.O., Lotia, A., *et al* (2010) The *Aspergillus* Genome Database, a curated comparative genomics resource for gene, protein and sequence information for the *Aspergillus* research community. *Nucleic Acids Research*. **38**: D420-D427.

Asano, Y., Hagiwara, D., Yamashino, T. and Mizuno, T. (2007) Characterization of the bZip-Type Transcription Factor NapA with Reference to Oxidative Stress Response in *Aspergillus nidulans*. *Bioscience, Biotechnology, and Biochemistry*. **71**: 1800-1803.

Asif, A.R., Oellerich, M., Armstrong, V.W., Gross, U. and Reichard, U. (2010) Analysis of the cellular *Aspergillus fumigatus* proteome that reacts with sera from rabbits developing an acquired immunity after experimental aspergillosis. *Electrophoresis*. **31**: 1947-1958.

Assaker, G., Ramel, D., Wculek, S.K., Gonzalez-Gaitan, M. and Emery, G. (2010) Spatial restriction of receptor tyrosine kinase activity through a polarized endocytic cycle controls border cell migration. *Proceedings of the National Academy of Sciences, USA*. **107**: 22558-22563.

Baars, T.L., Petri, S., Peters, C. and Mayer, A. (2007) Role of the V-ATPase in Regulation of the Vacuolar Fission-Fusion Equilibrium. *Molecular Biology of the Cell*. **18**: 3873-3882.

Back, S.H., Schröder, M., Lee, K., Zhang, K. and Kaufman, R.J. (2005) ER stress signaling by regulated splicing: IRE1/HAC1/XBP1. *Methods*. **35**: 395-416.

Baginski, M., Czub, J. and Sternal, K. (2006) Interaction of Amphotericin B and Its Selected Derivatives With Membranes: Molecular Modeling Studies. *The Chemical Record*. **6**: 320-332.

Bahn, Y.-S., Molenda, M., Staab, J.F., Lyman, C.A., Gordon, L.J. and Sundstrom, P. (2007) Genome-Wide Transcriptional Profiling of the Cyclic AMP-Dependent Signaling Pathway during Morphogenic Transitions of *Candida albicans*. *Eukaryotic Cell*. **6**: 2376-2390.

Bhabhra, R. and Askew, D.S. (2005) Thermotolerance and virulence of *Aspergillus fumigatus*: role of the fungal nucleus. *Medical Mycology Supplement*. **43**: 587-593.

Bhabhra, R., Richie, D.L., Kim, H.S., Nierman, W.C., Fortwendel, J., Aris, J.P., *et al* (2008) Impaired Ribosome Biogenesis Disrupts the Integration between

Morphogenesis and Nuclear Duplication during the Germination of *Aspergillus fumigatus*. *Eukaryotic Cell*. **7**: 575-583.

Bhabhra, R., Miley, M.D., Mylonakis, E., Boettner, D., Fortwendel, J., Panepinto, J.C., *et al* (2004) Disruption of the *Aspergillus fumigatus* Gene Encoding Nucleolar Protein CgrA Impairs Thermotolerant Growth and Reduces Virulence. *Infection and Immunity*. **72**: 4731-4740.

Billaut-Mulot, O., Fernandez-Gomez, R. and Ouaiissi, A. (1997) Phenotype of recombinant *Trypanosoma cruzi* which overexpresses elongation factor 1-gamma: possible involvement of EF-1gamma GST-like domain in the resistance to clomipramine. *Gene*. **198**: 259-267.

Biswas, S., Chida, A.S. and Rahman, I. (2006) Redox modifications of protein-thiols: Emerging roles in cell signaling. *Biochemical Pharmacology*. **71**: 551-564.

Biteau, B., Labarre, J. and Toledano, M.B. (2003) ATP-dependent reduction of cysteine-sulphinic acid by *S. cerevisiae* sulphiredoxin. *Nature*. **425**: 980-984.

Blatzer, M., Schrettl, M., Sarg, B., Lindner, H.H., Pfaller, K. and Haas, H. (2011) SidL, an *Aspergillus fumigatus* Transacetylase Involved in Biosynthesis of the Siderophores Ferricrocin and Hydroxyferricrocin. *Applied and Environmental Microbiology*. **77**: 4959-4966.

Blum, G., Perkhofer, S., Haas, H., Schrettl, M., Wurzner, R., Dierich, M.P. and Lass-Flörl, C. (2008) Potential Basis for Amphotericin B Resistance in *Aspergillus terreus*. *Antimicrobial Agents and Chemotherapy*. **52**: 1553-1555.

Boccalatte, F.E., Voena, C., Riganti, C., Bosia, A., D'Amico, L., Riera, L., *et al* (2009) The enzymatic activity of 5-aminoimidazole-4-carboxamide ribonucleotide formyltransferase/IMP cyclohydrolase is enhanced by NPM-ALK: new insights in ALK-mediated pathogenesis and the treatment of ALCL. *Blood*. **113**: 2776-2790.

Bos, J.L., Rehmann, H. and Wittinghofer, A. (2007) GEFs and GAPs: Critical Elements in the Control of Small G Proteins. *Cell*. **129**: 865-877.

Brakhage, A.A. and Langfelder, K. (2002) Menacing mold: the molecular biology of *Aspergillus fumigatus*. *Annual Review of Microbiology*. **56**: 433-455.

Brakhage, A.A., Andrianopoulos, A., Kato, M., Steidl, S., Davis, M.A., Tsukagoshi, N. and Hynes, M.J. (1999) HAP-Like CCAAT-Binding Complexes in Filamentous Fungi: Implications for Biotechnology. *Fungal Genetics and Biology*. **27**: 243-252.

Brennan, J.P., Miller, J.I.A., Fuller, W., Wait, R., Begum, S., Dunn, M.J. and Eaton, P. (2005) The Utility of N,N-Biotinyl Glutathione Disulfide in the Study of Protein S-Glutathiolation. *Molecular and Cellular Proteomics*. **5.2**: 215-225.

Bruns, S., Seidler, M., Albrecht, D., Salvenmoser, S., Remme, N., Hertweck, C., *et al* (2010a) Functional genomic profiling of *Aspergillus fumigatus* biofilm reveals enhanced production of the mycotoxin gliotoxin. *Proteomics*. **10**: 3097-3107.

Bruns, S., Kniemeyer, O., Hasenberg, M., Amanianda, V., Nietzsche, S., Thywissen, A., *et al* (2010b) Production of Extracellular Traps against *Aspergillus fumigatus* *In Vitro* and in Infected Lung Tissue Is Dependent on Invading Neutrophils and Influenced by Hydrophobin RodA. *PLoS Pathogens*. **6**: e1000873.

Bueid, A., Howard, S.J., Moore, C.B., Richardson, M.D., Harrison, E., Bowyer, P. and Denning, D.W. (2010) Azole antifungal resistance in *Aspergillus fumigatus*: 2008 and 2009. *Journal of Antimicrobial Chemotherapy*. **65**: 2116-2118.

Burns, C., Geraghty, R., Neville, C., Murphy, A., Kavanagh, K. and Doyle, S. (2005) Identification, cloning, and functional expression of three glutathione transferase genes from *Aspergillus fumigatus*. *Fungal Genetics and Biology*. **42**: 319-327.

Bursac, D. and Lithgow, T. (2009) Jid1 is a J-protein functioning in the mitochondrial matrix, unable to directly participate in endoplasmic reticulum associated protein degradation. *FEBS Letters*. **583**: 2954-2958.

Cagas, S.E., Jain, M.R., Li, H. and Perlin, D.S. (2011) Profiling the *Aspergillus fumigatus* Proteome in Response to Caspofungin. *Antimicrobial Agents and Chemotherapy*. **55**: 146-154.

Carberry, S. (2008) Proteomic Investigation of Gliotoxin Metabolism in *Aspergillus fumigatus*. *PhD Thesis*.

Carberry, S. and Doyle, S. (2007) Proteomic studies in biomedically and industrially relevant fungi. *Cytotechnology*. **53**: 95-100.

Carberry, S., Neville, C., Kavanagh, K. and Doyle, S. (2006) Analysis of major intracellular proteins of *Aspergillus fumigatus* by MALDI mass spectrometry: Identification and characterisation of an elongation factor 1B protein with glutathione transferase activity. *Biochemical and Biophysical Research communications*. **341**: 1096-1104.

- Carr, P.D., Tuckwell, D., Hey, P.M., Simon, L., d'Enfert, C., Birch, M., *et al* (2010) The Transposon *impala* Is Activated by Low Temperatures: Use of a Controlled Transposition System To Identify Genes Critical for Viability of *Aspergillus fumigatus*. *Eukaryotic Cell*. **9**: 438-448.
- Carvalho, N., Arentshorst, M., Jin Kwon, M., Meyer, V. and Ram, A. (2010) Expanding the ku70 toolbox for filamentous fungi: establishment of complementation vectors and recipient strains for advanced gene analyses. In *Applied Microbiology and Biotechnology*: Springer Berlin / Heidelberg, pp. 1463-1473.
- Cheng, D., Marner, J. and Rubenstein, P.A. (1999) Interaction in vivo and in vitro between yeast fimbrin, SAC6P, and polymerisation-defective yeast actin (V266G and L267G). *The Journal of Biological Chemistry*. **274**: 35873-35880.
- Choi, J.H., Lou, W. and Vancura, A. (1998) A Novel Membrane-bound Glutathione S-Transferase Functions in the Stationary Phase of the Yeast *Saccharomyces cerevisiae*. *Journal of Biological Chemistry*. **273**: 29915-29922.
- Collinson, E.J. and Grant, C.M. (2003) Role of Yeast Glutaredoxins as Glutathione S-transferases. *Journal of Biological Chemistry*. **278**: 22492-22497.
- Corbi, N., Batassa, E.M., Pisani, C., Onori, A., Di Certo, M.G., Strimpakos, G., *et al* (2010) The eEF1gamma subunit contacts RNA polymerase II and binds Vimentin promoter region. *PLOS one*. **5**.
- Costanzo, M., Baryshnikova, A., Bellay, J., Kim, Y., Spear, E.D., Sevier, C.S., *et al* (2010) The Genetic Landscape of a Cell. *Science*. **327**: 425-431.
- Cramer, R.A., Stajich, J.E., Yamanaka, Y., Dietrich, F.S., Steinbach, W.J. and Perfect, J.R. (2006a) Phylogenomic analysis of non-ribosomal peptide synthetases in the genus *Aspergillus*. *Gene*. **383**: 24-32.
- Cramer, R.A., Jr., Gamcsik, M.P., Brooking, R.M., Najvar, L.K., Kirkpatrick, W.R., Patterson, T.F., *et al* (2006b) Disruption of a Nonribosomal Peptide Synthetase in *Aspergillus fumigatus* Eliminates Gliotoxin Production. *Eukaryotic Cell*. **5**: 972-980.
- da Silva Ferreira, M.E., Colombo, A.L., Paulsen, I., Ren, Q., Wortman, J., Huang, J., *et al* (2005) The ergosterol biosynthesis pathway, transporter genes, and azole resistance in *Aspergillus fumigatus*. *Medical Mycology*. **S1 43**: S313-S319.
- da Silva Ferreira, M.E., Kress, M.R.V.Z., Savoldi, M., Goldman, M.H.S., Hartl, A., Heinekamp, T., *et al* (2006) The akuBKU80 Mutant Deficient for Nonhomologous

End Joining Is a Powerful Tool for Analyzing Pathogenicity in *Aspergillus fumigatus*. *Eukaryotic Cell*. **5**: 207-211.

Dagenais, T.R.T. and Keller, N.P. (2009) Pathogenesis of *Aspergillus fumigatus* in Invasive Aspergillosis. *Clinical Microbiology Reviews*. **22**: 447-465.

Davies, K.M., Strauss, M., Daum, B., Kief, J.H., Osiewacz, H.D., Rycovska, A., *et al* (2011) Macromolecular organization of ATP synthase and complex I in whole mitochondria. *Proceedings of the National Academy of Sciences, USA*. **108**: 14121-14126.

Davis, C. (2011b) The Glutathione *s*-transferase GliG Mediates Gliotoxin Biosynthesis, not Self-Protection in *Aspergillus fumigatus*: A Functional Genomic Investigation. *PhD Thesis*.

Davis, C., Carberry, S., Schrettl, M., Singh, I., Stephens, J.C., Barry, S.M., *et al* (2011a) The role of glutathione S-transferase GliG in gliotoxin biosynthesis in *Aspergillus fumigatus*. *Chemistry & Biology*. **18**: 542-552.

Denning, D.W., Anderson, M.J., Turner, G., Latgé, J.-P. and Bennett, J.W. (2002) Sequencing the *Aspergillus fumigatus* genome. *The Lancet Infectious Diseases*. **2**: 251-253.

Deplazes, A., Mockli, N., Luke, B., Auerbach, D. and Peter, M. (2009) Yeast Uri1p promotes translation initiation and may provide a link to cotranslational quality control. *The EMBO Journal*. **28**: 1429-1441.

Deveau, A., Piispanen, A.E., Jackson, A.A. and Hogan, D.A. (2010) Farnesol Induces Hydrogen Peroxide Resistance in *Candida albicans* Yeast by Inhibiting the Ras-Cyclic AMP Signaling Pathway. *Eukaryotic Cell*. **9**: 569-577.

Douglas, C., D'Ippolito, J., Shei, G., Mainz, M., Onishi, J., Marrinan, J., *et al* (1997) Identification of the FKS1 gene of *Candida albicans* as the essential target of 1,3-beta-D-glucan synthase inhibitors. *Antimicrobial Agents and Chemotherapy*. **41**: 2471-2479.

Dourado, D.F.â.A.â.R., Fernandes, P.A., Mannervik, B. and Ramos, M.J.o. (2008) Glutathione Transferase: New Model for Glutathione Activation. *Chemistry*. **14**: 9591-9598.

Doyle, S. (2011) Fungal proteomics: from identification to function. *FEMS Microbiology Letters*. **321**: 1-9.

Dumas, R., Biou, V., Halgand, F., Douce, R. and Duggleby, R.G. (2001) Enzymology, Structure, and Dynamics of Acetohydroxy Acid Isomeroreductase. *Accounts of Chemical Research*. **34**: 399-408.

Duncan, M.W., Roder, H. and Hunsucker, S.W. (2008) Quantitative matrix-assisted laser desorption/ionization mass spectrometry. *Briefings in functional genomics and proteomics*. **7**: 355-370.

Edmonds, B.T., Bell, A., Wyckoff, J., Condeelis, J. and Leyh, T.S. (1998) The Effect of F-actin on the Binding and Hydrolysis of Guanine Nucleotide by Dictyostelium Elongation Factor 1A. *Journal of Biological Chemistry*. **273**: 10288-10295.

Ejiri, S.-i. (2002) Moonlighting Functions of Polypeptide Elongation Factor 1: From Actin Bundling to Zinc Finger Protein R1-Associated Nuclear Localization. *Bioscience, Biotechnology, and Biochemistry*. **66**: 1-21.

Emri, T.s., Pocsi, I.n. and Szentirmai, A. (1998) Changes in the glutathione (GSH) metabolism of *Penicillium chrysogenum* grown on different nitrogen, sulphur and carbon sources. *Journal of Basic Microbiology*. **38**: 3-8.

Esakova, O.A., Meshalkina, L.E., Golbik, R., Hubner, G. and Kochetov, G.A. (2004) Donor substrate regulation of transketolase. *European Journal of Biochemistry*. **271**: 4189-4194.

Esposito, A.M. and Kinzy, T.G. (2010) The eukaryotic translation elongation factor 1Bgamma has a non-guanine nucleotide exchange factor role in protein metabolism. *The Journal of Biological Chemistry*. **285**: 37995-38004.

Farah, M.E., Sirotkin, V., Haarer, B., Kakhniashvili, D. and Amberg, D.C. (2011) Diverse Protective Roles of the Actin Cytoskeleton During Oxidative Stress. *Cytoskeleton*. **68**: 340-354.

Fedorova, N.D., Khaldi, N., Joardar, V.S., Maiti, R., Amedeo, P., Anderson, M.J., *et al* (2008) Genomic Islands in the Pathogenic Filamentous Fungus *Aspergillus fumigatus*. *PLoS Genetics*. **4**: e1000046 EP -.

Fleck, C.B. and Brock, M. (2010) *Aspergillus fumigatus* Catalytic Glucokinase and Hexokinase: Expression Analysis and Importance for Germination, Growth, and Conidiation. *Eukaryotic Cell*. **9**: 1120-1135.

Fontecave, M., Atta, M. and Mulliez, E. (2004) S-adenosylmethionine: nothing goes to waste. *Trends in Biochemical Sciences*. **29**: 243-249.

Fortwendel, J.R., Juvvadi, P.R., Rogg, L.E. and Steinbach, W.J. (2011) Regulatable Ras Activity Is Critical for Proper Establishment and Maintenance of Polarity in *Aspergillus fumigatus*. *Eukaryotic Cell*. **10**: 611-615.

Frova, C. (2006) Glutathione transferases in the genomics era: New insights and perspectives. *Biomolecular Engineering*. **23**: 149-169.

Fu, L. and Sztul, E. (2003) Traffic-Independent Function of the Sar1p/COPII Machinery in Proteasomal Sorting of the Cystic Fibrosis Transmembrane Conductance Regulator. *The Journal of Cell Biology*. **160**: 157-163.

Galagan, J.E., Calvo, S.E., Cuomo, C., Ma, L.-J., Wortman, J.R., Batzoglou, S., *et al* (2005) Sequencing of *Aspergillus nidulans* and comparative analysis with *A. fumigatus* and *A. oryzae*. *Nature*. **438**: 1105-1115.

Gallie, D.R. (2002) Protein-protein interactions required during translation. *Plant Molecular Biology*. **50**: 949-970.

Gao, X.-H., Bedhomme, M., Veyel, D., Zaffagnini, M. and Lemaire, S.D. (2009) Methods for Analysis of Protein Glutathionylation and their Application to Photosynthetic Organisms. *Molecular Plant*. **2**: 218-235.

Garcera, A., Barreto, L., Piedrafita, L., Tamarit, J. and Herrero, E. (2006) *Saccharomyces cerevisiae* cells have three Omega class glutathione S-transferases acting as 1-Cys thiol transferases. *The Biochemical Journal*. **398**: 187-196.

Gardiner, D.M., Waring, P. and Howlett, B.J. (2005) The epipolythiodioxopiperazine (ETP) class of fungal toxins: distribution, mode of action, functions and biosynthesis. *Microbiology*. **151**: 1021-1032.

Gaspar, M.L., Jesch, S.A., Viswanatha, R., Antosh, A.L., Brown, W.J., Kohlwein, S.D. and Henry, S.A. (2008) A Block in Endoplasmic Reticulum-to-Golgi Trafficking Inhibits Phospholipid Synthesis and Induces Neutral Lipid Accumulation. *The Journal of Biological Chemistry*. **283**: 25735-25751.

Gautam, P., Shankar, J., Madan, T., Sirdeshmukh, R., Sundaram, C.S., Gade, W.N., *et al* (2008) Proteomic and Transcriptomic Analysis of *Aspergillus fumigatus* on Exposure to Amphotericin B. *Antimicrobial Agents and Chemotherapy*. **52**: 4220-4227.

Gautam, P., Upadhyay, S., Hassan, W., Madan, T., Sirdeshmukh, R., Sundaram, C., *et al* (2011) Transcriptomic and Proteomic Profile of *Aspergillus fumigatus* on Exposure to Artemisinin. In *Mycopathologia*: Springer Netherlands, pp. 1-16.

Ghezzi, P. (2005) Review Regulation of protein function by glutathionylation. *Free Radical Research*. **39**: 573-580.

Goeckeler, J.L. and Brodsky, J.L. (2010) Molecular chaperones and substrate ubiquitination control the efficiency of endoplasmic reticulum-associated degradation. *Diabetes, Obesity and Metabolism*. **12**: 32-38.

Goldberg, A.L. (2003) Protein degradation and protection against misfolded or damaged proteins. *Nature*. **426**: 895-899.

Gomez, P., Hackett, T., Moore, M., Knight, D. and Tebbutt, S. (2010) Functional genomics of human bronchial epithelial cells directly interacting with conidia of *Aspergillus fumigatus* *BMC Genomics*. **11**: 358.

Gorg, A., Drews, O., Luck, C., Weiland, F. and Weiss, W. (2009) 2-DE with IPGs. *Electrophoresis*. **30**: S122-S132.

Greenbaum, D., Colangelo, C., Williams, K. and Gerstein, M. (2003) Comparing protein abundance and mRNA expression levels on a genomic scale. *Genome Biology*. **4**: 117.

Greetham, D. and Grant, C. (2009) Antioxidant activity of the yeast mitochondrial 1-Cys peroxiredoxin is dependent on thioredoxin reductase and glutathione in vivo. *Molecular and Cellular Biology*. **29**: 3229 - 3240.

Greetham, D., Vickerstaff, J., Shenton, D., Perrone, G., Dawes, I. and Grant, C. (2010) Thioredoxins function as deglutathionylase enzymes in the yeast *Saccharomyces cerevisiae*. *BMC Biochemistry*. **11**: 3.

Griffiths, W.J. and Wang, Y. (2009) Mass spectrometry: from proteomics to metabolomics and lipidomics. *Chemical Society Reviews*. **38**: 1882-1896.

Gross, S.R. and Kinzy, T.G. (2005) Translation elongation factor 1A is essential for regulation of the actin cytoskeleton and cell morphology. *Nature Structural and Molecular Biology*. **12**: 772-778.

Gross, S.R. and Kinzy, T.G. (2007) Improper organization of the actin cytoskeleton affects protein synthesis at initiation. *Molecular and Cellular Biology*. **27**: 1974-1989.

Guo, S., Wharton, W., Moseley, P. and Shi, H. (2007) Heat shock protein 70 regulates cellular redox status by modulating glutathione-related enzyme activities. *Cell Stress and Chaperones*. **12**: 245-254.

Han, K.H., Kim, J.H., Kim, W.S. and Han, D.M. (2005) The *snpA*, a temperature-sensitive suppressor of *npgAI*, encodes the eukaryotic translation release factor, eRF1, in *Aspergillus nidulans*. *FEMS Microbiology Letters*. **251**: 155-160.

Han, X., Aslanian, A. and Yates III, J.R. (2008) Mass Spectrometry for proteomics. *Current Opinion in Chemical Biology*. **12**: 483-490.

Harris, S.D., Hofmann, A.F., Tedford, H.W. and Lee, M.P. (1999) Identification and Characterization of Genes Required for Hyphal Morphogenesis in the Filamentous Fungus *Aspergillus nidulans*. *Genetics*. **151**: 1015-1025.

Hartmann, T., Sasse, C., Schedler, A., Hasenberg, M., Gunzer, M. and Krappmann, S. (2011) Shaping the fungal adaptome- Stress responses of *Aspergillus fumigatus*. *International Journal of Medical Microbiology Colonisation and infection by human-pathogenic fungi*. **301**: 408-416.

Hawkins, A.R., Lamb, H.K., Moore, J.D., Charles, I.G. and Roberts, C.F. (1993) Review Article: The pre-chorismate (shikimate) and quinate pathways in filamentous fungi: theoretical and practical aspects. *Journal of General Microbiology*. **139**: 2891-2899.

Hayes, J.D. and McLellan, L.I. (1999) Glutathione and Glutathione-dependent Enzymes Represent a Co-ordinately Regulated Defence Against Oxidative Stress. *Free Radical Research*. **31**: 273-300.

Hayes, J.D., Flanagan, J.U. and Jowsey, I.R. (2005) Glutathione transferases. *Annual Review of Pharmacology and Toxicology*. **45**: 51-88.

Henderson, B. (2010) Integrating the cell stress response: a new view of molecular chaperones as immunological and physiological homeostatic regulators. *Cell Biochemistry and Function*. **28**: 1-14.

Hieter, P. and Boguski, M. (1997) Functional Genomics: It's All How You Read It. *Science*. **278**: 601-602.

Hissen, A.H.T., Wan, A.N.C., Warwas, M.L., Pinto, L.J. and Moore, M.M. (2005) The *Aspergillus fumigatus* Siderophore Biosynthetic Gene *sidA*, Encoding L-Ornithine N5-Oxygenase, Is Required for Virulence. *Infection and Immunity*. **73**: 5493-5503.

Hohl, T.M. and Feldmesser, M. (2007) *Aspergillus fumigatus*: Principles of Pathogenesis and Host Defense. *Eukaryotic Cell*. **6**: 1953-1963.

Hondorp, E.R. and Matthews, R.G. (2004) Oxidative Stress Inactivates Cobalamin-Independent Methionine Synthase (MetE) in *Escherichia coli*. *PLoS Biology*. **2**: e336.

Hondorp, E.R. and Matthews, R.G. (2009) Oxidation of Cysteine 645 of Cobalamin-Independent Methionine Synthase Causes a Methionine Limitation in *Escherichia coli*. *Journal of Bacteriology*. **191**: 3407-3410.

Huet, C., Menendez, J., Gancedo, C. and Fran  ois, J.M. (2000) Regulation of pyc1 encoding pyruvate carboxylase isozyme I by nitrogen sources in *Saccharomyces cerevisiae*. *European Journal of Biochemistry*. **267**: 6817-6823.

Hynes, M.J. and Murray, S.L. (2010) ATP-Citrate Lyase Is Required for Production of Cytosolic Acetyl Coenzyme A and Development in *Aspergillus nidulans*. *Eukaryotic Cell*. **9**: 1039-1048.

Ibrahim-Granet, O.m., Dubourdeau, M., Latge, J.-P., Ave, P., Huerre, M., Brakhage, A.A. and Brock, M. (2008) Methylcitrate synthase from *Aspergillus fumigatus* is essential for manifestation of invasive aspergillosis. *Cellular Microbiology*. **10**: 134-148.

Inaba, T., Nagano, Y., Nagasaki, T. and Sasaki, Y. (2002) Distinct Localization of Two Closely Related Ypt3/Rab11 Proteins on the Trafficking Pathway in Higher Plants. *Journal of Biological Chemistry*. **277**: 9183-9188.

Jackson, R.J., Hellen, C.U.T. and Pestova, T.V. (2010) The mechanism of eukaryotic translation initiation and principles of its regulation. *Nature*. **11**: 113-127.

Jahn, B., Koch, A., Schmidt, A., Wanner, G., Gehringer, H., Bhakdi, S. and Brakhage, A. (1997) Isolation and characterization of a pigmentless-conidium mutant of *Aspergillus fumigatus* with altered conidial surface and reduced virulence. *Infection and Immunity*. **65**: 5110-5117.

Jancova, P., Anzenbacher, P. and Anzenbacherova, E. (2010) Phase II Drug Metabolising Enzymes. *Biomedical papers of the Medical Faculty of the University Palacky, Olomouc, Czechoslovakia*. **154**: 103-116.

Janssen, G.M.C. and Moller, W. (1988) Kinetic studies on the role of elongation factors 1   and 1   in protein synthesis. *Journal of Biological Chemistry*. **263**: 1773-1778.

Jeppesen, M.G., Ortiz, P., Shepard, W., Kinzy, T.G., Nyborg, J. and Andersen, G.R. (2003) The Crystal Structure of the Glutathione S-Transferase-like Domain of

Elongation Factor 1B γ from *Saccharomyces cerevisiae*. *The Journal of Biological Chemistry*. **278**: 47190-47198.

Jin, L.-T., Li, X.-K., Cong, W.-T., Hwang, S.-Y. and Choi, J.-K. (2008) Previsible silver staining of protein in electrophoresis gels with mass spectrometry compatibility. *Analytical Biochemistry*. **383**: 137-143.

Jin, Y., Bok, J.W., Guzman-de-Peña, D. and Keller, N.P. (2002) Requirement of spermidine for developmental transitions in *Aspergillus nidulans*. *Molecular Microbiology*. **46**: 801-812.

Jones, D.P. and Go, Y.-M. (2011) Mapping the cysteine proteome: analysis of redox-sensing thiols. *Current Opinion in Chemical Biology Omics*. **15**: 103-112.

Jonusiene, V., Sasnauskiene, S. and Juodka, B. (2005) The cloning and characterization of *Tetrahymena pyriformis* translation elongation factor 1B alpha and gamma subunits. *Cellular and Molecular Biology Letters*. **10**: 689-696.

Kambouris, N.G., Burke, D.J. and Creutz, C.E. (1993) Cloning and genetic characterisation of a calcium-binding and phospholipid-binding protein from *Saccharomyces cerevisiae* that is homologous to translation elongation factor-1gamma. *Yeast*. **9**: 151-163.

Kamiie, K., Nomura, Y., Kobayashi, S., Taira, H., Kobayashi, K., Yamashita, T., *et al* (2002) Cloning and Expression of Bombyx mori Silk Gland Elongation Factor 1 γ ; in *Escherichia coli*. *Bioscience, Biotechnology, and Biochemistry*. **66**: 558-565.

Kim, S. and Coulombe, P.A. (2010) Emerging role for the cytoskeleton as an organizer and regulator of translation. *Nature Reviews Molecular Cell Biology*. **11**: 75-81.

Kim, S., Kellner, J., Lee, C.-H. and Coulombe, P.A. (2007) Interaction between the keratin cytoskeleton and eEF1B γ affects protein synthesis in epithelial cells. *Nature Structural and Molecular Biology*. **14**: 982-983.

Kniemeyer, O. (2011) Proteomics of eukaryotic microorganisms: The medically and biotechnologically important fungal genus *Aspergillus*. *Proteomics*. **11**: 3232-3243.

Kniemeyer, O., Lessing, F. and Brakhage, A.A. (2009) Proteome analysis for pathogenicity and new diagnostic markers for *Aspergillus fumigatus*. *Medical Mycology*. **47 Suppl 1**: S248-254.

Kniemeyer, O., Lessing, F., Scheibner, O., Hertweck, C. and Brakhage, A.A. (2006) Optimisation of a 2-D gel electrophoresis protocol for the human-pathogenic fungus *Aspergillus fumigatus*. *Current Genetics*. **49**: 178-189.

Knutsen, A.P. and Slavin, R.G. (2011) Allergic Bronchopulmonary Aspergillosis in Asthma and Cystic Fibrosis. *Clinical and Developmental Immunology*. **Epub 2011**.

Kobayashi, S., Kidou, S. and Ejiri, S.-i. (2001) Detection and characterisation of glutathione S-transferase in rice EF-1betabeta'gamma and EF-1gamma expressed in *Escherichia coli*. *Biochemical and Biophysical Research communications*. **288**: 509-514.

Kochetov, G. and Sevostyanova, I. (2005) Binding of the Coenzyme and Formation of the Transketolase Active Center. *IUBMB Life*. **57**: 491-497.

Koonin, E.V., Tatusov, R.L., Altschul, S.F., Bryant, S.H., Mushegian, A.R., Bork, P. and Valencia, A. (1994) Eukaryotic translation elongation factor 1gamma contains a glutathione transferase domain-Study of a diverse, ancient protein super family using motif search and structural modeling. *Protein Science*. **3**: 2045-2055.

Krappmann, S., Sasse, C. and Braus, G.H. (2006a) Gene Targeting in *Aspergillus fumigatus* by Homologous Recombination Is Facilitated in a Nonhomologous End-Joining-Deficient Genetic Background
10.1128/EC.5.1.212-215.2006. *Eukaryotic Cell*. **5**: 212-215.

Krappmann, S., Sasse, C. and Braus, G.H. (2006b) Gene Targeting in *Aspergillus fumigatus* by Homologous Recombination Is Facilitated in a Nonhomologous End-Joining-Deficient Genetic Background. *Eukaryotic Cell*. **5**: 212-215.

Kubodera, T., Yamashita, N. and Nishimura, A. (2000) Pyrithiamine Resistance Gene (*ptrA*) of *Aspergillus oryzae*: Cloning, Characterization and Application as a Dominant Selectable Marker for Transformation. *Bioscience, Biotechnology, and Biochemistry*. **64**: 1416-1421.

Kubodera, T., Yanashita, N. and Nishimura, A. (2002) Transformation of *Aspergillus* sp. and *Trichoderma reesei* Using the Pyrithiamine Resistance Gene (*ptrA*) of *Aspergillus oryzae*. *Biosci. Biotechnol. Biochem.* **66**: 404-406.

Kummasook, A., Tzaphmaag, A., Thirach, S., Pongpom, M., Cooper Jr., C.R. and Vanittanakom, N. (2011) *Penicillium marneffe* actin expression during phase transition, oxidative stress, and macrophage infection. *Molecular Biology Reports*. **38**: 2813-2819.

Kwon-Chung, K.J. and Sugui, J.A. (2009) What do we know about the role of gliotoxin in the pathobiology of *Aspergillus fumigatus*? *Medical Mycology*. **47**: S97-S103.

Lamb, H.K., Bagshaw, C.R. and Hawkins, A.R. (1991) In vivo overproduction of the pentafunctional arom polypeptide in *Aspergillus nidulans* affects metabolic flux in the quinate pathway. *Molecular and General Genetics*. **227**: 187-196.

Lambou, K., Lamarre, C., Beau, R.m., Dufour, N. and Latge, J.-P. (2010) Functional analysis of the superoxide dismutase family in *Aspergillus fumigatus*. *Molecular Microbiology*. **75**: 910-923.

Latge, J.-P. (1999) *Aspergillus fumigatus* and Aspergillosis. *Clinical Microbiology Reviews*. **12**: 310-350.

Le Sourd, F., Boulben, S., Le Bouffant, R., Cormier, P., Morales, J., Belle, R. and Mulner-Lorillon, O. (2006) eEF1B: At the dawn of the 21st century. *Biochimica et Biophysica Acta*. **1759**: 13-31.

Lessing, F., Kniemeyer, O., Wozniok, I., Loeffler, J., Kurzai, O., Haertl, A. and Brakhage, A.A. (2007) The *Aspergillus fumigatus* transcriptional regulator AfYap1 represents the major regulator for defense against reactive oxygen intermediates but is dispensable for pathogenicity in an intranasal mouse infection model. *Eukaryotic Cell*. **6**: 2290-2302.

Li, S.C. and Kane, P.M. (2009) The yeast lysosome-like vacuole: Endpoint and crossroads. *Biochimica et Biophysica Acta (BBA) - Molecular Cell Research Lysosomes*. **1793**: 650-663.

Liu, G., Tang, J., Edmonds, B.T., Murray, J., Levin, S. and Condeelis, J. (1996) F-actin sequesters elongation factor 1 alpha from interaction with aminoacyl-tRNA in a pH-dependent reaction. *Journal of Cell Biology*. **135**: 953-963.

Longo, V.D. (1999) Mutations in signal transduction proteins increase stress resistance and longevity in yeast, nematodes, fruit flies, and mammalian neuronal cells. *Neurobiology of Aging*. **20**: 479-486.

Longo, V.D. and Fabrizio, P. (2002) Regulation of longevity and stress resistance: a molecular strategy conserved from yeast to humans? *Cellular and Molecular Life Sciences*. **59**: 903-908.

Lopez-Mirabal, H.R., Thorsen, M., Kielland-Brandt, M.C., Toledano, M.B. and Winther, J.R. (2007) Cytoplasmic glutathione redox status determines survival upon exposure to the thiol-oxidant 4,4'-dipyridyl disulfide. *FEMS Yeast Res.* **7**: 391-403.

López-Mirabal, H.R. and Winther, J.R. (2008) Redox characteristics of the eukaryotic cytosol. *Biochimica et Biophysica Acta (BBA) - Molecular Cell Research Redox regulation of protein folding.* **1783**: 629-640.

Lushchak, V.I. (2011) Adaptive response to oxidative stress: Bacteria, fungi, plants and animals. *Comparative Biochemistry and Physiology.* **153**: 175-190.

Ma, Y. and Hendershot, L.M. (2001) The Unfolding Tale of the Unfolded Protein Response. *Cell.* **107**: 827-830.

Mabey, J.E., Anderson, M.J., Giles, P.F., Miller, C.J., Attwood, T.K., Paton, N.W., *et al* (2004) CADRE: the Central *Aspergillus* Data REpository. *Nucleic Acids Research.* **32**: D401-D405.

Maeng, S., Ko, Y.-J., Kim, G.-B., Jung, K.-W., Floyd, A., Heitman, J. and Bahn, Y.-S. (2010) Comparative Transcriptome Analysis Reveals Novel Roles of the Ras and Cyclic AMP Signaling Pathways in Environmental Stress Response and Antifungal Drug Sensitivity in *Cryptococcus neoformans*. *Eukaryotic Cell.* **9**: 360-378.

Maiya, S., Grundmann, A., Li, S.-M. and Turner, G. (2006) The Fumitremorgin Gene Cluster of *Aspergillus fumigatus*: Identification of a Gene Encoding Brevianamide F Synthetase. *ChemBioChem.* **7**: 1062-1069.

Malhotra, J.D. and Kaufman, R.J. (2007) The endoplasmic reticulum and the unfolded protein response. *Seminars in Cell & Developmental Biology Degradation of Misfolded Glycoproteins Moving Stem Cells Towards the Clinic.* **18**: 716-731.

Mateyak, M.K. and Kinzy, T.G. (2010) eEF1A: Thinking Outside the Ribosome. *Journal of Biological Chemistry.* **285**: 21209-21213.

Mayer, M.P. and Bukau, B. (2005) Hsp70 chaperones: Cellular functions and molecular mechanism. *Cellular and Molecular Life Sciences.* **62**: 670-684.

McCormick, A., Loeffler, J.r. and Ebel, F. (2010) *Aspergillus fumigatus*: contours of an opportunistic human pathogen. *Cellular Microbiology.* **12**: 1535-1543.

- McGoldrick, S., O'Sullivan, S.M. and Sheehan, D. (2005) Glutathione transferase-like proteins encoded in genomes of yeasts and fungi: insights into evolution of a multifunctional protein superfamily. *FEMS Microbiology Letters*. **242**: 1-12.
- Melin, P., Schnurer, J. and Wagner, E.G.H. (2004) Disruption of the gene encoding the V-ATPase subunit A results in inhibition of normal growth and abolished sporulation in *Aspergillus nidulans*. *Microbiology*. **150**: 743-748.
- Merrick, W.C. (2010) Eukaryotic Protein Synthesis: Still a Mystery. *Journal of Biological Chemistry*. **285**: 21197-21201.
- Meyer, A. and Hell, R.d. (2005a) Glutathione homeostasis and redox-regulation by sulfhydryl groups. *Photosynthesis Research*. **86**: 435-457.
- Meyer, A. and Hell, R. (2005b) Glutathione homeostasis and redox-regulation by sulfhydryl groups. *Photosynthesis Research*. **86**: 435-457.
- Meyer, V. (2008) Genetic Engineering of filamentous fungi- progress, obstacles and future trends. *Biotechnology Advances*: 177-185.
- Meyer, V., Wu, B. and Ram, A. (2011) *Aspergillus* as a multi-purpose cell factory: current status and perspectives. *Biotechnology Letters*. **33**: 469-476.
- Michielse, C.B., Hooykaas, P.J.J., van den Hondel, C.A.M.J.J. and Ram, A.F.J. (2008) *Agrobacterium*-mediated transformation of the filamentous fungus *Aspergillus awamori*. *Nature Protocols*. **3**: 1671-1678.
- Minden, J.S., Dowd, S.R., Meyer, H.E. and Stuhler, K. (2009) Difference gel electrophoresis. *Electrophoresis*. **30**: S156-S161.
- Mirkes, P.E. (1974) Polysomes, Ribonucleic Acid, and Protein Synthesis During Germination of *Neurospora crassa* Conidia. *Journal of Bacteriology*. **117**: 196-202.
- Mootz, H.D., Schwarzer, D. and Marahiel, M.A. (2002) Ways of Assembling Complex Natural Products on Modular Nonribosomal Peptide Synthetases. *ChemBioChem*. **3**: 490-504.
- Morel, M.I., Ngadin, A., Droux, M., Jacquot, J.-P. and Gelhaye, E. (2009) The fungal glutathione S-transferase system. Evidence of new classes in the wood-degrading basidiomycete *Phanerochaete chrysosporium*. *Cellular and Molecular Life Sciences*. **66**: 3711-3725.

- Munro, C.A. (2010) Fungal echinocandin resistance. *F1 000 Biology Reports*. **2**.
- Neilson, K.A., Ali, N.A., Muralidharan, S., Mirzaei, M., Mariani, M., Assadourian, G., *et al* (2011) Less label, more free: Approaches in label-free quantitative mass spectrometry. *Proteomics*. **11**: 535-553.
- Nett, J.E., Sanchez, H., Cain, M.T. and Andes, D.R. (2010) Genetic Basis of *Candida* Biofilm Resistance Due to Drug-Sequestering Matrix Glucan. *Journal of Infectious Diseases*. **202**: 171-175.
- Neville, C., Murphy, A., Kavanagh, K. and Doyle, S. (2005) A 4'-Phosphopantetheinyl Transferase Mediates Non-Ribosomal Peptide Synthetase Activation in *Aspergillus fumigatus*. *ChemBioChem*. **6**: 679-685.
- Nielsen, A.L. (2009) The coat protein complex II, COPII, protein Sec13 directly interacts with presenilin-1. *Biochemical and Biophysical Research communications*. **388**: 571-575.
- Nielsen, J.B., Nielsen, M.L. and Mortensen, U.H. (2008) Transient disruption of non-homologous end-joining facilitates targeted genome manipulations in the filamentous fungus *Aspergillus nidulans*. *Fungal Genetics and Biology*. **45**: 165-170.
- Nielsen, M.L., Albertsen, L., Lettier, G., Nielsen, J.B. and Mortensen, U.H. (2006) Efficient PCR-based gene targeting with a recyclable marker for *Aspergillus nidulans*. *Fungal Genetics and Biology*. **43**: 54-64.
- Nierman, W.C., Pain, A., Anderson, M.J., Wortman, J.R., Kim, H.S., Arroyo, J., *et al* (2005) Genomic sequence of the pathogenic and allergenic filamentous fungus *Aspergillus fumigatus*. *Nature*. **438**: 1151-1156.
- Oakley, A.J. (2005) Glutathione transferases: new functions. *Current Opinion in Structural Biology*. **15**: 716-723.
- O'Gorman, C.M., Fuller, H.T. and Dyer, P.S. (2009) Discovery of a sexual cycle in the opportunistic fungal pathogen *Aspergillus fumigatus*. *Nature*. **457**: 471-474.
- O'Hanlon, K.A. (2010) A functional genomics approach: Characterisation of two Non-ribosomal peptide synthetase genes, and investigation of an adaptive response towards alkylating DNA damage in *Aspergillus fumigatus*. *PhD Thesis*.
- O'Hanlon, K.A., Cairns, T., Stack, D., Schrettl, M., Bignell, E.M., Kavanagh, K., *et al* (2011) Targeted Disruption of Non-Ribosomal Peptide Synthetase pes3 Augments the Virulence of *Aspergillus fumigatus*. *Infection and Immunity*. **79**: 3978-3992.

- Olarewaju, O., Ortiz, P.A., Chowdhury, W.Q., Chatterjee, I. and Kinzy, T.G. (2004) The translation elongation factor eEF1B plays a role in the oxidative stress response pathway. *RNA Biology*. **1**: 89-94.
- Ostrosky-Zeichner, L., Casadevall, A., Galgiani, J.N., Odds, F.C. and Rex, J.H. (2010) An insight into the antifungal pipeline: selected new molecules and beyond. *Nature Reviews. Drug Discovery*. **9**: 719-727.
- Ozturk, S.B. and Kinzy, T.G. (2008) Guanine nucleotide exchange factor independence of the G-protein eEF1A through novel mutant forms and biochemical properties. *Journal of Biological Chemistry*. **283**: 23244-23253.
- Pahlman, I.-L., Gustafsson, L., Rigoulet, M. and Larsson, C. (2001) Cytosolic redox metabolism in aerobic chemostat cultures of *Saccharomyces cerevisiae*. *Yeast*. **18**: 611-620.
- Panasenko, O.O., David, F.P.A. and Collart, M.A. (2009) Ribosome Association and Stability of the Nascent Polypeptide-Associated Complex Is Dependent Upon Its Own Ubiquitination. *Genetics*. **181**: 447-460.
- Paoletti, M., Rydholm, C., Schwier, E.U., Anderson, M.J., Szakacs, G., Lutzoni, F., *et al* (2005) Evidence for Sexuality in the Opportunistic Fungal Pathogen *Aspergillus fumigatus*. *Current Biology*. **15**: 1242-1248.
- Paris, S., Wysong, D., Debeaupuis, J.-P., Shibuya, K., Philippe, B., Diamond, R.D. and Latge, J.-P. (2003) Catalases of *Aspergillus fumigatus*. *Infection and Immunity*. **71**: 3551-3562.
- Paukstelis, P.J. and Lambowitz, A.M. (2008) Identification and evolution of fungal mitochondrial tyrosyl-tRNA synthetases with group I intron splicing activity. *Proceedings of the National Academy of Sciences, USA*. **105**: 6010-6015.
- Paulsen, C.E. and Carroll, K.S. (2009) Chemical Dissection of an Essential Redox Switch in Yeast. *Chemistry & Biology*. **16**: 217-225.
- Perrin, R.M., Fedorova, N.D., Bok, J.W., Cramer, R.A., Jr., Wortman, J.R., Kim, H.S., *et al* (2007) Transcriptional Regulation of Chemical Diversity in *Aspergillus fumigatus* by LaeA. *PLoS Pathogens*. **3**: e50 EP -.
- Peters, C., Baars, T.L., Bühler, S. and Mayer, A. (2004) Mutual Control of Membrane Fission and Fusion Proteins. *Cell*. **119**: 667-678.

Pfaller, M., Boyken, L., Hollis, R., Kroeger, J., Messer, S., Tendolkar, S. and Diekema, D. (2011) Comparison of the Broth Microdilution Methods of the European Committee on Antimicrobial Susceptibility Testing and the Clinical and Laboratory Standards Institute for Testing Itraconazole, Posaconazole, and Voriconazole against *Aspergillus* Isolates. *Journal of Clinical Microbiology*. **49**: 1110-1112.

Pisarev, A.V., Hellen, C.U.T. and Pestova, T.V. (2007) Recycling of Eukaryotic Posttermination Ribosomal Complexes. *Cell*. **131**: 286-299.

Pittman, Y.R., Kandl, K., Lewis, M., Valente, L. and Kinzy, T.G. (2009) Coordination of eukaryotic translation elongation factor 1A (eEF1A) function in actin organization and translation elongation by the guanine nucleotide exchange factor eEF1B α . *Journal of Biological Chemistry*. **284**: 4739-4747.

Pocsi, I., Miskei, M., Karanyi, Z., Emri, T., Ayoubi, P., Pusztahelyi, T., *et al* (2005) Comparison of gene expression signatures of diamide, H₂O₂ and menadione exposed *Aspergillus nidulans* cultures - linking genome-wide transcriptional changes to cellular physiology. *BMC Genomics*. **6**: 182.

Preiss, T. and Hentze, M., W. (2003) Starting the protein synthesis machine: eukaryotic translation initiation. *BioEssays*. **25**: 1201-1211.

Priebe, S., Linde, J.r., Albrecht, D., Guthke, R. and Brakhage, A.A. (2011) FungiFun: A web-based application for functional categorization of fungal genes and proteins. *Fungal Genetics and Biology*. **48**: 353-358.

Pusztahelyi, T., Klement, É., Szajli, E., Klem, J., Miskei, M., Karányi, Z., *et al* (2010) Comparison of transcriptional and translational changes caused by long-term menadione exposure in *Aspergillus nidulans*. *Fungal Genetics and Biology*. **48**: 92-103.

Qiao, J., Liu, W. and Li, R. (2010) Truncated Afyap1 Attenuates Antifungal Susceptibility of *Aspergillus fumigatus* to Voriconazole and Confers Adaptation of the Fungus to Oxidative Stress. In *Mycopathologia*: Springer Netherlands, pp. 155-160.

Qiao, J., Kontoyiannis, P., Calderone, R., Li, D., Ma, Y., Wan, Z., *et al* (2008) AfyapI, encoding a bZip transcriptional factor of *Aspergillus fumigatus*, contributes to oxidative stress response but is not essential to the virulence of this pathogen in mice immunosuppressed by cyclophosphamide and triacinelone. *Medical Mycology*. **46**: 773-782.

Rahman, I., Kode, A. and Biswas, S.K. (2006) Assay for quantitative determination of glutathione and glutathione disulfide levels using enzymatic recycling method. *Nature Protocols*. **1**: 3159-3165.

Rai, R., Tate, J.J. and Cooper, T.G. (2003) Ure2, a Prion Precursor with Homology to Glutathione S-Transferase, Protects *Saccharomyces cerevisiae* Cells from Heavy Metal Ion and Oxidant Toxicity. *Journal of Biological Chemistry*. **278**: 12826-12833.

Reeves, E.P., Reiber, K., Neville, C., Scheibner, O., Kavanagh, K. and Doyle, S. (2006) A nonribosomal peptide synthetase (Pes1) confers protection against oxidative stress in *Aspergillus fumigatus*. *FEBS Journal*. **273**: 3038-3053.

Richie, D.L., Hartl, L., Aimanianda, V., Winters, M.S., Fuller, K.K., Miley, M.D., *et al* (2009) A Role for the Unfolded Protein Response (UPR) in Virulence and Antifungal Susceptibility in *Aspergillus fumigatus*. *PLoS Pathogens*. **5**: e1000258.

Rodnina, M.V. and Wintermeyer, W. (2009) Recent mechanistic insights into eukaryotic ribosomes. *Current Opinion in Cell Biology Nucleus and gene expression*. **21**: 435-443.

Rodrigues-Pousada, C., Menezes, R.A. and Pimentel, C. (2010) The Yap family and its role in stress response. *Yeast*. **27**: 245-258.

Ron, D. and Walter, P. (2007) Signal integration in the endoplasmic reticulum unfolded protein response. *Nature Review Molecular Cell Biology*. **8**: 519-529.

Rooij, I.I.S.-d., Allwood, E.G., Aghamohammadzadeh, S., Hettema, E.H., Goldberg, M.W. and Ayscough, K.R. (2010) A role for the dynamin-like protein Vps1 during endocytosis in yeast. *Journal of Cell Science*. **123**: 3496-3506.

Saliola, M., Sponziello, M., D'Amici, S., Lodi, T. and Falcone, C. (2008) Characterization of KIGUT2, a gene of the glycerol-3-phosphate shuttle, in *Kluyveromyces lactis*. *FEMS Yeast Research*. **8**: 697-705.

Sanglard, D. and Odds, F.C. (2002) Resistance of *Candida* species to antifungal agents: molecular mechanisms and clinical consequences. *The Lancet Infectious Diseases*. **2**: 73-85.

Sato, I., Shimizu, M., Hoshino, T. and Takaya, N. (2009) The Glutathione System of *Aspergillus nidulans* Involves a Fungus-specific Glutathione S-Transferase. *Journal of Biological Chemistry*. **284**: 8042-8053.

Scharf, D.H., Remme, N., Heinekamp, T., Hortschansky, P., Brakhage, A.A. and Hertweck, C. (2010) Transannular Disulfide Formation in Gliotoxin Biosynthesis and Its Role in Self-Resistance of the Human Pathogen *Aspergillus fumigatus*. *Journal of the American Chemical Society*. **132**: 10136-10141.

Scharf, D.H., Remme, N., Habel, A., Chankhamjon, P., Scherlach, K., Heinekamp, T., *et al* (2011) A Dedicated Glutathione S-Transferase Mediates Carbon-Sulfur Bond Formation in Gliotoxin Biosynthesis. *Journal of the American Chemical Society*. **133**: 12322-12325.

Schluter, A., Fourcade, S.p., Ripp, R., Mandel, J.L., Poch, O. and Pujol, A. (2006) The Evolutionary Origin of Peroxisomes: An ER-Peroxisome Connection. *Molecular Biology and Evolution*. **23**: 838-845.

Schrettl, M. and Haas, H. (2011) Iron homeostasis-Achilles' heel of *Aspergillus fumigatus*? *Current Opinion in Microbiology*. **14**: 400-405.

Schrettl, M., Bignell, E., Kragl, C., Joechl, C., Rogers, T., Arst, H.N., *et al* (2004) Siderophore Biosynthesis But Not Reductive Iron Assimilation Is Essential for *Aspergillus fumigatus* Virulence. *The Journal of Experimental Medicine*. **200**: 1213-1219.

Schrettl, M., Bignell, E., Kragl, C., Sabiha, Y., Loss, O., Eisendle, M., *et al* (2007) Distinct Roles for Intra- and Extracellular Siderophores during *Aspergillus fumigatus* Infection. *PLoS Pathogens*. **3**: e128.

Schrettl, M., Carberry, S., Kavanagh, K., Haas, H., Jones, G.W., O'Brien, J., *et al* (2010) Self-Protection against Gliotoxin-A Component of the Gliotoxin Biosynthetic Cluster, GliT, Completely Protects *Aspergillus fumigatus* Against Exogenous Gliotoxin. *PLoS Pathogens*. **6**: e1000952.

Schrettl, M., Kim, H.S., Eisendle, M., Kragl, C., Nierman, W.C., Heinekamp, T., *et al* (2008) SreA-mediated iron regulation in *Aspergillus fumigatus*. *Molecular Microbiology*. **70**: 27-43.

Senior, A.E., Nadanaciva, S. and Weber, J. (2002) The molecular mechanism of ATP synthesis by F1F0-ATP synthase. *Biochimica et Biophysica Acta (BBA) - Bioenergetics*. **1553**: 188-211.

Sheehan, D. (2006) Detection of redox-based modification in two-dimensional electrophoresis proteomic separations. *Biochemical and Biophysical Research Communications*. **349**: 455-462.

Sheehan, D., Meade, G., Foley, V.M. and Dowd, C.A. (2001) Structure, function and evolution of glutathione transferases: implications for classification of non-mammalian members of an ancient enzyme superfamily. *The Biochemical Journal*. **360**: 1-16.

Shenton, D., Smirnova, J.B., Selley, J.N., Carroll, K., Hubbard, S.J., Pavitt, G.D., *et al* (2006) Global Translational Responses to Oxidative Stress Impact upon Multiple Levels of Protein Synthesis. *Journal of Biological Chemistry*. **281**: 29011-29021.

Shringarpure, R., Grune, T., Mehlhase, J. and Davies, K.J.A. (2003) Ubiquitin Conjugation Is Not Required for the Degradation of Oxidized Proteins by Proteasome. *Journal of Biological Chemistry*. **278**: 311-318.

Sies, H., Dafre, A.L., Ji, Y. and Akerboom, T.P.M. (1998) Protein S-thiolation and redox regulation of membrane-bound glutathione transferase. *Chemico-Biological Interactions*. **111-112**: 177-185.

Snelders, E., Huis in 't Veld, R.A.G., Rijs, A.J.M.M., Kema, G.H.J., Melchers, W.J.G. and Verweij, P.E. (2009) Possible Environmental Origin of Resistance of *Aspergillus fumigatus* to Medical Triazoles. *Applied Environmental and Microbiology*. **75**: 4053-4057.

Snelders, E., van der Lee, H.A.L., Kuijpers, J., Rijs, A.J.M.M., Varga, J., Samson, R.A., *et al* (2008) Emergence of Azole Resistance in *Aspergillus fumigatus* and Spread of a Single Resistance Mechanism. *PLoS Medicine*. **5**: e219.

Sokol-Anderson, M.L., Brajtburg, J. and Medoff, G. (1986) Amphotericin B-induced oxidative damage and killing of *Candida albicans*. *Journal of Infectious Diseases*. **154**: 76-83.

Son, H., Lee, J., Park, A.R. and Lee, Y.-W. (2011) ATP citrate lyase is required for normal sexual and asexual development in *Gibberella zeae*. *Fungal Genetics and Biology*. **48**: 408-417.

Stack, D., Neville, C. and Doyle, S. (2007) Nonribosomal peptide synthesis in *Aspergillus fumigatus* and other fungi. *Microbiology*. **153**: 1297-1306.

Stack, D., Frizzell, A., Tomkins, K. and Doyle, S. (2009) Solid Phase 4'-Phosphopantetheinylation: Fungal Thiolation Domains are Targets for Chemoenzymatic Modification. *Bioconjugate Chemistry*. **20**: 1514-1522.

Strieker, M., TanoviÄ‡, A. and Marahiel, M.A. (2010) Nonribosomal peptide synthetases: structures and dynamics. *Current Opinion in Structural Biology*

Theory and simulation / Macromolecular assemblages. **20**: 234-240.

Suliman, H.S., Appling, D.R. and Robertus, J.D. (2007) The gene for cobalamin-independent methionine synthase is essential in *Candida albicans*: A potential antifungal target. *Archives of Biochemistry and Biophysics.* **467**: 218-226.

Sundstrom, M., Lindqvist, Y., Schneider, G., Hellman, U. and Ronne, H. (1993) Yeast TKL1 gene encodes a transketolase that is required for efficient glycolysis and biosynthesis of aromatic amino acids. *Journal of Biological Chemistry.* **268**: 24346-24352.

Taylor, D.J., Nilsson, J., Merrill, A.R., Andersen, G.R., Nissen, P. and Frank, J. (2007) Structures of modified eEF2 80S ribosome complexes reveal the role of GTP hydrolysis in translocation. *The EMBO Journal.* **26**: 2421-2431.

Teutschbein, J., Albrecht, D., Potsch, M., Guthke, R., Aimaganianda, V., Clavaud, C.c., *et al* (2010) Proteome Profiling and Functional Classification of Intracellular Proteins from Conidia of the Human-Pathogenic Mold *Aspergillus fumigatus*. *Journal of Proteome Research.* **9**: 3427-3442.

Thön, M., Al Abdallah, Q., Hortschansky, P., Scharf, D.H., Eisendle, M., Haas, H. and Brakhage, A.A. (2010) The CCAAT-binding complex coordinates the oxidative stress response in eukaryotes. *Nucleic Acids Research.* **38**: 1098-1113.

Thornton, C.R. (2010) Chapter 6 - Detection of Invasive Aspergillosis
Advances in Applied Microbiology. In *Advances in Applied Microbiology*. Gadd, A.I.L.S.S.G.M. (ed.): Academic Press, pp. 187-216.

Tobaben, S.n., Varoqueaux, F., Brose, N., Stahl, B. and Meyer, G. (2003) A Brain-specific Isoform of Small Glutamine-rich Tetratricopeptide Repeat-containing Protein Binds to Hsc70 and the Cysteine String Protein. *Journal of Biological Chemistry.* **278**: 38376-38383.

Tone, Y., Tanahashi, N., Tanaka, K., Fujimuro, M., Yokosawa, H. and Toh-e, A. (2000) Nob1p, a new essential protein, associates with the 26S proteasome of growing *Saccharomyces cerevisiae* cells. *Gene.* **243**: 37-45.

Travers, K.J., Patil, C.K., Wodicka, L., Lockhart, D.J., Weissman, J.S. and Walter, P. (2000) Functional and Genomic Analyses Reveal an Essential Coordination between the Unfolded Protein Response and ER-Associated Degradation. *Cell.* **101**: 249-258.

Tyagi, R., Lee, Y.T., Guddat, L.W. and Duggleby, R.G. (2005) Probing the mechanism of the bifunctional enzyme ketol-acid reductoisomerase by site-directed mutagenesis of the active site. *FEBS Journal*. **272**: 593-602.

Unlu, M., Morgan, M.E. and Minden, J.S. (1997) Difference gel electrophoresis: a single gel method for detecting changes in protein extracts. *Electrophoresis*. **18**: 2071-2077.

Valdes-Santiago, L., Cervantes-Chavez, J.A. and Ruiz-Herrera, J. (2009) *Ustilago maydis* spermidine synthase is encoded by a chimeric gene, required for morphogenesis, and indispensable for survival in the host. *FEMS Yeast Research*. **9**: 923-935.

Valouev, I., Fominov, G., Sokolova, E., Smirnov, V. and Ter-Avanesyan, M. (2009) Elongation factor eEF1B modulates functions of the release factors eRF1 and eRF3 and the efficiency of translation termination in yeast. *BMC Molecular Biology*. **10**: 60.

Veal, E.A., Toone, W.M., Jones, N. and Morgan, B.A. (2002) Distinct roles for glutathione s-transferases in the oxidative stress response in *Schizosaccharomyces pombe*. *The Journal of Biological Chemistry*. **277**: 35523-35531.

Vizeacoumar, F.J., Vreden, W.N., Fagarasanu, M., Eitzen, G.A., Aitchison, J.D. and Rachubinski, R.A. (2006) The Dynamin-like Protein Vps1p of the Yeast *Saccharomyces cerevisiae* Associates with Peroxisomes in a Pex19p-dependent Manner. *Journal of Biological Chemistry*. **281**: 12817-12823.

Vodisch, M., Albrecht, D., Lessing, F., Schmidt, A.D., Winkler, R., Guthke, R., *et al* (2009) Two-dimensional proteome reference maps for the human pathogenic filamentous fungus *Aspergillus fumigatus*. *Proteomics*. **9**: 1407-1415.

Vodisch, M., Scherlach, K., Winkler, R., Hertweck, C., Braun, H.-P., Roth, M., *et al* (2011) Analysis of the *Aspergillus fumigatus* Proteome Reveals Metabolic Changes and the Activation of the Pseurotin A Biosynthesis Gene Cluster in Response to Hypoxia. *Journal of Proteome Research*. **10**: 2508-2524.

Walker, L.A., Munro, C.A., de Bruijn, I., Lenardon, M.D., McKinnon, A. and Gow, N.A.R. (2008) Stimulation of Chitin Synthesis Rescues *Candida albicans* from Echinocandins. *PLoS Pathogens*. **4**: e1000040.

Wang, W., Fridman, A., Blackledge, W., Connelly, S., Wilson, I.A., Pilz, R.B. and Boss, G.R. (2009) The Phosphatidylinositol 3-Kinase/Akt Cassette Regulates Purine Nucleotide Synthesis. *Journal of Biological Chemistry*. **284**: 3521-3528.

Wang, X., Yen, J., Kaiser, P. and Huang, L. (2010) Regulation of the 26S Proteasome Complex During Oxidative Stress. *Science Signalling*. **3**: ra88.

Wheeler, G.L. and Grant, C.M. (2004) Regulation of redox homeostasis in the yeast *Saccharomyces cerevisiae*. *Physiologia Plantarum*. **120**: 12-20.

Willger, S.D., Puttikamonkul, S., Kim, K.-H., Burritt, J.B., Grahl, N., Metzler, L.J., *et al* (2008) A Sterol-Regulatory Element Binding Protein Is Required for Cell Polarity, Hypoxia Adaptation, Azole Drug Resistance, and Virulence in *Aspergillus fumigatus*. *PLoS Pathogens*. **4**: e1000200 EP.

Winnik, W.M. and Kitchin, K.T. (2008) Measurement of oxidative stress parameters using liquid chromatography-tandem mass spectrometry (LC-MS/MS). *Toxicology and Applied Pharmacology*. **233**: 100-106.

Winyard, P.G., Moody, C.J. and Jacob, C. (2005) Oxidative activation of antioxidant defence. *Trends in Biochemical Sciences*. **30**: 453-461.

Woods, J.P., Heinecke, E.L. and Goldman, W.E. (1998) Electrotransformation and Expression of Bacterial Genes Encoding Hygromycin Phosphotransferase and beta - Galactosidase in the Pathogenic Fungus *Histoplasma capsulatum*. *Infection and Immunity*. **66**: 1697-1707.

Yu, J., Hamari, Z., Han, K.H., Seo, J.A., Reyes-Dominguez, Y. and Scazzocchio, C. (2004) Double-joint PCR: a PCR-based molecular tool for gene manipulations in filamentous fungi. *Fungal Genetics and Biology*. **41**: 973-981.

Yu, X. and Cai, M. (2004) The yeast dynamin-related GTPase Vps1p functions in the organization of the actin cytoskeleton via interaction with Sla1p. *Journal of Cell Science*. **117**: 3839-3853.

Zemp, I. and Kutay, U. (2007) Nuclear export and cytoplasmic maturation of ribosomal subunits. *FEBS Letters Vienna Special Issue: Molecular Machines*. **581**: 2783-2793.

Zhang, W., Li, F. and Nie, L. (2010) Integrating multiple "omics" analysis for microbial biology: application and methodologies. *Microbiology*. **156**: 287-301.

Zhu, D., Tan, K.S., Zhang, X., Sun, A.Y., Sun, G.Y. and Lee, J.C.-M. (2005) Hydrogen peroxide alters membrane and cytoskeleton properties and increases intercellular connections in astrocytes. *Journal of Cell Science*. **118**: 3695-3703.